FACULTAD DE INGENIERÍA

MODELAMIENTO Y PREDICCIÓN DE RIESGO FINANCIERO: UN ENFOQUE DINÁMICO DE VALORES EXTREMOS

FERNANDA STEPHANIE FUENTES LAGOS

Grado: Doctor en Sistemas de Ingeniería
Director de Tesis: Dr. Rodrigo Herrera Leiva

Enero 2021

CONSTANCIA

La Dirección del Sistema de Bibliotecas a través de su encargado Biblioteca Campus Curicó certifica que el autor del siguiente trabajo de titulación ha firmado su autorización para la reproducción en forma total o parcial e ilimitada del mismo.

Curicó, 2021

Título de la tesis	Modelamiento y predicción de Riesgo Financiero: Un enfoque dinámico de valores extremos
Thesis title	Modelling and Forecasting financial risk: A dynamic extreme value approach
Nombre estudiante	Fernanda Stephanie Fuentes Lagos
Fecha inicio tesis	Octubre 2016
Fecha término tesis	Diciembre 2019
Director de tesis	Dr. Rodrigo Herrera Leiva
	Universidad de Talca - Facultad de Economía y Negocios
	Escuela de Ingeniería Comercial
	Talca 3460000, Chile
	rodrigo.herrera@utalca.cl

Dr. Alfredo Candia Vejar

Dr. Miguel de Carvalho

Dr. Rodrigo Herrera Leiva

Dedicada a mis padres, con infinito amor,
impetuoso respeto y profundo agradecimiento.

"La ciencia no es perfecta, con frecuencia se utiliza mal, no es más que una herramienta, pero es la mejor herramienta que tenemos: se corrige a sí misma, está siempre evolucionando y se puede aplicar a todo. Con esta herramienta conquistamos lo imposible."

Carl Sagan.

Agradecimientos

Quiero expresar mis mayores agradecimientos a quien admiro y respeto como profesional y persona, mi supervisor de tesis doctoral el Dr. Rodrigo Herrera, por guiar mi trabajo de investigación y generosamente prodigar su conocimiento en interminables jornadas de aprendizaje, reflexión, y arduo trabajo. Además de jugar un rol fundamental en mi formación como investigadora a través de su constante motivación, plena confianza, asertivos consejos y apoyo incondicional.

Al PhD. Adam Clements, por darme la oportunidad de contar con su valiosa contribución a nivel científico para el desarrollo de mis investigaciones. Además y muy especialmente, por su tiempo, dedicación y hospitalidad durante mi visita de laboratorio en el *National Centre for Econometrics Research* de la *Queensland University of Technology.*

Finalmente agradecer a la Agencia Nacional de Investigación y Desarrollo de Chile (ANID), por el soporte económico proporcionado a través de la beca de doctorado nacional Folio: 21171244 y el proyecto FONDECYT: 1180672.

Índice

Resumen

Una amplia literatura proporciona herramientas econométricas para medir el riesgo financiero durante periodos de turbulencias. Sin embargo, hechos estilizados presentes en series de tiempo financieras, tales como clúster de eventos extremos, persistencia y colas pesadas, pueden no ser capturados a través de metodologías clásicas con parámetros estáticos, lo cual podría producir sesgos en las estimaciones y en consecuencia conclusiones erróneas. Por lo tanto, resulta importante contar con una metodología más flexible para la estimación, análisis y predicción del riesgo financiero extremo.

Esta tesis presenta un marco teórico que introduce conceptos y estrategias utilizadas para modelar el comportamiento dinámico de series de tiempo durante periodos de crisis. Un profundo entendimiento de las características intrínsecas entre los mercados financieros es obtenido por medio de aplicaciones empíricas que involucran, entre otros, índices de: productos básicos, tipos de cambio, productos energéticos, bancos, mercados globales etc.

Como principal resultado un modelo completamente dinámico, basado en teoría de valores extremos y procesos puntuales marcados, es introducido para cuantificar el riesgo unidimensional (riesgo de cola) y riesgo multidimensional (riesgo sistémico), extendiendo la literatura en modelos score-driven aplicados a eventos extremos. El desarrollo de esta metodología ofrece una sofisticada y poderosa herramienta econométrica que permite caracterizar las pérdidas extremas de forma dinámica a través de la intensidad y tamaño de los eventos extremos pasados.

Para ayudar a capturar de mejor forma el comportamiento dinámico de las series de tiempo, se evalúa incorporar variables exógenas al modelo, tales como medidas de volatilidad implícita o realizada, complementando la información otorgada por ambos procesos estocásticos. El desempeño de los distintos enfoques metodológicos considerados en esta tesis son comparados a través de medidas de riesgo, por medio de diferentes test estadísticos de ajuste en periodos de predicción. Los resultados de experimentos empíricos y teóricos muestran la superioridad la metodología propuesta en los mercados financieros analizados.

Este enfoque abre una línea de investigación futura para continuar explorando modelos dinámicos que permitan gestionar adecuadamente el riesgo financiero a niveles extremos. Importantes implicaciones para inversores y precursores de políticas públicas pueden ser obtenidas con los resultados de esta investigación, información clave que puede ser utilizada como proxy para el desarrollo de estrategias económicas y financieras.

Palabras Claves: Teoría de valores extremos, Modelos dinámicos, Medidas de riesgo financiero, Mercados financieros.

Abstract

An extensive literature provides econometric tools to measure financial risk during periods of turmoil. However, stylized facts present in financial time series, such as clusters of extreme events, persistence and heavy tails, may not be captured through classical methodologies with static parameters, which could produce biases in the estimates and consequently erroneous conclusions. Therefore, it is important to have a more flexible methodology to estimate, analyze, and predict extreme financial risk.

This thesis presents a theoretical framework that introduces concepts and strategies used to model the dynamic behavior of time series during crisis periods. A deep understanding of the intrinsic characteristics between financial markets is obtained through empirical applications involving indices of: commodities, exchange rates, energy products, banks, global markets, among others.

As a main result, a completely dynamic model based on the extreme value theory and marked point process, is introduced to quantify one-dimensional risk (tail risk) and multidimensional risk (systemic risk), extending the literature on score-driven models applied to extremes events. This methodology offers a sophisticated and powerful econometric tool that allows to characterize extreme losses dynamically through the intensity and size of past extreme events.

In order to capture the dynamic behavior of time series, we evaluate to incorporate exogenous variables into the model, such as implied or realized volatility measures, complementing the information provided by both stochastic processes. The performance of the methodologies considered in this thesis is compared using different risk measures through accuracy statistical tests during the forecasting period. The empirical results and theoretical experiments show the superiority of the methodology proposed in the financial markets analyzed.

This framework opens up future research lines to continue exploring dynamic models that allow adequate financial risk management at extreme levels. Thus, the results obtained in this research can have important implications for investors and precursors of public policies. Consequently, risk managers can utilize this information as a proxy for developing economic and financial strategies.

Palabras Claves: Extreme Value Theory, Dynamic Models, Financial Risk Measures, Financial Markets.

1. Introducción

El modelamiento de los eventos extremos ha recibido especial atención desde las recientes crisis financieras. Episodios como la crisis subprime y la crisis de la deuda soberana europea evidencian las catastróficas consecuencias económicas que subyacen a nivel global durante periodos de estrés en el mercado financiero. En este sentido, la teoría de valores extremos (EVT[1]) emerge como una disciplina estadística con un importante conjunto de técnicas que permiten caracterizar el complejo comportamiento de las series de tiempo financieras y cuantificar adecuadamente las pérdidas [34].

El desarrollo de los modelos fundamentales EVT tiene origen en las investigaciones de Fisher and Tippett [38] y Gnedenko [41] cuyo primer teorema derivó en la distribución asintótica para modelar los máximos, denominada distribución Generalizada del Valores Extremos (GEV). Más adelante, en los años 70, toma lugar el segundo teorema fundamental de EVT propuesto por Pickands [66] y Balkema and De Haan [3] que caracteriza la distribución asintótica de los excesos por encima de un umbral como una distribución de la familia Generalizada de Pareto (GPD).

Entre algunas de las primeras investigaciones EVT aplicadas en finanzas se encuentran Wiggins [76], Koedijk and Kool [50], Embrechts et al. [33]. A partir del año 2000 un incremento de nuevas metodologías se han desarrollado contibuyendo a enriquecer la literatura en riesgo financiero extremo. En este contexto, uno de las técnicas más ampliamente utilizadas es el modelo clásico de McNeil and Frey [60]. A través de un método en dos etapas, técnicas de EVT son aplicadas a los residuos estimados de un modelo de volatilidad condicional. Aunque esta metodología funciona bastante bien en la práctica, tiene un gran inconveniente, los resultados son sensibles al ajuste del modelo de volatilidad aplicado en la primera etapa [20, 29, 13].

Estudios empíricos muestran que solo modelos que contienen un término de apalancamiento, independientemente de si son modelos basados en rendimientos diarios (por ejemplo, SV o GARCH) o medidas de volatilidad realizadas (por ejemplo, HAR o HEAVY) han tenido éxito en explicar la dinámica de eventos extremos [55, 73]. En la misma línea, modelos construidos por medio de un *conditional quantil* y *expectile regressions* han sido extendidos incorporando refinamiento de EVT [58, 79, 28].

Enfoques más recientes propone modelar la intensidad y magnitud de los eventos extremos por medio de metodologías que combinan procesos puntuales marcados (MPP) y EVT [20]. En este contexto existe una relación natural entre la intensidad de ocurrencia de los eventos extremos y la volatilidad observada, como fue evidenciado por Engle and Russell [36], premio Nobel de Economía 2002. La principal ventaja de los modelos MPP es que permiten capturar el comportamiento dinámico de eventos extremos cuyos tiempos inter-excedencias evidencian autocorrelación. Además, centra el análisis solo en las colas de la distribución haciendo un uso eficiente de las observaciones.

En la búsqueda de una metodología más flexible para la estimación, análisis y predicción del riesgo financiero, recientes investigaciones han desarrollado una amplia variedad de nuevos modelos basados en el enfoque score-driven introducido por Creal et al. [27] y Harvey [44]. Esta metodología ha alcanzado popularidad en los últimos años, principalmente porque desarrolla un marco común y natural que permite construir una amplia variedad de modelos dinámicos. Una importante característica del enfoque score-driven es que la función de verosimilitud es conocida de forma cerrada, lo cual permite construir parámetros dinámicos de forma sencilla contribuyendo a incrementar la popularidad de estos modelos en econometría [52]. Por otro lado, el comportamiento dinámico de las series de tiempo es capturado a través de parámetros dinámicos cuyas ecuaciones de actualización siempre reduce la divergencia de Kullback-Leibler entre la densidad condicional verdadera y la implícita del modelo [9].

[1] Todas las abreviaciones consideran las siglas en inglés

En la actualidad, a pesar de la versatilidad del modelo score-driven, existen pocas investigaciones aplicadas a EVT, las cuales principalmente modelan un solo parámetro dinámico [59, 81, 5]. Esta tesis contribuye a disminuir esta brecha, extendiendo la literatura al introducir dos enfoques score-driven. El primero denominado score-driven Peak Over Threshold (SPOT) es una propuesta metodológica que sugiere caracterizar la intensidad y magnitud de los eventos extremos a través de dos parámetros dinámicos, uno para cada proceso estocástico. El segundo, denominado Generalized score-driven Peak Over Threshold (GSPOT), propone un modelo completamente dinámico MPP para las excedencias, donde todos los parámetros varían en el tiempo con una actualización basada solo en el score de las observaciones pasadas.

Además, esta tesis también plantea nuevos desafíos empíricos, para capturar el comportamiento de series de tiempo cruciales para la estabilidad financiera a nivel global, las cuales han mostrado ser frágiles durante periodos de turbulencias. Entre algunas aplicaciones se encuentran, los tipos de cambios de importantes mercados globales, los cuales a niveles extremos parecen ser dependientes de los principales productos básicos de exportación de cada país (*commodity currencies*). Además, se analizan hechos estilizados de compañías individuales de energía limpia y su relación con productos básicos (petróleo y oro) e índices globales (Estados Unidos y Europa), evidenciando la existencia de clúster entre compañías del mismo sector productivo. Por otro lado, un análisis empírico se desarrolla en torno a algunos de los denominados G-SIBS (*global systemically important banks*) quienes han evidenciado inestabilidad sistemática y elevados niveles de estrés durante periodos de crisis financieras. En este contexto a través de una extensión dinámica de una medida de riesgo sistémico se obtienen estrategias de optimización de portafolios.

A continuación se detallan las principales preguntas de investigación que motivan el desarrollo de esta tesis:

1.1. Preguntas de investigación

1. ¿Es posible obtener un mayor beneficio en el pronóstico de riesgo extremo al utilizar una metodología basada solo en las pérdidas extremas?
2. ¿Cuál es la relación entre la intensidad condicional y la volatilidad observada? ¿Aquellos modelos basados en intensidad, proveen una predicción superior del riesgo financiero extremo versus enfoques tradicionales de volatilidad?
3. ¿De qué manera factores estilizados de eventos extremos financieros y volatilidades pueden ser capturados utilizando procesos puntuales marcados y teoría de valores extremos? ¿Son homogéneos estos factores estilizados en los distintos mercados financieros tales como productos básicos, energía y banca?
4. ¿Podrían variables exógenas, como la volatilidad implícita o realizada, ayudar a predecir la tasa de ocurrencia y magnitud de eventos extremos futuros? ¿Contribuyen estas variables a mejorar el desempeño de diferentes medidas de riesgo?
5. ¿Es posible modelar la intensidad condicional de manera completamente dinámica y de esta forma capturar el comportamiento de las series de tiempo financieras en periodos de crisis? ¿Cuáles son las ventajas de utilizar un enfoque dinámico en el análisis de riesgo financiero extremo?

Para direccionar estas preguntas se propone una serie de objetivos específicos que son el esquema base de esta investigación y representan los lineamientos para el desarrollo del objetivo general, todos estos detallados a continuación:

1.2. Objetivos

1.2.1. Objetivos general

Desarrollar un modelo score-driven MPP para eventos extremos, utilizando la información dinámica de la intensidad de ocurrencia y la magnitud de las excedencias para capturar y predecir riesgo financiero extremo.

1.2.2. Objetivos específicos

- Evaluar empíricamente diferentes enfoques metodológicos para describir el comportamiento de series financieras cruciales para la economía (tales como índices de: productos básicos, tipos de cambio, productos energéticos, bancos, mercados globales etc).
- Identificar las ventajas de cuantificar el riesgo financiero analizando solo eventos extremos, versus los enfoques clásicos.
- Analizar la relación entre la volatilidad y la intensidad condicional de los eventos extremos en el contexto de crisis financieras.
- Desarrollar un enfoque score-driven multiparámetro para modelar dinámicamente el comportamiento eventos extremos.
- Examinar la capacidad predictiva del modelo cuantificando medidas de riesgo en diferentes periodos de predicción.
- Mejorar ajustes estadísticos de las medidas de riesgo financiero evaluando la pertinencia de incorporar variables exógenas de volatilidad.

2. Marco teórico

2.1. Teoría de Valores Extremos

La EVT es una disciplina estadística que desarrolla técnicas para describir lo inusual en lugar de lo habitual. Por definición, los valores extremos son escasos, por lo que la EVT proporciona el argumento asintótico que permite extrapolar de niveles observados a niveles no observados a partir de un conjunto de datos muy limitado [24].

Existen dos teoremas fundamentales que juegan un importante rol en EVT, el primero de Fisher and Tippett [38] y Gnedenko [41] que caracteriza la distribución asintótica del máximo observado como la distribución GEV. Mientras que el segundo teorema de Pickands [66] y Balkema and De Haan [3] da lugar a la distribución asintótica que concierne los excesos por encima de un umbral, como una distribución GPD. Estos son descritos a continuación:

2.1.1. Distribución Generalizada de Valores Extremos

Supongamos que $y_t \in \mathbb{R}$, son retornos negativos independiente e idénticamente distribuidos (iid) de una serie financiera, siguiendo una función de probabilidad común F. Si nos concentramos en investigar solo la distribución de probabilidad de los valores máximos de la serie de retornos $M_T = \max\{Y_t\}_{t=1}^{T}$, esta tiene una estandarización que permite obtener un límite no-degenerado cuando $T \to \infty$. Para este fin, la transformación propuesta por Fisher and Tippett [38], Gnedenko [40] propone utilizar las secuencias $a_T > 0$ y $b_T \in \mathbb{R}$, para la cual establece que si

$$\lim_{T\to\infty} T\{1 - F(a_T y + b_T)\} \to -\ln H_{\xi,\mu,\sigma}(y). \tag{1}$$

Entonces el límite de la función parametrizada $\lim_{T\to\infty} P\left(\frac{M_T - b_T}{a_T} \leq y\right) = H_{\xi,\mu,\sigma}(y)$ converge a una distribución GEV definida como

$$H_{\xi,\mu,\sigma}(y) = \begin{cases} \exp\left\{-\left(1+\xi\frac{y-\mu}{\sigma}\right)_+^{-1/\xi}\right\} & \xi \neq 0, \\ \exp\left\{-\exp\left(-\frac{y-\mu}{\sigma}\right)\right\} & \xi = 0. \end{cases}$$

Donde $(f)_+ = \max\{0, f\}$ corresponde a la parte positiva de la función y $\xi, \mu \in \mathbb{R}$ y $\sigma > 0$ son los parámetros de forma, localización y escala, respectivamente. A través del parámetro de forma ξ es posible determinar la distribución y en consecuencia el grosor de la cola. Cuanto mayor sea el índice, más gruesa será la cola:

- $\xi > 0$: Distribución de Fréchet
- $\xi < 0$: Distribución de Weibull
- $\xi = 0$: Distribución de Gumbel

2.1.2. Distribución Generalizada de Pareto

Como una alternativa diferente para modelar eventos extremos que sobrepasen un umbral suficientemente alto $u > 0$, surge la metodología Peak Over Threshold (POT). El teorema Pickand-Balkema-De Haan [3, 66] muestra que si la condición expuesta en Ec. (1) se cumple, entonces la distribución límite para los excesos sobre el umbral corresponde a la función GDP

$$P(Y - u \leq y \mid Y > u) \quad \approx \quad G_{\xi,\beta}(y)$$

donde

$$G_{\xi,\beta}(y) = \begin{cases} 1 - \left(1 + \xi \frac{(y-u)}{\beta}\right)_+^{-1/\xi}, & \xi \neq 0, \\ 1 - \exp\left(-\frac{(y-u)}{\beta}\right) & \xi = 0. \end{cases}$$

en esta distribución el parámetro de escala es definido como $\beta = \sigma + \xi(u - \mu) > 0$.

2.2. Procesos Puntuales

Alternativamente, es posible observar las serie de retornos iid $y_t \in \mathbb{R}$, como el par de variables aleatorias $\{(t_i, z_i)\}_{i \geq 1}$ que describe los dos procesos estocásticos. Por un lado la tasa de ocurrencia t_i como el i-ésimo evento extremo ocurrido en el tiempo t, y por otro lado la magnitud del evento extremo $z_i = y_{t_i} - u$ donde la observación y_{t_i} excede el umbral u.

Si definimos el proceso puntual $N(t) \equiv \sum \mathbb{1}_{\{t_i < t, z_i = z\}}$ como el contador de las observaciones (t_i, z_i) ocurridas hasta el tiempo t, es posible construir un proceso puntual bi-dimensional en el espacio $\Omega = (0,1) \times (u, \infty)^2$. Pickands [65] demostró que para todo el subespacio $A = [t_1, t_2) \times [y, \infty)$, donde t_1 y t_2 son coordenadas en el tiempo $0 < t_1, t_2 < 1$, este proceso puntual bidimensional puede ser visto como un proceso Poisson no-homogéneo con intensidad definida como sigue:

$$\lambda(t,z) = \begin{cases} \frac{1}{\sigma}\left(1 + \xi \frac{y-\mu}{\sigma}\right)_+^{-\frac{1}{\xi}-1}, & \xi \neq 0, \\ \frac{1}{\sigma}\exp\left(-\frac{y-\mu}{\sigma}\right), & \xi = 0 \end{cases} \tag{2}$$

donde μ, ξ y σ, corresponde a los parámetros definidos en la distribución GEV.

Considerando que la intensidad no depende del tiempo es posible re-escribirla en términos de un proceso Poisson unidimensional donde $N_g(t) \equiv \sum \mathbb{1}_{\{t_j < t\}}$ corresponde únicamente al proceso estocástico básico (Ground process) que contabiliza sólo los tiempos de ocurrencia de los eventos extremos hasta el tiempo t y cuya intensidad de ocurrencia es definida por $\tau(u) = -\ln H_{\xi,\mu,\sigma}(u)$. De esta forma, si consideramos que el proceso de Poisson de las excedencias es unidimensional, entonces tiene incrementos independientes, es decir, el número de eventos t_i que ocurren en intervalos de tiempo disjuntos son mutuamente independientes, lo que implica falta de memoria en la evolución del proceso. Consecuentemente, el número de eventos extremos t_i en cualquier intervalo de tiempo de largo $(t_2 - t_1)$ distribuye Poisson con media:

$$\Lambda(A) = \int\int_A \lambda(r,s)\, dr ds = -(t_2 - t_1) \ln H_{\xi,\mu,\sigma}(y).$$

Luego, es posible reescribir la función de intensidad en la ecuación (2) a través de dos procesos estocásticos. El primero $\tau(u)$ caracterizando la intensidad de los eventos extremos ocurridos sobre el umbral , mientras que el segundo $g(z)$ representa la función de densidad de las marcas

$$\lambda(t,z) = \tau(u) \cdot g(z), \tag{3}$$

donde $g(z)$ es la función de densidad de la GPD

$$g(z) = \begin{cases} \frac{1}{\beta}\left(1 + \xi \frac{z}{\beta}\right)_+^{-\frac{1}{\xi}-1}, & \xi \neq 0, \\ \frac{1}{\beta}\exp\left(-\frac{z}{\beta}\right) & \xi = 0. \end{cases}$$

Luego, como una extensión a los modelos MPP, la historia de eventos extremos pasados $\mathcal{H}_t = \{(t_i, z_i)\ \forall i : t_i < t\}$

[2] El tiempo ha sido re-escalado al intervalo (0,1) para facilitar la exposición de la metodología.

hasta el tiempo t sin incluir el tiempo t, puede ser incorporada fácilmente en ambos procesos estocásticos de la intensidad condicional como sigue:

$$\lambda\left(t_i, z_i \mid \mathcal{H}_t\right) = \tau\left(t_i \mid \mathcal{H}_t\right) g\left(z_i \mid t_i, \mathcal{H}_t\right), \tag{4}$$

a diferencia del proceso puntual bidimensional, esta intensidad corresponde a un MPP, donde la función densidad de probabilidad de las marcas, es condicional a la ocurrencia del último evento extremo en el tiempo t_i.

3. Métodos

3.1. Score-driven Peak Over Threshold framework

Utilizando el enfoque score-driven propuesto por Harvey [44] and Creal et al. [26], se desarrolla una especificación dinámica para la intensidad condicional descrita en Ec. (4)

$$\lambda\left(t_i, z_i \mid \mathcal{H}_t, f_i; \Theta\right) = \tau\left(t_i \mid \mathcal{H}_t, f_i^{\tau}; \theta^{\tau}\right) g\left(z_i \mid t_i, \mathcal{H}_t, f_i^{g}; \theta^{g}\right)$$

Donde $f_i := \left\{\left(f_i^{\tau}, f_i^{g}\right)\right\} \in \mathbb{R}^2$ es el vector bivariado de parámetros de tiempo variable y el $\Theta := \{(\theta^{\tau}, \theta^{g})\} \in \mathbb{R}^{k+1}$ el vector de parámetros estáticos. La principal característica de esta especificación, es que tanto la intensidad base como también la función densidad de probabilidad de las marcas, cuentan con un parámetro dinámico que captura el comportamiento de ambos procesos estocásticos. Para este fin, la metodología score-driven utiliza la información completa del log-likelihood dado por

$$\mathcal{L}_i\left(t_i, z_i \mid \mathcal{H}_t, f_i; \Theta\right) = \ln \tau\left(t_i \mid \mathcal{H}_t, f_i^{\tau}; \theta^{\tau}\right) - \int_{t_{i-1}}^{t_i} \tau\left(s \mid \mathcal{H}_s, f_{N(s)}^{\tau}; \theta^{\tau}\right) ds + \ln g\left(z_i \mid t_i, \mathcal{H}_t, f_i^{g}; \theta^{g}\right)$$

donde, $N(t) \equiv \sum \mathbb{1}_{\{t_i \le t, z_i = z\}}$ es la función de conteo de las observaciones estocásticas $\{(t_i, z_i)\}_{i \ge 1}$ ocurridas durante el intervalo $(0, t]$. La ecuación de actualización caracterizada por el factor dinámico que permite modelar el parámetro de tiempo variante definido por

$$f_{i+1}^{r} = \omega_r + \phi_r f_i^{r} + \psi_r s_i^{r}$$

donde ω_r, ϕ_r y ψ_r son coeficientes no restringidos para cada parámetro dinámico presente en la especificación. Mientras que, $s_i^{r} = S_{ri} \nabla_{ri}$ es el scaled score de la función densidad de probabilidad, que puede ser obtenido como

$$S_{ri} = E\left[\nabla_{ri}^2 \mid \mathcal{H}_t\right]^{-1} \qquad \nabla_{ri} = \frac{\partial \mathcal{L}_i}{\partial f_i^{r}}$$

donde la función scaling $S_{ri} = E\left[\nabla_{ri}^2 \mid \mathcal{H}_t\right]^{-1}$ es la inversa condicional de la información de Fisher y ∇_{ri} el score de la función densidad de probabilidad. A modo de simplificar la notación el índice $r = \{\tau, g\}$ representa el proceso estocástico de la intensidad o magnitud de los eventos extremos, según corresponda.

3.2. Generalized Score-driven Peak over Threshold framework

En el modelo completamente dinámico GSPOT, la intensidad condicional definida en Ec. (4) describe la probabilidad instantánea de observar un evento extremo en el tiempo t_i con magnitud z_i condicional a la historia de eventos extremos pasados $\mathcal{H}_t = \{(t_i, z_i)\ \forall i : t_i < t\}$, como sigue

$$\lambda\left(t_i, z_i \mid \mathcal{H}_t, \boldsymbol{f}_i\right) = \tau\left(t_i \mid \mathcal{H}_t, \boldsymbol{f}_i^{\star}\right) g\left(z_i \mid t_i, \mathcal{H}_t, \boldsymbol{f}_i^{*}\right),$$

para la cual $\tau\left(t_i \mid \mathcal{H}_t, \boldsymbol{f}_i^{\star}\right)$ corresponde al proceso estocástico de la intensidad del proceso base, caracterizada a través de una función hazard. Mientras que $g\left(z_i \mid t_i, \mathcal{H}_t, \boldsymbol{f}_i^{*}\right)$ denota la función densidad de probabilidad de las marcas como una GPD. A diferencia de la especificación SPOT, la presente metodología extiende la dinámica a todos los parámetros involucrados en la intensidad condicional presente en Ec. (4). Cabe destacar, que se trata del primer modelo que extiende la metodología score-driven a más de un parámetro.

En definitiva, la extensión GSPOT permite aprovechar toda la información de la función densidad de probabilidad, caracterizando ambos procesos estocásticos a través de un set de parámetros de tiempo variable $\boldsymbol{f}_i := \left\{\boldsymbol{f}_i^\star \cup \boldsymbol{f}_i^*\right\}$, con $\boldsymbol{f}_i^\star := \left(f_i^1, \ldots, f_i^{k_1}\right)$ y $\boldsymbol{f}_i^* := \left(f_i^{k_1+1}, \ldots, f_i^{k_1+k_2}\right)$. En este caso, la contribución de cada evento i a la función log-likelihood es

$$\mathcal{L}_i\left(\boldsymbol{f}_i\right) = \left\{\ln \tau\left(t_i \mid \mathcal{H}_t, \boldsymbol{f}_i^\star; \boldsymbol{\theta}^\star\right) - \int_{t_{i-1}}^{t_i} \tau\left(s \mid \mathcal{H}_s, \boldsymbol{f}_{N(s)}^\star; \boldsymbol{\theta}^\star\right) ds\right\} + \ln g\left(z_i \mid t_i, \mathcal{H}_t, \boldsymbol{f}_i^*; \boldsymbol{\theta}^*\right)$$

donde $\boldsymbol{\theta} := \left\{\boldsymbol{\theta}^\star \cup \boldsymbol{\theta}^*\right\}$, representa el conjunto de no restringidos coeficientes estáticos para cada parámetro de tiempo variable con $\boldsymbol{\theta}^\star := \left\{\left(\omega_j, \psi_j, \phi_j\right)\right\}_{j=1}^{j=k_1}$ y $\boldsymbol{\theta}^* := \left\{\left(\omega_j, \psi_j, \phi_j\right)\right\}_{j=k_1+1}^{j=k_1+k_2}$. Siguiendo el enfoque del score-driven, la función actualizadora es definida por

$$f_{i+1}^j = \omega_j + \psi_j s_i^j + \phi_j f_i^j$$

$$s_i^j = S_i^j \nabla_i^j = E_{i-1}\left[-\frac{\partial^2 \mathcal{L}_i\left(\boldsymbol{f}_i\right)}{\partial f_i^{j2}}\right]^{-1} \frac{\partial \mathcal{L}_i\left(\boldsymbol{f}_i\right)}{\partial f_i^j}$$

Donde el scaling S_i^j es la entrada diagonal de la inversa condicional de la matriz de información de Fisher $\boldsymbol{S}_i$ con respecto al parámetro j y $\nabla_i^j = \frac{\partial \mathcal{L}_i\left(\boldsymbol{f}_i\right)}{\partial f_i^j}$ es el j-th elemento del vector score $\boldsymbol{\nabla}_i$, obtenido por el gradiente de la función log-likelihood con respecto al parámetro j.

Una condición importante de la metodología propuesta es la ortogonalidad de los parámetros de tiempo variable con respecto a la matriz de información de Fisher, cada vez que se observa un evento extremo i. Para alcanzar esta condición se obtiene una nueva parametrización de la Ec. (4) utilizando la estrategia propuesta por [25].

4. Descripción de las publicaciones

4.1. Modeling Extreme Risks in Commodities and Commodity Currencies

En muchos países los productos básicos (*commodities)* dominan parte importante de las exportaciones. Los precios a los cuales estos productos son transados tienen un importante efecto en el comportamiento de los tipos de cambio, estas monedas son denominadas *"commodity currencies"*.

Estudios previos han analizado la relación entre los productos básicos y los tipos de cambio utilizando modelos de cointegración y corrección de error [51, 45, 77, 8], además de diferentes test de causalidad de Granger [18, 22]. Sin embargo a pesar de la extensa literatura, existe poco conocimiento acerca del comportamiento de este tipo de retornos a niveles extremos [21, 49, 16, 12, 10].

Este artículo propone análizar si existe co-movimiento entre productos básicos y tipos de cambio durante periodos de turbulencias financieras, desarrollando una extensión multivariada del modelo Hawkes-POT propuesto por Chavez-Demoulin et al. [20]. Alternativamente, los resultados de este modelo son comparados con la especificación Diagonal BEKK (DBEKK) introducido por Baba et al. [2], Engle and Kroner [35] con un refinamiento EVT, como una extensión del modelo clásico univariado de McNeil and Frey [60].

Las principales preguntas de investigación son: ¿Es posible obtener una mejor gestión de riesgo extremo basados en modelos de intensidad (multivariado Hawkes-POT) en contraste con modelos de volatilidad y correlación (DBEKK)? ¿Existe un vínculo unidireccional desde los productos básicos hacia las monedas? ¿Es más beneficioso gestionar el riesgo financiero en periodos de crisis a través de especificaciones que utilicen solo en eventos extremos y/o modelos basados en volatilidad?

El estudio empírico considera los retornos negativos de dos importantes tipos de cambio, conocidos y ampliamente estudiados en la literatura como *commodity currencies*, estos son el dólar australiano y dólar canadiense, vinculado a sus principales productos de exportación, el oro y petróleo, respectivamente [69, 67, 7, 4]. La base de datos fue obtenida de Bloomberg con observaciones diarias que van desde el 4 de enero 2005 al 31 de diciembre 2014, para el periodo de prueba y desde el 1 de enero del 2015 al 31 de diciembre 2016 para el periodo de predicción. Similar a Herrera [48], el umbral al cuantil del 0.90 fue escogido de forma pragmática, probando diferentes cuantiles desde el 0.90 al 0.94. La idea es seleccionar el umbral que permita obtener un mejor ajuste del *Value at Risk* (VaR) dentro del periodo de prueba, según algunos test estadísticos utilizados ampliamente en la literatura (LR_{uc}, LR_{ind}, LR_{cc} y DQ_{hit}), bajo tres niveles de confianza 0.95, 0.99 y 0.999 [23, 58].

Los resultados muestran que la intensidad y volatilidad siguen patrones similares a través del tiempo. Consecuente con la literatura previa, el modelo unidireccional Hawkes-POT revela una influencia desde los productos básicos a las monedas [21, 16, 12]. Durante el periodo de prueba, mejores resultados en los ajustes del VaR son obtenidos con el modelo Hawkes-POT, mientras que en el periodo de predicción los resultados son mixtos. En el caso de Australia el modelo Hawkes-POT muestra superioridad y mientras que en el caso de Canadá el modelo DBEKK-EVT permite un mejor ajuste.

En general ambos enfoques son complementarios y proporcionan información relavente para un más profundo entendimiento de la relación entre los principales productos básicos de cada país y sus tipos de cambio durante periodos de estrés. Por un lado, la intensidad condicional utiliza la intensidad de ocurrencia y tamaño de los eventos extremos para describir dinámicamente su comportamiento, mientras que, por otro lado, el modelo de volatilidad utiliza la información completa contenida en los retornos. A diferencia del modelo DBEKK, el beneficio principal del modelo Hawkes-POT es que permite evidenciar la existencia de *commodity currencies*, ya que captura la relación causal unidireccional de dependencia extrema desde los productos básicos hacia las monedas.

4.2. Dynamics of Connectedness in Clean Energy Stock Markets

Las problemáticas medioambientales y el incremento en el costo de los combustibles fósiles ha estimulado el desarrollo de la economía verde, logrando que negocios de energía renovable sean competitivos frente a los recursos de energía convencional y atrayendo participantes en mercados de energía limpia interesados en nuevas oportunidades de inversión [6, 80, 57].

Estudios previos han examinado la relación entre los índices de energía limpia y otros mercados financieros a través de modelos de GARCH multivariados [32, 54, 56] y modelos basados en cópulas multivariadas [11, 61, 68]. Si bien ambos enfoques proveen información útil en diferentes contextos, volatilidad y dependencia respectivamente, estas no permiten obtener conclusiones en términos de conectividad direccional, lo cual es relevante para el desarrollo de estrategias de inversión y políticas públicas.

Por otro lado, luego de una extensa revisión de la literatura financiera aplicada en mercados de energía limpia, es posible observar una importante limitación. La mayoría de las investigaciones desarrolladas analizan empíricamente índices globales, entre los cuales se destacan, S&P Global Clean Energy Index (SPGCE), WilderHill Clean Energy Index (ECO) y WilderHill New Energy Global Innovation Index (NEX). Por lo cual, estas investigaciones observan el comportamiento de los mercados de energía limpia desde un punto de vista más homogéneo, sin incluir la información desagregada a nivel de compañías individuales, lo cual podría proveer sesgos en las conclusiones obtenidas [64].

Esta investigación utiliza la metodología *Directional Conectedness* propuesta por Diebold and Yılmaz [31] para estimar medidas de volatilidad direccional entre índices individuales de compañías de energía limpia e índices de volatilidad implicada obtenida de opciones asociadas a productos básicos (oro y petróleo) e índices globales (Estados Unidos y Europa). Considerando primero una red estática de conectividad que resume la información de toda la muestra y una red dinámica de conectividad a través de un *rolling-window*, los resultados obtenidos son complementados a través de un análisis impulso-respuesta.

Las principales preguntas de investigación son: ¿Es posible evidenciar un comportamiento heterogéneo entre los distintos subsectores productivos en los mercados de energía limpia? ¿Existe una relación unidireccional entre las compañías de energía limpia y los productos básicos o mercados financieros? ¿Qué expectativas en términos de volatilidad implicada son más importantes para los mercados de energía limpia?

Para el análisis empírico se considera la volatilidad realizada (*realized range-based volatility*) de 16 compañías individuales de energía limpia constituyentes del índice SPGCE[3], y su relación con cuatro indices de volatilidad implicada, el Cboe Gold ETF Volatility Index (GVZ), Cboe Crude Oil ETF Volatility Index (OVX), CBOE Volatility Index based on options of the S&P 500 index (VIX) y Euro Stoxx 50 Volatility Index based on EURO STOXX 50 options prices (VSTOXX). Las primeras dos volatilidades implicadas son asociadas a productos básicos, el petróleo es un sustituto inherente de los mercados de energía limpia [68, 53]. Mientras que el oro es incluido por su rol como cobertura durante periodos de turbulencias [74, 70]. Las dos últimas volatilidades implicadas hacen referencia a los índices globales de Estados Unidos y Europa y son incluidas considerando los países de origen de las compañías analizadas.

Los resultados revelan que la conectividad es unidireccional, marcada fuertemente por la procedencia de un flujo significativo de información desde los índices de volatilidad implicada hacia las compañías de energía limpia, donde las expectativas de las volatilidades futuras del VIX y GVZ jue-

[3]Entre las treinta compañías constituyentes del SPGCE solo fueron consideradas dieciséis ya que estas contienen datos a partir de la fecha establecida en el periodo in-sample.

gan un rol fundamental. Al examinar la evolución de las medidas de volatilidad direccional en el tiempo es posible evidenciar la existencia de clúster de volatilidad entre compañías pertenecientes al mismo sub-sector productivo. En consecuencia, es posible identificar una relación heterogénea entre los sub-sectores productivos de las compañías de energía limpia (i.e., solar, eólica, hidroeléctricas, geotérmica, *fuel cell*, mixta) y los índices de volatilidad implicada.

Finalmente, el análisis impulso-respuesta permite confirmar los resultados obtenidos en la conectividad direccional, destacando el rol de los índices de volatilidad implicada VIX y GVZ sobre la volatilidad realizada de las compañías de energía limpia. Las respuestas de las compañías a los shocks de volatilidad implicada permite confirmar la existencia de clúster entre los distintos sub-sectores productivos de energía limpia. Como conclusión final, esta investigación evidencia que es necesario tener en cuenta las características específicas de cada sub-sector productivo para lograr estrategias de inversión más eficientes, contrario a la literatura previa que examina estas variables desde un punto de vista más agregado.

4.3. Forecasting Extreme Financial Risk: A Score-driven Approach

Los recientes avances en teoría econométrica han puesto énfasis en capturar el comportamiento de los factores estilizados de series de tiempo a través de modelos dinámicos. Una de las más prometedoras es la metodología score-driven introducida por Creal et al. [27] y Harvey [44], la cual ha alcanzado popularidad en muchas aplicaciones financieras. Sin embargo, en la literatura existen pocas investigaciones score-driven con enfoque EVT. Massacci [59] propone una metodología score-driven para la GPD, cuyos parámetros de tiempo variable están conjuntamente actualizados por la media de un modelo one-factor. Zhang and Bernd [81] propone una especificación en dos etapas, donde primero los datos son desvolatilizados y luego a través del enfoque score-driven, el parámetro de forma de la GPD es modelado de manera dinámica, manteniendo fijo el parámetro de escala. Recientemente, Bee et al. [5] propone un enfoque score-driven POT, basado en una medida realizada obtenida de retornos intra-diarios, incluyendo un término autoregresivo por medio del enfoque score-driven.

Este artículo considera una propuesta metodológica completamente diferente, donde el método score-driven es aplicado a un MPP para las excedencias, capturando dinámicamente dos procesos estocásticos, la intensidad de ocurrencia y la magnitud de los eventos extremos ocurridos sobre un umbral. Este modelo es denominado score-driven Peak Over Threshold (SPOT).

Cuatro diferentes funciones hazard no-monotónicas son empleadas para caracterizar la intensidad del proceso base: Weibull, gamma, Burr y generalizada gamma. Mientras que para la magnitud de los excesos es usada una GPD. La metodología propone modelar de forma dinámica un parámetro en intensidad del proceso base y otro en la magnitud de los eventos extremos, originando diferentes especificaciones de acuerdo a los parámetros seleccionados para ser dinámicos dentro de cada proceso estocástico, las cuales son comparadas en término de AIC y BIC.

Una de las ventajas del modelo SPOT, es que puede incorporar fácilmente variables exógenas. En el contexto financiero de riesgo extremo, recientes investigaciones proponen incluir medidas de volatilidad realizada para ayudar a explicar la dinámica de las excedencias [15, 78, 5]. Este artículo extiende la literatura en modelos score-driven EVT, proponiendo un SPOT realizado (rSPOT) que evalua el desempeño de cuatro medidas de volatilidad (simple realized variance, realized semivariance, jumps, negative jumps).

Las principales preguntas investigación son ¿En qué grado la dinámica de los eventos extremos es explicada por dos componentes estocásticos, intensidad y magnitud, conducidos por un parámetro score-driven?. ¿Existe alguna ventaja al incorporar medidas de volatilidad realizada en el análisis de la gestión de riesgo extremo?

El modelo es aplicado a los retornos negativos diarios de 10 conocidos índices globales. La base de datos es obtenida del *Oxford-Man Institute "realized library" version 0.3*. El periodo de prueba comprende observaciones que van desde el 3 de enero del 2000 al 29 de diciembre del 2016, mientras que el periodo de predicción, considera observaciones desde el 4 de enero 2017 al 27 de diciembre 2018. Consecuente con la literatura, consideramos el umbral a un cuantil del 0.90 [19, 5, 46].

El desempeño del modelo propuesto es comparado con otros dos enfoques score-driven EVT, los modelos de Bee et al. [5] y Massacci [59], en un periodo de predicción de uno y dos años. Diferentes pruebas estadísticas son evaluadas para cuantificar la exactitud del VaR. Complementariamente es estimada la función de pérdida de Fissler and Ziegel (FZL) que involucra el VaR y el expected shortfall (ES) conjuntamente. Luego, estas estimaciones son comparadas a través del modelo de ajuste *Model Confidence Set* propuesto por Hansen et al. [42]

En términos de los criterios de información AIC y BIC, mejores resultados son obtenidos con el parámetro de forma estimado dinámicamente en la especificación Burr que caracteriza la intensidad del proceso base, y con el parámetro de escala estimado dinámicamente en la GPD que modela la magnitud de los eventos extremos. En general, los resultados de la predicción muestran que la especificación SPOT logra un mejor desempeño en las pruebas del VaR. Mientras que para la medida FZL la especificación rSPOT lidera por sobre sus competidores.

4.4. Assessing Systemic Risk with Score-driven Extreme Value Models

La gestión del riesgo sistemático como elemento fundamental para entender las crisis financieras, ha motivado el interés de los investigadores por avanzar en el desarrollo de medidas globales que permitan integrar simultáneamente perspectivas tanto microprudenciales como macroproduciales [39, 71, 62]. En este sentido, las medidas de riesgo sistémico más ampliamente utilizadas en la literatura son; el marginal expected shortfall (MES) de Acharya et al. [1], el SRISK propuesto por Brownlees and Engle [14] y el CoVaR de Tobias and Brunnermeier [72].

En los últimos años el enfoque score-driven desarrollado por Creal et al. [27] y Harvey [44] ha alcanzado popularidad en la modelación del riesgo sistémico. Sin embargo, la literatura de estos modelos basados en EVT hasta el momento se limita principalmente a capturar la dinámica de un solo parámetro de tiempo variable (escala o forma).

Este artículo introduce el modelo Generalized score-driven Peaks Over Threshold (GSPOT), con base en MPP y EVT, donde todos los parámetros varían dinámicamente a través del tiempo. Una importante condición es que los parámetros son ortogonales a la matriz de información de Fisher. En particular, en esta especificación la ecuación de actualización de cada uno de los parámetros se encuentra basada en el pasado de las observaciones y no depende de los *spillovers* de los distintos procesos estocásticos. Un estudio de Monte-Carlo muestra el desempeño del modelo bajo diferentes escenarios, los cuales consideran tamaños muestrales dentro de un rango típico para retornos financieros y diferentes formas funcionales para los parámetros.

El modelo GSPOT es usado para extender dinámicamente la medida tail-β risk propuesta recientemente por van de Leur et al. [75]. A través de esta medida nosotros podemos obtener información del riesgo individual y capturar el riesgo sistémico asociado a la estabilidad del mercado financiero global. Luego, una versión dinámica del MES es estimada utilizando la información contenida en el tail-β risk dinámico.

El análisis empírico considera 16 bancos constituyentes del S&P Bank index, el cual considera a su vez los bancos más importantes de Estados Unidos. El periodo de prueba comprende observaciones entre el 4 de enero de 1999 y el 31 de diciembre de 2013, con un periodo de predicción que considera

observaciones desde el 4 de enero del 2014 al 31 de diciembre del 2018. Consecuente con una amplia literatura se utilizó un cuantil del 0.90 para definir el umbral [19, 5, 46].

Los resultados indican que el enfoque GSPOT es capaz de capturar hechos estilizados presentes en las series de retornos financieras, tales como clúster extremos, persistencia y colas pesadas. Complementariamente, la intensidad de ocurrencia de los eventos extremos y su magnitud proveen información conjunta importante para describir a través de los parámetros dinámicos el comportamiento de los eventos extremos en índices de bancos durante periodos de turbulencia financiera.

A través de la medida de riesgo sistémico tail-β risk dinámico y la medida MES obtenida a partir de la anterior, se muestra empíricamente que es posible diversificar portafolios de bancos en relación al riesgo financiero extremo, obteniendo ventajas en términos de los retornos esperados.

5. Conclusiones

Esta tesis se desarrolla en el contexto de riesgo financiero extremo, diferentes metodologías son analizadas para capturar el comportamiento de conocidas series de tiempo (tales como índices de: productos básicos, tipos de cambio, productos energéticos, bancos, mercados globales, etc.), cuyo productos y mercados subyacentes juegan un rol clave para la estabilidad económica a nivel global durante periodos de crisis. A través de las aplicaciones empíricas es posible obtener una comprensión más profunda del riesgo de cola y riesgo sistémico en periodos de turbulencia. Esta información puede ser aprovechada para desarrollar estrategias de prevención y diversificación de riesgo financiero.

Esta investigación introduce la primera propuesta que extiende el enfoque score-driven a más de un parámetro. Un modelo MPP para las excedencias es desarrollado con múltiples parámetros dinámicos en el proceso estocástico de la intensidad y tamaño de los eventos extremos, el cual denominamos GSPOT. Esta especificación metodológica contribuye a reducir la brecha en modelos econométricos score-driven aplicados a EVT.

Esta sección detalla una lista de las principales contribuciones metodológicas y conclusiones empíricas de esta tesis. Posteriormente en la subsección 5.1 se expone las limitaciones de la propuesta y contribuye a la discusión sobre futuras investigaciones.

5.1. Principales Contribuciones y Conclusiones

1. Conocidos mercados financieros muestran hechos estilizados asociados a las colas de la distribución de sus retornos que dificultan la modelación de las observaciones a niveles extremos. Estas series de tiempo evidencian características homogéneas de co-movimiento e inestabilidad sistémica durante periodos de crisis.
2. Modelos EVT basados en la intensidad condicional, parecen ser complementarios a los enfoques basados en modelos de volatilidad. Sin embargo, la intensidad condicional modelada a través de un modelo multivariado Hawkes-POT permite observar relaciones unidireccionales.
3. Existe una relación directa entre la intensidad condicional y la volatilidad observada, que se evidencia fuertemente durante periodos de crisis.
4. Incorporar variables exógenas, como la volatilidad realizada, ha mostrado ser relevante para mejorar el ajuste de diferentes medidas de riesgo derivadas de nuevas metodologías que se refleja en un mejor desempeño en términos estadísticos.
5. Las metodologías SPOT y rSPOT muestran superioridad por sobre los actuales modelos score-driven EVT. Mientras que el enfoque SPOT logra un mejor desempeño en gestión de riesgo de cola, el rSPOT es más adecuado en riesgo sistémico, de acuerdo a los datos analizados.
6. La metodología GSPOT, permite evidenciar que ambos procesos estocásticos proveen información conjunta importante para describir el comportamiento de los eventos extremos. Además, en un contexto de optimización de portafolios bancarios, es posible proponer estrategias de diversificación más flexibles y adecuadas para la gestión de riesgo financiero extremo por medio de este enfoque.

5.2. Limitaciones

La principal limitación de estrategias basadas en MPP y EVT, es que las estimaciones del modelo se centran solo en los eventos extremos, apartando estas observaciones de la muestra completa. Por lo tanto, es necesario contar con un número suficientemente largo de observaciones como periodo de ajuste. Un cuantil es definido para establecer el umbral que delimitará las observaciones extremas. La estrategia de elección del umbral debe tener en consideración el trade-off entre el sesgo que se

produce al considerar un número elevado de observaciones y a un aumento de la varianza asociada a un reducido número de observaciones extremas.

De manera particular, una condición importante del modelo GSPOT, es la ortogonalidad de los parámetros con respecto a la matriz de información de Fisher. Siguiendo la estrategia propuesta por Cox and Reid [25] la definición de ortogonalidad puede ser extendida a más de un parámetro, sin embargo, la complejidad incrementa con el número de parámetros.

5.3. Futuras Investigaciones

Variadas aristas se despliegan como investigaciones de trabajos futuros basado en las metodologías utilizadas en esta tesis. Por un lado, considerando la relación directa entre la intensidad condicional y la volatilidad, una propuesta inherente es la introducción de una medida de conectividad direccional basada en la intensidad condicional de los eventos extremos siguiendo el enfoque propuesto por Diebold and Yilmaz [30].

Desde el punto de vista dinámico, la estrategia de ortogonalización de parámetros puede ser utilizada en una infinidad de nuevas specificaciones score-driven basados en EVT como por ejemplo, las recientemente introducidas distribuciones Birbaum-Saunders model y extended generalized Pareto model de [37] y [63], respetivamente. En el caso multidimensional, se podría considerar la metodología score-driven en un modelo del tipo factor latente, con la idea de extender la metodología GSPOT a altas dimensiones, similar a la idea propuesta por Hautsch and Herrera [47]. Otra alternativa sería considerar modelos de regresión para la densidad angular de distribuciones bivariadas de valores extremos como las presentadas en Castro-Camilo et al. [17], Hanson et al. [43].

Referencias

[1] V. V. Acharya, L. H. Pedersen, T. Philippon, and M. Richardson, "Measuring systemic risk," *The Review of Financial Studies*, vol. 30, no. 1, pp. 2–47, 2017.

[2] Y. Baba, R. F. Engle, D. F. Kraft, and K. F. Kroner, "Multivariate simultaneous generalized arch," *Manuscript, University of California, San Diego, Department of Economics*, 1985.

[3] A. A. Balkema and L. De Haan, "Residual life time at great age," *The Annals of Probability*, vol. 5 (2), pp. 792 – 804, 1974.

[4] O. H. Bashar, I. M. Wadud, and H. J. A. Ahmed, "Oil price uncertainty, monetary policy and the macroeconomy: The canadian perspective," *Economic Modelling*, vol. 35, pp. 249–259, 2013.

[5] M. Bee, D. J. Dupuis, and L. Trapin, "Realized peaks over threshold: A time-varying extreme value approach with high-frequency-based measures," *Journal of Financial Econometrics*, vol. 17, no. 2, pp. 254–283, 2019.

[6] M. Bhattacharya, S. R. Paramati, I. Ozturk, and S. Bhattacharya, "The effect of renewable energy consumption on economic growth: Evidence from top 38 countries," *Applied Energy*, vol. 162, pp. 733–741, 2016.

[7] J. Białkowski, M. T. Bohl, P. M. Stephan, and T. P. Wisniewski, "The gold price in times of crisis," *International Review of Financial Analysis*, vol. 41, pp. 329–339, 2015.

[8] H. C. Bjørnland and H. Hungnes, "The commodity currency puzzle," *University of Oslo*, no. 32, 2005.

[9] F. Blasques, S. J. Koopman, and A. Lucas, "Maximum likelihood estimation for generalized autoregressive score models," Tinbergen Institute Discussion Paper, Tech. Rep., 2014.

[10] V. Bodart, B. Candelon, and J. F. Carpantier, "Real exchanges rates in commodity producing countries: A reappraisal," *Journal of International Money and Finance*, vol. 31, no. 6, pp. 1482–1502, 2012.

[11] E. Bouri, N. Jalkh, A. Dutta, and G. Salah, "Gold and crude oil as safe-haven assets for clean energy stock indices: Blended copulas approach," *Energy*, vol. 178, pp. 544–553, 2019.

[12] C. Bowman *et al.*, "Effective cross-hedging for commodity currencies," *Crawford School of Economics and Government, The Australian National University*, 2005.

[13] F. Breidt and R. Davis, "Extremes of stochastic volatility models," *Handbook of Financial Time Series*, pp. 355–364, 2008.

[14] C. Brownlees and R. F. Engle, "Srisk: A conditional capital shortfall measure of systemic risk," *The Review of Financial Studies*, vol. 30, no. 1, pp. 48–79, 2016.

[15] D. Buncic and K. I. Gisler, "Global equity market volatility spillovers: A broader role for the united states," *International Journal of Forecasting*, vol. 32, no. 4, pp. 1317–1339, 2016.

[16] P. Cashin, L. Céspedes, and S. Ratna, "Commodity currencies and the real exchange rate," *Journal of Development Economics*, vol. 75, pp. 239–268, 2004.

[17] D. Castro-Camilo, M. de Carvalho, J. Wadsworth *et al.*, "Time-varying extreme value dependence with application to leading european stock markets," *The Annals of Applied Statistics*, vol. 12, no. 1, pp. 283–309, 2018.

[18] K. Chan, Y. Tse, and M. Williams, "The Relationship between Commodity Prices and Currency Exchange Rates Evidence from the Futures Markets," *Commodity Prices and Markets*, vol. 20, no. February, pp. 47–71, 2011.

[19] V. Chavez-Demoulin and J. McGill, "High-frequency financial data modeling using hawkes processes," *Journal of Banking & Finance*, vol. 36, no. 12, pp. 3415–3426, 2012.

[20] V. Chavez-Demoulin, A. C. Davison, and A. J. McNeil, "Estimating value-at-risk: a point process approach," *Quantitative Finance*, vol. 5, no. 2, pp. 227–234, 2005.

[21] Y.-C. Chen and K. Rogoff, "Commodity currencies," *Finance and Development*, vol. 40, no. 1, pp. 45–48, 2003.

[22] Y.-C. Chen, S. K. Rogoff, and B. Rossi, "Can Exchange Rates Forecast Commodity Prices?" *Quarterly Journal of Economics*, vol. 125, no. 3, pp. 1145–1194, 2010.

[23] P. Christoffersen, "Evaluating interval forecasts," *International economic review*, pp. 841–862, 1998.

[24] S. Coles, *An introduction to Statistical Modeliing of Extreme Values*. Springer, 2001.

[25] D. R. Cox and N. Reid, "Parameter orthogonality and approximate conditional inference," *Journal of the Royal Statistical Society: Series B (Methodological)*, vol. 49, no. 1, pp. 1–18, 1987.

[26] D. Creal, S. J. Koopman, and A. Lucas, "A General Framework for Observation Driven Time-Varying Parameter Models," *SSRN Electronic Journal*, 2008.

[27] ——, "Generalized autoregressive score models with applications," *Journal of Applied Econometrics*, vol. 28, no. 5, pp. 777–795, 2013.

[28] A. Daouia, S. Girard, and G. Stupfler, "Estimation of tail risk based on extreme expectiles," *Journal of the Royal Statistical Society: Series B (Statistical Methodology)*, vol. 80, no. 2, pp. 263–292, 2018.

[29] R. Davis and T. Mikosch, "Extreme value theory for GARCH processes," in *Handbook of Financial Time Series*, J.-P. K. T. G. Andersen, R. A. Davis and T. Mikosch, Eds. Springer, 2009, vol. 6, pp. 187–200.

[30] F. X. Diebold and K. Yilmaz, "Better to give than to receive: Predictive directional measurement of volatility spillovers," *International Journal of Forecasting*, vol. 28, no. 1, pp. 57–66, 2012.

[31] F. X. Diebold and K. Yılmaz, "On the network topology of variance decompositions: Measuring the connectedness of financial firms," *Journal of Econometrics*, vol. 182, no. 1, pp. 119–134, 2014.

[32] A. Dutta, E. Bouri, and M. H. Noor, "Return and volatility linkages between CO2 emission and clean energy stock prices," *Energy*, vol. 164, pp. 803–810, 2018.

[33] P. Embrechts, C. Klüppelberg, and T. Mikosch, *Modelling Extremal Events for Insurance and Finance*. Springer,Berlin, 1998.

[34] P. Embrechts, S. I. Resnick, and G. Samorodnitsky, "Extreme value theory as a risk management tool," *North American Actuarial Journal*, vol. 3, no. 2, pp. 30–41, 1999.

[35] R. F. Engle and K. F. Kroner, "Multivariate simultaneous generalized arch," *Econometric theory*, pp. 122–150, 1995.

[36] R. F. Engle and J. R. Russell, "Autoregressive conditional duration: a new model for irregularly spaced transaction data," *Econometrica*, pp. 1127–1162, 1998.

[37] M. S. Ferreira, I. Gomes, and V. Leiva, "On an extreme value version of the birnbaum-saunders distribution," 2012.

[38] R. A. Fisher and L. H. C. Tippett, "Limiting forms of the frequency distribution of the largest or smallest member of a sample," in *Mathematical Proceedings of the Cambridge Philosophical Society*, vol. 24, no. 2. Cambridge University Press, 1928, pp. 180–190.

[39] X. Freixas, L. Laeven, and J.-L. Peydró, *Systemic risk, crises, and macroprudential regulation.* Mit Press, 2015.

[40] B. Gnedenko, "Sur la distribution limite du terme maximum d'une série aléatoire the annals of mathematics 44 (3), 423–453. translated and reprinted in: Breakthroughs in statistics, vol. i, 1992, eds. s. kotz and nl johnson," 1943.

[41] B. V. Gnedenko, "On a local limit theorem of the theory of probability," *Uspekhi Matematicheskikh Nauk*, vol. 3, no. 3, pp. 187–194, 1948.

[42] P. R. Hansen, Z. Huang, and H. H. Shek, "Realized garch: a joint model for returns and realized measures of volatility," *Journal of Applied Econometrics*, vol. 27, no. 6, pp. 877–906, 2012.

[43] T. E. Hanson, M. de Carvalho, and Y. Chen, "Bernstein polynomial angular densities of multivariate extreme value distributions," *Statistics & Probability Letters*, vol. 128, pp. 60–66, 2017.

[44] A. C. Harvey, *Dynamic models for volatility and heavy tails: with applications to financial and economic time series.* Cambridge University Press, 2013, vol. 52.

[45] D. Hatzinikolaou and M. Polasek, "The Commodity-Currency View of the Australian Dollar: A Multivariate Cointegration Approach," *Journal of Applied Economics*, vol. 13, no. 1, pp. 81–99, 2005.

[46] N. Hautsch and R. Herrera, "Multivariate dynamic intensity peaks-over-threshold models," *Journal of Applied Econometrics*, vol. 35, no. 2, pp. 248–272, dec 2020.

[47] ——, "Multivariate dynamic intensity peaks-over-threshold models," *Journal of Applied Econometrics*, vol. 35, no. 2, pp. 248–272, 2020.

[48] R. Herrera, "Energy risk management through self-exciting marked point process," *Energy Economics*, vol. 38, no. 0, pp. 64 – 76, 2013.

[49] H. Kato *et al.*, "Changes in the relationship between currencies and commodities," Bank of Japan, Tech. Rep., 2012.

[50] K. G. Koedijk and C. J. Kool, "Tail estimates of east european exchange rates," *Journal of Business & Economic Statistics*, vol. 10, no. 1, pp. 83–96, 1992.

[51] E. Kohlscheen, "Emerging floaters: pass-throughs and (some) new commodity currencies," *Journal of International Money and Finance*, vol. 29, no. 8, pp. 1580–1595, 2010.

[52] S. J. Koopman, A. Lucas, and M. Scharth, "Predicting time-varying parameters with parameter-driven and observation-driven models," *Review of Economics and Statistics*, vol. 98, no. 1, pp. 97–110, 2016.

[53] S. Kumar, S. Managi, and A. Matsuda, "Stock prices of clean energy firms, oil and carbon markets: A vector autoregressive analysis," *Energy Economics*, vol. 34, no. 1, pp. 215–226, 2012.

[54] E. Kyritsis and A. Serletis, "Oil Prices and the Renewable Energy Sector," *The Energy Journal*, vol. 40, pp. 337–364, 2019.

[55] Y. Liu and J. A. Tawn, "Volatility model selection for extremes of financial time series," *Journal of Statistical Planning and Inference*, vol. 143, no. 3, pp. 520–530, 2013.

[56] A. I. Maghyereh, B. Awartani, and H. Abdoh, "The co-movement between oil and clean energy stocks: A wavelet-based analysis of horizon associations," *Energy*, vol. 169, pp. 895–913, 2019.

[57] K. Malik, S. M. Rahman, A. N. Khondaker, I. R. Abubakar, Y. A. Aina, and M. A. Hasan, "Renewable energy utilization to promote sustainability in gcc countries: policies, drivers, and barriers," *Environmental Science and Pollution Research*, vol. 26, no. 20, pp. 20 798–20 814, 2019.

[58] S. Manganelli and R. F. Engle, "A comparison of value-at-risk models in finance," *Risk measures for the 21st century*, pp. 123–44, 2004.

[59] D. Massacci, "Tail risk dynamics in stock returns: Links to the macroeconomy and global markets connectedness," *Management Science*, vol. 63, no. 9, pp. 3072–3089, 2016.

[60] A. McNeil and R. Frey, "Estimation of tail-related risk measures for heteroscedastic financial time series: an extreme value approach," *Journal of Empirical Finance*, vol. 7, pp. 271–300, 2000.

[61] H. Mejdoub and A. Ghorbel, "Conditional dependence between oil price and stock prices of renewable energy : a vine copula approach," *Economic and Political Studies*, vol. 6, no. 2, pp. 176–193, 2018.

[62] A. Pais and P. A. Stork, "Bank size and systemic risk," *European Financial Management*, vol. 19, no. 3, pp. 429–451, 2013.

[63] I. Papastathopoulos and J. A. Tawn, "Extended generalised pareto models for tail estimation," *Journal of Statistical Planning and Inference*, vol. 143, no. 1, pp. 131–143, 2013.

[64] L. Pham, "Do all clean energy stocks respond homogeneously to oil price?" *Energy Economics*, vol. 81, pp. 355–379, 2019.

[65] J. Pickands, "The two-dimensional poisson process and extremal processes," *Journal of applied Probability*, pp. 745–756, 1971.

[66] ——, "Statistical inference using extreme order statistics," *The Annals of Statistics*, pp. 119 – 131, 1975.

[67] R. Ready, N. Roussanov, and C. Ward, "After the tide: Commodity currencies and global trade," *Journal of Monetary Economics*, vol. 85, pp. 69–86, 2017.

[68] J. C. Reboredo and A. Ugolini, "The impact of energy prices on clean energy stock prices. a multivariate quantile dependence approach," *Energy Economics*, vol. 76, pp. 136–152, 2018.

[69] E. Sanidas, "Four harmonic cycles explain and predict commodity currencies' wide long term fluctuations," *Technological Forecasting and Social Change*, vol. 87, pp. 135–151, 2014.

[70] S. J. H. Shahzad, N. Raza, M. Shahbaz, and A. Ali, "Dependence of stock markets with gold and bonds under bullish and bearish market states," *Resources Policy*, vol. 52, pp. 308–319, 2017.

[71] J. F. Slijkerman, D. Schoenmaker, and C. G. de Vries, "Systemic risk and diversification across european banks and insurers," *Journal of Banking & Finance*, vol. 37, no. 3, pp. 773–785, 2013.

[72] A. Tobias and M. K. Brunnermeier, "Covar," *The American Economic Review*, vol. 106, no. 7, p. 1705, 2016.

[73] L. Trapin, "Can volatility models explain extreme events?" *Journal of Financial Econometrics*, 2017.

[74] E. Tully and B. M. Lucey, "A power garch examination of the gold market," *Research in International Business and Finance*, vol. 21, no. 2, pp. 316–325, 2007.

[75] M. C. van de Leur, A. Lucas, and N. J. Seeger, "Network, market, and book-based systemic risk rankings," *Journal of Banking & Finance*, vol. 78, pp. 84–90, 2017.

[76] J. B. Wiggins, "Estimating the volatility of s&p 500 futures prices using the extreme-value method," *The Journal of Futures Markets (1986-1998)*, vol. 12, no. 3, p. 265, 1992.

[77] Y. Wu, "What explains movements in the peso dollar exchange rate?" IMF Working Papers, Tech. Rep., 2013.

[78] X. Yao, M. Izzeldin, and Z. Li, "A novel cluster har-type model for forecasting realized volatility," *International Journal of Forecasting*, vol. 35, no. 4, pp. 1318–1331, 2019.

[79] Y. Yi, X. Feng, and Z. Huang, "Estimation of extreme value-at-risk: An EVT approach for quantile GARCH model," *Economics Letters*, vol. 124, no. 3, pp. 378–381, 2014.

[80] P. Zeppini and J. C. Van Den Bergh, "Global competition dynamics of fossil fuels and renewable energy under climate policies and peak oil: A behavioural model," *Energy Policy*, vol. 136, p. 110907, 2020.

[81] X. Zhang and S. Bernd, "Tail risk in government bond markets and ECB unconventional policies," Working paper, Tech. Rep., 2016.

Apéndice A. Modeling Extreme Risks in Commodities and Commodity Currencies

Contiene

- Artículo original obtenido según DOI: https://doi.org/10.1016/j.pacfin.2018.06.003

Pacific-Basin Finance Journal 51 (2018) 108–120

Contents lists available at ScienceDirect

Pacific-Basin Finance Journal

journal homepage: www.elsevier.com/locate/pacfin

Modeling extreme risks in commodities and commodity currencies

Fernanda Fuentes[a], Rodrigo Herrera[b], Adam Clements[c,*]

[a] Facultad de Ingeniería, Universidad de Talca, Camino a los Niches km. 1, Curicó, Chile
[b] Facultad rde Economía y Negocios, Universidad de Talca, Av. Lircay s/n, Talca, Chile
[c] School of Economics and Finance, Queensland University of Technology, Australia

ARTICLE INFO

Keywords:
Commodity currency
BEKK
Hawkes model
Value at risk

JEL:
C11
C58
C22
F30

ABSTRACT

This paper examines extreme co-movements between the Australian and Canadian currencies, often known as commodity currencies, and gold and oil markets respectively. Here, two main approaches based on extreme value theory are compared in the context of explaining the co-movements between the markets in times of market instability. On the one hand, the intensity of the extreme events is represented by self-exciting marked point processes using a multivariate extension of the Hawkes-POT model, while contemporaneous co-movements are characterized utilizing a more traditional multivariate volatility model, the DBEKK-EVT model. It is found that intensity and volatility follow similar paths through time. The Hawkes-POT model reveals the unidirectional influence of the commodity on the currency, consistent with previous literature. Hawkes-POT model produces slightly more accurate Value at Risk results in the in-sample period, while the results are mixed in the backtesting period. Overall it seems as though the simpler multivariate volatility based approach produce forecasts of extreme risk that are comparable to the more complex Hawkes model.

1. Introduction

In many countries there are principal commodities that dominate a significant share of total exports. The prices at which these commodities are traded are crucial to the economic performance and generally have a significant effect on exchange rates behavior (Edwards, 1986). Because of the importance of this relationship these currencies are often called “commodity currencies”. Previous studies have analyzed the relationship between commodity prices and exchange rates, often using cointegration and error correction models (Hatzinikolaou and Polasek, 2005; Wu, 2013; Kohlscheen, 2010; Bjørnland and Hungnes, 2005), and tests for causality (Chen et al., 2010; Choudhri and Schembri, 2014; Chan et al., 2011). Overall, a relationship flowing from commodity to currency markets is often found to exist (Cashin et al., 2004; Chen and Rogoff, 2003; Bowman et al., 2005; Bodart et al., 2012; Kato et al., 2012). Nevertheless, despite the extensive research, there is little understanding of their joint behavior at extreme levels.

The underlying relationship between extreme events and comovements during financial turmoil periods is of growing interest among investors and researchers (Belhajjam et al., 2017). However, examining the complex behavior of these markets at extreme levels is not a straightforward task, mainly because it involves capturing stylized facts present in financial series, such as clustering of extreme events and heavy tails (Hung et al., 2008; Liu and Tang, 2011; Delatte and Lopez, 2013; Aboura and Chevallier, 2015). A large literature presents tools to measure risk in periods of stability, but these are not valid in turbulent times (Massacci, 2016). A drawback of the commonly used models is the potential misestimation of the tails of the probability distribution (Kellner and Gatzert, 2013). Therefore it is essential to employ methods that can adequately capture the complex relationship between these markets in

* Corresponding author.
E-mail address: a.clements@qut.edu.au (A. Clements).

https://doi.org/10.1016/j.pacfin.2018.06.003
Received 12 October 2017; Received in revised form 6 June 2018; Accepted 9 June 2018
Available online 18 June 2018
0927-538X/ © 2018 Elsevier B.V. All rights reserved.

extreme economic conditions.

While many studies have considered extreme risks across multiple assets such as stock indices, there is little understanding of how the different approaches performed when there are underlying causal links (commodity to currency here) between the assets. Here two main approaches to modeling extreme risk are compared. The first is an intensity based point process framework which is a multivariate extension of the Hawkes-Peaks over Threshold (POT) model of Chavez-Demoulin et al. (2005) and Chavez-Demoulin and Davison (2012) is proposed. This methodology, based on self-exciting point processes and Extreme Value Theory (EVT) permits the analysis of extreme events which are not necessarily iid, capturing the intrinsic characteristics of the return series during periods of crisis. This approach explicitly takes into account the unidirectional influence from the commodity to currency markets. The second approach is based on a more traditional method that uses volatility and correlation. Here the Diagonal BEKK (DBEKK) model of Baba et al. (1985) and Engle and Kroner (1995) is used, combined with refinements of EVT, extending the univariate conditional model proposed by McNeil and Frey (2000) to the multivariate case. The DBEKK approach is chosen as it is the only one that has an underlying stochastic process that leads to valid regularity conditions and asymptotic properties, see (Chang and McAleer, 2018; McAleer, 2018).

The main research question posed here is whether intensity based models (with causal links) provide superior forecasts of extreme risk relative to the volatility and correlation based approach (only contemporaneous links), or are these approaches complementary? In addressing this question it will become evident if the unidirectional link to currency markets is important when forecasting risk. This comparison will also shed light on the question of whether using the full set of returns (correlation) or focusing only on the extreme losses is most beneficial for forecasting extreme risk. The methodologies proposed here along with the empirical results will provide participants in the commodity and currency markets, commodity traders, producers and wholesale consumers, a deeper understanding of the extreme risks they face. The main conclusion is that both approaches complement each other in characterizing the relationship between currency and commodity.

The in-sample risk estimation results indicate that the Hawkes-POT models that take into account the casual links provide more accurate estimates of Value at Risk (VaR) relative to the DBEKK-EVT approach. It is found that the intensity of extreme events in the currency markets are influenced mainly by the rate of occurrence of the extreme events in the commodity markets and not by the magnitude of these events. However, when comparing predictions of risk in the backtesting period, the results are mixed. It is not clear if intensity or volatility plays a more important role in the prediction of the extreme events. In the Australian case the best model is the Hawkes-POT, and in the Canadian case the best model is the DBEKK-EVT.

This paper is organized as follows. In Section 2, we introduce the multivariate Hawkes-POT model and the DBEKK-EVT approach. Section 3 includes the empirical analysis, description of the models, estimation results and analysis of the risk measures. Finally, Section 4 presents the conclusions, study limitations and recommendations for future research.

2. Methodology

2.1. Multivariate Hawkes-POT

Here, the perspective of an investor concerned with losses is taken, therefore all subsequent analysis is based on the negative returns for both the commodities $\{X_t^1\}_{t\geq 0}$ and currencies $\{X_t^2\}_{t\geq 0}$. A popular method to model extreme events is the Peaks over Threshold (POT) methodology, with all values that are above a sufficiently high threshold considered to be extreme events. Fig. 1 gives a graphical description of this procedure for both markets. Under this framework, a vector of random variables $\{(t_i^m, Y_i^m)\}_{i\geq 1}$ is obtained in which the superscript $m = 1, \ldots, M$ represents the mth dimension of the model, t_i^m characterizes the time of the ith extreme event, and Y_i^m characterizes the mark, $Y_i^m = X_{t_i} - 0.0001pt^m - u^m$, with high threshold $u^m > 0$. Here, $N^m(t)$, $t \in \mathbb{R}$,

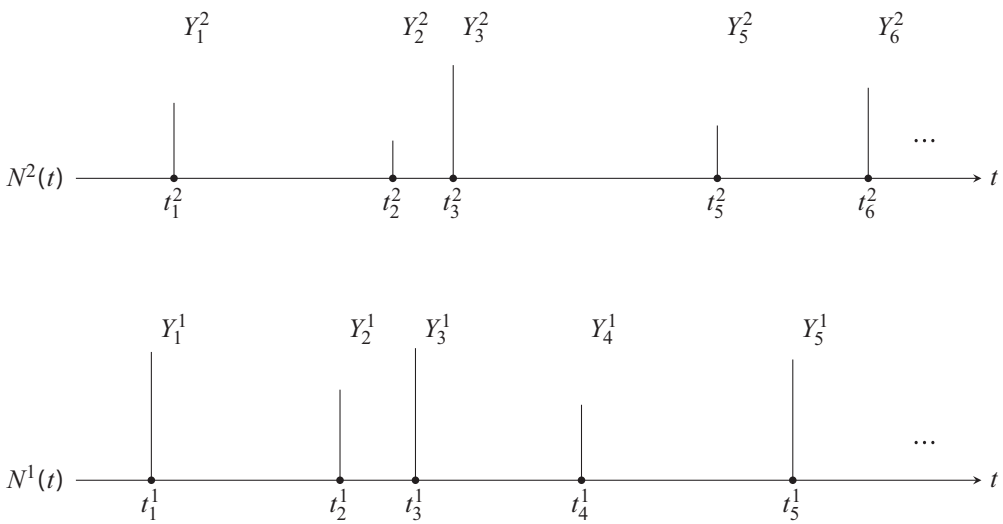

Fig. 1. The Peaks over Threshold procedure. The model considers the time of occurrence t_i of an extreme event i, where Y_i^m denotes the mark.

corresponds to the stochastic point process or left-continuous counting process describing the dynamic of occurrence of the stochastic process $\{(t_i^m, Y_i^m)\}_{i\geq 1}$ before time t.

Here the stochastic process $N^m(t)$ is modelled by means of an extension of a univariate self-exciting marked point process that capture the tendency of clustering in extreme events, the Hawkes-POT model Chavez-Demoulin and Mcgill, 2012). The conditional intensity of this process is defined as

$$\lambda^m(t, y|\mathcal{H}_t) = \lambda_g^m(t|\mathcal{H}_t) g^m(y|\mathcal{H}_t, t)$$

where $\lambda_g^m(t \mid \mathscr{H}_t)$ describes the intensity of occurrence of the extreme events, the self-exciting ground process, and $g^m(y \mid \mathscr{H}_t, t)$ the density function of the exceedances or marks, conditional on the history of the process $\mathscr{H}_t = \{(t_i^m, Y_i^m); \forall (m,i) : t_i^m < t\}$. According to the Pickands-Balkema-De Haan theorem (Balkema and de Haan, 1974; Pickands, 1975) the probability density function of the marks is well approximated by the density function of Generalized Pareto Distribution (GPD)

$$g^m(y|H_t, t) = \begin{cases} \frac{1}{\beta^m}\left(1 + \xi^m \frac{y}{\beta^m}\right)_+^{\frac{-1}{\xi^m}-1} & , \xi^m 1 0 \\ \frac{1}{\beta^m} \exp\left(\frac{-y}{\beta^m}\right) & , \xi^m = 0 \end{cases} \tag{1}$$

with scale and shape parameters, β^m and ξ^m, respectively, where $(f)_+ = \max\{0, f\}$ defines the positive part of the function. In a multivariate Hawkes process, an extreme event in the dimension or series m, increases the likelihood of future events of this type within the same dimension (self-excitation) and also in other dimensions (cross-excitation), a commonly observed pattern in financial markets. The intensity of a multivariate Hawkes process is given by

$$\lambda_g^m(t|\mathcal{H}_t) = \mu_m + \sum_{k=1}^{M} \eta_{mk} \sum_{i:t_i^k<t} h_{mk}(y_i^k, t - t_i^k)$$

where μ_m corresponds to the immigrant rate of extreme events in dimension m that occur independent of self-excitation and η_{mk} determines the influence of events in dimension k on the occurrence of extreme events in dimension m. In this sense, we say that extreme events in dimension m Granger causes extreme events in dimension k if η_{mk} is statistically different from zero. The exponential kernel $h_{mk}(y_i^k, t - t_i^k) = \alpha_k \exp(\delta_{mk} y_i^k - \alpha_k(t - t_i^k))$ represents the instant influence of events in series k on the intensity of m. Here, α_k is the rate of decay in the intensity from events in series k and δ_{mk} captures the impact of the size of events in series k on the intensity of m. When $m = k$ this is a self-exciting effect, otherwise it represents cross-excitation. The density function of the marks $g^m(y \mid \mathscr{H}_t, t)$ is conditional. Its scale parameter, $\beta^m(y \mid \mathscr{H}_t)$, is dependent on the internal history of the process through the exponential kernel and aims to capture the impact of the size of the extreme events on their subsequent distribution

$$\beta^m(y|H_t) = \beta_0^m + \sum_{k=1}^{M} \beta_k^m \sum_{i:t_i^k<t} h_{mk}(y_i^k, t\text{-}t_i^k)$$

The conditional intensity in the mth dimension in the multivariate Hawkes-POT model, assuming $\xi^m \neq 0$ is given by

$$\lambda^m(t, y|H_t) = \frac{\lambda_g^m(t|H_t)}{\beta^m(y|H_t)}\left(1 + \xi^m \frac{y}{\beta^m(y|H_t)}\right)^{\frac{1}{\xi^m}-1} \tag{2}$$

Under this specification all the parameters with exception of the shape parameter ξ^m are restricted to be positive. Finally, the log-likelihood for such processes in a range $(0, T]$ is given by:

$$\ln L = \sum_{m=1}^{M} \sum_{i=1}^{N^m(T)} \{\ln g(y|H_t) + \ln \lambda_g^m(t|H_t)\} - \sum_{m=1}^{M} \int_0^T \lambda_g^m(s|H_s) ds. \tag{3}$$

In its general form, this model for M dimensions has a rich structure due to its flexibility in permitting different forms of dependence. However, this flexibility is associated with a high cost in the number of parameters. For this reason, in Section 3, restricted alternatives of this general model are also estimated to capture the relationship between extreme risks in the commodity and currency markets.

2.2. Multivariate DBEKK-EVT

The multivariate DBEKK-EVT approach consists of three main steps. An AR specification is first used to model the conditional mean of each return series. Then, based on the residuals we model the cross dynamics of the conditional covariances through the DBEKK model. Finally, by applying EVT to the standardised residuals we obtain risk measures at extreme levels.

We consider $\{X_t^1\}_{t\geq 0}$ and $\{X_t^2\}_{t\geq 0}$ as the vectors of the negative returns of the commodity and the currency, respectively. We model the conditional mean of X_t^m as an AR (1) process as follows

$$X_t^m = \phi^m + \theta^m X_{t-1}^m + \varepsilon_t^m,$$

where ϕ^m and θ^m are constant terms and $\varepsilon_t^m = z_t^m \sqrt{h_t^m}$ is an error term of the mean in each series. The latter is composed of two

stochastic processes. The first process corresponds to a vector of random iid innovations ${z_t}^m$, here assumed to follow a multivariate *t*-Student distribution with mean and variance equal to zero and one, respectively. The second process ${h_t}^m$ is obtained from the diagonal of the (2 × 2) conditional covariance matrix $\mathbf{H_t}$, whose structure corresponds to the DBEKK model proposed by Engle et al. (1993),

$$\mathbf{H_t} = \mathbf{CC}' + \mathbf{A}\boldsymbol{\varepsilon}_{\mathbf{t-1}}\boldsymbol{\varepsilon}'_{\mathbf{t-1}}\mathbf{A}' + \mathbf{B}\mathbf{H_{t-1}}\mathbf{B}', \tag{4}$$

where $\mathbf{C}$ is a (2 × 2) lower triangular matrix $\mathbf{A}$ and $\mathbf{B}$ are both (2 × 2) diagonal matrices. As shown by Chang and McAleer (2018), the diagonality of the positive definite matrices $\mathbf{A}$ and $\mathbf{B}$ is indispensable so that standard statistical inference, as well as, consistence and asymptotic normality of the parameters would be valid.

In addition, to capture the dynamics of the extreme events we apply the refinement proposed by McNeil and Frey (2000). Specifically, the GPD defined in (1) is used to model the residuals ${z_t}^m$ above a threshold $u^m > 0$, as follows

$$\begin{aligned} g^m({z_t}^m - u^m) &= g^m\left(\frac{{\varepsilon_t}^m}{\sqrt{{h_t}^m}} - u^m\right) \\ &= g^m\left(\frac{{X_t}^m - \phi^m + \theta^m {X_{t-1}}^m - u^m\sqrt{{h_t}^m}}{\sqrt{{h_t}^m}}\right) \end{aligned}$$

2.3. Evaluating value-at-risk

In terms of understanding potential extreme losses, Value at Risk (VaR) represents the percentage loss that a portfolio will face over a predefined period of time, at a certain confidence level α is a popular measure of risk. The VaR is estimated in the period in-sample and backtesting for the returns in both markets. For the Hawkes-POT model, it can be directly obtained from the intensity of the ground process and the parameters of the GPD for the size of the events, given by:

$$VaR_\alpha^{t+1} = u + \frac{\beta(y\mathcal{H}_t)}{\xi}\left(\left(\frac{1-\alpha}{\lambda_g(t+1\mathcal{H}_t)}\right)^{-\xi} - 1\right), \tag{5}$$

where the superscript for dimension m has been removed for ease of exposition.[1]

In the case of DBEKK-EVT model, it can be obtained in terms of the conditional mean and volatility, denoted as:

$$VaR_\alpha^{t+1} = \phi^m + \theta^m {X_t}^m + {z_q}^m\sqrt{{h_t}^m} \tag{6}$$

where ${z_q}^m$ is the upper q-th quantile of the marginal distribution of z_t which, by assumption, does not depend on *t*. ${h_t}^m$ is a diagonal element from the covariance matrix $\mathbf{H_t}$ in (4).

Four widely used statistical tests are performed to evaluate the accuracy of the *V aR* from both models, with three of these tests based on the likelihood ratio tests of Christoffersen (1998). The first is the likelihood ratio unconditional coverage test (LR_{uc}) test which determines whether the number of exceptions, $I_t = I(X_t < -VaR - 0.0001pt_\alpha^t)$ (when the *V aR* prediction is breached) differ from its expected value at a given confidence level α. The second is a test of independence (LR_{ind}) that tests whether VaR exceptions are independent through time. The third statistic is the likelihood ratio test of conditional coverage (LR_{cc}), which simultaneously checks for independence and coverage. Finally, the dynamic quantile test (DQ_{hit}) of Engle and Manganelli (2004) is applied, which also tests for the presence of any dependence between the hits by defining $Hit_t = I_t - \alpha$, (therefore $E[Hit_t] = 0$). Then, the model to be estimated is $Hit_{t+1} = a + bHit_t + e_t$, and the null hypothesis $H_0 = a = b = 0$ tested (For details see (7)). Tests in the subsequent empirical analysis are undertaken at three levels of confidence: 0.95, 0.99, and 0.999.

3. Empirical analysis

The recent empirical evidence has focused on the currencies of Australia, Canada and New Zealand (Sanidas, 2014; Ready et al., 2017). Here, the Australian and Canadian markets are examined as both provide long historical records which is necessary for the analysis of extreme events. Gold and oil are centrally important commodities in these economies. Canada is the only country in the G-7 that is a net exporter of crude oil; it exports nearly 100% of its oil to the United States, the main consumer of the commodity (Bashar et al., 2013), with Australia the second-largest gold producer worldwide.

3.1. Data description and model specifications

The financial series are daily return observations on the Australian Dollar (AUD), Canadian Dollar (CAD), gold and Brent oil futures respectively. All series were obtained from Bloomberg. As extreme losses are analyzed here, negative logarithmic returns of the financial price series $X_t = -\ln\left(\frac{P_t}{P_{t-1}}\right)$ are utilized. In order to determine the predictive ability of the models, the database was divided into two periods. The first 10 years are used for estimation and model fit, with observations ranging from 4 January 2005 to

[1] See Chavez-Demoulin and McGill (2012) for details pertaining to the derivation of this risk measure under the Hawkes-POT model.

31 December 2014. For the backtesting sample, the period from 1 January 2015 until 31 December 2016 is used. Table B.1 presents the descriptive statistics for each of the series. The results show the existence of common stylized facts, such as an asymmetry in the losses and heavy tails. Jarque-Bera and Box-Pierce tests show that the returns are not normally distributed and auto-correlation is present in the returns. In addition, results of the LM-test indicate volatility persistence in both markets.

The multivariate Hawkes-POT model is specified in (2). In this model it is possible to characterize the stochastic process of the intensity and the magnitude or size of the extreme events. In order to capture dependency this approach contains six parameters that allow cross-excitation through their intensities (η_{12}, η_{21}), as well as, through the magnitudes of the extreme returns ($\beta_2{}^1$, δ_{12}, $\beta_1{}^2$, δ_{21}). A general model and two restricted versions are proposed to examine the nature of the links in extreme risk between the commodity and currency markets. Model 1, is the most general specification and forms a benchmark to which the restricted models will be compared. Consistent with previous studies in the literature (Cashin et al., 2004; Chen and Rogoff, 2003; Bowman et al., 2005; Bodart et al., 2012; Kato et al., 2012), Model 2 and Model 3 are unidirectional specifications where the currency is influenced by the commodity. Model 2 fully restricts the influence from the currency market to the commodity market but still retains all of the links from the commodity to the currency market (i.e., $\eta_{12} = \beta_2{}^1 = \delta_{12} = 0$). Finally, in addition to the Model 2 constraints, Model 3 allows only the intensity of the extreme commodity events to influence the intensity of the extreme currency movements (i.e., $\eta_{12} = \beta_2{}^1 = \delta_{12} = \beta_1{}^2 = \delta_{21} = 0$). Finally, the last approach corresponds to the DBEKK-EVT model. We consider an AR(1) to model the conditional means of the log-returns. Under this specification the conditional variance and covariance are estimated jointly.

To determine the fraction of observations in the tail of the distribution, an optimal threshold must be chosen. The choice of this threshold is subject to a balance between bias and variance. That is, increasing the sample size of extreme events will bias the approximation through the GPD of the tail's distribution, but the variance of the estimates will be reduced. While decreasing this proportion increases the variance of the estimators, unbiased parameters are obtained. Most techniques for selecting the threshold are based on graphical methods and bootstrap techniques (McNeil et al., 2005; Scarrott and MacDonald, 2012; Chavez-Demoulin and Davison, 2012). However, these techniques can be subjective in their interpretation. Similar to Herrera (2013), the threshold is chosen in a pragmatic way. The idea is to choose the threshold such that as many in-sample VaR tests (LR_{uc}, LR_{ind}, LR_{cc} and DQ_{hit}) are satisfied. It is expected that this method will lead to better results in backtesting analysis than others might. To this end, thresholds in the range of 0.90 to 0.94 quantiles are considered, with the number of VaR tests satisfied for each scenario recorded. The threshold that maximizes the accuracy of the in-sample VaR is the 0.90 quantile, as it is also suggested by McNeil and Frey (2000).

3.2. Relationship between extreme price intensity and volatility in commodity currencies

Engle and Russell (1998) was the first study to examine the close relationship between intensity and volatility in a high frequency framework. In this section, this idea is extended to the context extreme price intensity and its relationship with volatility in commodity currencies. One of the main features of our approach is that while volatility is defined using all returns, the intensity of extreme events is only defined by those that have exceeded a high threshold. Both approaches have their advantages and disadvantages, but analyzing them together they give a clear picture of the dynamics of this type of event.

Table B.2 reports the estimation results for the Hawkes-POT models, for both the Australian and Canadian markets. The results reveal the importance of the cross-exciting dependence between the commodity and the currency in terms of feedback between intensities and magnitudes. In both cases, Model 3 is superior in terms of Akaike information criterion (AIC), meaning that the intensity of the extreme currency events is influenced by the arrival rate of the events in the commodity market, although the magnitude of the extreme events is not important.

An important feature of the Hawkes-POT model is that it allows one to distinguish the proportion of extreme events that are due to exogenous events, represented by the immigration rates (μ_1 and μ_2), and the proportion of extreme events that are exclusively due to self-excitation (η_{11} and η_{22}) and cross-excitation (η_{12} and η_{21}) (Hardiman et al., 2013). Overall, low immigrant rates are found along with higher values of the branching coefficients. In the Australian case, the immigration rate is higher ($\mu_1 = 0.050$) for gold than for the Australian dollar ($\mu_2 = 0.044$), consistent with the common observation that commodities often exhibit higher volatility. The self-exciting coefficients, which corresponds to the probability that extreme events occur only by effects of the same market, are almost identical ($\eta_{11} = 0.283$ and $\eta_{22} = 0.284$). In addition, the cross-excitation coefficient, which indicates the proportion of extreme events in the Australian dollar that are caused by extreme losses occurring in the returns of gold, also shows evidence of cross-excitation ($\boldsymbol{\eta_{21} = 0.128}$).

Similarly for Canada, the immigration rate is higher ($\mu_1 = 0.060$) for oil than for the Canadian dollar ($\mu_2 = 0.048$) and the rate of self-excitation is lower in the Canadian dollar ($\eta_{22} = 0.160$) than for the oil ($\eta_{11} = 0.174$). Again, the cross-excitation coefficient is highly significant ($\boldsymbol{\eta_{21} = 0.151}$), so the rate of occurrence of extreme events in oil strongly influences the intensity in the currency, which is mainly due to the global commodity characteristics of oil (Chan et al., 2011; Ferraro et al., 2015).

On the other hand, the coefficient of the decay kernel function are stronger for the currency in both cases (Australia: $\alpha_2 = 0.080$, Canada: $\alpha_2 = 0.054$), implying that after a extreme commodity shock the effect on the currency market dissipates faster. Furthermore, the parameters δ_{11} and δ_{22} are also statistically significant in both countries, indicating that the magnitude of past events influence the intensity of future extreme events on the same market.

In relation to the process for the marks, the coefficients associated with the influence of the intensity on the magnitude of the marks in both markets are large and statistically significant. For instance, for the currency and commodity in the Australian case both coefficients are very similar ($\beta_1{}^1 = 1.953$, $\beta_2{}^2 = 1.931$), whilst in the Canadian case this value is high for the commodity ($\beta_1{}^1 = 1.698$) but somewhat lower for the currency ($\beta_2{}^2 = 0.885$), confirming the importance of the cross-sectional feedback between the intensity of occurrence of extreme events and their magnitudes. Regarding the tail behavior of the distribution functions, the

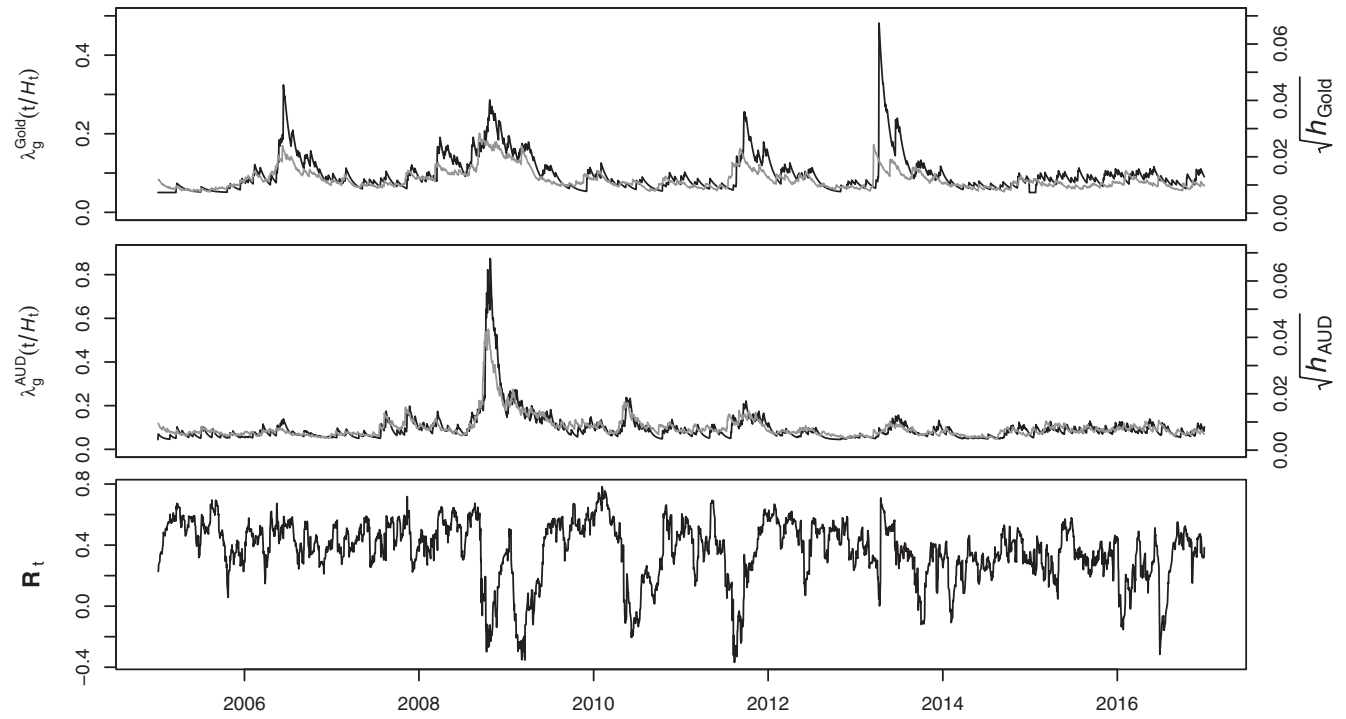

Fig. 2. Conditional intensity (Black line) and conditional variance (Gray line) obtained through the DBEKK-EVT approach are shown in the top two panels, for gold and Australian dollar respectively. Correlation (**R**t) between both markets is presented in the lower panel.

underlying distributions of the marks in all markets exhibit light tail distributions with shape parameters (ξ_1 and ξ_2) greater than zero.

Table B.3 displays the estimation results for the DBEKK-EVT model, for both the Australian and Canadian markets. The effect of lagged shocks (ARCH effects) are captured by the diagonal elements of the **A** matrix, while the effect of past volatility (GARCH effects) are captured by the diagonal elements of the **B** matrix of the multivariate BEKK model. In both cases and for both markets, the coefficients capturing the ARCH and GARCH effects are statistically significant, common empirical result. In particular, the diagonal

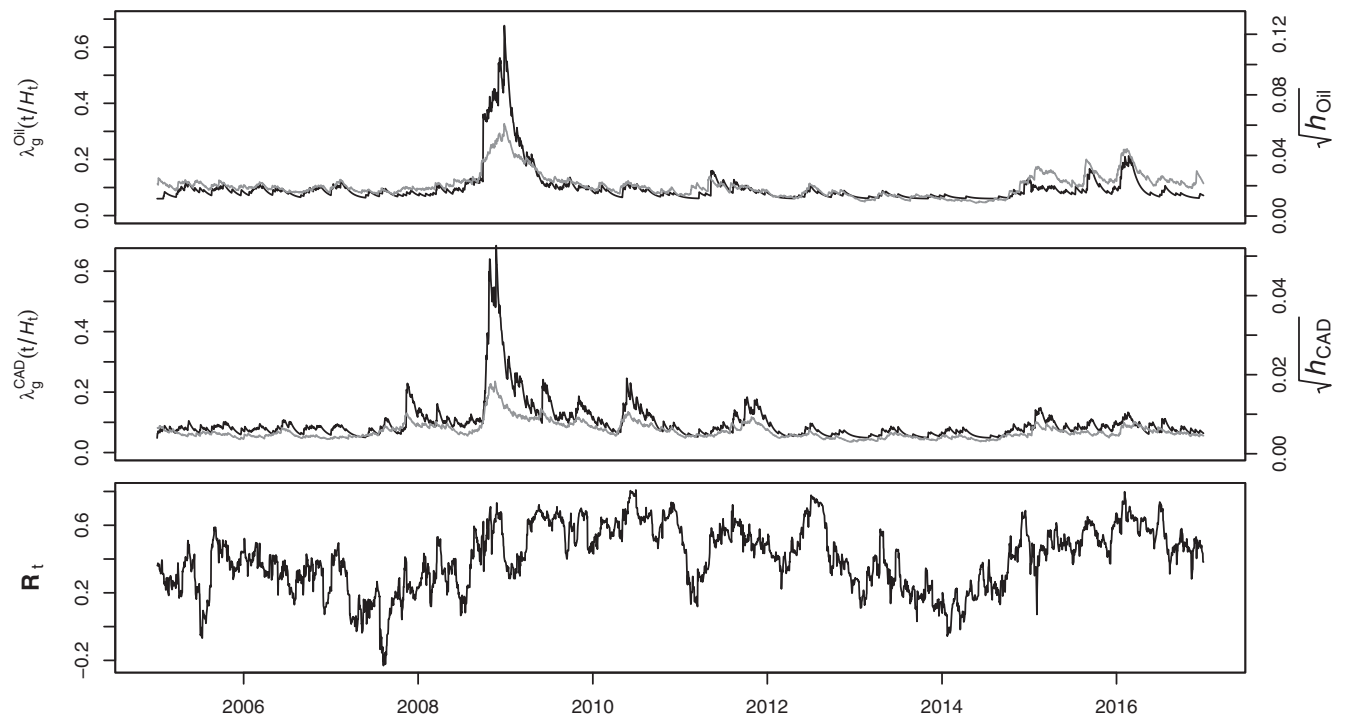

Fig. 3. Conditional intensity (Black line) and conditional variance (Gray line) obtained through the DBEKK-EVT approach are shown in the top two panels, for gold and Australian dollar respectively. Correlation (**R**t) between both markets is presented in the lower panel.

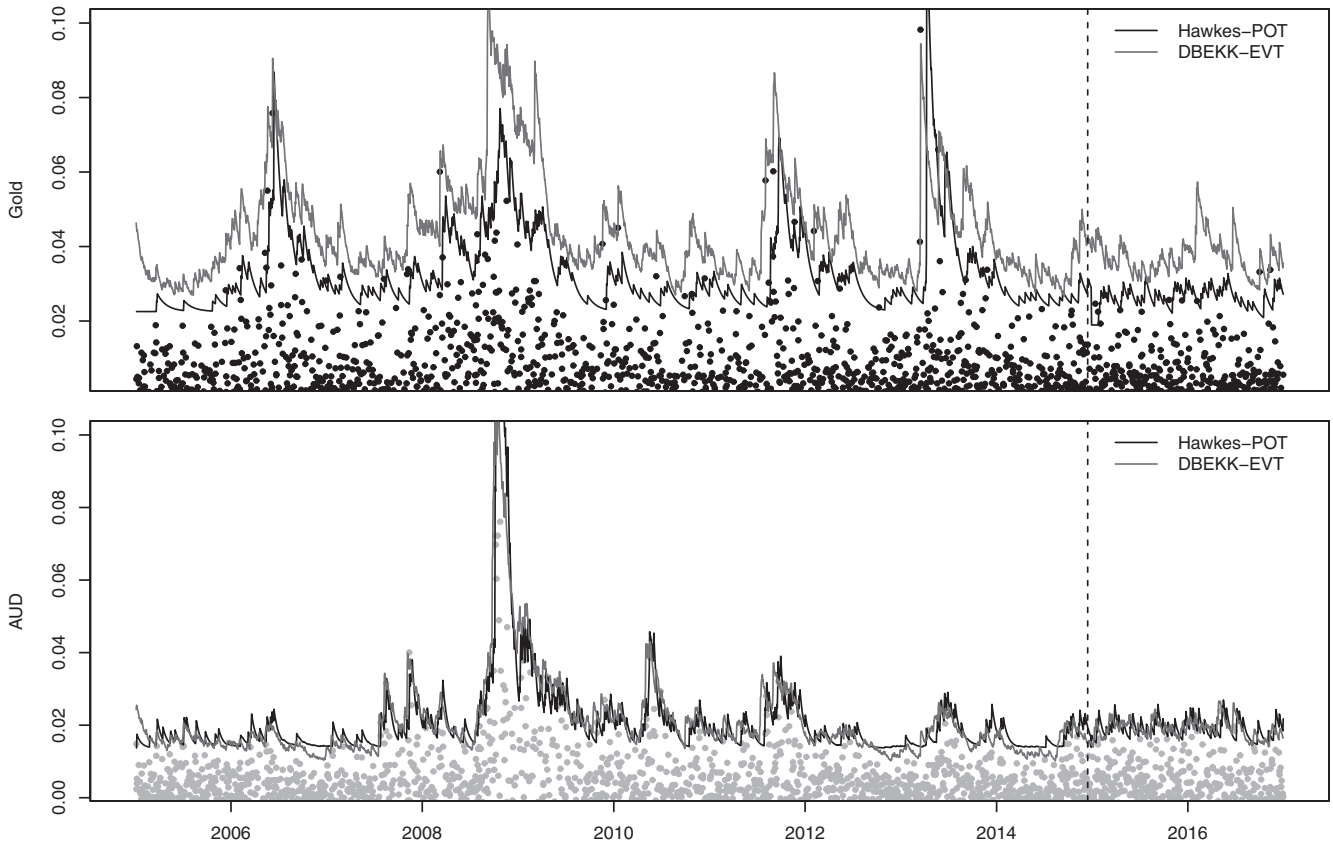

Fig. 4. VaR estimation to 99% with black line for the Hawkes-POT and DBEKK-EVT, applied to the negative log returns of the future gold prices (Top panel) and the Australian dollar (Below panel). The vertical dotted line indicates the division between the in-sample period from 4 January 2005 to 31 December 2014, and the backtesting period from 1 January 2015 until 31 December 2016. The dashed line in the graphic represents the beginning of the backtesting period.

elements of the **A** matrices are positive meaning that own lagged shocks largely affect the conditional variance between these markets. On the other hand, the sign of the diagonal elements of the **B** matrix indicates that the returns are negatively affected by own past volatility. In relation to the process for the marks, only the scale parameters are statistically significant. For instance, for the currency and commodity in the Australian case the scale coefficient is slightly higher for the commodity than the currency ($\beta_1 = 0.720$, $\beta_2 = 0.647$), whilst in the Canadian case this value is higher for the currency instead ($\beta_1 = 0.557$, $\beta_2 = 0.730$).

Figs. 2 and 3 exhibit the dynamic in-sample behaviour of the Hawkes-POT model together with the dynamic of the DBEKK-EVT approach. In both specifications, the two top panels display the conditional intensity (black line) and the volatility (gray line) for the commodity and currency markets. While the third panel shows the dynamic conditional correlation obtained by means of the DBEKK-EVT approach.

The first interesting result is that while the conditional intensity uses the occurrence of the extreme events to describe its dynamics, the volatility models uses all the information contained in the magnitude of its returns. However, both approaches seem to be complementary for describing the dynamics of such events. In the case of Australia, the intensity of extreme events and their underlying volatility is very similar throughout the entire period, with slight divergence in gold volatility during the global crisis of 2009. Further, the conditional correlation exhibit some sudden movements in this same period, showing a strong negative magnitude on separate occasions the 2009. This is probably due to the occurrence of a flight to quality from international investors in financial markets. Particularly in the gold market, large losses occur during 2013, when the price reached around US$1200 per troy ounce (Figuerola-Ferretti and McCrorie, 2016; Białkowski et al., 2015), and consequently an effect on the Australian dollar can be observed. On the other hand, in the case of Canada, the relationship between conditional intensity and volatility follows the same pattern, although with some differences during the global crisis of 2009, which is more pronounced in the conditional intensity of both markets. An interesting result is also the great jump in the conditional variance during 2009 that does not seem to strongly affect the dynamic conditional correlation, which remains high from 2009 to 2012, exhibiting its lowest value during 2014. According to the classification of Forbes and Rigobon (2002), this significant increase in correlation between the Brent market and the Canadian dollar during periods of turmoil would correspond to the definition of contagion, while for the Australian case, this corresponds to interdependence.

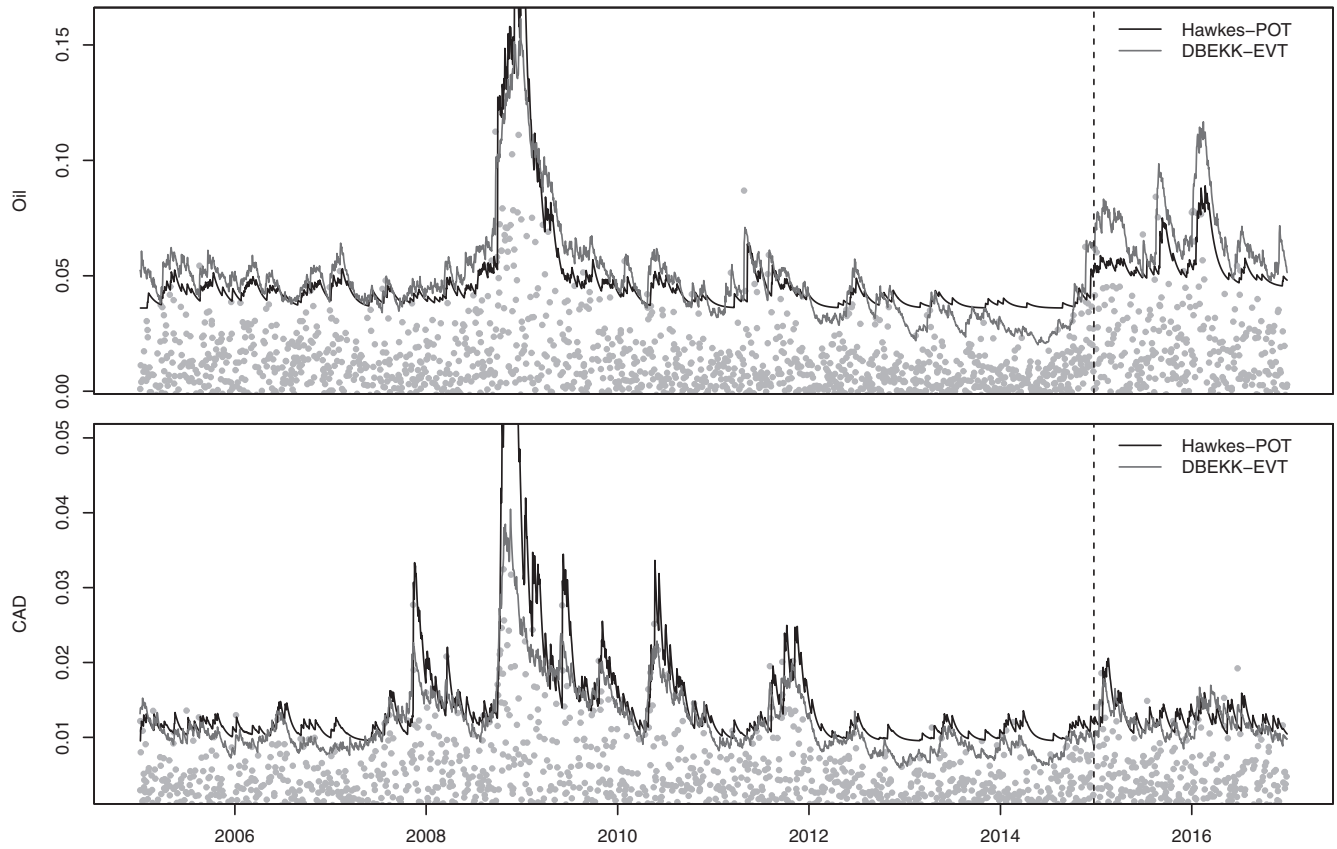

Fig. 5. VaR estimation to 99% with black line for the Hawkes-POT and DBEKK-EVT applied to the negative log returns of the future oil prices (Top panel) and the Canadian dollar (Below panel). The vertical dotted line indicates the division between the in-sample period from 4 January 2005 to 31 December 2014, and the backtesting period from 1 January 2015 until 31 December 2016. The dashed line in the graphic represents the beginning of the backtesting period.

3.3. VaR forecasting

Tables B.4 and B.5 report the results of the VaR accuracy tests for the in-sample period from 4 January 2005 to 31 December 2014, and the backtesting period from 1 January 2015 until 31 December 2016. We evaluated the ability of the proposed methodologies to estimate the VaR based on tests LR_{uc}, LR_{ind}, LR_{cc} and DQ_{hit}. The accuracy of the competing models is evaluated by investigating the dynamic of the VaR exceptions during these periods. Entries in the rows are the significance levels of the respective tests.

In relation to the in-sample period in the Australian and Canadian cases, slightly better results in VaR accuracy are obtained from using the Hawkes-POT with the VaR tests satisfied in > 89% of the cases. In comparison, the DBEKK-EVT performs slightly worse in the Australian case, but equally well in the Canadian case relative to the Hawkes-POT models.

In the Backtesting period the results are mixed. In the Australian case, Model 1 in the Hawkes-POT specification produces excellent results with all tests of VaR adequacy being passed, while in the Canadian case DBEKK-EVT produces a better fit, with 75% of the tests satisfied. In general, for Australia, shortcomings in the accuracy of the tests of the VaR are observed at a low confidence level (0.95), in the commodity for Canada, the tests are rejected mainly for the currency, at high confidence levels.

Figs. 4 and 5 display VaR estimates at the 0.99 confidence level with black and gray lines for the Hawkes-POT and DBEKK-EVT specifications respectively. The top panel shows the VaR estimates for the commodity, while the bottom panel for the currency. In the case of Australia for the gold market, we observe that in the in-sample and backtesting periods the DBEKK-EVT specification tends to overestimate the VaR, which is reflected in the unconditional and conditional coverage rejections in Table B.5. While in the currency market the dynamic of these VaR estimates are almost identical. For the Canadian market we observe that the behavior of the VaR estimates for the commodity is smoother for the Hawkes-POT specification than the competitive specifications, while in contrast, the VaR estimates from the Hawkes-POT approach tends to react more strongly during the crisis of 2009 than the DBEKK-EVT specification.

4. Conclusions

This paper has examined dependence at extreme levels in the relationship between two well-known commodity currencies, the Australian dollar and the Canadian dollar, and the movements in gold and crude oil prices respectively. Two approaches based on

extreme value theory were considered. We consider two perspectives based on extreme value theory, with a multivariate Hawkes-POT marked point process framework, based on intensity of extreme events and the DBEKK-EVT model based on correlation and volatility.

Overall, both the intensity and volatility based approaches can be considered to be complementary, and each offer participants in these markets a deeper understanding of the risks they face these markets in periods of market stress. The benefit of the Hawkes point process approach is that it captures the causal unidirectional dependence between both markets and a feedback between the intensity and magnitude of extreme events. However from a very practical view, while point process models have often found to provide superior predictions in an univariate setting, the multivariate volatility models provides forecasts of similar quality in the backtesting period. While the point process framework offers interesting economic insights into the causal linkages between the markets, the volatility models which is generally practically easier to implement provides adequate forecast in the multivariate setting.

Appendix A. Accuracy of the VaR

A.1. Likelihood ratio unconditional coverage test (LR_{uc})

The aim of the LR_{uc} test is to determine whether the number of errors obtained differs from the expected value, remaining consistent with the stated confidence level α in the risk quantification. Consider $H_t = \mathrm{I}(r_t < -VaR_\alpha^t)$ as being the sequence of efficient predictions of the VaR; if $[H_t] = \alpha$ with $H_t \overset{iid}{\sim} Bernoulli(\alpha)$, then under the null hypothesis H_0: $E[H_t] = \alpha$, for which the likelihood is defined as

$$\ln L(\alpha; H_1, H_2, \ldots, H_T) = (1-\alpha)^{n_0}\alpha^{n_1}$$

where n_0 is the number of correct predictions, whilen_1 is the number of violations of VaR. On the other hand, the alternative hypothesis is defined as H_1: $E[H_t] \neq \alpha$,

$$\ln L(\hat{\pi}; H_1, H_2, \ldots, H_T) = (1-\pi)^{n_0}\pi^{n_1}$$

where $\hat{\pi} = \frac{n_1}{n_0 + n_1}$ is the likelihood of π. Then, by means of a likelihood ratio test, one can test the unconditional coverage.

$$LR_{uc} = 2[\ln L(\hat{\pi}; H_1, H_2, \ldots, \mathrm{H_T}) - \ln \mathrm{L}(\alpha; \mathrm{H_1}, \mathrm{H_2}, \ldots, \mathrm{H_T})] \overset{asy}{\sim} \chi_1^2$$

with L being the likelihood of the binomial distribution and ${\chi_1}^2$ the Chi-squared distribution with one degree of freedom.

A.2. Likelihood ratio test of independence (LR_{ind})

Repeated mistakes result in significant losses for the investor, the LR_{ind} test verifies that there is no dependence over time between violations. Since H_t is a series of binary variables, we can model the dependence as a Markov chain whose first order transition matrix is defined by

$$\prod = \begin{bmatrix} 1-\pi_{01} & \pi_{01} \\ 1-\pi_{11} & \pi_{11} \end{bmatrix}$$

where $n_{ij} = \Sigma I(H_t = j | H_{t-1} = i)$ represents the number of transitions of state i to state j. Under the null hypothesis, we observe that $\pi_{01} = \pi_{11} = \pi_0$, so the conditional likelihood at the first state has to be.

$$L(\Pi_1; H_2, \ldots, H_T \mid H_1) = (1-\pi_{01})^{n_{00}+n_{10}}\pi_{01}^{n_{01}+n_{11}}$$

Under the alternative hypothesis, we have that $\hat{\pi}_{01} = \frac{n_{00}}{n_{01}+n_{01}}$ and $\hat{\pi}_{11} = \frac{n_{11}}{n_{10}+n_{11}}$ with likelihood.

$$L(\Pi_2; H_2, \ldots, H_T \mid H_1) = (1-\pi_{01})^{n_{00}}\pi_{01}^{n_{01}}(1-\pi_{11})^{n_{10}}\pi_{11} - 0.0001pt^{n_{11}}$$

Finally, the likelihood ratio test of independence for this statistic is defined by.

$$LR_{ind} = 2[\ln L(\Pi_2; H_2, \ldots, H_T \mid H_1) - \ln L(\Pi_1; H_2, \ldots, H_T \mid H_1)] \overset{asy}{\sim} \chi_1^2$$

which is asymptotically Chi-square distributed with one degree of freedom.

A.3. Likelihood ratio test of conditional coverage(LR_{cc})

Providing a more global perspective, the LR_{cc} simultaneously checks the previous two tests

$$LR_{cc} = LR_{uc} + LR_{ind}$$

where the likelihood ratio test is defined as.

$$LR_{cc} = 2[\ln L(\Pi_2; H_2, \ldots, H_T \mid H_1) - \ln L(\alpha; H_2, \ldots, H_T \mid H_1)] \overset{asy}{\sim} \chi_2^2$$

which is asymptotically Chi-squared distributed with two degrees of freedom. For further details regarding these three tests, see Christoffersen (1998).

A.4. Dynamic quantile test (DQ_{hit})

Evaluate the existence of a correlation between VaR violations based on logit models. The number of violations of the VaR with mean equal to 0 we defined as the Hit in time t, (i.e.,$Hit_t = H_t - \alpha$ with $E[Hit_t] = 0$). Then, the model to be estimated is as follows:

$$Hit_{t+1} = a + bHit_t + e_t,$$

where e_t are discrete random iid. Under the null hypothesis $H_0 = a = b = 0$, regressors should not have explanatory power and are asymptotically Chi-squared distributed with one degree of freedom.

Appendix B. Tables

Table B.1
Descriptive statistics of the logarithmic returns of the series and the p-value of the Jarque-Bera and Box-Pierce tests (10 lags).

Country		Mean ($\times$1E − 03)	Standard deviation	Min	Max	Skewness	Kurtosis	Jarque-Bera	Box-Pierce	LM-Test
Australia	Currency	0.020	0.009	−0.076	0.082	−0.488	12.569	0.00	0.00	0.00
	Commodity	0.400	0.013	−0.098	0.086	−0.398	5.048	0.00	0.02	0.00
	Currency	0.020	0.006	−0.032	0.039	−0.132	3.212	0.00	0.00	0.00
	Commodity	0.130	0.020	−0.113	0.135	−0.068	3.467	0.00	0.00	0.00

Table B.2
Results of the Hawkes-POT models for Australia and Canada for the in-sample period. Negative logarithmic returns are applied to future prices of gold (subscript 1) and the Australian dollar (subscript 2), and Oil (subscript 1) and the Canadian dollar (subscript 2), respectively. Standard errors are in parentheses. Log-lik corresponds to the log-likelihood, while AIC corresponds to the value of the Akaike information criterion.

Model	Ground process											
	Commodity						Currency					
	μ_1	η_{11}	η_{12}	α_1	δ_{11}	δ_{12}	δ_{22}	δ_{21}	μ_2	η_{22}	η_{21}	α_2
Australia												
1	0.060	0.118	0.083	0.061	0.487	0.493	0.380	0.001	0.046	0.315	0.071	0.072
	(0.014)	(0.116)	(0.081)	(0.042)	(0.091)	(0.170)	(0.053)	(0.003)	(0.010)	(0.098)	(0.013)	(0.021)
2	0.050	0.283		0.041	0.416		0.389	0.001	0.044	0.284	0.128	0.080
	(0.010)	(0.074)		(0.012)	(0.050)		(0.054)	(0.002)	(0.010)	(0.091)	(0.013)	(0.022)
3	0.050	0.283		0.041	0.416		0.389	0.389	0.044	0.284	0.128	0.080
	(0.010)	(0.074)		(0.012)	(0.050)		(0.054)	(0.054)	(0.010)	(0.091)	(0.013)	(0.022)
Canada												
1	0.057	0.136	0.066	0.046	0.406	0.750	1.305	0.077	0.049	0.157	0.133	0.055
	(0.011)	(0.071)	(0.107)	(0.013)	(0.069)	(1.422)	(0.183)	(0.460)	(0.011)	(0.063)	(0.015)	(0.013)
2	0.060	0.174		0.044	0.389	0.074	1.304		0.049	0.157	0.136	0.054
	(0.010)	(0.071)		(0.011)	(0.064)	(0.452)	(0.183)		(0.011)	(0.063)	(0.015)	(0.013)
3	0.060	0.174		0.044	0.389		1.303		0.048	0.160	0.151	0.054
	(0.010)	(0.071)		(0.011)	(0.064)		(0.181)		(0.010)	(0.060)	(0.012)	(0.012)

Model	Generalized Pareto distribution function								Log-Lik	
	Commodity				Currency					
	$\beta_0{}^1$	$\beta_1{}^1$	$\beta_2{}^1$	ξ_1	$\beta_0{}^2$	$\beta_2{}^2$	$\beta_1{}^2$	ξ_2		AIC
Australia										
1	0.617	1.523	0.001	0.123	0.320	1.993	0.001	0.209	1950.822	−3861.644
	(0.110)	(0.577)	(0.001)	(0.062)	(0.058)	(0.339)	(0.001)	(0.069)		
2	0.561	1.953		0.094	0.332	1.931	0.001	0.221	1954.675	−3875.349
	(0.091)	(0.442)		(0.063)	(0.057)	(0.324)	(0.001)	(0.068)		
3	0.561	1.953		0.094	0.332	1.931		0.221	1954.675	−3879.350
	(0.091)	(0.442)		(0.063)	(0.057)	(0.324)		(0.068)		

Canada										
1	0.870	1.564	0.001	0.156	0.178	0.881	0.001	0.186	1940.332	−3840.664
	(0.116)	(0.588)	(0.001)	(0.044)	(0.033)	(0.230)	(0.001)	(0.046)		
2	0.853	1.698		0.150	0.178	0.883	0.001	0.187	1940.927	−3847.854
	(0.114)	(0.587)		(0.044)	(0.033)	(0.231)	(0.001)	(0.046)		
3	0.853	1.698		0.150	0.177	0.885		0.187	1940.984	−3851.968
	(0.114)	(0.587)		(0.044)	(0.033)	(0.230)		(0.046)		

Table B.3
Results of the DBEKK-EVT models for Australia and Canada in the period In-Sample. Negative logarithmic returns are applied to future prices of gold (subscript 1) and the Australian dollar (subscript 2), and Oil (subscript 1) and the Canadian dollar (subscript 2), respectively. Standard errors are in parentheses. Log-lik corresponds to the log-likelihood, while AIC corresponds to the value of the Akaike information criterion.

	AR(1)		DBEKK						EVT		Log-Lik	AIC
	ϕ^m	θ^m	**C**		**A**		**B**		β_m	ξ_m		
Australia												
Commodity	−4E−04	0.003	0.006	0.001	0.366		−0.792		0.720	0.029	16,103.594	−32,177.187
	(2E−04)	(0.026)	(0.000)	(0.000)	(0.021)		(0.021)		(0.063)	(0.061)		
Currency	6E−05	−0.040		0.001		0.496		−0.883	0.647	−0.041		
	(1E−04)	(0.021)		(0.000)		(0.018)		(0.008)	(0.056)	(0.060)		
Canada												
Commodity	−3E−05	−0.041	0.008	0.005	0.399		−0.825		0.557	0.030	16,115.982	−32,201.964
	(3E−04)	(0.020)	(0.000)	(0.000)	(0.018)		(0.014)		(0.048)	(0.061)		
Currency	1E−05	−0.030		0.003		0.421		−0.159	0.730	−0.041		
	(1E−04)	(0.020)		(0.000)		(0.025)		(0.061)	(0.071)	(0.074)		

Table B.4
VaR accuracy tests for the in-sample period. Entries in the rows are the significance levels (p-values) of the respective tests, with the exception of the confidence level α for the VaR and the number of exceptions (Excep).

		α level	Australia					Canada				
			Excep	LR_{uc}	*LRind*	LR_{cc}	DQ_{hit}	Excep	LR_{uc}	*LRind*	LR_{cc}	DQ_{hit}
Hawkes-POT												
Model 1	Commodity	0.95	123	0.78	0.41	0.69	0.43	135	0.56	0.07	0.17	0.08
		0.99	31	0.26	0.40	0.37	0.40	25	0.89	0.48	0.77	0.49
		0.999	7	**0.02**	0.84	0.07	0.84	5	0.18	0.89	0.40	0.89
	Currency	0.95	128	0.86	0.32	0.60	0.33	126	0.82	0.73	0.92	0.74
		0.99	28	0.58	0.32	0.52	0.32	29	0.52	0.34	0.51	0.34
		0.999	9	**0.00**	0.80	**0.01**	0.80	10	**0.00**	0.78	**0.00**	0.78
Model 2	Commodity	0.95	132	0.59	0.42	0.62	0.43	129	0.96	0.17	0.40	0.19
		0.99	30	0.35	0.37	0.43	0.37	23	0.59	0.52	0.70	0.52
		0.999	7	**0.02**	0.84	0.07	0.84	5	0.18	0.89	0.40	0.89
	Currency	0.95	127	0.93	0.16	0.36	0.17	126	0.82	0.73	0.92	0.74
		0.99	29	0.46	0.34	0.49	0.35	29	0.52	0.34	0.51	0.34
		0.999	10	**0.00**	0.78	**0.00**	0.78	10	**0.00**	0.78	**0.00**	0.78
Model 3	Commodity	0.95	132	0.59	0.42	0.62	0.43	129	0.96	0.17	0.40	0.19
		0.99	30	0.35	0.37	0.43	0.37	23	0.59	0.52	0.70	0.52
		0.999	7	**0.02**	0.84	0.07	0.84	5	0.18	0.89	0.40	0.89
	Currency	0.95	127	0.93	0.16	0.36	0.17	126	0.82	0.73	0.92	0.74
		0.99	29	0.46	0.34	0.49	0.35	28	0.65	0.31	0.54	0.31
		0.999	10	**0.00**	0.78	**0.00**	0.78	10	**0.00**	0.78	**0.00**	0.78

DBEKK-EVT												
Model 1	Commodity	0.95	58	**0.00**	0.20	**0.00**	0.21	118	0.33	0.06	0.11	0.07
		0.99	9	**0.00**	**0.02**	**0.00**	**0.02**	24	0.73	0.50	0.75	0.50
		0.999	1	0.27	0.98	0.55	0.98	3	0.80	0.93	0.96	0.93
	Currency	0.95	99	**0.01**	0.30	**0.02**	0.31	139	0.36	0.86	0.64	0.85
		0.99	25	0.95	0.25	0.51	0.25	40	**0.01**	0.65	**0.03**	0.66
		0.999	8	**0.01**	0.82	**0.02**	0.82	8	**0.01**	0.82	**0.03**	0.82

Table B.5
VaR accuracy tests for the out-sample period. Entries in the rows are the significance levels (p-values) of the respective tests, with the exception of the confidence level α for the VaR and the number of exceptions (Excep).

		α level	Australia					Canada				
			Excep	LR_{uc}	*LRind*	LR_{cc}	DQ_{hit}	Excep	LR_{uc}	*LRind*	LR_{cc}	DQ_{hit}
Hawkes-POT												
Model 1	Commodity	0.95	31	0.27	0.05	0.08	0.05	34	0.10	0.33	0.16	0.33
		0.99	7	0.42	0.68	0.66	0.68	10	0.05	0.55	0.13	0.53
		0.999	1	0.54	0.95	0.83	0.95	4	**0.00**	0.83	**0.01**	0.80
	Currency	0.95	31	0.27	0.48	0.42	0.46	36	**0.04**	0.73	0.12	0.74
		0.99	6	0.69	0.05	0.14	0.05	10	0.05	**0.01**	**0.01**	**0.01**
		0.999	0	0.31	1.00	0.60	1.00	3	**0.02**	0.85	0.06	0.85
Model 2	Commodity	0.95	33	0.14	**0.03**	**0.04**	**0.04**	34	0.10	0.33	0.16	0.33
		0.99	7	0.42	0.68	0.66	0.68	9	0.11	0.59	0.25	0.57
		0.999	1	0.54	0.95	0.83	0.95	4	**0.00**	0.83	**0.01**	0.80
	Currency	0.95	31	0.27	0.48	0.42	0.46	36	**0.04**	0.73	0.12	0.74
		0.99	6	0.69	0.05	0.14	0.05	10	0.05	**0.01**	**0.01**	**0.01**
		0.999	0	0.31	1.00	0.60	1.00	3	**0.02**	0.85	0.06	0.85
Model 3	Commodity	0.95	33	0.14	**0.03**	**0.04**	**0.04**	34	0.10	0.33	0.16	0.33
		0.99	7	0.42	0.68	0.66	0.68	9	0.11	0.59	0.25	0.57
		0.999	1	0.54	0.95	0.83	0.95	4	**0.00**	0.83	**0.01**	0.80
	Currency	0.95	31	0.27	0.48	0.42	0.46	36	**0.04**	0.73	0.12	0.74
		0.99	6	0.69	0.05	0.14	0.05	10	0.05	**0.01**	**0.01**	**0.01**
		0.999	0	0.31	1.00	0.60	1.00	3	**0.02**	0.85	0.06	0.85
DBEKK-EVT												
Model 1	Commodity	0.95	10	**0.00**	0.53	**0.00**	0.54	28	0.71	0.68	0.86	0.69
		0.99	2	0.11	0.90	0.27	0.90	5	0.92	0.76	0.95	0.76
		0.999	0	0.31	1.00	0.59	1.00	1	0.56	0.95	0.84	0.95
	Currency	0.95	26	0.99	0.77	0.96	0.78	30	0.44	0.83	0.73	0.83
		0.99	4	0.58	0.80	0.83	0.80	11	**0.03**	0.22	**0.04**	0.22
		0.999	1	0.56	0.95	0.84	0.95	4	**0.00**	**0.02**	**0.00**	**0.02**

References

Aboura, S., Chevallier, J., 2015. Volatility returns with vengeance: financial markets vs. commodities. Res. Int. Bus. Financ. 33, 334–354.

Baba, Y., Engle, R., Kraft, D., Kroner, K., 1985. Multivariate Simultaneous Generalized Arch. Unpublished manuscript. Department of Economics, University of California, San Diego, CA, USA.

Balkema, A.A., de Haan, L., 1974. Residual life time at great age. Ann. Probab. 2 (5), 792–804.

Bashar, O.H., Wadud, I.M., Ali Ahmed, H.J., 2013. Oil price uncertainty, monetary policy and the macroeconomy: the Canadian perspective. Econ. Model. 35, 249–259.

Belhajjam, A., Belbachir, M., El Ouardirhi, S., 2017. Robust multivairiate extreme value at risk allocation. Finan. Res. Lett. 23, 1–11.

Białkowski, J., Bohl, M.T., Stephan, P.M., Wisniewski, T.P., 2015. The gold price in times of crisis. Int. Rev. Financ. Anal. 41, 329–339.

Bjørnland, H.C., Hungnes, H., 2005. The Commodity Currency Puzzle. Statistics Norway, Research Department.

Bodart, V., Candelon, B., Carpantier, J.F., 2012. Real exchanges rates in commodity producing countries: a reappraisal. J. Int. Money Financ. 31 (6), 1482–1502.

Bowman, C., et al., 2005. Effective Cross-Hedging for Commodity Currencies. Crawford School of Economics and Government, The Australian National University.

Cashin, P., Céspedes, L., Ratna, S., 2004. Commodity currencies and the real exchange rate. J. Dev. Econ. 75, 239–268.

Chan, K., Tse, Y., Williams, M., 2011. The relationship between commodity prices and currency exchange rates evidence from the futures markets. Commodity Pric. Markets 20 (February), 47–71.

Chang, C.-L., McAleer, M., 2018. The fiction of full BEKK: pricing fossil fuels and carbon emissions. Finan. Res. Lett. http://dx.doi.org/10.1016/j.frl.2018.03.008. in press, available online March 17.

Chavez-Demoulin, V., Davison, A.C., 2012. Modelling time series extremes. Rev. Stat. Stat. J. 10 (1), 109–133.

Chavez-Demoulin, V., McGill, J.a., 2012. High-frequency financial data modeling using Hawkes processes. J. Bank. Financ. 36 (12), 3415–3426.

Chavez-Demoulin, V., Davison, R.A.C., McNeil, A.J., 2005. Estimating value-at-risk: a point process approach. Quant. Finan. 5 (2), 227–234.
Chen, Y.-C., Rogoff, K., 2003. Commodity currencies. Finan. Dev. 40 (1), 45–48.
Chen, Y.-C., Rogoff, S.K., Rossi, B., 2010. Can exchange rates forecast commodity prices? Q. J. Econ. 125 (3), 1145–1194.
Choudhri, E.U., Schembri, L.L., 2014. Productivity, commodity prices and the real exchange rate: the long-run behavior of the Canada-US exchange rate. Int. Rev. Econ. Financ. 29, 537–551.
Christoffersen, P., 1998. Evaluating interval forecasts. Int. Econ. Rev. 39, 841–862.
Delatte, A.L., Lopez, C., 2013. Commodity and equity markets: some stylized facts from a copula approach. J. Bank. Financ. 37 (12), 5346–5356.
Edwards, S., 1986. Commodity export prices and the real exchange rate in developing countries. In: Coffee in Colombia.
Engle, R.F., Kroner, K.F., 1995. Multivariate simultaneous generalized arch. Econom. Theory 11 (1), 122–150.
Engle, R.F., Manganelli, S., 2004. Caviar: conditional autoregressive value at risk by regression quantiles. J. Bus. Econ. Stat. 22 (4), 367–381.
Engle, R.F., Russell, J.R., 1998. Autoregressive conditional duration: a new model for irregularly spaced transaction data. Econometrica 1127–1162.
Engle, R.F., Engle, R.F., Kroner, K.F., Kroner, K.F., 1993. Multivariate simultaneous generalized arch.
Ferraro, D., Rogoff, K., Rossi, B., 2015. Can oil prices forecast exchange rates? An empirical analysis of the relationship between commodity prices and exchange rates. J. Int. Money Financ. 54, 116–141.
Figuerola-Ferretti, I., McCrorie, J.R., 2016. The shine of precious metals around the global financial crisis. J. Empir. Financ. 38, 717–738.
Forbes, K.J., Rigobon, R., 2002. No contagion, only interdependence: measuring stock market comovements. J. Financ. 57 (5), 2223–2261.
Hardiman, S.J., Bercot, N., Bouchaud, J.P., 2013. Critical reflexivity in financial markets: a Hawkes process analysis. Eur. Phys. J. B 86 (10).
Hatzinikolaou, D., Polasek, M., 2005. The commodity-currency view of the Australian dollar: a multivariate cointegration approach. J. Appl. Econ. 13 (1), 81–99.
Herrera, R., 2013. Energy risk management through self-exciting marked point process. Energy Econ. 38, 64–76.
Hung, J.C., Lee, M.C., Liu, H.C., 2008. Estimation of value-at-risk for energy commodities via fat-tailed GARCH models. Energy Econ. 30 (3), 1173–1191.
Kato, H., et al., 2012. Changes in the Relationship between Currencies and Commodities. Tech. Rep.. Bank of Japan.
Kellner, R., Gatzert, N., 2013. Estimating the basis risk of index-linked hedging strategies using multivariate extreme value theory. J. Bank. Financ. 37 (11), 4353–4367.
Kohlscheen, E., 2010. Emerging floaters: pass-throughs and (some) new commodity currencies. J. Int. Money Financ. 29 (8), 1580–1595.
Liu, P., Tang, K., 2011. The stochastic behavior of commodity prices with heteroskedasticity in the convenience yield. J. Empir. Financ. 18 (2), 211–224.
Massacci, D., 2016. Tail risk dynamics in stock returns: links to the macroeconomy and global markets connectedness. Manag. Sci. 63, 3072–3089.
McAleer, M., 2018. Stationarity and invertibility of a dynamic correlation matrix. Kybernetika 54, 363–374.
McNeil, A.J., Frey, R., 2000. Estimation of tail-related risk measures for heteroscedastic financial time series: an extreme value approach. J. Empir. Financ. 7 (3–4), 271–300.
McNeil, A.J., Frey, R., Embrechts, P., 2005. Quantitative risk management: concepts, techniques and tools. Risk Manage. 101 (476), 30.
Pickands, J., 1975. Statistical inference using extreme order statistics. Instit. Math. Stat. Stable 3 (1), 119–131.
Ready, R., Roussanov, N., Ward, C., 2017. After the tide: commodity currencies and global trade. J. Monet. Econ. 85, 69–86.
Sanidas, E., 2014. Four harmonic cycles explain and predict commodity currencies' wide long term fluctuations. Technol. Forecast. Soc. Chang. 87, 135–151.
Scarrott, C., MacDonald, A., 2012. A review of extreme value threshold estimation and uncertainty quantification. Rev. Stat. Stat. J. 10 (1), 33–60.
Wu, Y., 2013. What explains movements in the peso/dollar exchange rate? IMF Working Papers 13 (171), 1.

Apéndice B. Dynamics of Connectedness in Clean Energy Stock Markets

Contiene

- Artículo original obtenido según DOI: https://doi.org/10.3390/en13143705

energies

MDPI

Article

Dynamics of Connectedness in Clean Energy Stocks

Fernanda Fuentes [1,†] and Rodrigo Herrera [2,*,†]

[1] DSc Program on Complex Engineering Systems, Institute of Mathematics and Physics, University of Talca, Talca 3460000, Chile; fefuentes@utalca.cl
[2] Faculty of Business and Economics, University of Talca, Talca 3460000, Chile
* Correspondence: rodrigo.herrera@utalca.cl
† These authors contributed equally to this work.

Received: 3 June 2020; Accepted: 16 July 2020; Published: 18 July 2020

Abstract: This paper examines the dynamics of connectedness among the realized volatility indices of 16 clean energy stocks belonging to the SPGCE and the implied volatility indices of two important stock markets—the S&P 500 and the STOXX50—and two commodities markets—the crude oil and gold markets. The empirical results show a unidirectional connectedness from the implied volatility indices to the clean energy stocks. Our analysis further reveals similar volatility connectedness behaviors among companies in the same energy production subsector. However, there exists heterogeneous behavior between different energy production subsectors over time. Further, we identify pairwise directional connectedness clusters among related companies, indicating that there are few possibilities for portfolio diversification within the energy production subsectors. Finally, through an impulse–response analysis, we confirm that the expectation of future market volatility of the S&P 500 index and the gold price plays a leading role in volatility connectedness with clean energy stocks.

Keywords: renewable energy markets; realized volatility; implied volatility; directional connectedness

1. Introduction

Global economic development is intricately tied to the supply and demand of energy. At present, the largest source of energy is fossil fuels, the use of which accounts for 87% of global carbon dioxide CO_2 emissions [1–3]. Over the last few years, national governments have taken a variety of actions to reduce greenhouse gas emissions and to help make renewable energy competitive with conventional energy sources [4–6]. Within these new stock markets, clean energy stocks have attracted the attention of both investors and energy policy analysts, who are interested in understanding the behavior of these stocks and determining whether these new investment opportunities hold promise [7–9].

The literature on clean energy stocks is scarce, and the majority of research has used global clean energy indices to represent the behavior of these markets. The S&P Global Clean Energy Index (SPGCE), WilderHill Clean Energy Index (ECO), and WilderHill New Energy Global Innovation Index (NEX) are the main indices used (see Table 1). Nevertheless, conducting analyses using only global clean energy indices—thereby excluding company-level information—can lead to flaws in the conclusions of studies [10]. Commonly, the relationships between clean energy indices and other financial markets have been studied using multivariate volatility models [7,11–13] and multivariate copulas models [1,14,15]. While both of these methodologies provide researchers with useful information in different contexts, neither provides any insights related to directional connectedness.

Our study extends the current literature in several ways: (i) We analyze the volatility connectedness among individual clean energy stocks from distinct subsectors of production; (ii) we include implied volatility indices to investigate the expectations of financial markets regarding

individual clean energy stocks; (iii) we determine whether the clean energy stocks are more affected by expectations from financial markets (i.e., the USA or Europe) or commodity markets (i.e., oil or gold); (iv) we analyze volatility connectedness to determine the magnitude and direction of volatility spillovers and observe the dynamics of connectedness between markets; and (v) we complement our results with an impulse–response analysis to determine the impact of a shock in the implied volatility indices on the volatility of clean energy stocks.

The motivation to include implied volatility indices from commodity and global stock markets is because these two markets have become important economic and financial indicators representing market consensus on the expected future uncertainty [15–17]. Therefore, the estimated volatility connectedness of commodity and stock markets with the realized volatility of the clean energy stocks is informative of the different nature of risk transfer associated with trading activity and cross-market sentiments of the market participants. In particular, energy stock prices have different effects across industries or sectoral stock markets; for instance, energy-intensive firms should be more influenced by large oil volatility shocks, indicating a negative relationship between increasing oil prices and stock prices [18,19]. As oil prices rise, economic agents are motivated to seek alternative energy sources, such as clean energy markets. On the other hand, technology stocks are susceptible to the business cycle; influencing also clean energy firms that, at the same time, depend on inputs from technology companies [20,21]. Hence, clean energy stocks and technology stocks are closely related to the business cycle. Thus, the results of this research provide useful information to risk managers looking for diversification strategies using derivatives on an investment portfolio during periods of financial turmoil.

Our analysis includes the realized range-based volatility of 16 individual clean energy stocks, all belonging to the SPGCE index. These companies include solar, wind, and hydroelectric energy producers located in countries such as the United States, Canada, Brazil, Denmark, and China. Our study provides a more detailed vision of the behavior of clean energy stocks by using the information from four implied volatility indices to define the expectations for future volatilities in clean energy stocks. The following indices have been identified in the existing literature as having important links with clean and conventional energy stocks: CBOE Gold ETF Volatility Index (GVZ), CBOE Crude Oil ETF Volatility Index (OVX), CBOE Volatility Index based on options of the S&P 500 index (VIX), and EURO STOXX 50 Volatility Index based on EURO STOXX 50 options prices $(VSTOXX)$. The CBOE acronym refers to Chicago Board Options Exchange. The first two implied volatility indices are associated with commodities; oil is known as an inherent substitute in clean energy stocks [22,23], while gold is included for its role as an effective safe haven in the face of stressful financial situations [15,24,25]. The second two are global indices, from the United States and Europe, respectively. These indices were included due to the countries of origin of the companies. Unlike the previous literature, which examined these indices from an aggregate point of view, our research shows that, if we want to find the most efficient investment strategies, we must acknowledge that each subsector of energy production has specific characteristics. In this context, the main research questions posed are: Are the volatility prices of clean energy stocks heterogeneous across the different clean energy production subsectors? And how clean energy stock prices, of different production subsectors, relate to the changes in prices of the main financial and commodity markets? This information is relevant to investors and energy policy analysts who are interested in understanding the behavior of clean energy stocks, in order to determine whether these new investment opportunities are attractive [7–9]

To estimate the directional volatility spillover measures between the realized volatility of clean energy stocks and the implied volatility indices, we use the Diebold–Yilmaz connectedness methodology (see [26]). This methodology provides a useful framework for estimating directional connectedness between individual series and offers important summary measures of network connectedness. We chose this methodology for several reasons. First, this approach can be easily implemented by means of a vector autoregression model through forecast error variance decomposition. More importantly, this framework quantifies both the direction and strength of dynamic connectedness

among different variables. Second, it allows the use of different time horizons, facilitating selection suitable for each context. Third, it overcomes the dimensionality problem that arises from an increase in the number of variables included in the analysis.

Our results reveal that connectedness is unidirectional, marked by the strong flow of information from the implied volatility indices toward the clean energy stocks, where the future volatility expectations of VIX and GVZ play fundamental roles. By examining the dynamics of the volatility connectedness, it is possible to identify cross-sectional patterns among companies from the same subsector of production. As a result, we can identify a heterogeneous relationship between subsectors of clean energy production (i.e., solar, wind, hydroelectric, geothermal, fuel cell, and mixed) and the implied volatility indices. Finally, an impulse–response analysis allows us to confirm the results of directional connectedness, highlighting the impact of shocks in VIX and GVZ on the realized volatility of the clean energy stocks. Furthermore, using this analysis method, we can once again observe cross-sectional patterns among the connectedness measures of distinct subsectors of clean energy production.

The remainder of this paper is organized as follows. Section 2 presents a review of the literature. In Section 3, we provide a description of the data. Then, in Section 4, we present the methodology and, in Section 5, we analyze the empirical results of this study. Finally, we offer some concluding remarks in Section 6.

2. Literature Review

A growing interest in sustainable development has led to increasing investor awareness of clean energy stocks and expanding research on the relationship between those stocks and other financial markets. Table 1 presents a detailed overview of the literature on clean energy stocks, identifying the main methodologies and indices used in each study.

The first studies on clean energy stocks used VAR models; for instance, Kumar et al. [23] used a VAR model to show that the price behavior of clean energy stocks can be explained by past movements in oil prices, stock prices of high-technology firms, and interest rates. In this study, carbon price returns are not a significant factor in stock price movements for clean energy firms. Managi and Okimoto [27] proposed a Markov Switching VAR model to examine the relationships between clean energy, oil, and technology stock prices. Their results indicated a positive relationship between these stock's market indices, a relationship that started with a structural change in late 2007.

Another strand of literature focuses more on the interdependence of volatility than on its price returns. For example, Sadorsky [28] compared different multivariate GARCH models (BEKK, Diagonal, DCC, and CCC) to model conditional correlations and to analyze volatility spillovers between oil prices and the stock prices of clean energy and technology companies. The results indicated that the stock prices of clean energy companies were more highly correlated with technology stock prices than with oil prices. Ahmad et al. [16] used DCC, ADCC, and GO-GARCH models to examine how crude oil, US bonds, gold, VIX, OVX, and European carbon prices can be used to hedge an investment in clean energy equities. Their study shows that VIX is the best asset for protecting clean energy equities, followed by oil and gold. Dutta et al. [11], using a bivariate VAR-GARCH approach, studied the relationship between the carbon emissions market and renewable energy stock returns. They found a significant volatility linkage between the carbon emission returns and the prices of clean energy in European markets; however, this relationship did not hold for US markets. Kyritsis and Serletis [12] used VAR-GARCH-in-mean to estimate an impulse–response analysis of clean energy stock markets and technology company stocks with the different sized shocks in oil price shocks. The results suggested that there was a symmetric relationship between oil and the returns of clean energy stocks. Maghyereh et al. [13] proposed a wavelet MGARCH-DCC method to analyze the bidirectional relationships between the returns and volatilities from oil and technology to the clean energy market using multiple time horizons. Their main finding was that, over long time horizons, the returns and volatilities of oil significantly and positively affected clean energy stock markets. When considering all

time horizons, there exists a bidirectional relationship between the returns and volatilities of technology and clean energy stocks. Dutta et al. [7], through a DCC-GARCH model, showed that commodity volatilities and clean energy equity prices move in opposite directions, suggesting the possibility of using implied volatility indices as an effective tool for hedging clean energy stock indices.

More recent literature has analyzed the behavior of clean energy stocks and their contemporary relationships with other markets using multivariate copula functions. Mejdoub and Ghorbel [1] used a TGARCH-Vine copula to determine how changes in oil prices affect renewable energy stock markets. Their results indicated a significant and symmetric dependence between both markets, which were coupled in the same direction. Reboredo and Ugolini [14] carried out a study based on a multivariate vine copula to characterize the dependence between different classes of energy (i.e., oil, gas, coal, and electricity) and the price of clean energy. Their analysis showed that oil and electricity were the main contributors to the dynamics of clean energy prices. Bouri et al. [15] carries out a two-stage study: First, they utilized a mixture specification copula and, then, they performed an analysis of parametric and non-parametric tail dependence measures. The objective of their study was to verify the role of gold and oil as potential safe havens for clean energy indices in times of crisis. Their results showed that both commodities were no more than weak safe-haven stocks for clean energy indices, where oil was better during extreme price movements. Reboredo [22] used TGARCH-copulas to characterize the structural dependence between oil and three international clean energy indices (ECO, SPGCE, ERIX), incorporating the indices of different production sectors as well (i.e., solar, wind, smart technologies). His results showed a symmetric tail dependence in almost all of the clean energy indices; except for the solar energy index, which was asymmetrically affected by extreme movements in oil prices.

Recent studies have used the Diebold–Yilmaz methodology (see [26]) to analyze the connectedness between clean energy stocks and other markets. Connectedness is central for risk mediation and management, thus playing a pivotal role in risk markets, credit risk, counter-party and gridlock risk, and systemic risk [29]. In this vein, Ahmad [30] determined that technology and clean energy indices are the dominant emitters of return and volatility spillovers to crude oil. Furthermore, the authors showed evidence that clean energy indices can provide a profitable hedging opportunity in combination with oil and technology indices. Ahmad and Rais [31] determined the existence of directional spillover from technologies to clean energy markets and a bidirectional dependence with global stock markets. Pham [10] identified the subsectors of production to analyze the connectedness between oil and different clean energy indices. The results showed that biofuel and energy management stocks (NASDAQ OMX Energy Management Index) were more connected with oil price, while wind, geothermal, and fuel cell stocks were among the least connected to oil price. The study asserted that disaggregating the analysis to the level of the production subsector is necessary for effectively studying the behavior of clean energy stocks.

Finally, there also exist other methodologies to analyze the dependence among clean energy markets which are not classified among the previously mentioned ones; for instance, Sadorsky [32] used an extension of the capital asset pricing model to investigate the determinants of risk in clean energy stocks. The results showed that increased oil prices have a positive impact on the financial risk of clean energy stocks. Bondia et al. [33] analyzed cointegration and causality, providing evidence that clean energy stocks are affected by technology stock prices, oil prices, and interest rates in the short term. Dutta [17] used a realized volatility model to demonstrate that clean energy stocks are highly sensitive to shocks in the OVX. Reboredo et al. [34] proposed a wavelet analysis and Granger causality test to examine co-movement and causality between oil and renewable energy indices. Their results indicated that there is a weak relationship in the short term that gradually gets stronger over the long term. Yahşi et al. [35] developed a prediction model for future carbon prices using explanatory variables. Their main findings indicated that the variable with the most influence on future carbon prices is clean energy stocks.

Table 1. Methodologies and indices used for empirical analyses in different articles.

Econometric Methodology	Reference	Specification	Indices
VAR	Kumar et al. [23]	VAR	ECO, SPGCE, NEX, PSE, Oil, Carbon, Interest Rate, S&P 500
	Managi and Okimoto [27]	Markov Switching VAR	ECO, PSE, Oil, Interest Rate
Volatility	Sadorsky [28]	BEKK, Diagonal, DCC, CCC	ECO, PSE, Oil
	Ahmad et al. [16]	DCC, ADCC, GO-GARCH	ECO, Oil, Gold, VIX, OVX, Carbon, Bond
	Dutta et al. [11]	VAR-GARCH, DCC-GARCH	ECO, ERIX, Carbon
	Maghyereh et al. [13]	waveled MGARCH-DCC	ECO, Oil, FTSE ET50
	Kyritsis and Serletis [12]	VAR-GARCH in mean	ECO, SPGCE, NEX, PSE, Oil
	Dutta et al. [7]	DCC-GARCH	ECO, SPGCE, MAC, OVX, GVZ, VXSLV
Copulas	Reboredo [22]	TGARCH- Copula	ECO, SPGCE, ERIX, WIND, SOLAR, TECH, Oil
	Mejdoub and Ghorbel [1]	TGARCH-Vine Copula	ECO, SPGCE, NEX, Oil
	Reboredo and Ugolini [14]	Multivariate Vine Copula	ECO, ERIX, Oil, Natural Gas, Coal, Electricity, S&P 500, Euro Stoxx 50
	Bouri et al. [15]	EVT-Copulas	ECO, SPGCE, Oil, Gold
Mixed	Sadorsky [32]	Beta model (CAPME extension)	PBW, Oil
	Bondia et al. [33]	Threshold Cointegration Test, Granger Causality.	NEX, PSE, Oil, Interest Rate
	Reboredo et al. [34]	Wavelet based-test, Granger Causality	ECO, SPGCE, ERIX, Oil, WIND, SOLAR, TECH
	Dutta [17]	Range-based volatility measures.	ECO, Oil, OVX, Carbon
	Yahşi et al. [35]	Random Forest, Regression	SPGCE, DAX, Oil, Natural Gas, Coal, Carbon, Electricity
Diebold-Yilmaz Connectedness	Ahmad [30]	Diebold-Yilmaz connectedness, BEKK, DCC, CCC	ECO, PSE, Oil
	Ahmad and Rais [31]	Diebold-Yilmaz connectedness, ADCC	NEX, PSE, Oil, Heating, Gasoline, DJIMI, Market Indexes: WORLD-DS, US-DS, EUROPE-DS.
	Pham [10]	Diebold-Yilmaz connectedness, DCC, ADCC, GO-GARCH	Oil, NASDAQ OMX Clean Energy Indices.

Notes: ECO: Wilder Hill Clean Energy Index. NEX: Wilder Hill New Energy Global Innovation Index. SPGCE: S&P Global Clean Energy Index. PBW: Wilder Hill Clean Energy ETF. PSE: NYSE Arca Technology Index. EUA: European Union Allowances. ERIX: European renewable energy index. NE: China's new energy index. WIND: NYSE Bloomberg Global Wind Energy Index, SOLAR: NYSE Bloomberg Global Solar Energy, TECH: NYSE Bloomberg Global Energy Smart Technologies Index, MAC: MAC global solar energy stock.

One important weakness in the recent literature is that most studies have used global indices to represent the general behavior of clean energy markets. To the best of our knowledge, the only studies that have shown differences in their results after identifying subsectors of production are those of Reboredo [22] and Pham [10]. In particular, Pham [10] was the first to identify that using global indices of clean energy is a weakness when attempting to capture the heterogeneity of the subsectors of clean energy production. For this reason, our study offers a more detailed understanding of the behavior of clean energy stocks at the company level, thereby differentiating clean energy companies from different subsectors of production.

3. Data Description

Volatility, as a quantitative indicator of risk or uncertainty, is one of the most important measures for describing market expectations. The connectedness of volatility is known as the "connectedness of fear,"which has become an interesting area of study [36,37]. Quantifying these effects could inform early alert systems to warn of emerging crises [11].

This study uses the daily realized volatility indices for 16 clean energy stocks belonging to the SPGCE as its time-series. To obtain the realized volatility indices, we constructed the realized range-based volatility following Garman and Klass [38]:

$$\begin{aligned}\hat{\sigma}_{it}^2 &= 0.511\left(H_{it}-L_{it}\right)^2-0.019\left[\left(C_{it}-O_{it}\right)\left(H_{it}+L_{it}-2O_{it}\right)-2\left(H_{it}-O_{it}\right)\left(L_{it}-O_{it}\right)\right] \\ &\quad -0.383\left(C_{it}-O_{it}\right)^2,\end{aligned} \tag{1}$$

where H_{it}, L_{it}, O_{it}, and C_{it} are the high, low, opening, and closing prices, respectively, using the logs of stock prices i over time t.

In Table 2, we give a description of the companies, including the name, abbreviation, origin (country and year that it was founded), and the sector of production of each company. Representative in the sample are solar energy, wind energy, geothermic energy, fuel cell, and hydroelectric producers located in countries such as the United States, Canada, Brazil, Denmark, and China (The companies that operate in more than one sector of production are labeled "mixture" in Table 2). We also include four implied volatility indices: CBOE Gold ETF Volatility Index (GVZ), CBOE Crude Oil ETF Volatility Index (OVX), CBOE Volatility Index based on options of the S&P 500 index (VIX), and EURO STOXX 50 Volatility Index based on EURO STOXX 50 options prices $(VSTOXX)$. The first two implied volatility indices are associated with commodities; oil is known as an inherent substitute in clean energy stock prices [22,23], while gold is included for its role as an effective safe haven in the face of stressful financial situations [15,24,25]. The second two are global indices, from the United States and Europe, respectively. These indices were included because of the countries of origin of the companies. All data were obtained from the Thomson Reuters Datastream, with daily observations from 3 June 2008 to 3 June 2019. Because the OVX index has been published since the middle of the year 2008, only 16 of the 30 stock indices that make up the SPGCE were used for this study, as these were the only ones with information available for the whole sample period.

Figure 1 shows the implied volatility and realized volatility indices. In most cases, we observe an increase in volatility during the 2008 subprime crisis. Among the implied volatility indices in the left column, OVX stands out as having several spikes in volatility over the full sample period. In the case of the realized volatility estimations for the clean energy stocks, they show a more stable behavior over time than those exhibited by the implied volatility indices. In particular, if we focus on the sector of production of each company, we observe similar patterns and trends for companies whose production source is the same; for instance, CIG, ELP, and VER are all hydroelectric energy companies, whose returns exhibit similar stylized facts.

Table 2. Description of the 16 individual clean energy stock prices belonging to the SPGCE index.

Name	Ticker	Founded	Subsector
Cia Energetica de Minas Gerais Prf ADR	CIG	Brazil, 1952	Hydro (Electric power)
Companhia Paranaense de Energia	ELP	Brazil, 1954	Hydro (Electric power)
VERBUND AG	VER	Austria, 1947	Hydro (Electric power)
Nordex SE	NDX1	Germany, 1985	Wind
Vestas Wind Systems AS	VWS	Denmark, 1945	Wind
Siemens Gamesa Renewable Energy	SGRE	Spain, 1976	Wind
Falckrenewables	AA4	Italy, 2002	Mixture
Plugpower	PLUG	USA, 1997	Fuell Cell
Ormat Technologies	ORA	USA, 1965	Geotermal
First Solar Inc	FSLR	USA, 1999	Solar
Sunpower	SPWR	USA, 1985	Solar
Canadian Solar Inc	CSIQ	Canada, 2001	Solar
Boralex Inc. 'A'	BLX	Canada, 1982	Mixture
Innergex Renewable Energy Inc	INE	Canada, 1990	Mixture
Contact Energy Ltd	CEN	New Zealand, 1996	Mixture
GCL Poly Energy Holdings Ltd	GCLP	China, 2006	Mixture

Note: the table shows the name of the company, the country and year in which it was founded, and the sector of production or activity it is involved in. Companies that produce different types of energy have been labelled as 'mixture'.

Table 3 provides a wide descriptive statistics for both types of volatilities. The implied volatility indices show higher medians and standard deviations than those observed in the realized volatility indices of the clean energy stocks. Furthermore, all of the volatility indices have positive asymmetry and show a leptokurtic distribution. These results were confirmed by the Jarque–Bera test, which rejected the normality of the observations. The Box–Pierce test statistic, estimated with 10 lags, showed evidence of persistence. The Phillips–Perron test was used to examine the stationarity of the price volatilities. The results showed that all volatilities were stationary at the 0.05 significance level.

Table 3. Descriptive statistics of daily implied volatility indices and realized volatility indices.

Ticker	Mean	Standard Deviation	Min	Max	Skewness	Kurtosis	Jarque–Bera	Box–Pierce	Phillips–Perron
OVX	36.221	13.762	14.500	98.930	1.340	2.375	0.00	0.00	0.02
GVZ	19.145	7.801	8.880	64.530	2.062	5.917	0.00	0.00	0.01
VIX	19.378	9.624	9.150	80.860	2.543	8.362	0.00	0.00	0.01
VSTOXX	29.951	13.245	11.990	117.310	1.793	4.706	0.00	0.00	0.01
CIG	2.094	1.287	0.160	8.947	5.913	93.894	0.00	0.00	0.01
ELP	1.881	1.128	0.362	14.575	3.661	24.027	0.00	0.00	0.01
VER	1.630	0.978	0.156	12.743	2.877	17.235	0.00	0.00	0.01
NDX1	2.362	1.563	0.000	12.322	2.083	6.580	0.00	0.00	0.01
VWS	2.127	1.477	0.303	15.802	2.854	13.427	0.00	0.00	0.01
SGRE	2.285	1.303	0.427	15.425	2.126	9.381	0.00	0.00	0.01
AA4	2.189	1.283	0.294	11.997	1.943	5.977	0.00	0.00	0.01
PLUG	4.301	2.921	0.375	26.365	2.385	8.742	0.00	0.00	0.01
ORA	1.585	1.110	0.304	19.499	4.536	42.995	0.00	0.00	0.01
FSLR	2.599	1.537	0.566	19.270	3.018	16.715	0.00	0.00	0.01
SPWR	3.199	1.782	0.657	18.315	2.733	12.521	0.00	0.00	0.01
CSIQ	3.581	2.139	0.567	23.410	2.764	14.836	0.00	0.00	0.01
BLX	1.399	1.186	0.000	16.806	4.847	42.237	0.00	0.00	0.01
INE	1.217	1.182	0.000	16.579	5.533	46.376	0.00	0.00	0.01
CEN	0.863	0.505	0.000	5.473	1.823	7.434	0.00	0.00	0.01
GCLP	2.815	1.633	0.000	18.025	2.514	12.395	0.00	0.00	0.01

Note: the last two columns show the p-values of the Jarque–Bera and Box–Pierce tests with 10 lags.

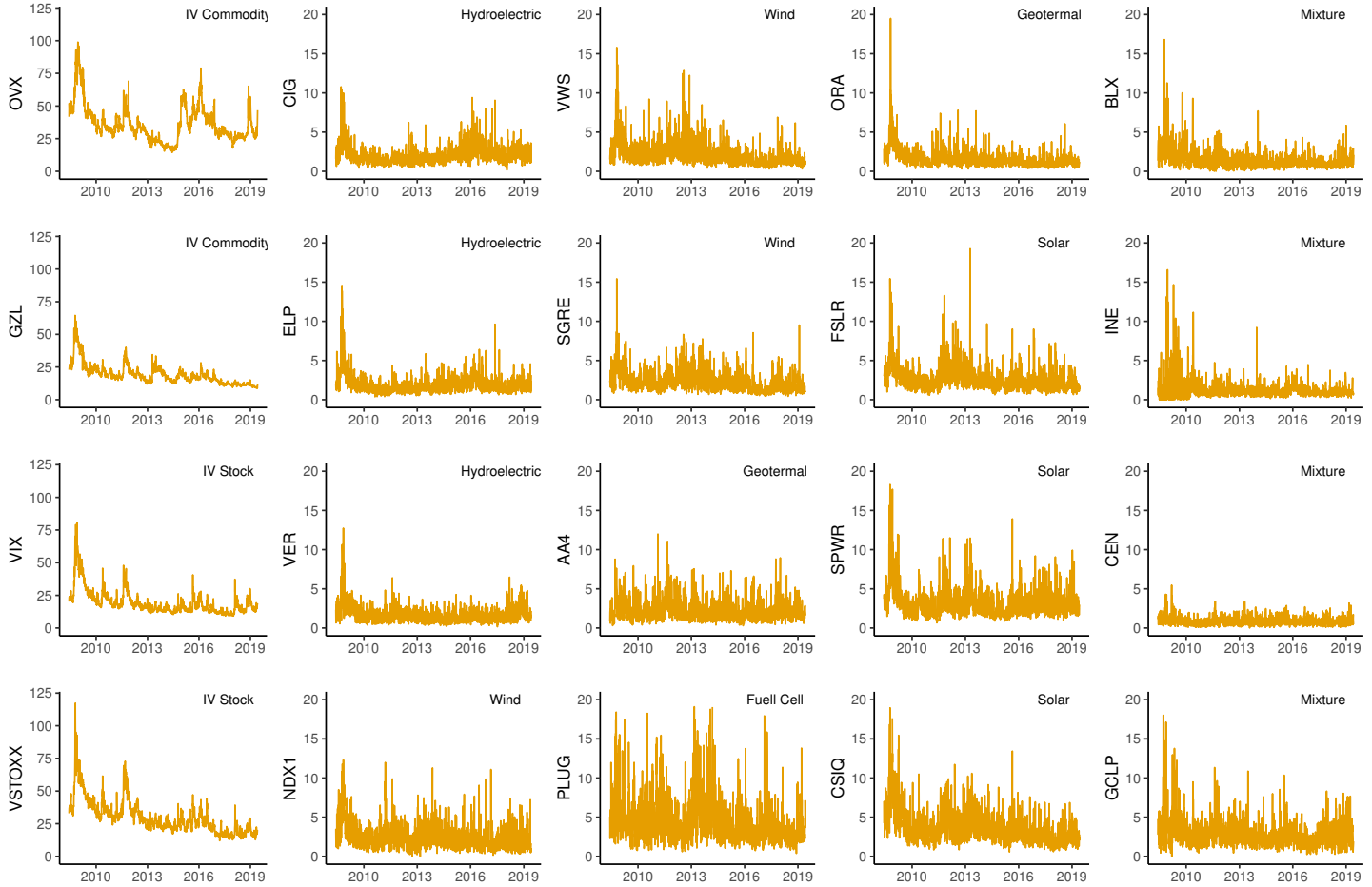

Figure 1. Daily implied volatility time-series (IV of commodities and stocks) and the daily realized volatility time-series for 16 clean energy stocks belonging to the SPGCE (highlighting the sector of production) of each company over the full sample period extending from June 2008 to June 2019. The labels utilized for the description of the companies are detailed in Table 2.

4. Methodology

To quantify the causal relationship between the realized volatility of clean energy stocks and the implied volatility of the global stock markets and commodity indices, we applied the Diebold–Yilmaz connectedness methodology [26]. This approach is based on a forecast error variance decomposition, employing a generalized VAR framework [39] of order p,

$$y_t = \sum_{i=1}^{p} \Phi y_{t-i} + \varepsilon_t, \tag{2}$$

where y_t is an M-dimensional vector of endogenous variables containing the set of realized volatility and implied volatility indices, $\varepsilon_t \sim N(0, \Sigma)$ is a vector of disturbances, and t is the daily time index.

The ijth H-step-ahead generalized forecast error variance decomposition is defined by

$$\theta_{ij}^{g}(H) = \frac{\sigma_{jj}^{-1} \sum_{h=0}^{H-1} (e_i' A_h \Sigma e_j)^2}{\sum_{h=0}^{H-1} (e_i' A_h \Sigma A_h' e_i)^2}, \; H = 1, 2, ..., \tag{3}$$

with $i, j = 1, ..., M$, where Σ is the variance–covariance matrix of the disturbance vector ε_t in the VAR, σ_{jj} is the jjth diagonal element of Σ, A_h is the coefficient matrix of the h-lagged perturbations vector in the infinite moving average representation of the VAR model, and e_i is the selection vector, which is equal to 1 in the ith element and zero otherwise. The error terms are not orthogonal; therefore, $\sum_{j=1}^{M} \theta_{ij}^{g}(H) \neq 1$. Hence, to compare individual pairwise directional connectedness, the estimates have to be normalized:

$$\tilde{\theta}_{ij}^{g}(H) = \frac{\theta_{ij}^{g}(H)}{\sum_{j=1}^{M} \theta_{ij}^{g}(H)}, \tag{4}$$

in which, by construction, $\sum_{j=1}^{M} \tilde{\theta}_{ij}^{g}(H) = 1$ and $\sum_{i,j=1}^{M} \tilde{\theta}_{ij}^{g}(H) = M$. As a matter of notation, we now convert from $\tilde{\theta}_{ij}^{g}(H)$ to $C_{i \leftarrow j}^{H}$ to describe the pairwise directional connectedness across different series, which is less cumbersome and more directly informative.

The measure of total directional connectedness from all other series to a series i is defined as follows:

$$C_{i \leftarrow \bullet}^{H} = \frac{\sum_{\substack{j=1 \\ j \neq i}}^{M} \tilde{\theta}_{ij}^{g}(H)}{M}. \tag{5}$$

Similarly, a total directional connectedness from a series j to all other series i is given by

$$C_{\bullet \leftarrow j}^{H} = \frac{\sum_{\substack{i=1 \\ i \neq j}}^{M} \tilde{\theta}_{ji}^{g}(H)}{M}. \tag{6}$$

The net total directional connectedness corresponds to the difference between directional connectedness, given as:

$$C_{i}^{H} = C_{\bullet \leftarrow i}^{H} - C_{i \leftarrow \bullet}^{H}. \tag{7}$$

Finally, the "total connectedness" (or "system-wide connectedness"), summarized in a single index (C^H), is given by:

$$C^{H} = \frac{\sum_{\substack{i,j=1 \\ i \neq j}}^{M} \tilde{\theta}_{ij}^{g}(H)}{M}. \tag{8}$$

Thus, total connectedness is the ratio of the sum of the off-diagonal elements of the variance decomposition matrix to the sum of all its elements.

5. Empirical Results and Discussion

There are three stages in our empirical application. First, a full-sample analysis provides a general overview of the measures of interdependence. This network connectedness is summarized in a total connectedness table. In the second stage, we estimate a rolling-sample connectedness specification, in order to analyze the dynamic behavior of volatilities by utilizing connectedness plots. Finally, we carry out an impulse–response analysis to graphically represent how shock in the implied volatility indices affects the volatility of clean energy stocks The results of this research were obtained using R version 3.4.4. Data and R Code are freely available at: https://github.com/FernandaFuentes/Dynamics-of-Connectedness-in-Clean-Energy-Stocks.

5.1. Full-Sample Analysis

To estimate the network connectedness, we used a VAR model of order 1 and examined the variance decomposition with a 10-step-ahead prediction horizon. Selection is based on the Schwarz Information Criterion. Table 4 corresponds to the total connectedness table. The total connectedness index C^H defined in (8) achieved a value of 38.31% for the full sample period of 2008–2019. This result is in line with the empirical findings of different studies, which obtained total connectedness indices of similar magnitudes when analyzing global equity markets, commodity markets, and foreign exchange markets [40–42].

To obtain a quick overview of the network connectedness, the last column in Table 4 lists the net total directional connectedness C_i^H in (7). Positive (negative) values indicate that the volatility indices are transmitters (receptors) of volatility spillovers. We observe that the implied volatility indices are transmitters, while the realized volatility indices seem to be receptors of volatility spillovers.

These results are confirmed when we focus on the results of the total directional connectedness measures "to" $C_{\bullet \leftarrow j}^H$, as defined in (6), shown in the last row of Table 4. In particular, if we look at the global implied volatility indices of the United States and Europe, the role of VIX becomes immediately apparent, with a total directional connectedness of $C_{\bullet \leftarrow VIX}^H$ = 139.4%. This value is possible as the index $C_{\bullet \leftarrow j}^H$ is not restricted in its dimension. Of this total, VIX transmits 28.09% to $VSTOXX$ and 15.75% to OVX. The total directional connectedness of $VSTOXX$ is $C_{\bullet \leftarrow VSTOXX}^H$ = 97.4%, primarily composed of VIX (20.49%) and GVZ (14.41%). These results show the strong connectedness between the four implied volatility indices. However, the informative capacity of VIX stands out over other equity volatility indices, a finding that has been well-supported by recent literature [43–45]

In the case of clean energy stocks, the total directional connectedness for most of the estimations was greater from VIX than from $VSTOXX$ (see columns 3 and 4). $VSTOXX$ was more crucial for only three European companies: Falckrenewables from Italy ($C_{AA4 \leftarrow VSTOXX}^H$ = 4.81%), Siemens Gamesa Energy from Spain ($C_{SGRE \leftarrow VSTOXX}^H$ = 6.44%), and Vestas Wind Systems AS of Denmark ($C_{VWS \leftarrow VSTOXX}^H$ = 6.03%). These results were consistent with the findings of Shu and Chang [45] and Sarwar [46], who showed that VIX has a higher impact than other implied volatility indices on financial markets. Meanwhile, if we compare the influence of the implied volatility of commodities on clean energy stocks, the most significant impact on other markets came from GVZ and, to a lesser extent, OVX, with total directional connectedness of $C_{\bullet \leftarrow GVZ}^H$ = 97.6% and $C_{\bullet \leftarrow OVX}^H$ = 40.40%, respectively. Only the Canadian company Innergex Renewable Energy Inc (INE) had a stronger directional connectedness from OVX. This may have been influenced by the fall in oil prices in mid 2014, which led to a drop of over 20% in the price of stocks in the Canadian market [36]. In terms of magnitude, volatility spillovers from OVX to hydroelectric energy companies were greater than those to companies in other subsectors of production.

Table 4. Full-Sample Connectedness.

	OVX	**GVZ**	**VIX**	**VSTOXX**	**CIG**	**ELP**	**VER**	**NDX1**	**VWS**	**SGRE**	**AA4**	**PLUG**	**ORA**	**FSLR**	**SPWR**	**CSIQ**	**BLX**	**INE**	**CEN**	**GCLP**	$C^H_{i\leftarrow\bullet}$	C^H_i
OVX	61.09	7.08	15.75	7.81	2.38	1.29	0.70	0.40	0.41	0.34	0.20	0.16	0.83	0.10	0.39	0.28	0.44	0.33	0.01	0.00	39.00	1.4
GVZ	4.84	52.39	13.54	14.41	1.84	1.75	0.11	1.73	1.66	1.36	0.41	0.50	0.92	1.37	1.24	1.64	0.25	0.02	0.01	0.01	47.60	50.0
VIX	8.75	12.13	45.58	20.49	0.79	0.94	0.94	1.93	1.58	1.86	0.34	0.22	1.79	0.59	0.91	0.43	0.51	0.05	0.12	0.05	54.40	85.0
VSTOXX	6.19	13.21	28.09	40.66	0.79	0.47	0.37	1.95	1.99	2.35	0.89	0.20	0.74	0.71	0.47	0.41	0.29	0.12	0.10	0.01	59.40	38.0
CIG	3.46	4.26	3.41	2.77	52.32	19.97	1.27	1.53	1.01	0.27	0.27	0.19	1.79	1.70	2.31	1.77	1.50	0.07	0.03	0.09	47.60	−2.8
ELP	2.83	7.19	4.83	1.72	18.66	47.57	1.44	2.30	0.97	0.64	0.04	0.48	3.43	1.65	2.48	2.59	0.85	0.15	0.03	0.17	52.40	−7.2
VER	2.58	3.05	9.98	3.29	3.21	2.99	59.08	2.55	1.02	1.54	0.56	0.45	2.68	1.01	2.01	0.71	2.39	0.13	0.36	0.42	41.00	−25.6
NDX1	0.78	5.29	5.30	4.67	1.49	1.85	1.64	60.13	3.32	3.94	0.94	1.03	2.93	1.52	1.95	2.24	0.20	0.09	0.16	0.52	39.80	−6.8
VWS	0.34	4.46	5.89	6.03	1.12	0.57	0.78	3.41	58.25	11.07	0.17	0.42	2.62	1.97	0.87	1.13	0.09	0.33	0.16	0.31	41.80	−3.8
SGRE	0.80	3.98	6.16	6.44	0.39	0.52	1.00	4.18	11.36	59.17	0.29	0.21	1.65	1.52	1.06	0.94	0.05	0.07	0.05	0.18	40.80	−7.6
AA4	1.08	0.67	2.41	4.81	0.50	0.16	0.37	1.58	0.59	0.54	84.45	0.12	0.23	0.80	0.96	0.06	0.05	0.22	0.15	0.26	15.60	−10.0
PLUG	0.44	3.83	1.75	1.27	0.25	0.47	0.03	1.42	0.93	0.33	0.08	83.70	1.07	0.34	1.44	2.22	0.13	0.10	0.08	0.12	16.20	−5.2
ORA	1.86	7.53	10.67	6.00	3.17	4.04	1.30	2.87	3.39	2.03	0.16	0.78	47.55	2.29	2.05	2.44	1.34	0.37	0.13	0.04	52.40	−20.8
FSLR	0.58	4.68	4.66	3.58	1.63	1.44	0.63	1.14	3.84	2.39	0.28	0.53	2.26	50.93	12.71	6.92	0.35	0.73	0.11	0.61	49.00	−10.6
SPWR	0.85	5.19	6.95	2.18	1.70	2.19	0.60	1.33	1.62	1.77	0.42	1.04	1.72	12.56	51.16	7.43	0.33	0.64	0.09	0.21	48.80	−7.6
CSIQ	1.04	7.20	6.67	4.85	1.66	2.65	0.55	2.31	2.31	1.62	0.09	2.01	3.07	7.71	8.12	47.00	0.29	0.33	0.11	0.41	53.00	−18.6
BLX	1.93	5.70	5.47	3.16	4.39	2.48	2.64	0.95	0.30	0.31	0.04	1.53	2.47	0.35	1.31	1.17	65.12	0.53	0.10	0.08	34.80	−25.4
INE	1.30	0.23	2.42	1.11	0.35	0.08	0.07	0.09	0.53	0.07	0.14	0.78	0.40	0.04	0.10	0.49	0.13	91.43	0.19	0.06	8.60	−4.2
CEN	0.37	0.60	1.27	0.47	0.19	0.22	0.63	0.81	0.57	0.26	0.05	0.10	0.52	0.39	0.22	0.55	0.23	0.05	92.34	0.16	7.60	−5.6
GCLP	0.47	1.29	4.12	2.26	0.28	1.12	0.27	0.44	0.52	0.54	0.32	0.25	0.44	1.81	0.65	1.01	0.07	0.13	0.09	83.92	16.00	−12.2
$C^H_{\bullet\leftarrow j}$	40.40	97.60	139.4	97.40	44.80	45.20	15.40	33.00	38.00	33.20	5.60	11.00	31.60	38.40	41.20	34.40	9.40	4.40	2.00	3.80	$VSI^H = 38.31\%$	

Note: C^H corresponds to the total Volatility Spillover Index connectedness. Model based on a VAR of order 1. Each component (i, j) of the table is the estimated contribution from stock volatility j to the 10-step-ahead forecast error variance of stock volatility i. $C^H_{\bullet\leftarrow j}$ is the contribution from stock market j to others. $C^H_{i\leftarrow\bullet}$ is the contribution from other markets to stock volatility i.

Similarly, considering the clean energy stocks, we identified where they were receiving volatility spillover from. To do this, we focused on measuring directional connections "from" $C^H_{i\leftarrow\bullet}$, as defined in (5), shown in the penultimate column in Table 4. Canadian Solar Inc received the most volatility shocks from other stocks ($C^H_{CSIQ\leftarrow\bullet}$ = 53%). This company was primarily affected by the US solar energy companies Sunpower and First Solar ($C^H_{CSIQ\leftarrow SPWR}$ = 8.12%, $C^H_{CSIQ\leftarrow FSLR}$ = 7.71%), followed by contributions from GVZ ($C^H_{CSIQ\leftarrow GVZ}$ = 7.2%).

Finally, our estimations allowed us to identify connectedness clusters among related companies, by observing high values in pairwise directional connectedness measures. For example, there was bi-directional connectedness between the Brazilian hydroelectric companies Companhia Energetica de Minas Gerais and Companhia Paranaense de Energia ($C^H_{CIG\leftarrow ELP}$ = 19.97, $C^H_{ELP\leftarrow CIG}$ = 18.66%), the US solar energy companies First Solar and Sunpower ($C^H_{FSLR\leftarrow SPWR}$ = 12.71%, $C^H_{SPWR\leftarrow FSLR}$ = 12.56%), and the European wind energy companies Siemens Gamesa Renewable Energy and Vestas Wind Systems AS ($C^H_{SGRE\leftarrow VWS}$ = 11.36%, $C^H_{VWS\leftarrow SGRE}$ = 11.07%). These findings confirm that companies in the same production subsector are strongly related.

5.2. Rolling-Sample Analysis: Spillover Plots

In this section, we show the advantages of studying the dynamic behavior between volatility indices. We also present evidence that the dynamic total connectedness index C^H_t can distinguish peaks and falls in financial markets. Figure 2 shows a plot of the dynamic total connectedness index for the full sample. These results were obtained from a VAR model of order 1 with a rolling window of 500 days (two years). We examined the variance decomposition with a 10-step-ahead horizon. In order to determine the prediction horizon and the span of the rolling window, we followed the robustness analysis proposed by Antonakakis and Kizys [47].

Figure 2. The total connectedness index (C^H_t), indicating total connectedness among the stock volatilities for the time period from June 2008 to June 2019. A two-year rolling estimation window is utilized and a 10-step-ahead predictive horizon is used for the underlying variance decomposition.

Throughout the period under analysis, many changes can be observed. These changes indicate the evolution of total directional connectedness, which fluctuated widely between 25% and 65%. In the 2008 subprime crisis, we can observe the highest rate of interdependence, showing that volatility shocks are transmitted quickly through markets in times of financial stress [37]. The first period of the sample also captured the effect of the European debt crisis at the end of 2009. Subsequently, the total directional connectedness of the systems began to decrease. In the middle of 2014, political confrontations between the United States and Russia led to an increase in market tensions, spurring another rise in the index.

Saudi Arabia helped the United States to pressure the Russian government by changing its policy of keeping oil prices high. As a result, the price of oil began to fall from US$100/barrel in July 2014 to US$44 in March 2015. "Black Monday", on 24 August 2015 can be observed in Figure 2. This episode of financial turmoil led to the highest increase in oil volatility since the Subprime Crisis and tensions across global financial markets [13,16,36,41].

Figure 3 shows the estimation results, for the clean energy stocks in different subsectors, of the total directional connectedness measures "to" and "from" with gray and orange lines, respectively. In both cases, it is possible to observe that the patterns of transmission varied over time and differed between subsectors. Cross-sectional patterns are clear and particularly evident in the dynamic of "from" volatility spillovers. This result is to be expected, as clean energy stocks are receptors of shocks produced by the implied volatility indices and not the other way around. Among the main subsectors displaying the same patterns of total directional connectedness were CIG, ELP, and VER in hydroelectric energy; NDX1, VWS, and SGRE in wind energy; and FSLR, SPWR, and CSIQ in solar energy.

In summary, the total directional connectedness measures between companies in the same energy production subsector showed similar behavior; however, this behavior was very heterogeneous between different energy production subsectors over time. Thus, total directional connectedness measures in clean energy stocks are affected by inherent patterns in each subsector of production. From this finding, we conclude that it is inadvisable to characterize the behavior of clean energy stocks by simply using a global index.

5.3. Impulse–Response Analysis

We used the estimations from our VAR model to run an impulse–response analysis between the realized volatilities of the clean energy stocks and the implied volatility indices. In the previous section, we found evidence of cross-sectional connectedness in clean energy stocks from the same subsector of production. Accordingly, we focused our impulse–response analysis on identifying whether there was similar response behaviors, in the clusters previously identified, when faced with an impulse in the implied volatilities of commodities and when faced with an impulse in the implied volatilities of the global stock market indices. The results are significant at the 95% level and shown in Figures 4 and 5, respectively. Graphics including the confidence interval are available from the author upon request.

On one hand, the left and center columns of Figure 4 exhibit the impulse–response functions for solar and wind energy companies, respectively. We can observe that shocks coming from the implied volatility of gold generated higher and more persistent impacts than shocks coming from the implied volatility of oil; for instance, the impulse–response functions seemed to stabilize after five months for GVZ. For many companies, their response to a shock in OVX had a more abrupt rate of decline, decaying after one month. On the other hand, in the right column of Figure 4, we show the impulse–response functions for hydroelectric companies. In this case, the estimations show a similar response to shocks coming from both commodities, GVZ and OVX, typically stabilizing after four months. This finding implies that, for this subsector of production, both the future market expectations of the price of gold and oil can be considered as relevant factors. In Table 4, it is possible to observe that, among the clean energy stocks, connectedness with OVX was only higher in the hydroelectric energy companies.

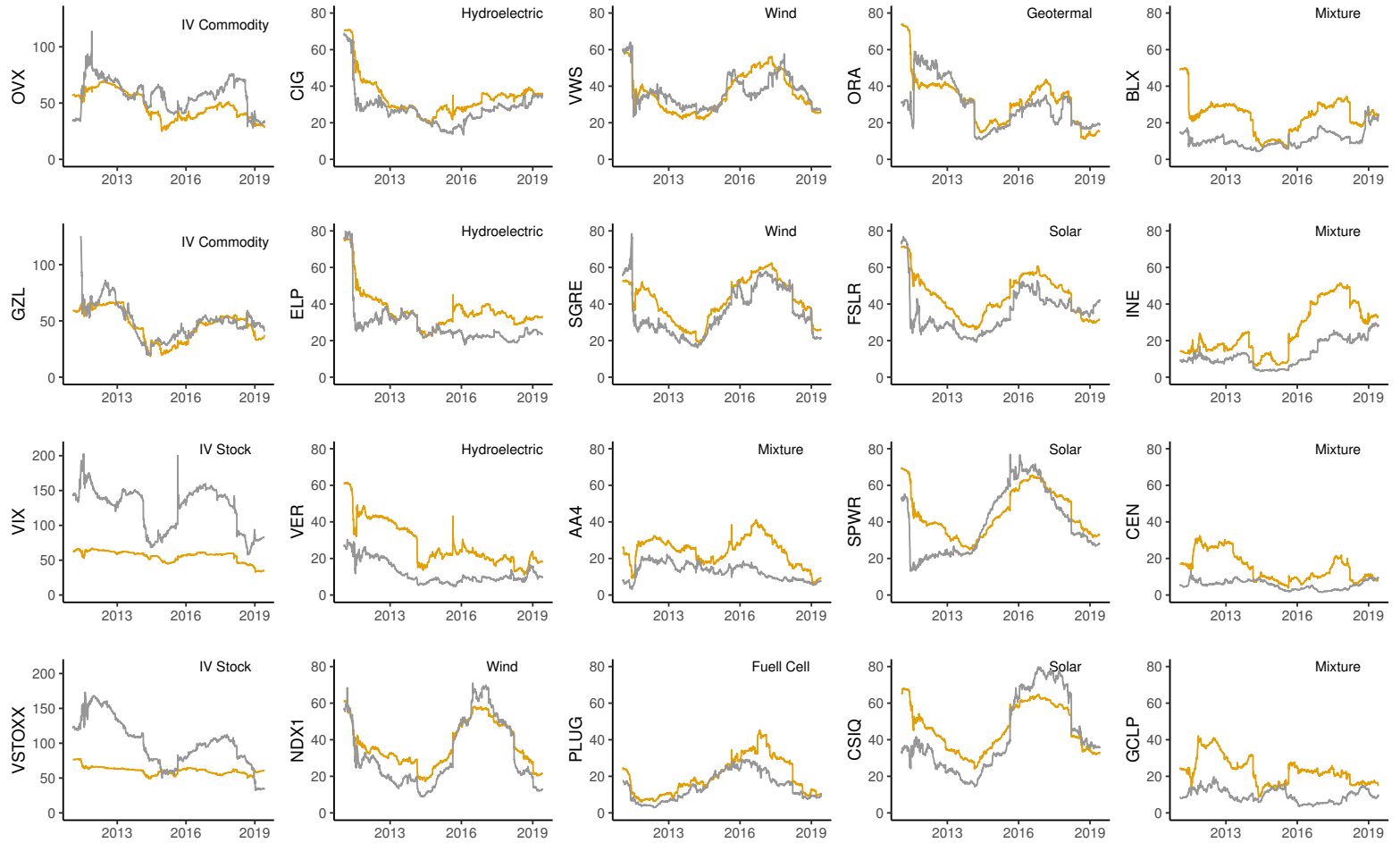

Figure 3. Total directional connectedness $C^{H}_{\bullet \leftarrow j}$ transmitted ("to", gray line) from the market j to the rest of the system and total directional connectedness $C^{H}_{i \leftarrow \bullet}$ received ("from", orange line) by market i from the rest of the system for the period June 2008 to June 2019. A two-year rolling estimation window is utilized and a 10-step-ahead predictive horizon is used for the underlying variance decomposition.

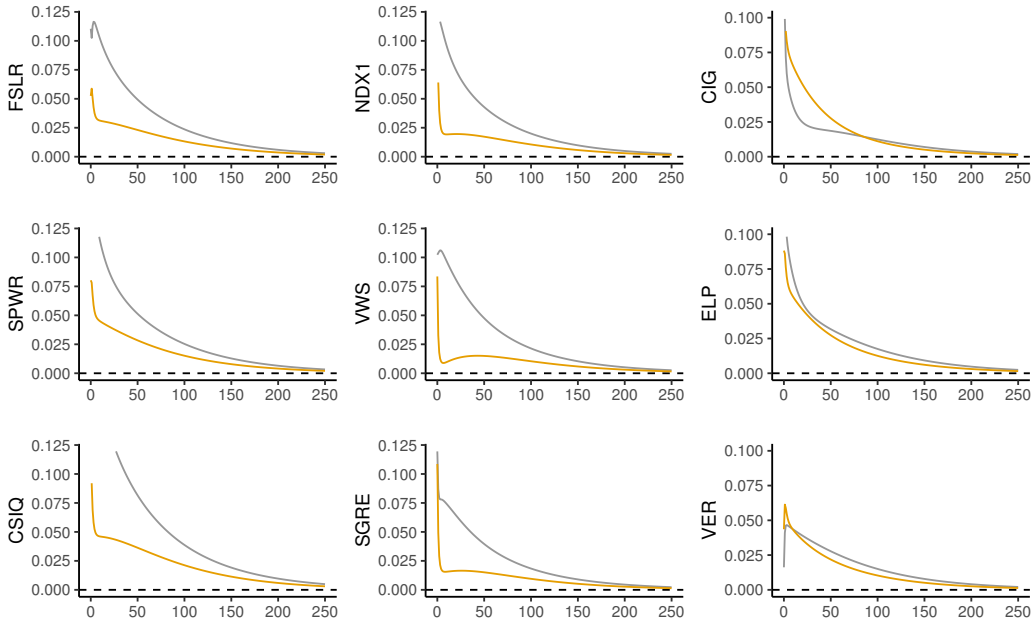

Figure 4. Impulse–response analysis of clean energy stocks, clustered by sector of production, when faced with a shock in GVZ (gray line) and in OVX (orange line) one year ahead (250 days). Left, center, and right columns correspond to solar, wind, and hydroelectric energy companies, respectively.

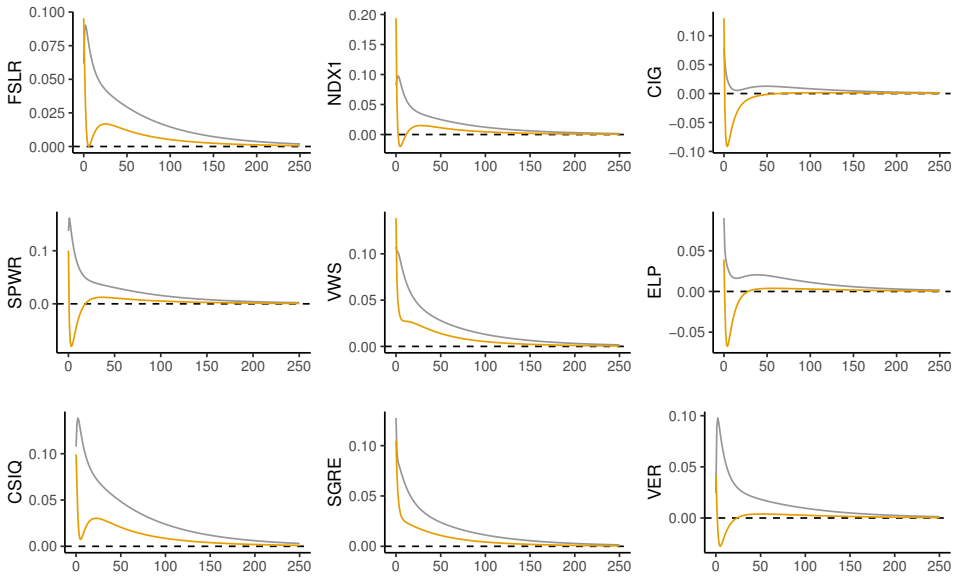

Figure 5. Impulse–response analysis of clean energy stocks, clustered by sector of production, when faced with a shock in VIX (gray line) and in VSTOXX (orange line) one year ahead (250 days). The left, center, and right columns correspond to solar, wind, and hydroelectric energy companies, respectively.

The impulse–response functions relating to the implied volatilities of the global indices and the clean energy stocks are shown in Figure 5. We observe that shocks originating in VIX had a significant impact on clean energy stocks in all subsectors of production. For solar and wind energy companies, the response Was more persistent over time; in particular, the impulse–response functions for VIX seemed to stabilize after four months, while the hydroelectric companies recuperated faster. Shocks coming from $VSTOXX$ generated a negative response in hydroelectric energy companies and a sharper decay rate in solar and wind energy companies, stabilizing at around two months.

6. Conclusions

Clean energy is a dynamic and promising industry which has experienced rapid growth over the last decade. We used the Diebold–Yilmaz connectedness methodology to examine the connectedness between the daily realized volatility indices of 16 clean energy stocks belonging to the SPGCE and implied volatility indices of two global stock markets—the S&P 500 and the STOXX50—and two commodities—the crude oil and gold markets. In this way, we provided a detailed characterization of the connectedness of clean energy markets by investigating the heterogeneity among different subsectors of clean energy production.

The empirical findings showed that there was a unidirectional connectedness from the implied volatility indices to the realized volatility indices of clean energy stocks. Among the implied volatility indices, the future expectations of VIX and GVZ played a leading role in volatility spillovers to the clean energy stocks.

In the dynamic analysis, the time-varying total connectedness index was shown to be able to capture rises and falls in financial price volatilities, as evidenced by the interdependence of volatilities during times of financial crisis. Answering our research questions, the results revealed the heterogeneous behavior between different energy production subsectors over time. Thus, to gain complete knowledge of the interdependence between clean energy stocks, it is necessary to separately examine the volatility dynamics of clean energy stocks from different subsectors of production. Furthermore, relating how clean energy stock prices of different production subsectors are influenced by changes in prices of the main financial and commodity markets, we obtained the following results: Through an impulse–response analysis, we confirmed the impact of shocks in VIX on the realized volatility of clean energy stocks. In terms of commodities, volatility shocks in GVZ produced higher and more persistent responses in the realized volatility of clean energy stocks.

As a policy implication of our research findings, portfolio managers can gain a better understanding of the complex behavior of each clean energy stock by incorporating stylized facts related to each production subsector, in order to effectively promote clean energy investment promoting economic development in this sector. Thus, the construction of optimal diversification strategies should consider the management of investment portfolios at a disaggregated level, taking into account each productive subsector's distinctive characteristics. Our research findings are consistent with Reboredo [22] and Pham [10], who are the first empirical studies to document the heterogeneity of the different clean energy production subsectors.

Author Contributions: All authors contributed equally to all aspects of the research reported in this paper. All authors have read and agreed to the published version of the manuscript.

Funding: The authors acknowledge the Chilean CONICYT funding agency for its financial support (FONDECYT 1180672) for this project.

Conflicts of Interest: The authors declare no conflict of interest.

References

1. Mejdoub, H.; Ghorbel, A. Conditional dependence between oil price and stock prices of renewable energy: A vine copula approach. *Econ. Political Stud.* **2018**, *6*, 176–193. [CrossRef]
2. Amran, Y.A.; Amran, Y.M.; Alyousef, R.; Alabduljabbar, H. Renewable and sustainable energy production in Saudi Arabia according to Saudi Vision 2030; Current status and future prospects. *J. Clean. Prod.* **2019**, *247*, 119602. [CrossRef]
3. Valadkhani, A.; Smyth, R.; Nguyen, J. Effects of primary energy consumption on CO2 emissions under optimal thresholds: Evidence from sixty countries over the last half century. *Energy Econ.* **2019**, *80*, 680–690. [CrossRef]
4. Bhattacharya, M.; Paramati, S.R.; Ozturk, I.; Bhattacharya, S. The effect of renewable energy consumption on economic growth: Evidence from top 38 countries. *Appl. Energy* **2016**, *162*, 733–741. [CrossRef]

5. Zeppini, P.; Van Den Bergh, J.C. Global competition dynamics of fossil fuels and renewable energy under climate policies and peak oil: A behavioural model. *Energy Policy* **2020**, *136*, 110907. [CrossRef]
6. Malik, K.; Rahman, S.M.; Khondaker, A.N.; Abubakar, I.R.; Aina, Y.A.; Hasan, M.A. Renewable energy utilization to promote sustainability in GCC countries: Policies, drivers, and barriers. *Environ. Sci. Pollut. Res.* **2019**, *26*, 20798–20814. [CrossRef] [PubMed]
7. Dutta, A.; Bouri, E.; Das, D.; Roubaud, D. Assessment and optimization of clean energy equity risks and commodity price volatility indexes: Implications for sustainability. *J. Clean. Prod.* **2020**, *243*, 118669. [CrossRef]
8. Kocaarslan, B.; Soytas, U. Asymmetric pass-through between oil prices and the stock prices of clean energy firms: New evidence from a nonlinear analysis. *Energy Rep.* **2019**, *5*, 117–125. [CrossRef]
9. Webb, J. New lamps for old: Financialised governance of cities and clean energy. *J. Cult. Econ.* **2019**, *12*, 286–298. [CrossRef]
10. Pham, L. Do all clean energy stocks respond homogeneously to oil price? *Energy Econ.* **2019**, *81*, 355–379. [CrossRef]
11. Dutta, A.; Bouri, E.; Noor, M.H. Return and volatility linkages between CO2 emission and clean energy stock prices. *Energy* **2018**, *164*, 803–810. [CrossRef]
12. Kyritsis, E.; Serletis, A. Oil Prices and the Renewable Energy Sector. *Energy J.* **2019**, *40*, 337–364. [CrossRef]
13. Maghyereh, A.I.; Awartani, B.; Abdoh, H. The co-movement between oil and clean energy stocks: A wavelet-based analysis of horizon associations. *Energy* **2019**, *169*, 895–913. [CrossRef]
14. Reboredo, J.C.; Ugolini, A. The impact of energy prices on clean energy stock prices. A multivariate quantile dependence approach. *Energy Econ.* **2018**, *76*, 136–152. [CrossRef]
15. Bouri, E.; Jalkh, N.; Dutta, A.; Salah, G. Gold and crude oil as safe-haven assets for clean energy stock indices: Blended copulas approach. *Energy* **2019**, *178*, 544–553.
16. Ahmad, W.; Sadorsky, P.; Sharma, A. Optimal hedge ratios for clean energy equities. *Econ. Model.* **2018**, *72*, 278–295. [CrossRef]
17. Dutta, A. Oil price uncertainty and clean energy stock returns: New evidence from crude oil volatility index. *J. Clean. Prod.* **2017**, *164*, 1157–1166. [CrossRef]
18. Park, J.; Ratti, R.A. Oil price shocks and stock markets in the US and 13 European countries. *Energy Econ.* **2008**, *30*, 2587–2608. [CrossRef]
19. Kilian, L.; Park, C. The impact of oil price shocks on the US stock market. *Int. Econ. Rev.* **2009**, *50*, 1267–1287. [CrossRef]
20. Ahmad, W. An analysis of directional spillover between crude oil prices and stock prices of clean energy and technology companies. *Res. Int. Bus. Financ.* **2017**, *42*, 376–389. [CrossRef]
21. Henriques, I.; Sadorsky, P. Oil prices and the stock prices of alternative energy companies. *Energy Econ.* **2008**, *30*, 998–1010. [CrossRef]
22. Reboredo, J.C. Is there dependence and systemic risk between oil and renewable energy stock prices? *Energy Econ.* **2015**, *48*, 32–45. [CrossRef]
23. Kumar, S.; Managi, S.; Matsuda, A. Stock prices of clean energy firms, oil and carbon markets: A vector autoregressive analysis. *Energy Econ.* **2012**, *34*, 215–226. [CrossRef]
24. Tully, E.; Lucey, B.M. A power GARCH examination of the gold market. *Res. Int. Bus. Financ.* **2007**, *21*, 316–325. [CrossRef]
25. Shahzad, S.J.H.; Raza, N.; Shahbaz, M.; Ali, A. Dependence of stock markets with gold and bonds under bullish and bearish market states. *Resour. Policy* **2017**, *52*, 308–319. [CrossRef]
26. Diebold, F.X.; Yılmaz, K. On the network topology of variance decompositions: Measuring the connectedness of financial firms. *J. Econom.* **2014**, *182*, 119–134. [CrossRef]
27. Managi, S.; Okimoto, T. Does the price of oil interact with clean energy prices in the stock. *Jpn. World Econ.* **2013**, *27*, 1–9. [CrossRef]
28. Sadorsky, P. Correlations and volatility spillovers between oil prices and the stock prices of clean energy and technology companies. *Energy Econ.* **2012**, *34*, 248–255. [CrossRef]
29. Demirer, M.; Diebold, F.X.; Liu, L.; Yilmaz, K. Estimating global bank network connectedness. *J. Appl. Econom.* **2018**, *33*, 1–15. [CrossRef]
30. Ahmad, W. On the dynamic dependence and investment performance of crude oil and clean energy stocks. *Res. Int. Bus. Financ.* **2017**, *42*, 376–389. [CrossRef]

31. Ahmad, W.; Rais, S. Time-varying spillover and the portfolio diversification implications of clean energy equity with commodities and financial assets. *Emerg. Mark. Financ. Trade* **2018**, *54*, 1837–1855. [CrossRef]
32. Sadorsky, P. Modeling renewable energy company risk. *Energy Policy* **2012**, *40*, 39–48. [CrossRef]
33. Bondia, R.; Ghosh, S.; Kanjilal, K. International crude oil prices and the stock prices of clean energy and technology companies: Evidence from non-linear cointegration tests with unknown structural breaks. *Energy* **2016**, *101*, 558–565. [CrossRef]
34. Reboredo, J.C.; Rivera-Castro, M.A.; Ugolini, A. Wavelet-based test of co-movement and causality between oil and renewable energy stock prices. *Energy Econ.* **2017**, *61*, 241–252. [CrossRef]
35. Yahşi, M.; Çanakoğlu, E.; Ağralı, S. Carbon price forecasting models based on big data analytics. *Carbon Manag.* **2019**, *10*, 175–187. [CrossRef]
36. Maghyereh, A.I.; Awartani, B.; Bouri, E. The directional volatility connectedness between crude oil and equity markets: New evidence from implied volatility indexes. *Energy Econ.* **2016**, *57*, 78–93. [CrossRef]
37. Awartani, B.; Aktham, M.; Cherif, G. The connectedness between crude oil and financial markets: Evidence from implied volatility indices. *J. Commod. Mark.* **2016**, *4*, 56–69. [CrossRef]
38. Garman, M.B.; Klass, M.J. On the estimation of security price volatilities from historical data. *J. Bus.* **1980**, pp. 67–78. [CrossRef]
39. Pesaran, H.H.; Shin, Y. Generalized impulse response analysis in linear multivariate models. *Econ. Lett.* **1998**, *58*, 17–29. [CrossRef]
40. Diebold, F.X.; Yilmaz, K. Measuring financial asset return and volatility spillovers, with application to global equity markets. *Econ. J.* **2009**, *119*, 158–171. [CrossRef]
41. Diebold, F.X.; Liu, L.; Yilmaz, K. *Commodity Connectedness*; Technical Report; National Bureau of Economic Research: Cambridge, MA, USA, 2017.
42. Polat, O. Systemic risk contagion in FX market: A frequency connectedness and network analysis. *Bull. Econ. Res.* **2019**, *71*, 585–598. [CrossRef]
43. Gupta, D.; Kamilla, U. Dynamic linkages between implied volatility indices of developed and emerging financial markets: An econometric approach. *Glob. Bus. Rev.* **2015**, *16*, 46S–57S. [CrossRef]
44. Ding, L.; Huang, Y.; Pu, X. Volatility linkage across global equity markets. *Glob. Financ. J.* **2014**, *25*, 71–89. [CrossRef]
45. Shu, H.C.; Chang, J.H. Spillovers of volatility index: Evidence from US, European, and Asian stock markets. *Appl. Econ.* **2019**, *51*, 2070–2083. [CrossRef]
46. Sarwar, G. Interrelations in market fears of US and European equity markets. *N. Am. J. Econ. Financ.* **2020**, *41*, 101136. [CrossRef]
47. Antonakakis, N.; Kizys, R. Dynamic spillovers between commodity and currency markets. *Int. Rev. Financ. Anal.* **2015**, *41*, 303–319. [CrossRef]

© 2020 by the authors. Licensee MDPI, Basel, Switzerland. This article is an open access article distributed under the terms and conditions of the Creative Commons Attribution (CC BY) license (http://creativecommons.org/licenses/by/4.0/).

Apéndice C. Forecasting Extreme Financial Risk: A Score-driven Approach

Contiene

- Correo electrónico confirmación artículo enviado a la revista
- Artículo enviado

Forecasting Extreme Financial Risk: A Score-driven Approach

October 29, 2020

Abstract

This paper develops a new class of dynamic models for forecasting extreme financial risk, driven by the score of the conditional distribution with respect to both the duration between extreme events and the magnitude of these events. This data-driven framework is a feasible method for modelling their time-varying arrival intensity, and magnitude. It is also shown how exogenous variables such as realized measures of volatility can easily be incorporated. An empirical analysis based on a set of major equity indices shows that both the arrival intensity and the size of extreme events vary greatly during times of market turmoil. The proposed framework performs well relative to competing approaches in terms of forecasting extreme tail risk measures.

JEL classification: C11; C58; G17; Q47; Q02

Keywords: Forecasting, Score-driven models, Time-varying parameters, Extreme value theory, Value at Risk, Expected Shortfall, Realized Volatility.

1 Introduction

Since the Global Financial Crisis and more recent sovereign debt crisis in several European countries, numerous new econometric approaches have been developed to quantify, model and forecast tail risk dynamics (see for instance Nieto & Ruiz 2016, Agarwal et al. 2017, Lucas et al. 2017, Chiu et al. 2017, Taylor 2019). One common approach is based on a combination of volatility models and extreme value theory (EVT), which typically consists of first estimating a conditional volatility model, followed by modeling the dynamics of the tail of the distribution through the standardized residuals obtained in the first step (e.g. McNeil & Frey 2000, Bee et al. 2016, Sahamkhadam et al. 2018, Karmakar & Paul 2019). The main shortcoming of this approach is that volatility specifications based on only past returns do not accurately capture tail risk during financial market turmoil (see Longin 2000, Bali 2000, Hong et al. 2007). Only models that contain a leverage term, irrespective of whether they are models based on daily returns (e.g., SV or GARCH) or realized measures of volatility (e.g., HAR or HEAVY) have been successful in explaining the dynamics of extreme events (see Liu & Tawn 2013, Trapin 2017). Alternative approaches that build on conditional quantile and expectile regressions have also been proposed. For instance, the CAViaR model introduced by Engle & Manganelli (2004) and the CARE approach by Taylor (2008) are examples of these methodologies. However, due to sparsity in the tails, more recent approaches (see Manganelli & Engle 2004, Yi et al. 2014, Daouia et al. 2018) incorporate refinements from EVT which improves parameter estimation and stability.

The class of score-driven models introduced by Creal et al. (2013) and Harvey (2013) have become popular in recent years in many financial applications (see Lucas & Zhang 2016, Calvori et al. 2017, Delle Monache & Petrella 2017, Gorgi et al. 2019, Bernardi & Catania 2019), mainly because these are the only models with time-varying parameters whose updating equations will always reduce the local Kullback-Leibler divergence between the true conditional density and the model-implied conditional density (Blasques et al. 2015). In the case of score-driven approaches applied to EVT, the literature is scarce. Massacci (2016) propose a score-driven Generalized

Pareto specification to model the magnitude of extreme events whose parameter dynamics are jointly updated by means of a one-factor model. Zhang & Bernd (2016) propose an alternative specification in two stage, given that the use of the one-factor model does not seem to be empirically justified. First, the data are de-volatilized and keeping the scale parameter fixed, through the score-driven approach, time-variation is introduced into the tail shape parameter of the Generalized Pareto distribution. Recently, Bee et al. (2019) propose a Peaks over Threshold (POT) approach based on realized measures obtained from intra-daily returns, including autoregressive terms by means of the score-driven framework.

We consider a completely different approach based on a novel score-driven marked point process (MPP) for extreme events, which takes into account the information provided by the timing and the magnitude of large losses occurring over a high threshold. The main advantage of using MPP modes on extreme events, is that in order to understand the tail risk behavior in financial markets, the dynamics of extreme events can be split into two conditionally independent stochastic components. One is associated with their irregularly spaced occurrence through time, and another associated with the severity of these events. Most of the recent literature on MPP related to extreme financial risk have considered the class of Hawkes processes to model the conditional intensity of extreme events exceeding a threshold, the so-called Hawkes-POT (e.g. Chavez-Demoulin & McGill 2012, Herrera & González 2014, Gresnigt et al. 2016, Herrera & Clements 2018). Unlike these models, where the parameters do not vary over time, we propose a new class of MPP models for extreme events with time-varying parameters whose dynamics are functions of the observations through the score function of the predictive density given the time and magnitude of each observed extreme event. These models will be denoted as Score-driven Peaks Over Threshold (SPOT) models.

Additionally, an extension denoted here as the realized SPOT (rSPOT) model which includes realized volatility measures (e.g., simple realized variance, realized semi variance, jumps, negative jumps) is proposed. The use of realized volatility measures has been rapidly gaining popularity, and they have been also utilized in the context of financial extreme risk in recent years

(Buncic & Gisler 2016, Yao et al. 2019, Bee et al. 2019).

The main question of interest is to what degree can the dynamic behaviour of extreme events (and hence tail risk) be explained by the two stochastic components, their occurrence times and/or their magnitudes. In addressing this issue, the question of whether there any gains from using realized measurements to produce more accurate forecasts of extreme market risk will also be addressed.

The benefits of the SPOT framework is illustrated in an empirical analysis of tail risk for a set of major world stock indices from 2000 to 2018. The estimation results confirm that using the information on the occurrence times and the magnitude of extreme events by means of the score-driven approach is helpful for describing tail risk dynamics. In particular, by decomposing the tail risk dynamics, financial crises are almost simultaneously reflected in the dynamics of both stochastic processes; the arrival times of extreme events and their associated magnitudes. In fact, both the Subprime crisis and the European debt crisis can be clearly distinguished. In addition, the dynamic parameter that best describes the behavior of the inter-exceedance times is the shape parameter of the conditional hazard function, exhibiting heavy-tailed behavior. The dynamics of the magnitudes is best described by a time varying scale parameter of the conditional probability distribution function. Further, it is observed that incorporating realized measures of volatility into the SPOT framework leads to gains in terms of goodness of fit.

Finally, the performance of the SPOT framework is examined under two measures of risk, Expected Shortfall (ES) and Value at Risk (VaR), considering two different backtesting periods. The forecast performance of the SPOT models are compared with other two competing models that utilize a score-driven approach in the context of extreme financial risk. The models proposed by Bee et al. (2019) and by Massacci (2016). The results of the out-of-sample forecasting exercise show that the SPOT specifications outperform both alternatives over one- and two year VaR backtesting periods, for most of the markets considered. In terms of a joint test of ES and VaR, the realized version of SPOT model outperforms the competing models.

The remainder of the paper is organized as follows: Section 2 the SPOT framework is intro-

duced. Section 3 provides the empirical results. Here the SPOT models are applied to a range of major equity indices and the role of realized measures is considered. Forecast comparisons are also undertaken. Section 4 provides concluding comments. Additional technical details are presented in the Appendix.

2 Methodology

2.1 Extreme Events via Marked Point Processes

Let $(\Omega, \mathcal{F}, \{\mathcal{F}_t\}, \mathbb{P})$ be a filtered probability space with respect to the right-continuos filtration $\mathcal{F}_t$. Suppose $y_t \in \mathbb{R}$ are random variables representing losses with a continuous distribution function F and upper support point of y_0 such that $\lim_{y \to y_0} F(y) = 1$. Extreme events will be defined as those observations that have exceeded some high threshold $u > 0$ previously defined. In particular, let $N(\cdot)$ be a regular Marked Point Process (MPP) with sequence of random variables $\{(t_i, z_i) : i = 1, \ldots n\}$ in a subset $A \subset \mathbb{R}_+ \times \mathbb{R}_+$ where t_i is the occurrence time of the extreme event i (with $t_i \to \infty$ almost surely when $i \to \infty$) and $z_i = y_{t_i} - u$ is its magnitude or mark for which the observation y_{t_i} exceeds the threshold u ($0 < u < y_0$) with available information set $\mathcal{F}_t = \{(t_i, z_i) : t_i < t\}$[1]. Observe that z_i is $\mathcal{F}_{t_i}-$measurable. In order to avoid ambiguity, we denote by $N(\{t\})$, the number of extreme events at time t (see Schoenberg 2006).

As is well known, the dynamics of this MPP can be completely characterized by means of its conditional intensity function

$$\lambda(t, z \mid \mathcal{F}_t)\, \mathtt{d}t\mathtt{d}z \;\approx\; E\left[N(\mathtt{d}t \times \mathtt{d}z) \mid \mathcal{F}_t\right] \approx \tau(t \mid \mathcal{F}_t)\, g(z \mid t, \mathcal{F}_t)\, \mathtt{d}t\mathtt{d}z \tag{1}$$

where $\tau(t \mid \mathcal{F}_t)$ is the conditional intensity of the occurrence of extreme events, the so-called *ground conditional intensity* while $g(z \mid t, \mathcal{F}_t)$ corresponds to the density probability function of

[1]This method is commonly known as the Peaks over Threshold (POT) approach (see Smith 1989, Davison & Smith 1990).

the exceedances, the so-called *marks*. Note that we are assuming that $N(\cdot)$ has separable conditional intensity following the terminology of Daley & Vere-Jones (2003)[2]. Thus, the contribution to the log-likelihood of extreme event i, related to the conditional intensity (1), is given by

$$\mathcal{L}(t_i, z_i \mid \mathcal{F}_t) = \ln \tau(t_i \mid \mathcal{F}_t) - \int_{t_{i-1}}^{t_i} \tau(s \mid \mathcal{F}_s)\, ds + \ln g(z_i \mid t_i, \mathcal{F}_t). \tag{2}$$

In the empirical section we will analyze daily observations of stock markets returns, and therefore, extreme observations will occur at discrete points in time. Thus, the construction of the SPOT approach begins with the specification of a discrete-time version for the conditional intensity function defined in (1).

2.2 The Score-driven Peaks Over Threshold (SPOT) framework

In this section we develop the class of SPOT models. The key quantities of interest are a bivariate vector of unobserved time-varying parameters f_i^τ and f_i^g, and information sets $T^i = \{t_1, \ldots, t_i\}$, $Z^i = \{z_1, \ldots, z_i\}$, $F_\tau^i = \{f_1^\tau, \ldots, f_i^\tau\}$ and $F_g^i = \{f_1^g, \ldots, f_i^g\}$ for $i = 1, \ldots n$ capturing all the dynamic features of the occurrence of, and magnitude related to the extreme events.

Let $\mathcal{F}_i^\tau = \{T^{i-1}, F_\tau^{i-1}\}$ and $\mathcal{F}_i^g = \left\{Z^{i-1}, F_g^{i-1}\right\}$ be the information set generated by the daily extreme returns with $\mathcal{F}_i = \mathcal{F}_i^\tau \cup \mathcal{F}_i^g$, with $\mathcal{F}_i \subseteq \mathcal{F}_t$. The conditional intensity of the SPOT model is governed by the following observation-driven specification

$$\lambda(t_i, z_i \mid \mathcal{F}_i, \boldsymbol{f}_i; \boldsymbol{\Theta}) = \tau(t_i \mid \mathcal{F}_i^\tau, f_i^\tau; \theta^\tau)\, g(z_i \mid t_i, \mathcal{F}_i^g, f_i^g; \theta^g). \tag{3}$$

Here, the ground conditional intensity is defined by means of conditional hazard functions $h(\cdot)$ as follows

$$\tau(t_i \mid \mathcal{F}_i^\tau, f_i^\tau; \theta^\tau) = \; h(t_i - t_{i-1} \mid \mathcal{F}_i^\tau, f_i^\tau; \theta^\tau) \quad i \geq 2, \tag{4}$$

[2]See Definition 7.3.II

where $h(t_1)$ is the conditional hazard function for the occurrence time of the first extreme event, $h(t_2 - t_1 \mid \mathcal{F}_2^\tau, f_2^\tau; \theta^\tau)$ the hazard function for the occurrence time of the second extreme event, conditioned by the occurrence time of the first extreme event and so on[3]. In the case of the process for the marks, as usual in EVT, they are assumed to follow a generalized Pareto distribution[4]. Moreover, $\boldsymbol{f}_i := \{(f_i^\tau, f_i^g)\} \in \mathbb{R} \times \mathbb{R}$ denotes a bivariate vector of time-varying parameters and $\boldsymbol{\Theta} := \{(\theta^\tau, \theta^g)\}$ a vector of static parameters[5]. Consequently, the log-likelihood introduced in (2) can now be written as the sum of two terms

$$\mathcal{L}(t_i, z_i \mid \mathcal{F}_i, \boldsymbol{f}_i; \boldsymbol{\Theta}) = \mathcal{L}_\tau(t_i \mid \mathcal{F}_i^\tau, f_i^\tau; \theta^\tau) + \mathcal{L}_g(z_i \mid t_i, \mathcal{F}_i^g, f_i^g; \theta^g),$$

where

$$\mathcal{L}_\tau(t_i \mid \mathcal{F}_i^\tau, f_i^\tau; \theta^\tau) = \ln \tau(t_i \mid \mathcal{F}_i^\tau, f_i^\tau; \theta^\tau) - \int_{t_{i-1}}^{t_i} \tau\left(s \mid \mathcal{F}_{N(\{s\})}^\tau, f_{N(\{s\})}^\tau; \theta^\tau\right) ds \tag{5}$$

and

$$\mathcal{L}_g(z_i \mid t_i, \mathcal{F}_i^g, f_i^g; \theta^g) = \ln g(z_i \mid t_i, \mathcal{F}_i^g, f_i^g; \theta^g). \tag{6}$$

The formal demonstration that the SPOT formulation in (3) and the standard MPP approach in (1) share identical likelihood functions follows the same arguments of the Autorregresive Conditional Hazard model, which is a discrete version of the Autoregressive Conditional Duration model (see the appendix in Hamilton & Jordà 2002). We provide a discussion about the connection between the both log-likelihood functions in Appendix A.1.

The specifications for the time-varying parameters in (3) are based on the score-driven approach proposed by Harvey (2013) and Creal et al. (2013) in terms of a scaled score of the

[3]For further discussion and examples of processes defined through their conditional intensity function see Definition 7.3.II in

[4]This result is consequence of the Pickages-Balked-de Haaf theorem (see Balkema & De Haan 1974, Pickands 1975), which essentially states that the generalized Pareto distribution is the limit distribution of scaled losses over a high threshold $u > 0$, for a wide class of distributions used in empirical finance.

[5]There is considerable computational complexity if we allow all parameters to vary simultaneously. For this reason, a parsimonious way of capturing the behavior of both stochastic processes is to allow only one time-varying parameter in the conditional intensity process and another in the process for the marks.

conditional probability density of the occurrence time t_i and the size of the marks z_i of the event i, respectively. That is

$$f_{i+1}^{\tau} = \omega_{\tau} + \phi_{\tau} f_i^{\tau} + \psi_{\tau} s_i^{\tau} \tag{7}$$

where $\{(\omega_{\tau}, \phi_{\tau}, \psi_{\tau})\} \subseteq \theta^{\tau}$ are (unknown) unrestricted coefficients , $s_i^{\tau} = S_{\tau i} \nabla_{\tau i}$ is the scaled score of the observed probability density function of the occurrence times of the extreme event i with

$$\begin{aligned} \nabla_{\tau i} = \frac{\partial \mathcal{L}\left(t_i, z_i \mid \mathcal{F}_i, \boldsymbol{f}_i; \boldsymbol{\Theta}\right)}{\partial f_i^{\tau}} &= \frac{\partial \mathcal{L}_{\tau}\left(t_i \mid \mathcal{F}_i^{\tau}, f_i^{\tau}; \theta^{\tau}\right)}{\partial f_i^{\tau}} \\ &= \frac{\partial}{\partial f_i^{\tau}} \left\{ \ln \tau\left(t_i \mid \mathcal{F}_i^{\tau}, f_i^{\tau}; \theta^{\tau}\right) - \int_{t_{i-1}}^{t_i} \tau\left(s \mid \mathcal{F}_{N(\{s\})}^{\tau}, f_{N(\{s\})}^{\tau}; \theta^{\tau}\right) ds \right\} \end{aligned}$$

and scaling function given by the inverse conditional Fisher information $S_{\tau i} = E\left[\nabla_{\tau i}^2 \mid \mathcal{F}_i^{\tau}\right]^{-1}$. Likewise, the dynamics of the time varying parameter f_i^g is given by

$$f_{i+1}^{g} = \omega_g + \phi_g f_i^g + \psi_g s_i^g, \tag{8}$$

where $\{(\omega_g, \phi_g, \psi_g)\} \subseteq \theta^g$ are again unrestricted coefficients, $s_i^g = S_{gi} \nabla_{gi}$ is the scaled score of the observed probability density function of the size of the extreme event i with scaling function $S_{gi} = E\left[\nabla_{gi}^2 \mid \mathcal{F}_i^g\right]^{-1}$ and score

$$\begin{aligned} \nabla_{gi} = \frac{\mathcal{L}\left(t_i, z_i \mid \mathcal{F}_i, \boldsymbol{f}_i; \boldsymbol{\Theta}\right)}{\partial f_i^g} &= \frac{\mathcal{L}_g\left(z_i \mid t_i, \mathcal{F}_i^g, f_i^g; \theta^g\right)}{\partial f_i^g} \\ &= \frac{\partial \ln g\left(z_i \mid t_i, \mathcal{F}_i^g, f_i^g; \theta^g\right)}{\partial f_i^g}. \end{aligned}$$

It is clear that the scaled score of the likelihood function is the key mechanism underpinning the dynamics of the parameters. An important advantage of this approach is its flexibility to include other informative measures associated with extreme events in (7) and (8), for example in the context of financial risk, a generic realized or implied measure of volatility.

2.2.1 Different SPOT specifications

To summarise the different possible structures within the SPOT framework, Table 1 reports which parameters, shapes or scales, of the different hazard and density functions are time-varying. Four types of (non)-monotonic hazard functions are employed: Weibull (W), gamma (G), Burr (B) and generalized gamma (GG) , while for the marks, the generalized Pareto distribution is used. In addition to each of these specifications, the score of the likelihood function and the scaling function utilized to update the parameters over time are provided. The following notation scheme for the SPOT models will be used. The first upper-case letter describes the type of hazard function utilized, the following two lower-case letters denote the time varying parameters (scale: s or shape: p) in the conditional ground intensity and the density function of the marks, respectively. In the case that we decide to work with a hazard function with two or more shape parameters, then a subindex with a number will also be included. For instance, foreshadowing the empirical results in Section 3, we find that a SPOT specification with Burr (B) conditional hazard function with time-varying shape (p_1) parameter and dynamic scale (s) parameter for the conditional density function of the marks, denoted as the Bp_1s-SPOT specification, provides the best fit in terms of AIC and BIC for most of the stock markets analyzed. All combinations are shown in Table 1 where the time varying parameters in either the hazard or the distribution for the marks, governed by equations 7 and 8 are highlighted.

2.2.2 A toy example: the Weibull SPOT approach

In order to highlight the rich structure of this framework, consider a SPOT specification whose conditional ground intensity is driven by the scale (s) parameter δ_i of a Weibull (W) hazard function, while for the dynamics of the marks the usual assumption of the conditional Generalized Pareto density on its scale (s) parameter β_i is utilized. This specification is denoted as the Wss-SPOT approach. The ground conditional intensity in this case is given by

Ground Intensity					
Specification	hazard function	$\exp(f_i^\tau)$	$\nabla_{\tau i}$	$S_{\tau i}$	Notation
Weibull	$\frac{k}{\delta}\left(\frac{t_i-t_{i-1}}{\delta}\right)^{k-1}$	δ_i	$k\left(\frac{t_i-t_{i-1}}{\delta_i}\right)^{k}-k$	$\frac{1}{k^2}$	Ws
		k_i	$k_i \ln\left(\frac{t_i-t_{i-1}}{\delta}\right)\left[1-\left(\frac{t_i-t_{i-1}}{\delta}\right)^{k_i}\right]+1$	$\frac{6}{6(\gamma-1)^2+\pi^2}$	Wp
Burr	$\frac{\frac{kb}{\delta}\left(\frac{t_i-t_{i-1}}{\delta}\right)^{b-1}}{1+\left(\frac{t_i-t_{i-1}}{\delta}\right)^{b}}$	δ_i	$b\left(\frac{t_i-t_{i-1}}{\delta_i}\right)^{b}\left[\frac{k+1}{1+\left(\frac{t_i-t_{i-1}}{\delta_i}\right)^{-b}}-1\right]$	$\frac{k+2}{b^2k}$	Bs
		k_i	$1-k_i \ln\left[\left(\frac{t_i-t_{i-1}}{\delta}\right)^{b}+1\right]$	1	Bp_1
		b_i	$1+b_i \ln\left(\frac{t_i-t_{i-1}}{\delta}\right)\left[1-\frac{k+1}{1+\left(\frac{t_i-t_{i-1}}{\delta}\right)^{-b_i}}\left(\frac{t_i-t_{i-1}}{\delta}\right)^{b_i}\right]$	$\frac{k+2}{\Upsilon}$	Bp_2
Gamma	$\frac{(t_i-t_{i-1})^{k-1}}{\delta^k\Gamma\left(k,\frac{t_i-t_{i-1}}{\delta}\right)}\exp\left\{-\frac{t_i-t_{i-1}}{\delta}\right\}$	δ_i	$\frac{t_i-t_{i-1}}{\delta_i}-k$	$\frac{1}{k}$	Gs
		k_i	$k_i \ln\left(\frac{t_i-t_{i-1}}{\delta}\right)-k_i\psi^{(0,k_i)}$	$\frac{1}{k_i^2\psi^{(1,k_i)}}$	Gp
G.Gamma	$\frac{\frac{b}{\delta}\left(\frac{t_i-t_{i-1}}{\delta}\right)^{bk-1}}{\Gamma\left(k,\left(\frac{t_i-t_{i-1}}{\delta}\right)^{b}\right)}\exp\left\{-\left(\frac{t_i-t_{i-1}}{\delta}\right)^{b}\right\}$	δ_i	$b\left(\frac{t_i-t_{i-1}}{\delta_i}\right)^{b}-bk$	$\frac{1}{b^2k}$	Gss
		k_i	$k_i b \ln\left(\frac{t_i-t_{i-1}}{\delta}\right)-k_i\psi^{(0,k_i)}$	$\frac{1}{k_i^2\psi^{(1,k_i)}}$	GGp_1
		b_i	$1+b_i \ln\left(\frac{t_i-t_{i-1}}{\delta}\right)\left[k-\left(\frac{t_i-t_{i-1}}{\delta}\right)^{b_i}\right]$	$\frac{1}{1+\psi^{(0,k)}\left(2+k\psi^{(0,k)}\right)+k\psi^{(1,k)}}$	GGp_2
Mark process					
Specification	density function	$\exp(f_i^g)$	∇_{gi}	S_{gi}	Notation
Generalized Pareto	$\frac{1}{\beta_i}\left(1+\xi\frac{z_i}{\beta_i}\right)^{-\frac{1}{\xi}-1}$	β_i	$\frac{z_i-\beta_i}{\xi z_i+\beta_i}$	$2\xi+1$	$s-$SPOT
		ξ_i	$\frac{\ln\left(\frac{\xi_i z_i}{\beta}+1\right)}{\xi_i}-\frac{z_i\xi_i+z_i}{z_i\xi_i+\beta}$	$\frac{(2\xi_i+1)(\xi_i+1)}{2\xi_i^2}$	p-SPOT

Table 1: Description of the SPOT specifications. We introduce four hazard functions for the ground conditional intensity (Weibull, Burr, gamma, generalized gamma) and one density probability function for the marks (Generalized Pareto). The columns with symbols $\exp(f_i^\tau)$ and $\exp(f_i^g)$ indicate the time-varying parameters in the ground conditional intensity and the density function of the marks, respectively. In the same way $\nabla_{\tau i}$,∇_{gi} and $S_{\tau i}$,S_{gi} correspond to the score functions and scale functions utilized in both processes for each score-driven specification. The parameter Υ is defined as $\Upsilon = 2\gamma+(\gamma-1)^2k+\frac{\pi^2k}{6}+k\psi^{(1,k)}+\psi^{(0,k)}\left(2+2k(\gamma-1)+k\psi^{(0,k)}\right)$, where $\psi^{(m,k)}=\psi^{(m)}(k)$ is the polygamma function of order m, while γ is the Euler–Mascheroni constant.

$$\tau\left(t_i \mid \mathcal{F}_i^\tau, f_i^\tau; k\right) = \exp\left(f_i^\tau\right)^k k\left(t_i - t_{i-1}\right)^{k-1},$$

where $k > 0$ is a shape parameter and $\delta_i = \exp\left(f_i^\tau\right)$ is the time varying scale parameter. Similarly, the conditional Pareto density function of the mark z_i conditional on its scale parameter $\beta_i = \exp\left(f_i^g\right)$ is defined as follows

$$g\left(z_i \mid \mathcal{F}_i^g, t_i, f_i^g; \xi\right) = \frac{1}{\exp\left(f_i^g\right)}\left(1 + \xi\frac{z_i}{\exp\left(f_i^g\right)}\right)^{-\frac{1}{\xi}-1},$$

where $\xi > 0$ is the shape parameter. This leads to the following Wss-SPOT specification

$$\lambda\left(t_i, z_i \mid \mathcal{F}_i, \boldsymbol{f}_i; \boldsymbol{\Theta}\right) = \frac{\exp\left(f_i^\tau\right)^k k\left(t_i - t_{i-1}\right)^{k-1}}{\exp\left(f_i^g\right)}\left(1 + \xi\frac{z_i}{\exp\left(f_i^g\right)}\right)^{-\frac{1}{\xi}-1}, \tag{9}$$

where $\boldsymbol{\Theta} := \{(\theta^\tau, \theta^g)\}$ is a vector of static parameters with $\theta^\tau := \{k, \omega_\tau, \phi_\tau, \psi_\tau\}$ and $\theta^g := \{\xi, \omega_g, \phi_g, \psi_g\}$. The dynamics of both scale parameters are linked to the score and are described in the following proposition.

Proposition 1. *For the Wss-SPOT with conditional intensity (9) the scaled scores becomes*

$$s_i^\tau = \frac{1}{k}\left\{\left(\frac{t_i - t_{i-1}}{\exp\left(f_i^\tau\right)}\right)^k - 1\right\} \quad \textit{and} \quad s_i^g = \frac{\left(z_i - \exp\left(f_i^g\right)\right)(2\xi + 1)}{\exp\left(f_i^g\right) + \xi z_i},$$

where $f_i^\tau = \ln\delta_i$ *and* $f_i^g = \ln\beta_i$.

Proofs of all propositions are provided in the Appendix A.2.

In both cases, under the correct model specification, the condition $\phi < 1$ is required to ensure that f_i is mean-reverting around its long-term mean value $\omega^{-1}(1-\phi)$ due to the fact that s_i is a martingale difference[6]. Alternatively, it is also possible to work with a specification with dynamic shape (p) parameters instead, the resulting time varying Weibull shape-shape SPOT

[6]However, explicit conditions for stationarity and ergodicity for this class of processes are much more involved and beyond the scope of this paper. For instance, the variance of s_i can be unbounded, and therefore, precise conditions have to be imposed for stability. For more details and discussion see Blasques et al. (2014).

model (Wpp-SPOT) would be

$$\lambda\left(t_i, z_i \mid \mathcal{F}_i, \boldsymbol{f}_i; \boldsymbol{\Theta}\right) = \frac{\delta^{\exp\left(f_i^\tau\right)} \exp\left(f_i^\tau\right) \left(t_i - t_{i-1}\right)^{\exp\left(f_i^\tau\right)-1}}{\beta} \left(1 + \exp\left(f_i^g\right) \frac{z_i}{\beta}\right)^{-\frac{1}{\exp\left(f_i^g\right)}-1}, \tag{10}$$

where $\boldsymbol{f}_i := \{(f_i^\tau, f_i^g)\} = \{(\ln k_i, \ln \xi_i)\}$ and $\boldsymbol{\Theta} := \{(\theta^\tau, \theta^g)\}$ with $\theta^\tau := \{\delta, \omega_\tau, \phi_\tau, \psi_\tau\}$ and $\theta^g := \{\beta, \omega_g, \phi_g, \psi_g\}$, leading to the following result.

Proposition 2. *For the Wpp-SPOT conditional intensity (10) the scaled scores are given by*

$$s_i^\tau = \nu + \nu \exp\left(f_i^\tau\right) \left(1 - \left(\frac{t_i - t_{i-1}}{\delta}\right)^{\exp\left(f_i^\tau\right)}\right) \ln\left(\frac{t_i - t_{i-1}}{\delta}\right) \quad \textit{where} \quad \nu = \frac{1}{(\gamma - 1)^2 + \pi^2/6},$$

γ is the Euler-Mascheroni constant and

$$s_i^g = \frac{\left(2\exp\left(f_i^g\right) + 1\right)\left(\exp\left(f_i^g\right) + 1\right)}{2\exp\left(2f_i^g\right)} \left\{\frac{\ln\left(z_i \exp\left(f_i^g\right)\beta^{-1} + 1\right)}{\exp\left(f_i^g\right)} - \frac{z_i\left(\exp\left(f_i^g\right) + 1\right)}{z_i \exp\left(f_i^g\right) + \beta}\right\},$$

where $f_i^\tau = \ln k_i$ and $f_i^g = \ln \xi_i$ define the time varying shape parameters.

It is also possible to specify a scale-shape (sp) or shape-scale (ps) SPOT model, or assume a different distributional assumption for the ground intensity, which demonstrates the flexibility of the proposed approach.

Furthermore, under the SPOT framework it is possible to compute conditional risk measures that are not restricted to a particular model specification. As the functional form for either the hazard, or the marks changes, it is possible to always directly obtain conditional risk measures. The next theorem gives the expressions for the VaR and ES explicitly for the Wss-SPOT model. Similar results can be obtained under others specifications.

Proposition 3. *For the Wss-SPOT specification (9) the VaR and ES, at the confidence level α, are given in closed form by the following expressions:*

$$VaR_{\alpha}\left(t_i, z_i \mid \mathcal{F}_i, \boldsymbol{f}_i; \boldsymbol{\Theta}\right) = \frac{\xi u + \exp\left(f_i^g\right)}{\xi}\left\{\left(\frac{\exp\left(f_i^{\tau}\right)^k k\left(t_i - t_{i-1}\right)^{k-1}}{1-\alpha}\right)^{\xi} - 1\right\}$$

and

$$ES_{\alpha}\left(t_i, z_i \mathcal{F}_i, \boldsymbol{f}_i; \boldsymbol{\Theta}\right) = \frac{VaR_{\alpha}\left(t_i, z_i \mid \mathcal{F}_i, \boldsymbol{f}_i; \boldsymbol{\Theta}\right) + \exp\left(f_i^g\right) - u\xi}{(1-\xi)}$$

where $\boldsymbol{f}_i := \{(f_i^{\tau}, f_i^g)\}$ *and* $\boldsymbol{\Theta} := \{(\theta^{\tau}, \theta^g)\}$ *with* $\theta^{\tau} := \{k, \omega_{\tau}, \phi_{\tau}, \psi_{\tau}\}$ *and* $\theta^g := \{\xi, \omega_g, \phi_g, \psi_g\}$.

Proof is provided in the Appendix A.2.

3 Tail Risk Dynamics in Major Stock Market Indices

We illustrate the benefit of the SPOT framework by applying the models to daily negative log-returns of ten well known world stock market indices.

3.1 Data Description

The sample spans January 3, 2000 to December 27, 2018, which is divided into an in-sample period from January 3, 2000 to December 29, 2016; and a backtesting period from January 4, 2017 until December 27, 2018.[7] Table 2 reports the descriptive statistics for each one of the indices. For each index, the common stylized facts, such as asymmetry and heavy tails are observed. In addition, the Jarque-Bera and Box-Pierce tests show that the returns are not normally distributed and auto-correlation is present in the returns.

Threshold selection is a critical issue in order to determine which observations should be considered extremes. In practice, it involves a trade-off between bias and variance. This means that the lower the threshold, the higher the bias of the estimates due to model misspecification,

[7]The data were obtained from the Oxford-Man Institute database "Realized Library" version 0.3.

while a high threshold increases the variance of parameter estimates. A comprehensive review of the literature that considers threshold selection in the context of EVT can be found in Scarrott & MacDonald (2012). However, most studies in empirical finance have shown that a threshold of about the 90th quantile of the distribution of negative returns is a reasonable choice with typically little impact on the model estimation (e.g., Chavez-Demoulin & McGill 2012, Bee et al. 2019, Hautsch & Herrera 2020). We proceed similarly and set a threshold at the 90th quantile.

3.2 Preliminary Estimates of Tail Risk Dynamics

As a starting point, a detailed comparison of all SPOT model specifications using only the DAX returns is presented. The first important question is to determine the preferred hazard function and whether a scale-scale, scale-shape, shape-scale, or shape-shape-SPOT specification is more suitable to model the dynamic behavior of extreme events. Table 3 presents the estimation results. Overall, the parameter estimates indicate that in all specifications, the time varying parameters of the ground conditional intensity, and the density of the marks are both persistent (ϕ_τ and ϕ_g are close to but less than 1). According to AIC and BIC, the Bp_1s-SPOT (shape-scale) specification provides the best fit for the DAX returns.

A complete analysis using all specifications was also applied to all stock markets[8]. Overall, the Bp_1s-SPOT specification also provides the most suitable fit among all markets considered. Table 4 displays the parameter estimates for Bp_1s-SPOT specification for all stock markets. It is evident that the estimates are remarkably similar across all of the indices. Strong persistence in the autoregressive process is observed for the ground conditional intensity, characterized by the ϕ_τ estimates being over 0.8. In the case of the process of the marks, this persistence is not quite so strong with values ψ_g around 0.65 for most of the markets.

In the case of the Burr distribution, both shape parameters are directly related to the tail index of the distribution, which is an important measure to gauge the heavy-tailed nature of

[8]These results can be obtained from the authors upon request.

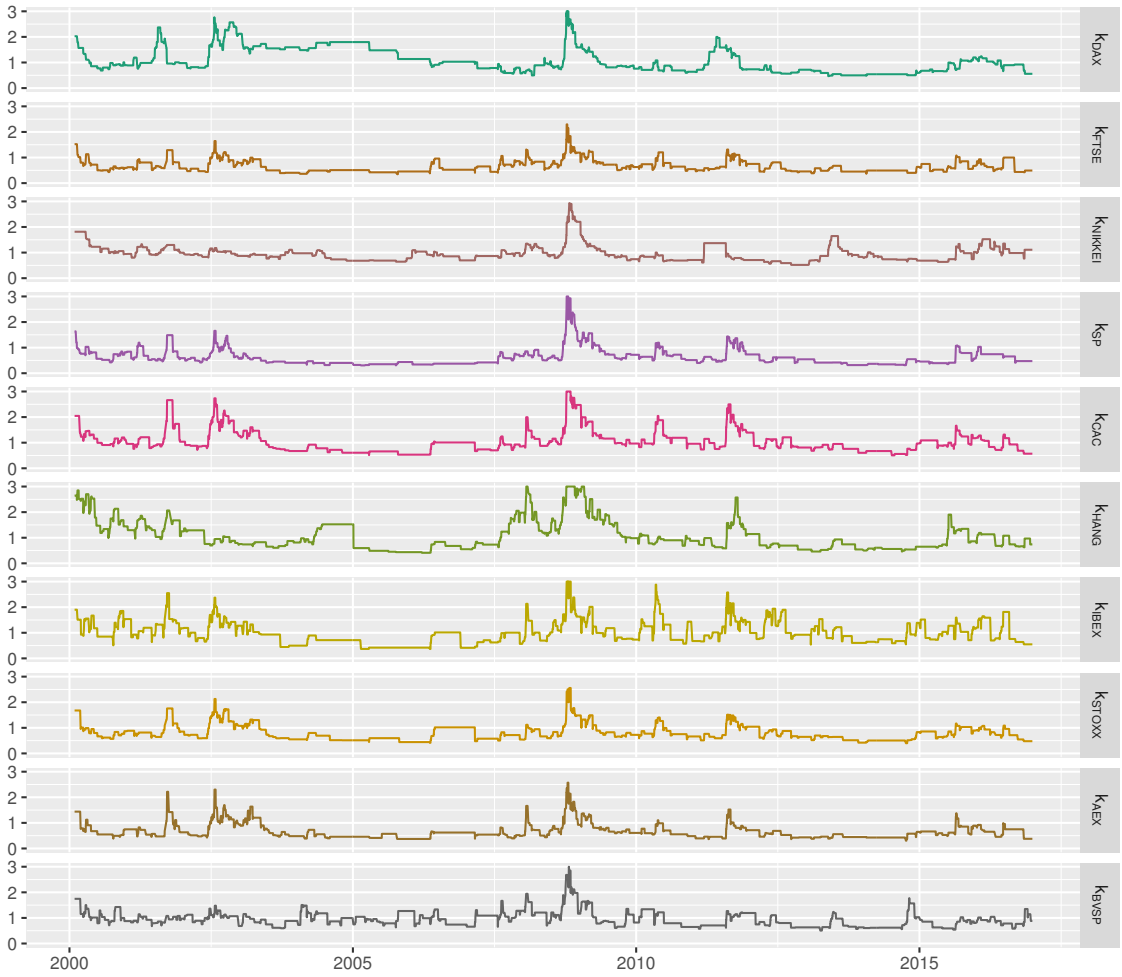

Figure 1: From top to bottom the time-varying shape parameter k_i of the ground conditional intensity of the point process of exceedances for a set of world major stock market indices over the In-sample period January 3, 2000 until December 29, 2016.

a distribution, given that it restricts the number of finite moments[9]. Across all markets, the tail distribution of the inter-exceedance times is heavy-tailed, with tail indices higher than one, implying that only a finite first moment exists. Therefore, it is clear that a typical risk measure based on the tail distribution of the inter-exceedance times, such as the variance or the standard deviation, may not exist.

Figures 1 and 2 provide additional evidence regarding the behavior of extreme events across

[9]In the case of the Burr distribution the tail index parameter corresponds to bk_i.

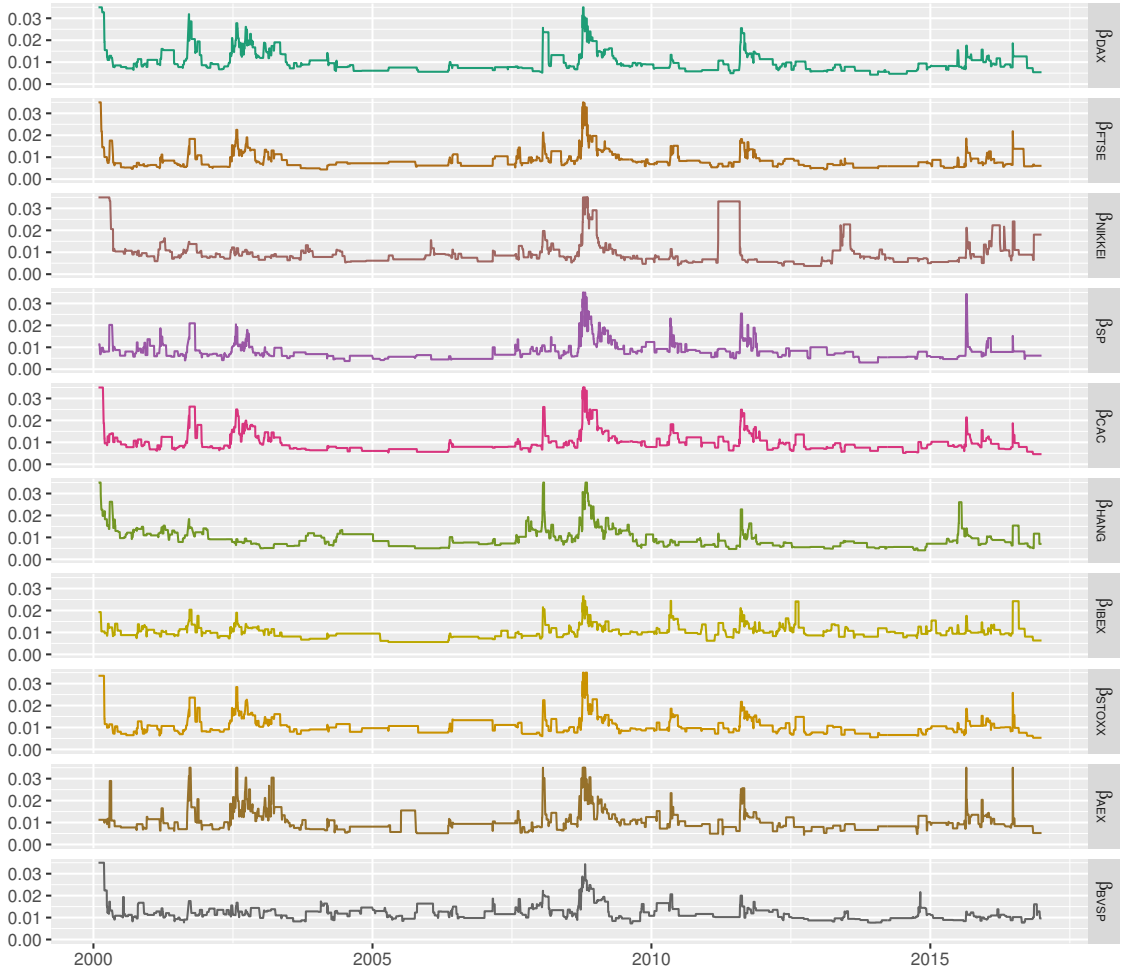

Figure 2: From top to bottom the time-varying scale parameter β_i of the generalized Pareto density function of the marks of the point process of exceedances for a set of world major stock market indexes over the In-sample period January 3, 2000 until December 29, 2016.

time as captured by the time varying shape k_i and scale β_i parameters, of the ground conditional intensity and the conditional density function of the marks, respectively. In fact, they illustrate two key aspects of the behavior of extreme returns: (i) clustering behavior during periods of turmoil as evidenced by increases in the shape parameter implying lower expected inter-exceedance times and (ii) the comovement effects among financial markets, which are almost simultaneously reflected in both stochastic processes. In fact, the recent subprime crisis and European debt crisis can be clearly distinguished in both figures, although with a very smooth dynamic. An erratic be-

havior could be a sign of model misspecification, as it might indicate that the conditional density is not sufficiently heavy-tailed. We return to this discussion in more detail in subsection 3.4.2.

3.3 Realized measures and extreme events

The SPOT framework can be extended in a number of ways. Most importantly, it is possible to include exogenous covariates in the updating equation of the score-driven parameters f_i^τ and f_i^g to help explain the dynamics of extreme events. High-frequency based realized measures are now widely available and have been used for modeling and forecasting future tail risk. For instance, Bee et al. (2016) proposed the RPOT model including the realized volatility in the classic POT approach, while Bee et al. (2018) used realized measures in the conditional extreme value theory framework proposing the Realized Extreme Quantile (REQ) approach, combining quantile regression with realized measures of volatility to forecast extreme quantiles. It is argued that there is a strong link between the dynamics of extreme events and the daily variance.

Existing models that combine MPP and EVT have just typically only employed the history of the process to capture the dynamics of the extreme events. So far, the information contained in realized measures has not been exploited. This work contributes to the recent literature on realized EVT models by considering SPOT specifications whose dynamics are not only driven by the score, but also by realized volatility measures. These measures are included in the updating equations (7) and (8) of the score-driven parameters f_i^τ and f_i^g, associated to the ground conditional intensity and the conditional Pareto density function of the marks, respectively. Models within this framework are denoted as realized SPOT (rSPOT) models and the influence of the realized measures in the updating equations for both processes are captured by the coefficients θ_τ and θ_g. The updating equations (7) and (8) are now replaced by:

$$\begin{aligned} f_{i+1}^\tau &= \omega_\tau + \phi_\tau f_i^\tau + \psi_\tau s_i^\tau + \varsigma_\tau RM_i^\tau \\ f_{i+1}^g &= \omega_g + \phi_g f_i^g + \psi_g s_i^g + \varsigma_g RM_i^g \end{aligned}$$

where RM_i^{τ} and RM_i^{g} are the realized measure utilized, which can be the same.

To illustrate the rSPOT models, four realized measures of volatility are considered, including realized variance, realized semi variance, jumps and negative jumps (e.g. Andersen & Bollerslev 1998, Barndorff-Nielsen & Shephard 2002, Andersen et al. 2005, Corsi 2009, Andersen et al. 2011, Corsi et al. 2013, Gorgi et al. 2018). With the exception of the jump measures, the others are included in logarithmic form. Table 5 presents the results of the estimates when the realized measures are included in the Bp_1s-SPOT. It can be seen that incorporating any of these measures of volatility into the standard model leads to improvements in the log-likelihood. These results are consistent with the existing literature, which demonstrates that there is a relationship between extreme events and the volatility of returns (Bali & Weinbaum 2007, Trapin 2017, Fuentes et al. 2018, Herrera & Clements 2018). Among the four realized measures of volatility, the simple realized variance is preferred, and only in the case of CAC 40 and AEX markets better results are obtained utilizing the realized semi variance. In the case of the autoregressive parameters, ϕ_τ and ϕ_g, are less persistent, a similar result to empirical results found in the existing literature in volatility models including realized measures (see Engle & Gallo 2006, Brownlees & Gallo 2009, Hansen et al. 2012, Noureldin et al. 2012).

3.4 Forecasting extreme tail risk

The Basel III standards have been a major international development since the Global Financial Crisis between 2007 and 2009. One of the most important changes is the adoption of the risk measure Expected Shortfall (ES) over the commonly used Value at Risk (VaR), mainly due to its ability to capture tail risk. This ability is intimately linked to its fundamental properties of being a coherent and comonotonically additive risk measure. As shown by Gneiting (2011) ES is not an elicitable risk measure[10], which is necessary in comparative backtesting procedures. However, a recent result from Fissler & Ziegel (2016) shows that ES jointly elicitable with VaR.

In this section, the out-of-sample predictive accuracy of the SPOT framework and its realized

[10]That simply means that there is no strictly consistent scoring function that elicits ES

version are examined in the context of forecasting VaR and ES. The Bp_1s-SPOT models, denoted below as simply SPOT for ease of notation, are compared to other two alternatives that utilize a score-driven approach in the context of extreme financial risk.

The first model, proposed by Bee et al. (2019), combines a Logit specification for the occurrence times and a GPD for the magnitude of the extreme events whose parameter dynamic is captured by means of a score-driven approach which includes realized measures. This specificaction is denoted as the BPOT model. The second model introduced by Massacci (2016) also utilizes also a GPD specification for modelling the conditional cumulative distribution function of magnitudes and a power law for the conditional probability of an exceedance, denoted here as the MPOT specification. Additionally, we also consider realized versions of these two alternatives (rBPOT and rMPOT), by incorporating realized measures of the daily asset price variation obtained from high-frequency data into their dynamic processes. A short description of both models can be found in the Appendix A.3. The major difference between the two alternatives and the SPOT specification is the way in which the dynamics of the occurrence of extreme events is incorporated. On the one hand, the SPOT framework is a natural dynamic extension to the standard POT approach, where only the information contained during the occurrence of extreme events is considered to build the conditional intensity function, which takes positive values but not restricted to be less than one, as in the other two alternatives. In addition, in both alternatives the observations that are below the threshold are also used in the log-likelihood function during the estimation, which under misspecification could provide a poor fit since most of the observations correspond to this subset of the sample.

3.4.1 Accuracy of VaR predictions

The estimation results of the rSPOT model in Table 5 are used here, and held fixed throughout the out-of-sample VaR forecast period. Table 6,7, and 8 reports the results of the accuracy for this risk measures for one (only 2017) and two (from 2017 to 2018) year out-of-sample periods across a range of confidence levels α: 0.95, 0.975, 0.99 and 0.999. The column labeled *Exc.* represents

the number of VaR exceptions, while the next columns report the results for a set of widely used statistical tests in order to determine the accuracy of the VaR. These tests are the likelihood ratio unconditional coverage test (LR_{uc}), which examines whether the proportion of VaR exceptions differ from its expected value at a given confidence level α. The second test is known as the Markov test of independence (LR_{ind}) that tests the independence property of VaR exceptions. The third statistic is a joint likelihood ratio test of conditional coverage (LR_{cc}), which performs simultaneously the independence and coverage tests (see Kupiec 1995, Christoffersen 1998). To ensure our results are robust to the choice of evaluation criteria, we also apply another powerful range of likelihood ratio tests introduced by Ziggel et al. (2014), whose main advantage is that all critical values are obtained utilizing Monte Carlo simulations increasing their power. These tests are the unconditional coverage test (MCS_{uc}), a new test of independent and identically distributed VaR exceptions (MCS_{iid}), and a test of conditional coverage (MCS_{cc}), where the abbreviation MCS is because critical values of the test statistic are computed via Monte Carlo simulations. Finally, as an overall goodness-of-fit test we utilize the dynamic quantile hit (DQ_{hit}) and dynamic quantile VaR (DQ_{VaR}) tests proposed by Engle & Manganelli (2004). Details on the implementation of these tests can be found in (e.g. Christoffersen 1998, Engle & Manganelli 2004, Ziggel et al. 2014).

In the case of the SPOT specification, it is found that specifications including information of realized measures outperform the alternative in out-of-sample forecasting for most of the markets considered. However, for the other two competing models it is not true. For the two years backtesting period, it is observed that the best results in terms of VaR accuracy (in terms of fewest test rejections) are obtained from the rSPOT specification, followed by the SPOT and the BPOT specifications. In the one year backtesting period, all models improves somewhat and exhibits similar results relative to those from the two years backtesting period. We notice that both realized versions of our competing models tend to overestimate the VaR for the sample period, and therefore, the unconditional coverage tests LR_{uc} reject the null hypothesis that the proportion of VaR exceptions are equal to the confidence level α. This result could be a sign that

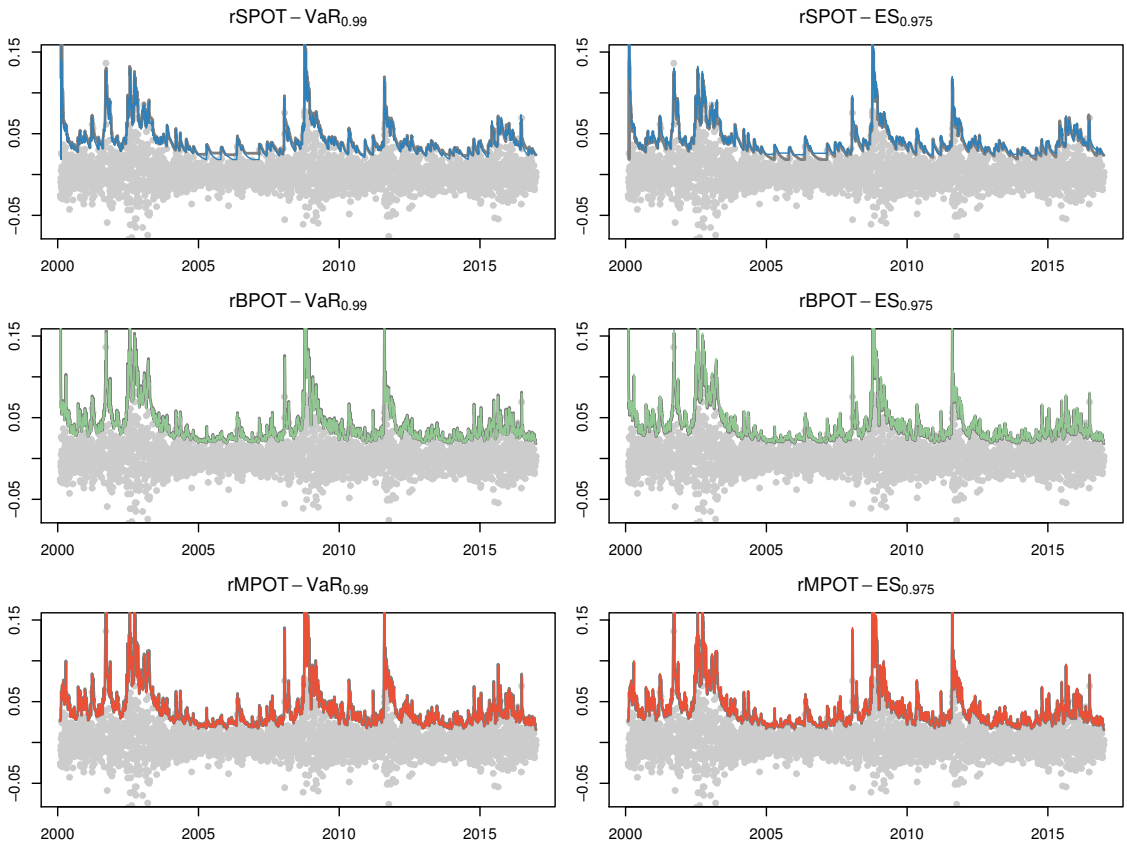

Figure 3: VaR and ES in-sample for the DAX negative log-returns over the period from January 3, 2000 until December 29, 2016. Left panel: estimated 99% -VaR for the rSPOT model (left panel-blue line), rBPOT model (left panel-green line) and rMPOT model (left panel-red line). Right panel: estimated 97.5% -ES for the rSPOT model (right panel-blue line), rBPOT model (right panel-green line) and rMPOT model (right panel-red line). Thick gray line in each plot indicates the alternative risk measure (left panel-gray line for the 97.5% -ES and right panel-gray line for the 99% -VaR).

both specifications seem to be more sensitive to the selection of the threshold at which extreme events are defined, and therefore, both approximations are estimated. Alternatively, this may be due to a misspecification problem, as discussed below.

3.4.2 Backtesting the Expected Shortall

A key point of Basel III standards is moving to ES from VaR reducing the confidence levels from 0.99 to 0.975 in order to capture tail risk. As an illustration, Figure 3 displays the fitted

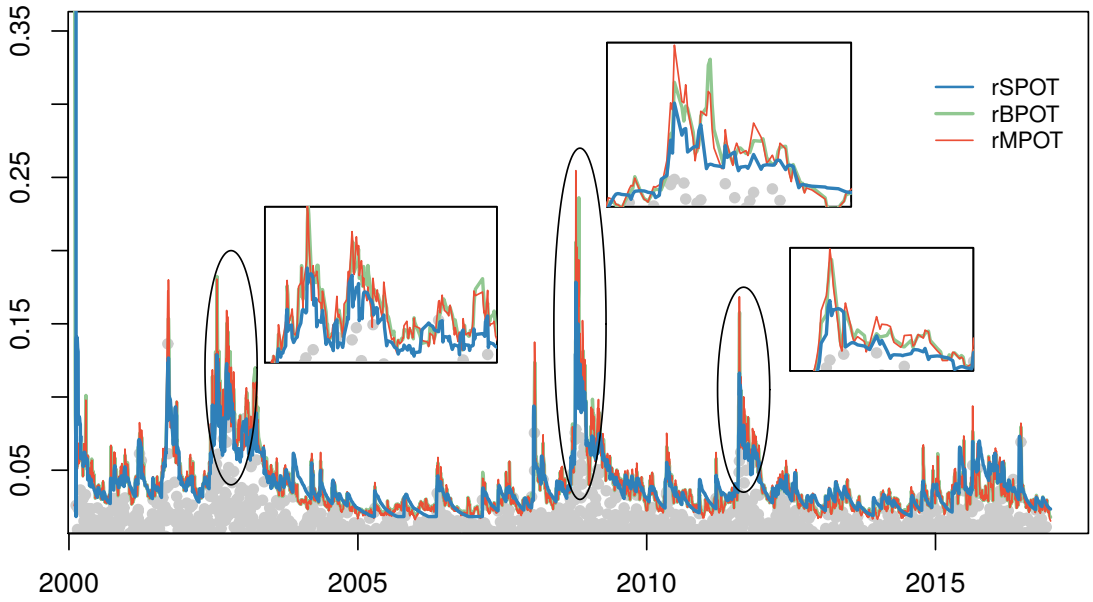

Figure 4: In-sample VaR for the DAX negative log-returns over the period from January 3, 2000 until December 29, 2016. Estimated 99% -VaR for the rSPOT model (blue line), rBPOT model (green line) and rMPOT model (red line). Rectangles correspond to zoomed-in panels of the (left hand) sample time periods in ellipsoids.

VaR (left panel) and ES (right panel) for the in-sample period for the DAX return series, using the rSPOT specification and the competing rBPOT and rMPOT models. Thick gray line in each plot indicates the alternative risk measure, left panel-gray line for the 97.5%-ES and right panel-gray line for the 99%-VaR. At first glance, comparing both VaR estimates at 0.99 confidence level, it seems that on average that both competing specifications are almost identical, while rSPOT approach exhibits a slightly different dynamic. Furthermore, for the in-sample period, on average, ES at 0.975 is higher than VaR at 0.99 for circa of 2%[11].

However, taking a closer look at the risk measures estimates there are clearly key differences.

[11]Results for the averages of both measures for all stock markets for the in- and out-sample period can be obtained from authors upon request.

We focus on VaR estimates in Figure 4 but similar results are obtained for the ES. The blue line gives the estimated VaR for the rSPOT specification, while red and green lines give the estimates based on the competing approaches rMPOT and rBPOT, respectively. As both competing specifications do not directly model the dynamic of occurrence time of the extreme events, the clustering behavior of extreme events must be fully attributed to the dynamic of the magnitude of these, and therefore, to the dynamic of the time-varying parameters. This causes larger spikes in VaR that are observed during periods of crisis in the zoomed-in panels in rectangles from sample time periods in ellipsoids in Figure 4. While in the rSPOT approach this occurs in a much smoother way, since one of the advantages of our specification is the modeling of the occurrence of events independently of the dynamics of the mark process.

Concerning the accuracy results of the ES risk measure, there is no loss function available for which the ES can be elicited, i.e., there is no valid loss function to backtest this risk measure. However, as was demostrated by Fissler & Ziegel (2016) and Patton et al. (2019) VaR and ES can be jointly elicited through the so-called *Fissler and Ziegel loss* (FZL) function, for strictly negative estimates. The main advantage of this framework is that there is not need to specify a conditional density, which removes the possibility that such a model is misspecified. Assuming that losses correspond to negative log-returns the FZL function is defined as follows

$$FZL_t^{\alpha} = -\frac{1}{\alpha ES_{\alpha}^t}\left\{y_t \leq VaR_{\alpha}^t\right\}\left(VaR_{\alpha}^t - y_t\right) + \frac{VaR_{\alpha}^t}{ES_{\alpha}^t} + \ln\left(-ES_{\alpha}^t\right) - 1. \tag{11}$$

In order to compare the estimates of the FZL function for the different models we assess the statistically significant differences in forecast performance by means of the Model Confident Set framework introduced by Hansen et al. (2011). We briefly describe how the Model Confidence Set framework works. First, we compute the average of the FZL functions across all the competing models for each stock market returns at the different confidence levels α. This statistics are collected in a set $\mathcal{M}_0$ indexed by $k = 1, \ldots, m_0$ for each stock market returns at the different confidence levels α. All the differences between the average of FZL functions are estimated

$\Delta_{kl}^{\alpha} = \overline{FZL_k^{\alpha}} - \overline{FZL_l^{\alpha}}$ for all competing models k and l. We then test $H_0 : \mathbb{E}\left[\Delta_{kl}^{\alpha}\right] = 0$ for equal predictive accuracy (The EPA statistic). If the null hypothesis is rejected at the significant level α' a smaller set is obtained by eliminating the worst model, the superior set is then $\hat{\mathcal{M}}^{*}{}_{1-\alpha'}$ with $m^* \leq m_0$. This procedure is repeated until the null hypothesis can not be rejected, being the most discriminating scenario when the final set consists of a single model.

Table 9 exhibits the ratios of the average FZL functions for the rSPOT approach with respect to the (realized) competing models at different confidence levels α. Values smaller than one indicate that the rSPOT model outperforms the competing models in terms of the FZL function. The results for the Model Confidence Set procedure are highlighted in gray color for the best performing specifications included in the superior set at the $\alpha' = 0.05$ significant level.

Overall, the realized versions of all models exhibit the best results in terms of the FZL functions. Indeed, almost only realized versions of all models belong to the superior set according to the Model Confidence Set procedure. For the two years backtesting period, it is observed that the best results in terms of FZL functions are obtained from the rSPOT specification, followed by the rMPOT specification. In the one year backtesting period, the best performance of all models is given by the rSPOT approach where in the 90% of all estimations, for all the stock markets analyzed at the different VaR confidence level, the specification is part of the superior set.

An important result is that unlike the best specifications obtained for the VaR risk measure, where the specifications without including realized measures prevailed, the FZL function shows that the realized version of all models seem to be the most appropriate when it comes to minimizing losses in terms of VaR and ES simultaneously. Finally, the results for the backtesting period confirm that the rSPOT provides superior forecasts relative to the competing approaches producing lower values for the FZL loss function in the majority of cases. This improvement may be due to the way in which the information on the occurrence of extreme events is modeled and incorporated in the specification.

Acknowledgments

The authors acknowledge the Chilean CONICYT funding agency for its financial support (FONDECYT 1180672) for this project.

4 Conclusions

This paper proposed a novel approach for modeling and forecasting the occurrence of extreme events in asset returns by means of a score-driven MPP framework of extreme events: the Score-driven Peaks over Threshold (SPOT) approach. The dynamics of the parameters in the SPOT framework are based on updating functions that are driven by the score of the conditional distribution with respect to both the duration between extreme events and their magnitudes. It was shown that these models are flexible in their structure and can easily accommodate exogenous variables such as realized measures of volatility. An empirical analysis showed that variation in both the conditional intensity function for the duration between events, and magnitude of the extreme returns are important features in relation to periods of market turmoil. Including realized measures of volatility improve the in-sample fit and out-of-sample forecast performance, leading to more accurate tail risk forecasts than recently developed competing models.

References

Agarwal, V., Ruenzi, S. & Weigert, F. (2017), 'Tail risk in hedge funds: A unique view from portfolio holdings', *Journal of Financial Economics* **125**(3), 610–636.

Andersen, T. G. & Bollerslev, T. (1998), 'Deutsche Mark–Dollar volatility: Intraday activity patterns, macroeconomic announcements, and longer run dependencies', *The Journal of Finance* **53**(1), 219–265.

Andersen, T. G., Bollerslev, T. & Meddahi, N. (2005), 'Correcting the errors: Volatility forecast evaluation using high-frequency data and realized volatilities', *Econometrica* **73**(1), 279–296.

Andersen, T. G., Bollerslev, T. & Meddahi, N. (2011), 'Realized volatility forecasting and market microstructure noise', *Journal of Econometrics* **160**(1), 220–234.

Bali, T. G. (2000), 'Testing the empirical performance of stochastic volatility models of the short-term interest rate', *Journal of Financial and Quantitative Analysis* **35**(2), 191–215.

Bali, T. G. & Weinbaum, D. (2007), 'A conditional extreme value volatility estimator based on high-frequency returns', *Journal of Economic Dynamics and Control* **31**(2), 361–397.

Balkema, A. A. & De Haan, L. (1974), 'Residual life time at great age', *The Annals of Probability* **5 (2)**, 792 – 804.

Barndorff-Nielsen, O. E. & Shephard, N. (2002), 'Econometric analysis of realized volatility and its use in estimating stochastic volatility models', *Journal of the Royal Statistical Society: Series B (Statistical Methodology)* **64**(2), 253–280.

Bee, M., Dupuis, D. J. & Trapin, L. (2016), 'Realizing the extremes: Estimation of tail-risk measures from a high-frequency perspective', *Journal of Empirical Finance* **36**, 86–99.

Bee, M., Dupuis, D. J. & Trapin, L. (2018), 'Realized extreme quantile: A joint model for conditional quantiles and measures of volatility with EVT refinements', *Journal of Applied Econometrics* **33**(3), 398–415.

Bee, M., Dupuis, D. J. & Trapin, L. (2019), 'Realized peaks over threshold: A time-varying extreme value approach with high-frequency-based measures', *Journal of Financial Econometrics* **17**(2), 254–283.

Bernardi, M. & Catania, L. (2019), 'Switching generalized autoregressive score copula models with application to systemic risk', *Journal of Applied Econometrics* **34**(1), 43–65.

Blasques, F., Koopman, S. J. & Lucas, A. (2014), 'Stationarity and ergodicity of univariate generalized autoregressive score processes', *Electronic Journal of Statistics* **8**(1), 1088–1112.

Blasques, F., Koopman, S. J. & Lucas, A. (2015), 'Information-theoretic optimality of observation-driven time series models for continuous responses', *Biometrika* **102**(2), 325–343.

Brownlees, C. T. & Gallo, G. M. (2009), 'Comparison of volatility measures: A risk management perspective', *Journal of Financial Econometrics* **8**(1), 29–56.

Buncic, D. & Gisler, K. I. (2016), 'Global equity market volatility spillovers: A broader role for the united states', *International Journal of Forecasting* **32**(4), 1317–1339.

Calvori, F., Creal, D., Koopman, S. J. & Lucas, A. (2017), 'Testing for parameter instability across different modeling frameworks', *Journal of Financial Econometrics* **15**(2), 223–246.

Chavez-Demoulin, V. & McGill, J. (2012), 'High-frequency financial data modeling using Hawkes processes', *Journal of Banking & Finance* **36**(12), 3415–3426.

Chiu, C.-W. J., Mumtaz, H. & Pinter, G. (2017), 'Forecasting with var models: Fat tails and stochastic volatility', *International Journal of Forecasting* **33**(4), 1124–1143.

Christoffersen, P. (1998), 'Evaluating interval forecasts', *International Economic Review* **39**(4), 841–62.

Corsi, F. (2009), 'A simple approximate long-memory model of realized volatility', *Journal of Financial Econometrics* **7**(2), 174–196.

Corsi, F., Fusari, N. & La Vecchia, D. (2013), 'Realizing smiles: Options pricing with realized volatility', *Journal of Financial Economics* **107**(2), 284–304.

Creal, D., Koopman, S. J. & Lucas, A. (2013), 'Generalized autoregressive score models with applications', *Journal of Applied Econometrics* **28**(5), 777–795.

Daley, D. & Vere-Jones, D. (2003), *An Introduction to the Theory of Point Processes*, Springer Series in Statistics.

Daouia, A., Girard, S. & Stupfler, G. (2018), 'Estimation of tail risk based on extreme expectiles', *Journal of the Royal Statistical Society: Series B (Statistical Methodology)* **80**(2), 263–292.

Davison, A. & Smith, R. (1990), 'Models for exceedances over high thresholds', *Journal of the Royal Statistical Society. Series B (Methodological)* **52**(3), 393–425.

Delle Monache, D. & Petrella, I. (2017), 'Adaptive models and heavy tails with an application to inflation forecasting', *International Journal of Forecasting* **33**(2), 482–501.

Engle, R. F. & Gallo, G. M. (2006), 'A multiple indicators model for volatility using intra-daily data', *Journal of Econometrics* **131**(1-2), 3–27.

Engle, R. F. & Manganelli, S. (2004), 'Caviar: Conditional autoregressive value at risk by regression quantiles', *Journal of Business & Economic Statistics* **22**(4), 367–381.

Engle, R. & Russell, J. (1998), 'Autoregressive conditional duration: A new model for irregularly spaced transaction data', *Econometrica* **66**, 1127–1162.

Fissler, T. & Ziegel, J. F. (2016), 'Higher order elicitability and Osband's principle', *The Annals of Statistics* **44**(4), 1680–1707.

Fuentes, F., Herrera, R. & Clements, A. (2018), 'Modeling extreme risks in commodities and commodity currencies', *Pacific-Basin Finance Journal* **51**, 108–120.

Gneiting, T. (2011), 'Making and evaluating point forecasts', *Journal of the American Statistical Association* **106**(494), 746–762.

Gorgi, P., Hansen, P., Janus, P. & Koopman, S. (2018), 'Realized Wishart-GARCH: A score-driven multi-asset volatility model', *Journal of Financial Econometrics* **17**(1), 1–32.

Gorgi, P., Koopman, S. J. & Li, M. (2019), 'Forecasting economic time series using score-driven dynamic models with mixed-data sampling', *International Journal of Forecasting* .

Gresnigt, F., Kole, E. & Franses, P. H. (2016), 'Specification testing in Hawkes models', *Journal of Financial Econometrics* **15**(1), 139–171.

Hamilton, J. D. & Jordà, Ò. (2002), 'A model of the federal funds rate target', *Journal of Political Economy* **110**(5), 1135–1167.

Hansen, P. R., Huang, Z. & Shek, H. H. (2012), 'Realized GARCH: A joint model for returns and realized measures of volatility', *Journal of Applied Econometrics* **27**(6), 877–906.

Hansen, P. R., Lunde, A. & Nason, J. M. (2011), 'The model confidence set', *Econometrica* **79**(2), 453–497.

Harvey, A. C. (2013), *Dynamic models for volatility and heavy tails: with applications to financial and economic time series*, Vol. 52, Cambridge University Press.

Hautsch, N. & Herrera, R. (2020), 'Multivariate dynamic intensity peaks-over-threshold models', *Journal of Applied Econometrics* **35**(2), 248–272.

Herrera, R. & Clements, A. (2018), 'Point process models for extreme returns: Harnessing implied volatility', *Journal of Banking & Finance* **88**, 161–175.

Herrera, R. & González, N. (2014), 'The modeling and forecasting of extreme events in electricity spot markets', *International Journal of Forecasting* **30**(3), 477–490.

Hong, Y., Li, H. & Zhao, F. (2007), 'Can the random walk model be beaten in out-of-sample density forecasts? Evidence from intraday foreign exchange rates', *Journal of Econometrics* **141**(2), 736–776.

Karmakar, M. & Paul, S. (2019), 'Intraday portfolio risk management using var and cvar: A cgarch-evt-copula approach', *International Journal of Forecasting* **35**(2), 699–709.

Kupiec, P. H. (1995), 'Techniques for verifying the accuracy of risk measurement models', *The Journal of Derivates* **3**(2).

Liu, Y. & Tawn, J. A. (2013), 'Volatility model selection for extremes of financial time series', *Journal of Statistical Planning and Inference* **143**(3), 520–530.

Longin, F. M. (2000), 'From value at risk to stress testing: The extreme value approach', *Journal of Banking & Finance* **24**(7), 1097–1130.

Lucas, A., Schwaab, B. & Zhang, X. (2017), 'Modeling financial sector joint tail risk in the euro area', *Journal of Applied Econometrics* **32**(1), 171–191.

Lucas, A. & Zhang, X. (2016), 'Score-driven exponentially weighted moving averages and value-at-risk forecasting', *International Journal of Forecasting* **32**(2), 293–302.

Manganelli, S. & Engle, R. F. (2004), 'A comparison of value-at-risk models in finance', *Risk measures for the 21st century* pp. 123–44.

Massacci, D. (2016), 'Tail risk dynamics in stock returns: Links to the macroeconomy and global markets connectedness', *Management Science* **63**(9), 3072–3089.

McNeil, A. & Frey, R. (2000), 'Estimation of tail-related risk measures for heteroscedastic financial time series: an extreme value approach', *Journal of Empirical Finance* **7**(3-4), 271–300.

Nieto, M. R. & Ruiz, E. (2016), 'Frontiers in var forecasting and backtesting', *International Journal of Forecasting* **32**(2), 475–501.

Noureldin, D., Shephard, N. & Sheppard, K. (2012), 'Multivariate high-frequency-based volatility (heavy) models', *Journal of Applied Econometrics* **27**(6), 907–933.

Patton, A. J., Ziegel, J. F. & Chen, R. (2019), 'Dynamic semiparametric models for expected shortfall (and value-at-risk)', *Journal of Econometrics* **211**(2), 388–413.

Pickands, J. (1975), 'Statistical inference using extreme order statistics', *The Annals of Statistics* **3**(1), 119 – 131.

Sahamkhadam, M., Stephan, A. & Östermark, R. (2018), 'Portfolio optimization based on GARCH-EVT-Copula forecasting models', *International Journal of Forecasting* **34**(3), 497–506.

Scarrott, C. & MacDonald, A. (2012), 'A review of extreme value threshold es-timation and uncertainty quantification', *REVSTAT–Statistical Journal* **10**(1), 33–60.

Schoenberg, F. P. (2006), 'On non-simple marked point processes', *Annals of the Institute of Statistical Mathematics* **58**(2), 223–233.

Smith, R. (1989), 'Extreme value analysis of environmetal time series: An application to trend detection in ground-level ozone', *Statistical Science* **4**(4), 367–377.

Taylor, J. W. (2008), 'Estimating value at risk and expected shortfall using expectiles', *Journal of Financial Econometrics* **6**(2), 231–252.

Taylor, J. W. (2019), 'Forecast combinations for value at risk and expected shortfall', *International Journal of Forecasting* .

Trapin, L. (2017), 'Can volatility models explain extreme events?', *Journal of Financial Econometrics* **16**(2), 297–315.

Yao, X., Izzeldin, M. & Li, Z. (2019), 'A novel cluster har-type model for forecasting realized volatility', *International Journal of Forecasting* **35**(4), 1318 – 1331.

Yi, Y., Feng, X. & Huang, Z. (2014), 'Estimation of extreme value-at-risk: An EVT approach for quantile GARCH model', *Economics Letters* **124**(3), 378–381.

Zhang, X. & Bernd, S. (2016), Tail risk in government bond markets and ECB unconventional policies, Technical report, Working paper.

Ziggel, D., Berens, T., Weiß, G. N. & Wied, D. (2014), 'A new set of improved value-at-risk backtests', *Journal of Banking & Finance* **48**, 29–41.

A Appendix

A.1 Impact of the discretization of time duration between extreme events in the maximum-likelihood inference

In section 2 we introduce the SPOT approach utilizing the framework of extreme vents via marked point process theory, which arises in continuous time. However, this type of models, where the time between extreme events is discrete, have been used extensively in recent literature on extreme financial risk (see Chavez-Demoulin & McGill 2012, Herrera & González 2014, Gresnigt et al. 2016). In this section we provide the formal connection between the discrete-time log-likelihood function proposed in (5) and (6) applied to the SPOT specification, and the continuos-time version of this log-likelihood function introduced in (2). We show that the continuos log-likelihood function is indeed a limiting result of the discrete-time version. The result is direct consequence of the arguments of the connection between the Autorregresive Conditional Hazard model by Hamilton & Jordà (2002), which is a discrete version of the Autoregressive Conditional Duration model introduced by Engle & Russell (1998).

Let t_i and t_{i-1} be the occurrence times of the last and penultimate extreme event, Δ be a discrete time interval at which the time is sampled. Further, let ϵ_η be an indicator function taking the value 1 if an extreme event is observed in the η-th time interval with $\eta \in \{t_{i-1}+\Delta, t_{i-1}+2\Delta \ldots, t_i\}$ and zero otherwise. Notice that according to the definition of the conditional ground intensity in (4) the conditional probability of observing an extreme event at the η-th time interval is $\tau\left(\eta \mid \mathcal{F}_i^\tau, f_i^\tau; \theta^\tau\right) = h\left(\eta - t_{i-1} \mid \mathcal{F}_i^\tau, f_i^\tau; \theta^\tau\right)$ for $i \geq 2$. Following Hamilton & Jordà (2002), the probability of observing ϵ_η given $\mathcal{F}_i^\tau$ is

$$p\left(\epsilon_\eta \mid \mathcal{F}_i^\tau, f_i^\tau; \theta^\tau\right) = h\left(\eta - t_{i-1} \mid \mathcal{F}_i^\tau, f_i^\tau; \theta^\tau\right)^{\epsilon_\eta} \left\{1 - h\left(\eta - t_{i-1} \mid \mathcal{F}_i^\tau, f_i^\tau; \theta^\tau\right)\right\}^{(1-\epsilon_\eta)}.$$

Then, the conditional log-likelihood of observing an extreme event between the inter-exceedance

times t_i and t_{i-1} can be calculated as

$$\sum_{\eta=t_{i-1}+\Delta}^{t_i} \epsilon_\eta \ln h\left(\eta - t_{i-1} \mid \mathcal{F}_i^\tau, f_i^\tau; \theta^\tau\right) + (1-\epsilon_\eta) \ln\left\{1 - h\left(\eta - t_{i-1} \mid \mathcal{F}_i^\tau, f_i^\tau; \theta^\tau\right)\right\}. \tag{12}$$

Notice that the term ϵ_η is zero for all the intervals but the last η. Then, last equation can be reduced to

$$\begin{aligned} &\ln h\left(t_i - t_{i-1} \mid \mathcal{F}_i^\tau, f_i^\tau; \theta^\tau\right) + \sum_{\eta=t_{i-1}+\Delta}^{t_i-\Delta} \ln\left\{1 - h\left(\eta - t_{i-1} \mid \mathcal{F}_i^\tau, f_i^\tau; \theta^\tau\right)\right\} \\ \approx &\ln h\left(t_i - t_{i-1} \mid \mathcal{F}_i^\tau, f_i^\tau; \theta^\tau\right) - \sum_{\eta=t_{i-1}+\Delta}^{t_i-\Delta} h\left(\eta - t_{i-1} \mid \mathcal{F}_i^\tau, f_i^\tau; \theta^\tau\right), \end{aligned}$$

where last expression is obtained by Taylor's theorem[12]. Observe that by letting $\Delta \to 0$ we get the limit of the sum

$$\ln h\left(t_i - t_{i-1} \mid \mathcal{F}_i^\tau, f_i^\tau; \theta^\tau\right) - \int_{t_{i-1}}^{t_i} h\left(s \mid \mathcal{F}_{N(\{s\})}^\tau, f_{N(\{s\})}^\tau; \theta^\tau\right) ds,$$

which is nothing more than the log-likelihood function for the continuos-time model in (2).

A.2 Proofs

Let (t_i, z_i) be a pair of random variables describing the occurrence time $t_i \in \mathbb{R}_+$ and the magnitude $z_i \in \mathbb{R}_+$ of an extreme event i, while

$$p\left(t_i - t_i\right) \;=\; \frac{k}{\delta}\left(\frac{t_i - t_{i-1}}{\delta}\right)^{k-1} \exp\left\{-\left(\frac{t_i - t_{i-1}}{\delta}\right)^{k}\right\}, \quad i \geq 2,$$

is the Weibull density probability function describing the dynamic of the duration between the time t and the time of last observed extreme event t_{i-1} with scale and shape parameters $\delta > 0$

[12]Observe that $f(x) = \ln(1-x) = -x + O\left(x^2\right)$ for x in the neighborhood of zero.

and $k > 0$, respectively, and

$$g(z_i) = \frac{1}{\beta}\left(1+\xi\frac{z_i}{\beta}\right)^{-\frac{1}{\xi}-1}$$

be the generalized Pareto density function of the mark z_i with scale parameter $\beta > 0$ and shape parameter $\xi > 0$. Following, we provide the details of the score-driven model as introduced for the Wss-SPOT and the Wpp-SPOT specification. The results for other hazard functions for the ground conditional intensity follow similar steps and are resumed in Table 1.

Proof. **Proposition 1**

The Wss-SPOT conditional intensity consists of both scale parameters being time varying. Let $f_i^\tau = \ln \delta_i$ and $f_i^g = \ln \beta_i$ be the time varying scale parameters, and $\theta^\tau := \{k, \omega_\tau, \phi_\tau, \psi_\tau\}$ and $\theta^g := \{\xi, \omega_g, \phi_g, \psi_g\}$ be the static parameters, where k and ξ correspond to the shape coefficients. The score function of (5) with respect to f_i^τ is given by

$$\begin{aligned}
\nabla_{\tau i} &= \frac{\partial \mathcal{L}_\tau\left(t_i \mid \mathcal{F}_i^\tau, f_i^\tau; \theta^\tau\right)}{\partial f_i^\tau} \\
&= \frac{\partial \mathcal{L}_\tau\left(t_i \mid \mathcal{F}_i^\tau, \delta_i; \theta^\tau\right)}{\partial \delta_i}\frac{\mathsf{d}\delta_i}{\mathsf{d}f_i^\tau} \\
&= k\left\{\left(\frac{t_i - t_{i-1}}{\delta_i}\right)^k - 1\right\}
\end{aligned}$$

where

$$\frac{\partial \mathcal{L}_\tau\left(t_i \mid \mathcal{F}_i^\tau, \delta_i; \theta^\tau\right)}{\partial \delta_i} = \frac{k}{\delta_i}\left(\frac{t_i - t_{i-1}}{\delta_i}\right)^k - \frac{k}{\delta_i} \tag{13}$$

$$\frac{\mathsf{d}\delta_i}{\mathsf{d}f_i^\tau} = \exp(f_i^\tau) = \delta_i.$$

Similarly, the score function of (6) with respect to f_i^g is given by

$$\begin{aligned}\nabla_{gi} &= \frac{\partial \mathcal{L}_g\left(z_i \mid t_i, \mathcal{F}_i^g, f_i^g; \theta^g\right)}{\partial f_i^g} \\ &= \frac{\partial \mathcal{L}_g\left(z_i \mid t_i, \mathcal{F}_i^g, \beta_i; \theta^g\right)}{\partial \beta_i} \frac{\mathsf{d}\beta_i}{\mathsf{d}f_i^g} \\ &= \frac{z_i - \beta_i}{\xi z_i + \beta_i}\end{aligned}$$

where

$$\frac{\partial \mathcal{L}_g\left(z_i \mid t_i, \mathcal{F}_i^g, \beta_i; \theta^g\right)}{\partial \beta_i} = \frac{z_i\left(1+\xi\right)}{\beta_i\left(\xi z_i + \beta_i\right)} - \frac{1}{\beta_i} \tag{14}$$

$$\frac{\mathsf{d}\beta_i}{\mathsf{d}f_i^g} = \exp(f_i^g) = \beta_i.$$

Under certain regularity conditions the expected value of the score is zero, applying this result to (13) and (14) we get

$$\int_0^\infty \left\{\frac{k}{\delta_i}\left(\frac{t_i - t_{i-1}}{\delta_i}\right)^k\right\} p\left(t_i - t_{i-1} \mid \mathcal{F}_i^\tau, \delta_i; \theta^\tau\right) \mathsf{d}t_i = \int_0^\infty \left\{\frac{k}{\delta_i}\right\} p\left(t_i - t_{i-1} \mid \mathcal{F}_i^\tau, \delta_i; \theta^\tau\right) \mathsf{d}t_i, \tag{15}$$

$$\int_0^\infty \left\{\frac{z_i + z_i\xi}{z_i\beta_i\xi + \beta_i^2}\right\} g\left(z_i \mid t_i, \mathcal{F}_i^g, \beta_i; \theta^g\right) \mathsf{d}z_i = \int_0^\infty \left\{\frac{1}{\beta_i}\right\} g\left(z_i \mid t_i, \mathcal{F}_i^g, \beta_i; \theta^g\right) \mathsf{d}z_i. \tag{16}$$

Furthermore, in order to obtain scaling functions of the ground intensity and density probability function of the mark i, we need to estimate the second derivatives

$$\begin{aligned}\frac{\partial^2 \mathcal{L}_\tau\left(t_i \mid \mathcal{F}_i^\tau, \delta_i; \theta^\tau\right)}{\partial \delta_i^2} &= \frac{k}{\delta_i^2} + \frac{1-k}{\delta_i}\left\{\frac{k}{\delta_i}\left(\frac{t_i - t_{i-1}}{\delta_i}\right)^k\right\} - \frac{2}{\delta_i}\left\{\frac{k}{\delta_i}\left(\frac{t_i - t_{i-1}}{\delta_i}\right)^k\right\}, \\ \frac{\partial^2 \mathcal{L}_g\left(z_i \mid t_i, \mathcal{F}_i^g, \beta_i; \theta^g\right)}{\partial \beta_i^2} &= \frac{1}{\beta_i^2} - \frac{2}{\beta_i}\left(\frac{z_i + z_i\xi}{\beta_i\xi z_i + \beta_i^2}\right) + \frac{\xi}{\xi+1}\left(\frac{z_i + z_i\xi}{\beta_i\xi z_i + \beta_i^2}\right)^2.\end{aligned}$$

With the above results in the obtained in (15) and (16) we use the conditional Fisher information to get the scaling functions

$$
\begin{aligned}
S_{\tau i} &= E\left[\left(\frac{\partial \mathcal{L}_\tau\left(t_i \mid \mathcal{F}_i^\tau, \delta_i; \theta^\tau\right)}{\partial f_i^\tau}\right)^2\right]^{-1} \\
&= E\left[\left(\frac{\partial \mathcal{L}_\tau\left(\mathcal{F}_i^\tau, \delta_i; \theta^\tau\right)}{\partial \delta_i}\right)^2\left(\frac{\mathsf{d}\delta_i}{\mathsf{d}f_i^\tau}\right)^2\right]^{-1} \\
&= E\left[-\frac{\partial^2 \mathcal{L}_\tau\left(t_i \mid \mathcal{F}_i^\tau, \delta_i; \theta^\tau\right)}{\partial \delta_i^2}\right]^{-1} \exp\left\{-2f_i^\tau\right\} \\
&= \left[\int_0^\infty \left\{\frac{k}{\delta_i^2} + \frac{1-k}{\delta_i}\left(\frac{k}{\delta_i}\right) - \frac{2}{\delta_i}\left(\frac{k}{\delta_i}\right)\right\} p\left(t_i - t_{i-1} \mid \mathcal{F}_i^\tau, \delta_i; \theta^\tau\right) \mathsf{d}t_i\right]^{-1} \frac{1}{\delta_i^2} \\
&= \left(\frac{\delta_i}{k}\right)^2 \frac{1}{\delta_i^2} \\
&= \frac{1}{k^2}
\end{aligned}
$$

and

$$
\begin{aligned}
S_{gi} &= E\left[\left(\frac{\partial \mathcal{L}_g\left(z_i \mid t_i, \mathcal{F}_i^g, \beta_i; \theta^g\right)}{\partial f_i^g}\right)^2\right]^{-1} \\
&= E\left[-\frac{\partial^2 \mathcal{L}_g\left(z_i \mid t_i, \mathcal{F}_i^g, \beta_i; \theta^g\right)}{\partial \beta_i^2}\right]^{-1} \exp\left\{-2f_i^g\right\} \\
&= \left[\int_0^\infty \left\{\frac{1}{\beta_i^2} - \frac{2}{\beta_i}\left(\frac{1}{\beta_i}\right) + \frac{\xi}{\xi+1}\left(\frac{1}{\beta_i}\right)^2\right\} g\left(z_i \mid t_i, \mathcal{F}_i^g, \beta_i; \theta^g\right) \mathsf{d}z_i\right]^{-1} \frac{1}{\beta_i^2} \\
&= \beta_i^2\left(2\xi+1\right)\frac{1}{\beta_i^2} \\
&= 2\xi + 1
\end{aligned}
$$

Finally, the scaled score functions $s_i^\tau = S_{\tau i}\nabla_{\tau i}$ and $s_i^g = S_{gi}\nabla_{gi}$ are given by

$$
s_i^\tau = \frac{1}{k}\left\{\left(\frac{t_i - t_{i-1}}{\delta_i}\right)^k - 1\right\}, \quad \text{and} \quad s_i^g = \frac{\left(z_i - \beta_i\right)\left(2\xi+1\right)}{\beta_i + \xi z_i}
$$

or alternatively in terms of the time varying parameters f_i^τ and f_i^g

$$s_i^\tau = \frac{1}{k}\left\{\left(\frac{t_i - t_{i-1}}{\exp\left(f_i^\tau\right)}\right)^k - 1\right\} \quad \text{and} \quad s_i^g = \frac{\left(z_i - \exp\left(f_i^g\right)\right)(2\xi + 1)}{\exp\left(f_i^g\right) + \xi z_i}$$

□

Proof. **Proposition 2**

The Wpp-SPOT conditional intensity consists of being both dynamic shape parameters. Similar to the above specification, let $f_i^\tau = \ln k_i$ and $f_i^g = \ln \xi_i$ be the time varying shape parameters, and $\theta^\tau := \{\delta, \omega_\tau, \phi_\tau, \psi_\tau\}$ and $\theta^g := \{\beta, \omega_g, \phi_g, \psi_g\}$ be the static parameters, where δ and β correspond to the scale coefficients. The score functions of (5) are given by

$$\begin{aligned}
\nabla_{\tau i} &= \frac{\partial \mathcal{L}_\tau\left(t_i \mid \mathcal{F}_i^\tau, k_i; \theta^\tau\right)}{\partial k_i}\frac{\mathsf{d}k_i}{\mathsf{d}f_i^\tau} \\
&= 1 + k_i \ln\left(\frac{t_i - t_{i-1}}{\delta}\right)\left\{1 - \left(\frac{t_i - t_{i-1}}{\delta}\right)^{k_i}\right\} \\
\nabla_{gi} &= \frac{\mathcal{L}_g\left(z_i \mid t_i, \mathcal{F}_i^g, \xi_i; \theta^g\right)}{\partial \xi_i}\frac{\mathsf{d}\xi_i}{\mathsf{d}f_i^g} \\
&= \frac{\ln\left(1 + \frac{\xi_i z_i}{\beta}\right)}{\xi_i} - \frac{z_i\xi_i + z_i}{\beta + \xi_i z_i},
\end{aligned}$$

respectively, where

$$\begin{aligned}
\frac{\partial \mathcal{L}_\tau\left(t_i \mid \mathcal{F}_i^\tau, k_i; \theta^\tau\right)}{\partial k_i} &= \frac{1}{k_i} + \ln\left(\frac{t_i - t_{i-1}}{\delta}\right)\left\{1 - \left(\frac{t_i - t_{i-1}}{\delta}\right)^{k_i}\right\} \\
\frac{\mathsf{d}k_i}{\mathsf{d}f_i^\tau} &= \exp(f_i^\tau) = k_i \\
\frac{\mathcal{L}_g\left(z_i \mid t_i, \mathcal{F}_i^g, \xi_i; \theta^g\right)}{\partial \xi_i} &= \frac{\ln\left(1 + \frac{\xi_i z_i}{\beta}\right)}{\xi_i^2} - \frac{z_i + \frac{z_i}{\xi_i}}{\beta + \xi_i z_i} \\
\frac{\mathsf{d}\xi_i}{\mathsf{d}f_i^g} &= \exp(f_i^g) = \xi_i
\end{aligned}$$

Again, the scaling functions of the ground intensity and density function of the mark i are obtained by means of second derivatives of the following log-likelihood functions

$$\begin{aligned}
\frac{\partial^2 \mathcal{L}_\tau \left(t_i \mid \mathcal{F}_i^\tau, k_i; \theta^\tau\right)}{\partial k_i^2} &= -\frac{1}{k_i^2} - \ln\left(\frac{t_i - t_{i-1}}{\delta}\right)^2 \left(\frac{t_i - t_{i-1}}{\delta}\right)^{k_i} \\
\frac{\partial^2 \mathcal{L}_g \left(z_i \mid t_i, \mathcal{F}_i^g, \xi_i; \theta^g\right)}{\partial \xi_i^2} &= -\frac{2}{\xi_i}\left\{\frac{\ln\left(1 + \frac{\xi_i z_i}{\beta}\right)}{\xi_i^2}\right\} + \frac{z_i^2 + \frac{z_i^2}{\xi_i}}{\beta^2\left(1 + \frac{z_i \xi_i}{\beta}\right)^2} + \frac{2 z_i}{\xi_i^2\left(\beta + z_i \xi_i\right)}.
\end{aligned}$$

With these results we use Fisher information to obtain the scaling functions

$$\begin{aligned}
S_{\tau i} &= E\left[\left(\frac{\partial \mathcal{L}_\tau \left(t_i \mid \mathcal{F}_i^\tau, k_i; \theta^\tau\right)}{\partial f_i^\tau}\right)^2\right]^{-1} \\
&= E\left[-\frac{\partial^2 \mathcal{L}_\tau (t_i \mid \mathcal{F}_i^\tau, k_i; \theta^\tau)}{\partial k_i^2}\right]^{-1} \exp\left\{-2 f_i^\tau\right\} \\
&= \left[\int_0^\infty \left(\frac{1}{k_i^2} + \ln\left(\frac{t_i - t_{i-1}}{\delta}\right)^2 \left(\frac{t_i - t_{i-1}}{\delta}\right)^{k_i}\right) p\left(t_i - t_{i-1} \mid \mathcal{F}_i^\tau, k_i; \theta^\tau\right) \mathsf{d}t_i\right]^{-1} \frac{1}{k_i^2} \\
&= \frac{k_i^2}{(\gamma - 1)^2 + \pi^2/6} \frac{1}{k_i^2} \\
&= \frac{1}{(\gamma - 1)^2 + \pi^2/6}
\end{aligned}$$

and

$$\begin{aligned}
S_{gi} &= E\left[\left(\frac{\partial \mathcal{L}_g\left(z_i \mid t_i, \mathcal{F}_i^g, \xi_i; \theta^g\right)}{\partial f_i^g}\right)^2\right]^{-1} \\
&= E\left[-\frac{\partial^2 \mathcal{L}_g\left(z_i \mid t_i, \mathcal{F}_i^g, \xi_i; \theta^g\right)}{\partial \xi_i^2}\right]^{-1} \exp\left\{-2 f_i^g\right\} \\
&= \left[\int_0^\infty \left(\frac{2}{\xi_i}\left\{\frac{\ln\left(1+\frac{\xi_i z_i}{\beta}\right)}{\xi_i^2}\right\} - \frac{z_i^2 + \frac{z_i^2}{\xi_i}}{\beta^2\left(1+\frac{z_i\xi_i}{\beta}\right)^2} - \frac{2z_i}{\xi_i^2\left(\beta + z_i\xi_i\right)}\right) g\left(z_i \mid t_i, \mathcal{F}_i^g, \xi_i; \theta^g\right) \mathsf{d}z_i\right]^{-1} \frac{1}{\xi_i^2} \\
&= \frac{\left(1+\xi_i\right)\left(1+2\xi_i\right)}{2}\frac{1}{\xi_i^2} \\
&= \frac{\left(1+\xi_i\right)\left(1+2\xi_i\right)}{2\xi_i^2}.
\end{aligned}$$

Finally, the scaled score functions $s_i^\tau = S_{\tau i}\nabla_{\tau i}$ and $s_i^g = S_{gi}\nabla_{gi}$ are obtained as follows

$$s_i^\tau = \nu + \nu k_i \ln\left(\frac{t_i - t_{i-1}}{\delta}\right)\left\{1 - \left(\frac{t_i - t_{i-1}}{\delta}\right)^{k_i}\right\}$$

and

$$s_i^g = \frac{\left(1+\xi_i\right)\left(1+2\xi_i\right)}{2\xi_i^2}\left\{\frac{\ln\left(1+\frac{\xi_i z_i}{\beta}\right)}{\xi_i} + \frac{z_i + z_i\xi_i}{\beta + \xi_i z_i}\right\},$$

where $\nu = \frac{1}{(\gamma-1)^2+\pi^2/6}$ and γ is the Euler-Mascheroni constant. Alternatively in terms of the time varying parameters f_i^τ and f_i^g the scaled score are given by

$$s_i^\tau = \nu + \nu\exp\left(f_i^\tau\right)\left(1 - \left(\frac{t_i - t_{i-1}}{\delta}\right)^{\exp\left(f_i^\tau\right)}\right)\ln\left(\frac{t_i - t_{i-1}}{\delta}\right),$$

and

$$s_i^g = \frac{\left(2\exp\left(f_i^g\right)+1\right)\left(\exp\left(f_i^g\right)+1\right)}{2\exp\left(2f_i^g\right)}\left\{\frac{\ln\left(z_i\exp\left(f_i^g\right)\beta^{-1}+1\right)}{\exp\left(f_i^g\right)} - \frac{z_i\left(\exp\left(-f_i^g\right)+1\right)}{z_i\exp\left(f_i^g\right)+\beta}\right\}.$$

□

Proof. **Proposition 3**

Suppose $y_t \in \mathbb{R}$ are random variables representing losses with continuous distribution function F and $z_i = y_{t_i} - u$ the magnitude i for which an observation y_{t_i} exceeds the threshold $u > 0$ at time t_i. The VaR at time t_i with conditional information $\mathcal{F}_i$ and confidence level α is such that

$$F^{-1}_{y_{t_i}|\mathcal{F}_i}(\alpha) := VaR^{t_i}_{\alpha},$$

which is solution to

$$1 - \alpha = \mathbb{P}(y_{t_i} > y \mid \mathcal{F}_i) = \mathbb{P}(y_{t_i} > u \mid \mathcal{F}_i)\, \mathbb{P}(y_{t_i} - u > y - u \mid \mathcal{F}_i). \tag{17}$$

In terms of point process representation the probability $\mathbb{P}(y_{t_i} > u \mid \mathcal{F}_i)$ indicates the probability of observing an extreme event in the interval $(t_{i-1}, t_i]$

$$\begin{aligned}\mathbb{P}(N(\{t_i\}) - N(\{t_{i-1}\}) > 0 \mid \mathcal{F}_i) &= 1 - \exp\left(-\int_{t_{i-1}}^{t_i} \tau\left(s \mid \mathcal{F}^{\tau}_{N(\{s\})}, f^{\tau}_{N(\{s\})}; \theta^{\tau}\right) ds\right), \\ &\approx \tau(t_i \mid \mathcal{F}^{\tau}_i, f^{\tau}_i; \theta^{\tau}) = \exp(f^{\tau}_i)^k\, k\,(t_i - t_{i-1})^{k-1}\end{aligned} \tag{18}$$

since $-\ln(1-x) \sim x$ for $x \to 0$. For the Wss-SPOT specification (9) the conditional probability of exceedances is then computed as

$$\mathbb{P}(y_{t_i} - u > y - u \mid \mathcal{F}_t) = \left(1 + \xi \frac{y_{t_i} - u}{\exp(f^g_i)}\right)^{-1/\xi}.$$

Replacing both results in (17) and the required quantile $y_{t_i} = VaR^{t_i}_{\alpha}$ we obtain

$$\mathbb{P}(y_{t_i} > VaR^{t_i}_{\alpha} \mid \mathcal{F}_i) = 1 - \alpha = \exp(f^{\tau}_i)^k\, k\,(t_i - t_{i-1})^{k-1} \left(1 + \xi \frac{VaR^{t}_{\alpha} - u}{\exp(f^g_i)}\right)^{-1/\xi}.$$

Solving this equation for VaR_α^t we get the wished result for VaR

$$VaR_\alpha\left(t_i, z_i \mid \mathcal{F}_i, \boldsymbol{f}_i; \boldsymbol{\Theta}\right) := VaR_\alpha^t = \frac{\xi u + \exp\left(f_i^g\right)}{\xi}\left\{\left(\frac{\exp\left(f_i^\tau\right)^k k\left(t_i - t_{i-1}\right)^{k-1}}{1-\alpha}\right)^\xi - 1\right\},$$

while the conditional ES is obtained by estimating the expectation of extreme losses beyond VaR_α^t

$$\begin{aligned}
ES_\alpha\left(t_i, z_i \mid \mathcal{F}_i, \boldsymbol{f}_i; \boldsymbol{\Theta}\right) &:= \frac{1}{1-\alpha}\int_\alpha^1 VaR_s^{t_i} ds. \\
&= u + \frac{\exp\left(f_i^g\right)\left\{(1-\alpha) + (\alpha-1)\left(\frac{\exp\left(f_i^\tau\right)^k k\left(t_i - t_{i-1}\right)^{k-1}}{1-\alpha}\right)^\xi - (1-\alpha)\,\xi\right\}}{(1-\alpha)\,(\xi-1)\,\xi} \\
&= \frac{\frac{\exp\left(f_i^g\right)}{\xi}\left(\left(\frac{\exp\left(f_i^\tau\right)^k k\left(t_i - t_{i-1}\right)^{k-1}}{1-\alpha}\right)^\xi - 1\right) + u}{(1-\xi)} + \frac{\exp\left(f_i^g\right) - \xi u}{(1-\xi)} \\
&= \frac{VaR_\alpha^t + \exp\left(f_i^g\right) - u\xi}{(1-\xi)}
\end{aligned}$$

where $\boldsymbol{f}_i := \{(f_i^\tau, f_i^g)\}$ is the vector of time-varying parameters and $\boldsymbol{\Theta} := \{(\theta^\tau, \theta^g)\}$ is a vector of static parameters with $\theta^\tau := \{k, \omega_\tau, \phi_\tau, \psi_\tau\}$ and $\theta^g := \{\xi, \omega_g, \phi_g, \psi_g\}$

□

A.3 Competing Models

We describe briefly the competing models introduced in section 3.4. Again, let $y_t \in \mathbb{R}$ be random variables representing losses and $u > 0$ some high threshold previously defined. The extreme events z_t will be defined as those observations that have exceeded this threshold u, whose magnitude is $z_t = \max\left(y_t - u, 0\right)$

A.3.1 The Bee et al.(2019) POT model (BPOT)

The first model combines a Logit specification for the occurrence times and a GPD for the magnitude of the extreme events whose parameter dynamic is captured by means of a score-driven approach. Under this framework the tail distribution of these events is described by the following censored specification whose cumulative distribution function is given by

$$H_t\left(z_t \mid \mathcal{F}_t, \beta_t, \rho_t; \xi\right) = \begin{cases} 1-\rho_t & z_t = 0 \\ 1-\rho_t\left(1+\xi\frac{z_t}{\beta_t}\right)^{-1/\xi} & z_t > 0. \end{cases} \tag{19}$$

Let $\rho_t = \exp p_t$ be the time-varying parameters harnessing the dynamic of the exceedance probability in the Logit model and $\beta_t = \exp f_t$ the scale parameter of the size of the extreme events in the GPD distribution, whose score-driving mechanisms is given by the following dynamics

$$\begin{aligned} f_{t+1} &= \omega_f + \phi_f f_t + \psi_f s_t^f \\ p_{t+1} &= \omega_p + \phi_p p_t + \psi_p s_t^p \end{aligned}$$

which include realized measures in the case of the realized version of this model. Here, s_t^f and s_t^p are the scaled score of the log-likelihood function of the distribution function in (19). For more details in the implementation of the BPOT model see Bee et al. (2019).

A.3.2 The Massacci (2016) POT model (MPOT)

The second model introduced by Massacci (2016) is a dynamic censored regression model for extreme events. The cumulative distribution function for the magnitudes is in this case given by

$$\begin{aligned} H_t\left(z_t \mid \mathcal{F}_t, \beta_t, \xi_t\right) = \mathbb{1}\left(z_t = 0\right)&\left[1-\left(\frac{1}{1+u}\right)^{\xi_t}\right] \\ &+ \mathbb{1}\left(z_t > 0\right)\left[1-\left(\frac{1}{1+u}\right)^{\xi_t}\left(1+\frac{z_t}{\beta_t}\right)^{-\xi_t}\right], \end{aligned} \tag{20}$$

where $\mathbb{1}(\cdot)$ is the indicator function. Unlike the other specifications, this approach combines a GPD specification for modelling the magnitude of the extreme events and a power law for the conditional probability of an exceedance. In addition, both the scale parameter $\beta_t = \exp f_t$ and the shape parameter $\xi_t = \exp p_t$ follow a score-driven updating. However, this specification assumes that the scaled score of the shape parameter also drives the dynamics of the scale parameter as follows

$$\begin{aligned} f_{t+1} &= \omega_f + \phi_f p_t + \psi_f s_t \\ p_{t+1} &= \omega_p + \phi_p p_t + \psi_p s_t, \end{aligned}$$

where again s_t is the scaled score with respect to $\xi_t$of the log-likelihood function of the distribution function in (20). In Massacci (2016) the derivation of each one of the quantities is discussed in more detail.

B Tables

	Mean	Standard Deviation	Min	Max	Skewness	Kurtosis	Jarque Bera	Box Pierce
DAX	0.0001	0.0167	-0.1363	0.1523	0.0387	7.3386	0.0000	0.0000
FTSE 100	0.0000	0.0129	-0.0893	0.1046	-0.0258	6.8049	0.0000	0.0000
NIKKEI 225	0.0000	0.0167	-0.1292	0.1323	-0.5680	7.0968	0.0000	0.0000
S&P 500	0.0001	0.0132	-0.0969	0.1033	-0.2373	6.8128	0.0000	0.0000
CAC 40	-0.0001	0.0161	-0.1098	0.1409	0.0540	5.9708	0.0000	0.0000
HANG SENG	0.0001	0.0166	-0.1470	0.1341	-0.2110	9.9489	0.0000	0.0000
IBEX 35	-0.0001	0.01664	-0.1272	0.1313	-0.1194	6.3219	0.0000	0.0000
STOXX 50	-0.0001	0.0164	-0.1041	0.1411	0.0448	5.8213	0.0000	0.0000
AEX	-0.0001	0.0159	-0.1271	0.1041	-0.1396	6.9787	0.0000	0.0000
BVSP	0.0004	0.0199	-0.1503	0.1547	0.0399	4.6854	0.0000	0.0000

Table 2: Descriptive statistics of daily logarithmic returns of the series and the p-value of the Jarque-Bera and Box-Pierce tests (10 lags).

	Ground Intensity							Mark process								
Specification	$exp(f_i^\tau)$	ω_τ	ψ_τ	ϕ_τ	k	δ	b	$\exp(f_i^g)$	ω_g	ψ_g	ϕ_g	ξ	β	Log-Lik	AIC	BIC
$Wss - SPOT$	δ_i	0.107	0.144	0.951	0.894			β_i	-1.216	0.246	0.731	0.057		107.756	-199.512	-150.014
		(0.048)	(0.028)	(0.022)	(0.034)				(0.310)	(0.045)	(0.069)	(0.044)				
$Wsp - SPOT$	δ_i	0.107	0.144	0.951	0.894			ξ_i	-0.386	0.035	0.786		0.010	88.618	-161.236	-111.738
		(0.048)	(0.028)	(0.022)	(0.034)				(0.268)	(0.015)	(0.127)		(0.001)			
$Wps - SPOT$	k_i	-0.020	0.060	0.909		7.546		β_i	-1.216	0.246	0.731	0.057		85.735	-155.47	-105.972
		(0.009)	(0.022)	(0.034)		(0.546)			(0.310)	(0.045)	(0.069)	(0.044)				
$Wpp - SPOT$	k_i	-0.020	0.060	0.909		7.546		ξ_i	-0.386	0.035	0.786		0.010	66.597	-117.194	-67.696
		(0.009)	(0.022)	(0.034)		(0.546)			(0.268)	(0.015)	(0.127)		(0.001)			
$Bss - SPOT$	δ_i	0.093	0.106	0.918	0.696		1.718	β_i	-1.216	0.246	0.731	0.057		126.642	-235.284	-179.598
		(0.055)	(0.033)	(0.045)	(0.212)		(0.242)		(0.310)	(0.045)	(0.069)	(0.044)				
$Bsp - SPOT$	δ_i	0.093	0.106	0.918	0.696		1.718	ξ_i	-0.386	0.035	0.786		0.010	107.504	-197.008	-141.322
		(0.055)	(0.033)	(0.045)	(0.212)		(0.242)		(0.268)	(0.015)	(0.127)		(0.001)			
$Bp_1s - SPOT$	k_i	-0.008	0.156	0.934		3.983	1.579	β_i	-1.216	0.246	0.731	0.057		132.514	**-247.028**	**-191.342**
		(0.022)	(0.037)	(0.035)		(1.136)	(0.172)		(0.310)	(0.045)	(0.069)	(0.044)				
$Bp_1p - SPOT$	k_i	-0.008	0.156	0.934		3.983	1.579	ξ_i	-0.386	0.035	0.786		0.010	113.376	-208.752	-153.066
		(0.022)	(0.037)	(0.035)		(1.136)	(0.172)		(0.268)	(0.015)	(0.127)		(0.001)			
$Bp_2s - SPOT$	b_i	0.560	0.129	0.283	-2.105	0.969		β_i	-1.216	0.246	0.731	0.057		72.772	-127.544	-71.858
		(0.001)	(0.037)	(0.001)	(0.500)	(0.001)			(0.310)	(0.045)	(0.069)	(0.044)				
$Bp_2p - SPOT$	b_i	0.560	0.129	0.283	-2.105	0.969		ξ_i	-0.386	0.035	0.786		0.010	53.634	-89.268	-33.582
		(0.001)	(0.037)	(0.001)	(0.500)	(0.001)			(0.268)	(0.015)	(0.127)		(0.001)			
$Gss - SPOT$	δ_i	0.112	0.143	0.952	0.919			β_i	-1.216	0.246	0.731	0.057		104.072	-192.144	-142.646
		(0.045)	(0.025)	(0.020)	(0.060)				(0.310)	(0.045)	(0.069)	(0.044)				
$Gsp - SPOT$	δ_i	0.112	0.143	0.952	0.919			ξ_i	-0.386	0.035	0.786		0.010	84.934	-153.868	-104.370
		(0.045)	(0.025)	(0.020)	(0.060)				(0.268)	(0.015)	(0.127)		(0.001)			
$Gps - SPOT$	k_i	-0.036	0.130	0.845		12.088		β_i	-1.216	0.246	0.731	0.057		69.861	-123.722	-74.224
		(0.025)	(0.039)	(0.088)		(1.060)			(0.310)	(0.045)	(0.069)	(0.044)				
$Gpp - SPOT$	k_i	-0.036	0.130	0.845		12.088		ξ_i	-0.386	0.035	0.786		0.010	50.723	-85.446	-35.948
		(0.025)	(0.039)	(0.088)		(1.060)			(0.268)	(0.015)	(0.127)		(0.001)			
$GGss - SPOT$	δ_i	-0.056	0.157	0.923	0.477		3.377	β_i	-1.216	0.246	0.731	0.057		122.641	-227.282	-171.596
		(0.074)	(0.038)	(0.041)	(0.049)		(0.644)		(0.310)	(0.045)	(0.069)	(0.044)				
$GGsp - SPOT$	δ_i	-0.056	0.157	0.923	0.477		3.377	ξ_i	-0.386	0.035	0.786		0.010	103.503	-189.006	-133.320
		(0.074)	(0.038)	(0.041)	(0.049)		(0.644)		(0.268)	(0.015)	(0.127)		(0.001)			
$GGp_1s - SPOT$	k_i	-0.688	0.292	0.286		-2.331	1.578	β_i	-1.216	0.246	0.731	0.057		112.898	-207.796	-152.110
		(0.063)	(0.061)	(0.077)		(0.602)	(0.132)		(0.310)	(0.045)	(0.069)	(0.044)				
$GGp_1p - SPOT$	k_i	-0.688	0.292	0.286		-2.331	1.578	ξ_i	-0.386	0.035	0.786		0.010	93.76	-169.52	-113.834
		(0.063)	(0.061)	(0.077)		(0.602)	(0.132)		(0.268)	(0.015)	(0.127)		(0.001)			
$GGp_2s - SPOT$	b_i	0.403	0.120	0.789	-3.423	-1.000		β_i	-1.216	0.246	0.731	0.057		27.004	-36.008	19.678
		(0.259)	(0.035)	(0.117)	(1.327)	(0.125)			(0.310)	(0.045)	(0.069)	(0.044)				
$GGp_2p - SPOT$	b_i	0.403	0.120	0.789	-3.423	-1.000		ξ_i	-0.386	0.035	0.786		0.010	7.866	2.268	57.954
		(0.259)	(0.035)	(0.117)	(1.327)	(0.125)			(0.268)	(0.015)	(0.127)		(0.001)			

Table 3: Parameter estimates of the SPOT model and its corresponding standard error. Log-Lik is the log-likelihood function and the AIC and BIC are the Akaike and the Schwartz information criterion. Best AIC and BIC values across models are printed in boldface. The data analyzed correspond to the DAX daily returns from January 3, 2000 to December 29, 2016.

Bp_1s-SPOT												
Stocks	Ground Intensity					Mark process						
	ω_τ	ψ_τ	ϕ_τ	δ	b	ω_g	ψ_g	ϕ_g	ξ	Log-Lik	AIC	BIC
DAX	-0.008	0.156	0.934	3.983	1.579	-1.216	0.246	0.731	0.057	132.514	-247.028	-191.342
	(0.022)	(0.037)	(0.035)	(1.136)	(0.172)	(0.296)	(0.044)	(0.066)	(0.044)			
FTSE 100	-0.055	0.180	0.843	3.211	1.835	-1.756	0.220	0.628	0.059	214.291	-410.582	-354.896
	(0.049)	(0.046)	(0.081)	(0.637)	(0.189)	(0.444)	(0.044)	(0.095)	(0.048)			
NIKKEI 225	-0.006	0.104	0.930	4.904	1.710	-1.780	0.207	0.620	0.167	126.265	-234.530	-178.844
	(0.020)	(0.039)	(0.058)	(1.111)	(0.168)	(0.432)	(0.045)	(0.092)	(0.053)			
S&P 500	-0.021	0.194	0.932	3.588	1.967	-0.941	0.207	0.801	0.040	234.649	-451.298	-395.612
	(0.023)	(0.039)	(0.033)	(0.694)	(0.198)	(0.260)	(0.041)	(0.056)	(0.055)			
CAC 40	0.011	0.164	0.915	5.471	1.535	-1.502	0.197	0.670	0.064	134.622	-251.244	-195.558
	(0.026)	(0.037)	(0.043)	(1.545)	(0.146)	(0.407)	(0.041)	(0.090)	(0.043)			
HANG SENG	0.002	0.155	0.963	5.501	1.696	-1.204	0.209	0.739	0.123	135.793	-253.586	-197.900
	(0.013)	(0.036)	(0.022)	(1.179)	(0.143)	(0.387)	(0.046)	(0.085)	(0.048)			
IBEX 35	0.012	0.221	0.837	5.045	1.588	-2.490	0.144	0.450	0.103	123.673	-229.346	-173.660
	(0.045)	(0.048)	(0.075)	(1.315)	(0.152)	(1.063)	(0.047)	(0.235)	(0.051)			
STOXX 50	-0.016	0.171	0.888	3.786	1.636	-1.713	0.181	0.620	0.066	133.43	-248.860	-193.174
	(0.035)	(0.041)	(0.056)	(1.005)	(0.179)	(0.484)	(0.040)	(0.108)	(0.050)			
AEX	-0.041	0.191	0.911	2.774	1.930	-1.594	0.225	0.644	0.073	146.848	-275.696	-220.010
	(0.037)	(0.046)	(0.052)	(0.570)	(0.217)	(0.408)	(0.044)	(0.091)	(0.044)			
BVSP	0.002	0.181	0.802	5.188	1.614	-2.607	0.156	0.406	0.040	60.515	-103.030	-47.344
	(0.050)	(0.047)	(0.114)	(1.215)	(0.150)	(1.372)	(0.051)	(0.314)	(0.041)			

Table 4: For all global stock markets, estimation of the parameters of the selected Bp_{1s}-SPOT model and its corresponding standard error in parenthesis. Log-Lik is the log-likelihood function and the AIC and BIC are the Akaike and Schwartz information criterion.

Bp_1s-rSPOT (or simply rSPOT)														
Stocks	Ground Intensity						Mark process							
	ω_τ	ψ_τ	ϕ_τ	δ	b	ς_τ	ω_g	ψ_g	ϕ_g	ξ	ς_g	Log-Lik	AIC	BIC
DAX	1.268	0.038	0.751	4.617	1.527	0.155	-0.223	0.087	0.488	0.052	0.259	145.731	-269.462	-201.402
	(0.472)	(0.057)	(0.092)	(1.368)	(0.154)	(0.057)	(0.390)	(0.060)	(0.125)	(0.044)	(0.078)			
FTSE 100	0.953	0.125	0.651	3.285	1.835	0.125	-0.269	0.052	0.420	0.011	0.289	228.111	-434.222	-366.162
	(0.493)	(0.051)	(0.130)	(0.652)	(0.185)	(0.061)	(0.454)	(0.056)	(0.116)	(0.048)	(0.068)			
NIKKEI 225	1.093	0.039	0.731	5.105	1.706	0.126	0.265	0.026	0.436	0.122	0.333	144.216	-266.432	-198.372
	(0.389)	(0.044)	(0.099)	(1.092)	(0.156)	(0.045)	(0.472)	(0.057)	(0.101)	(0.056)	(0.072)			
S&P 500	1.295	0.104	0.700	3.383	2.040	0.163	-0.372	-0.001	0.112	0.000	0.444	256.752	-491.504	-423.444
	(0.733)	(0.064)	(0.156)	(0.637)	(0.210)	(0.092)	(0.558)	(0.061)	(0.208)	(0.060)	(0.097)			
CAC 40	1.632	0.076	0.672	5.489	1.550	0.179	0.111	0.019	0.364	0.024	0.340	150.571	-279.142	-211.082
	(0.677)	(0.057)	(0.122)	(1.538)	(0.146)	(0.075)	(0.475)	(0.054)	(0.163)	(0.047)	(0.091)			
HANG SENG	1.229	0.125	0.806	6.034	1.664	0.135	0.130	0.043	0.424	0.077	0.314	151.475	-280.950	-212.890
	(0.580)	(0.043)	(0.092)	(1.413)	(0.140)	(0.063)	(0.439)	(0.057)	(0.139)	(0.050)	(0.079)			
IBEX 35	1.295	0.208	0.627	5.444	1.568	0.149	-1.204	-0.035	0.113	0.060	0.336	134.645	-247.290	-179.230
	(0.671)	(0.052)	(0.154)	(1.478)	(0.147)	(0.076)	(0.796)	(0.066)	(0.226)	(0.049)	(0.089)			
STOXX 50	0.765	0.120	0.758	3.835	1.641	0.098	-0.535	0.005	0.320	0.039	0.311	146.084	-270.168	-202.108
	(0.432)	(0.048)	(0.108)	(1.004)	(0.174)	(0.055)	(0.542)	(0.058)	(0.205)	(0.051)	(0.094)			
AEX	1.898	0.087	0.592	3.205	1.829	0.226	-0.068	0.019	-0.012	0.001	0.526	167.458	-312.916	-244.856
	(0.749)	(0.061)	(0.152)	(0.693)	(0.189)	(0.086)	(0.589)	(0.059)	(0.166)	(0.049)	(0.105)			
BVSP	1.044	0.125	0.624	5.186	1.630	0.124	-1.133	0.028	0.308	0.026	0.227	71.876	-121.752	-53.692
	(0.516)	(0.050)	(0.158)	(1.209)	(0.151)	(0.062)	(0.708)	(0.057)	(0.218)	(0.039)	(0.069)			

Table 5: For all global stock markets, estimation of the parameters of the Bp_{1s}-rSPOT model and its corresponding standard error in parenthesis. Log-Lik is the log-likelihood function and the AIC and BIC are the Akaike and Schwartz information criterion.

			2017									2017-2018								
		α	Exc.	LR_{uc}	LR_{ind}	LR_{cc}	DQ_{hit}	DQ_{VaR}	MCS_{uc}	MCS_{ind}	MCS_{cc}	Exc.	LR_{uc}	LR_{ind}	LR_{cc}	DQ_{hit}	DQ_{VaR}	MCS_{uc}	MCS_{ind}	MCS_{cc}
SPOT	DAX	0.95	2	0.00	0.85	0.00	0.85	0.83	0.00	0.82	0.37	12	0.03	0.35	0.06	0.36	0.65	0.04	0.29	0.57
		0.975	2	0.10	0.85	0.24	0.85	1.00	0.10	0.81	0.38	9	0.65	0.53	0.74	0.53	0.82	0.70	0.63	0.71
		0.99	1	0.39	0.92	0.68	0.92	1.00	0.52	0.51	0.98	3	0.54	0.83	0.81	0.84	0.94	0.73	0.71	0.58
		0.999	0	0.51	1.00	0.81	1.00	1.00	1.00	1.00	1.00	0	0.36	1.00	0.66	1.00	1.00	1.00	1.00	1.00
	FTSE 100	0.95	4	0.02	0.69	0.05	0.70	0.62	0.03	0.62	0.79	14	0.10	0.45	0.20	0.46	0.49	0.11	0.35	0.69
		0.975	3	0.27	0.77	0.52	0.77	1.00	0.28	0.67	0.67	9	0.65	0.18	0.36	0.18	0.03	0.70	0.55	0.87
		0.99	1	0.39	0.92	0.68	0.92	0.65	0.48	0.71	0.59	5	0.69	0.04	0.12	0.04	0.08	0.64	0.27	0.52
		0.999	0	0.51	1.00	0.81	1.00	1.00	1.00	1.00	1.00	1	0.44	0.94	0.74	0.94	1.00	0.39	0.44	0.86
	NIKKEI 225	0.95	3	0.00	0.77	0.02	0.78	0.56	0.00	0.09	0.17	13	0.06	0.41	0.12	0.42	0.70	0.08	0.05	0.10
		0.975	3	0.27	0.77	0.52	0.77	1.00	0.30	0.08	0.16	9	0.65	0.18	0.36	0.18	0.24	0.57	0.23	0.45
		0.99	1	0.39	0.92	0.68	0.92	1.00	0.57	0.06	0.12	5	0.69	0.04	0.12	0.04	0.04	0.68	0.32	0.61
		0.999	0	0.51	1.00	0.81	1.00	1.00	1.00	1.00	1.00	0	0.36	1.00	0.66	1.00	1.00	1.00	1.00	1.00
	S&P 500	0.95	3	0.00	0.77	0.02	0.78	1.00	0.00	0.93	0.12	12	0.03	0.04	0.01	0.05	0.07	0.03	0.12	0.24
		0.975	3	0.27	0.77	0.52	0.77	1.00	0.33	0.93	0.13	9	0.65	0.01	0.03	0.01	0.04	0.63	0.39	0.77
		0.99	3	0.57	0.77	0.82	0.77	0.43	0.35	0.94	0.13	7	0.20	0.00	0.01	0.00	0.00	0.15	0.41	0.85
		0.999	0	0.51	1.00	0.81	1.00	1.00	1.00	1.00	1.00	1	0.44	0.94	0.74	0.94	1.00	0.54	0.44	0.88
	CAC 40	0.95	2	0.00	0.85	0.00	0.85	0.81	0.00	0.72	0.57	11	0.02	0.28	0.03	0.30	0.23	0.02	0.24	0.48
		0.975	2	0.10	0.85	0.24	0.85	0.84	0.09	0.72	0.58	7	0.25	0.10	0.13	0.10	0.14	0.34	0.59	0.83
		0.99	1	0.39	0.92	0.68	0.92	1.00	0.25	0.64	0.74	3	0.54	0.83	0.81	0.84	0.97	0.58	0.62	0.74
		0.999	0	0.51	1.00	0.81	1.00	1.00	1.00	1.00	1.00	0	0.36	1.00	0.66	1.00	1.00	1.00	1.00	1.00
	HANG	0.95	1	0.00	0.92	0.00	0.92	0.94	0.00	0.07	0.12	14	0.10	0.32	0.16	0.34	0.25	0.09	0.00	0.00
		0.975	1	0.02	0.92	0.07	0.92	1.00	0.04	0.06	0.13	5	0.06	0.73	0.16	0.73	0.62	0.08	0.22	0.41
		0.99	1	0.39	0.92	0.68	0.92	1.00	0.32	0.06	0.12	2	0.23	0.89	0.49	0.89	0.72	0.23	0.66	0.71
		0.999	0	0.51	1.00	0.81	1.00	1.00	1.00	1.00	1.00	0	0.36	1.00	0.66	1.00	1.00	1.00	1.00	1.00
	IBEX 35	0.95	3	0.00	0.77	0.02	0.78	0.67	0.01	0.12	0.23	13	0.06	0.41	0.12	0.42	0.45	0.06	0.08	0.16
		0.975	3	0.27	0.77	0.52	0.77	0.95	0.39	0.12	0.24	8	0.43	0.13	0.24	0.14	0.06	0.50	0.32	0.63
		0.99	1	0.39	0.92	0.68	0.92	1.00	0.67	0.23	0.45	3	0.54	0.83	0.81	0.84	0.65	0.65	0.59	0.80
		0.999	0	0.51	1.00	0.81	1.00	1.00	1.00	1.00	1.00	0	0.36	1.00	0.66	1.00	1.00	1.00	1.00	1.00
	STOXX 50	0.95	1	0.00	0.92	0.00	0.92	0.96	0.00	0.51	0.99	10	0.01	0.48	0.02	0.49	0.62	0.01	0.21	0.42
		0.975	1	0.02	0.92	0.07	0.92	1.00	0.04	0.51	0.99	7	0.25	0.62	0.46	0.63	0.62	0.33	0.53	0.95
		0.99	1	0.39	0.92	0.68	0.92	1.00	0.33	0.50	0.99	4	0.93	0.78	0.96	0.78	0.82	0.95	0.85	0.30
		0.999	0	0.51	1.00	0.81	1.00	1.00	1.00	1.00	1.00	0	0.36	1.00	0.66	1.00	1.00	1.00	1.00	1.00
	AEX	0.95	1	0.00	0.92	0.00	0.92	0.96	0.00	0.51	1.00	9	0.00	0.53	0.01	0.54	0.80	0.00	0.24	0.48
		0.975	1	0.02	0.92	0.07	0.92	1.00	0.04	0.50	1.00	6	0.13	0.68	0.29	0.68	0.50	0.14	0.67	0.66
		0.99	1	0.39	0.92	0.68	0.92	1.00	0.59	0.50	1.00	5	0.69	0.73	0.87	0.73	0.86	0.70	0.81	0.39
		0.999	0	0.51	1.00	0.81	1.00	1.00	1.00	1.00	1.00	1	0.44	0.94	0.74	0.94	0.40	0.41	0.44	0.87
	BVSP	0.95	3	0.00	0.77	0.02	0.78	1.00	0.00	0.74	0.53	8	0.00	0.58	0.00	0.59	0.84	0.00	0.72	0.56
		0.975	3	0.27	0.77	0.52	0.77	1.00	0.40	0.73	0.54	5	0.06	0.73	0.16	0.73	0.04	0.04	0.98	0.06
		0.99	2	0.93	0.85	0.98	0.85	0.81	0.74	0.79	0.43	3	0.54	0.83	0.81	0.84	0.30	0.61	0.99	0.03
		0.999	0	0.51	1.00	0.81	1.00	1.00	1.00	1.00	1.00	0	0.36	1.00	0.66	1.00	1.00	1.00	1.00	1.00

			2017									2017-2018								
		α	Exc.	LR_{uc}	LR_{ind}	LR_{cc}	DQ_{hit}	DQ_{VaR}	MCS_{uc}	MCS_{ind}	MCS_{cc}	Exc.	LR_{uc}	LR_{ind}	LR_{cc}	DQ_{hit}	DQ_{VaR}	MCS_{uc}	MCS_{ind}	MCS_{cc}
rSPOT	DAX	0.95	12	0.68	0.70	0.85	0.70	1.00	0.55	0.78	0.43	18	0.51	0.20	0.35	0.21	1.00	0.50	0.16	0.32
		0.975	8	0.27	0.43	0.40	0.44	1.00	0.27	0.74	0.51	8	0.43	0.58	0.62	0.58	1.00	0.44	0.01	0.02
		0.99	2	0.93	0.85	0.98	0.85	1.00	0.91	0.06	0.13	2	0.23	0.89	0.49	0.89	0.75	0.35	0.44	0.90
		0.999	0	0.51	1.00	0.81	1.00	1.00	1.00	1.00	1.00	0	0.36	1.00	0.66	1.00	1.00	1.00	1.00	1.00
	FTSE 100	0.95	8	0.38	0.43	0.50	0.44	1.00	0.32	0.96	0.08	19	0.67	0.84	0.90	0.84	0.18	0.76	0.39	0.77
		0.975	7	0.48	0.49	0.62	0.50	1.00	0.49	0.99	0.01	9	0.65	0.53	0.74	0.53	1.00	0.63	0.64	0.72
		0.99	5	0.09	0.62	0.22	0.63	1.00	0.13	0.86	0.28	6	0.40	0.68	0.64	0.68	1.00	0.32	0.63	0.76
		0.999	2	0.02	0.85	0.07	0.85	1.00	0.02	0.41	0.81	1	0.44	0.94	0.74	0.94	1.00	0.28	0.03	0.06
	NIKKEI 225	0.95	12	0.68	0.23	0.45	0.24	1.00	0.65	0.43	0.87	15	0.17	0.29	0.22	0.30	0.42	0.15	0.53	0.94
		0.975	5	0.89	0.62	0.88	0.63	1.00	0.90	0.67	0.67	4	0.02	0.78	0.07	0.78	0.92	0.01	0.16	0.32
		0.99	4	0.25	0.69	0.48	0.70	1.00	0.19	0.77	0.46	1	0.06	0.94	0.17	0.94	0.88	0.13	0.08	0.16
		0.999	2	0.02	0.85	0.07	0.85	1.00	0.02	0.89	0.23	0	0.36	1.00	0.66	1.00	1.00	1.00	1.00	1.00
	S&P 500	0.95	5	0.05	0.62	0.13	0.63	1.00	0.03	0.93	0.15	17	0.37	0.18	0.27	0.19	0.02	0.39	0.07	0.15
		0.975	5	0.89	0.62	0.88	0.63	1.00	0.97	0.92	0.15	6	0.13	0.68	0.29	0.68	0.25	0.17	0.54	0.92
		0.99	2	0.93	0.85	0.98	0.85	1.00	1.00	0.49	0.97	0	0.00	1.00	0.02	1.00	1.00	0.03	0.00	0.00
		0.999	1	0.22	0.92	0.47	0.92	1.00	0.23	0.62	0.73	0	0.36	1.00	0.66	1.00	1.00	1.00	1.00	1.00
	CAC 40	0.95	10	0.84	0.32	0.60	0.33	1.00	0.96	0.91	0.18	24	0.49	0.18	0.32	0.19	0.28	0.43	0.34	0.66
		0.975	6	0.77	0.55	0.80	0.56	1.00	0.76	0.67	0.66	13	0.44	0.06	0.12	0.06	1.00	0.47	0.23	0.46
		0.99	2	0.93	0.85	0.98	0.85	1.00	0.90	0.42	0.84	2	0.23	0.89	0.49	0.89	1.00	0.39	0.23	0.45
		0.999	0	0.51	1.00	0.81	1.00	1.00	1.00	1.00	1.00	0	0.36	1.00	0.66	1.00	1.00	1.00	1.00	1.00
	HANG	0.95	5	0.05	0.62	0.13	0.63	1.00	0.06	0.99	0.03	11	0.02	0.44	0.04	0.45	1.00	0.02	0.07	0.14
		0.975	3	0.27	0.77	0.52	0.77	1.00	0.35	0.95	0.11	6	0.13	0.68	0.29	0.68	1.00	0.16	0.05	0.11
		0.99	1	0.39	0.92	0.68	0.92	1.00	0.26	0.78	0.43	4	0.93	0.78	0.96	0.78	1.00	0.86	0.12	0.24
		0.999	1	0.22	0.92	0.47	0.92	1.00	0.35	0.77	0.45	0	0.36	1.00	0.66	1.00	1.00	1.00	1.00	1.00
	IBEX 35	0.95	12	0.68	0.23	0.45	0.24	1.00	0.76	0.53	0.95	19	0.67	0.24	0.46	0.25	1.00	0.64	0.71	0.58
		0.975	10	0.07	0.32	0.11	0.33	1.00	0.06	0.70	0.58	11	0.86	0.44	0.73	0.45	1.00	0.79	0.69	0.62
		0.99	6	0.03	0.55	0.08	0.56	1.00	0.04	0.35	0.71	5	0.69	0.73	0.87	0.73	1.00	0.52	0.34	0.66
		0.999	5	0.00	0.62	0.00	0.62	1.00	0.00	0.50	0.99	1	0.44	0.94	0.74	0.94	1.00	0.43	0.03	0.05
	STOXX 50	0.95	10	0.84	0.48	0.76	0.49	1.00	0.98	0.82	0.35	20	0.85	0.30	0.57	0.31	0.17	0.97	0.06	0.11
		0.975	8	0.27	0.29	0.31	0.29	1.00	0.19	0.69	0.63	7	0.25	0.62	0.46	0.63	1.00	0.24	0.49	0.99
		0.99	5	0.09	0.09	0.06	0.09	1.00	0.08	0.54	0.93	2	0.23	0.89	0.49	0.89	1.00	0.36	0.23	0.46
		0.999	0	0.51	1.00	0.81	1.00	1.00	1.00	1.00	1.00	0	0.36	1.00	0.66	1.00	1.00	1.00	1.00	1.00
	AEX	0.95	8	0.38	0.43	0.50	0.44	1.00	0.32	0.55	0.87	15	0.17	0.11	0.10	0.11	0.24	0.15	0.25	0.50
		0.975	5	0.89	0.62	0.88	0.63	1.00	0.99	0.30	0.61	7	0.25	0.00	0.01	0.00	1.00	0.27	0.24	0.46
		0.99	4	0.25	0.69	0.48	0.70	1.00	0.14	0.48	0.94	3	0.54	0.01	0.03	0.01	1.00	0.54	0.17	0.36
		0.999	2	0.02	0.85	0.07	0.85	1.00	0.03	0.61	0.75	0	0.36	1.00	0.66	1.00	1.00	1.00	1.00	1.00
	BVSP	0.95	8	0.38	0.43	0.50	0.44	0.44	0.39	0.44	0.86	19	0.67	0.18	0.37	0.19	0.22	0.74	0.12	0.25
		0.975	5	0.89	0.62	0.88	0.63	0.65	0.81	0.67	0.67	7	0.25	0.62	0.46	0.63	0.63	0.34	0.62	0.76
		0.99	1	0.39	0.92	0.68	0.92	1.00	0.29	0.54	0.91	1	0.06	0.94	0.17	0.94	0.97	0.05	0.81	0.39
		0.999	0	0.51	1.00	0.81	1.00	1.00	1.00	1.00	1.00	1	0.44	0.94	0.74	0.94	0.97	0.37	0.81	0.38

Table 6: VaR accuracy tests of the SPOT (top-panel) and the rSPOT (bottom-panel) models for the out-sample periods, i.e, from January 4, 2017 until December 29, 2017 (only year 2017), and from January 4, 2017 until December 27, 2018 (2017-2018). Entries in the rows are the significance levels (p-values) of the respective tests, with the exception of the confidence level α for the VaR and the number of exceptions (Exc.).

			2017								2017-2018								
	α	Exc.	LR_{uc}	LR_{ind}	LR_{cc}	DQ_{hit}	DQ_{VaR}	MCS_{uc}	MCS_{ind}	MCS_{cc}	Exc.	LR_{uc}	LR_{ind}	LR_{cc}	DQ_{hit}	DQ_{VaR}	MCS_{uc}	MCS_{ind}	MCS_{cc}
BPOT																			
DAX	0.95	16	0.12	0.89	0.29	0.90	0.01	0.13	0.01	0.01	32	0.02	0.68	0.06	0.68	0.22	0.02	0.05	0.10
	0.975	11	0.03	0.58	0.08	0.59	0.02	0.04	0.08	0.17	20	0.01	0.32	0.02	0.33	0.04	0.01	0.04	0.09
	0.99	3	0.57	0.77	0.82	0.77	0.40	0.63	0.53	0.96	9	0.04	0.53	0.10	0.53	0.29	0.03	0.51	0.99
	0.999	0	0.51	1.00	0.81	1.00	1.00	1.00	1.00	1.00	1	0.44	0.94	0.74	0.94	0.98	0.20	0.02	0.05
FTSE 100	0.95	26	0.00	0.10	0.00	0.11	0.00	0.00	0.05	0.10	47	0.00	0.04	0.00	0.04	0.00	0.00	0.00	0.00
	0.975	12	0.01	0.16	0.02	0.16	0.00	0.01	0.07	0.15	25	0.00	0.01	0.00	0.01	0.00	0.00	0.13	0.24
	0.99	2	0.93	0.85	0.98	0.85	0.73	0.91	0.97	0.05	7	0.20	0.62	0.40	0.63	0.09	0.15	0.27	0.52
	0.999	0	0.51	1.00	0.81	1.00	1.00	1.00	1.00	1.00	1	0.44	0.94	0.74	0.94	1.00	0.18	0.03	0.05
NIKKEI 225	0.95	12	0.68	0.23	0.45	0.24	0.44	0.70	0.41	0.82	28	0.13	0.93	0.31	0.93	0.95	0.14	0.35	0.69
	0.975	4	0.54	0.69	0.77	0.70	0.77	0.51	0.42	0.84	12	0.63	0.35	0.57	0.35	0.63	0.57	0.08	0.17
	0.99	2	0.93	0.85	0.98	0.85	0.93	0.96	0.23	0.47	5	0.69	0.04	0.12	0.04	0.04	0.75	0.12	0.26
	0.999	0	0.51	1.00	0.81	1.00	1.00	1.00	1.00	1.00	1	0.44	0.94	0.74	0.94	0.69	0.32	0.10	0.19
S&P 500	0.95	16	0.12	0.11	0.08	0.12	0.01	0.12	0.27	0.56	26	0.26	0.76	0.51	0.76	0.94	0.26	0.03	0.06
	0.975	7	0.48	0.49	0.62	0.50	0.46	0.46	0.59	0.83	11	0.86	0.28	0.55	0.29	0.46	0.73	0.14	0.28
	0.99	3	0.57	0.77	0.82	0.77	0.60	0.46	0.72	0.57	7	0.20	0.10	0.11	0.10	0.09	0.15	0.35	0.72
	0.999	0	0.51	1.00	0.81	1.00	1.00	1.00	1.00	1.00	2	0.08	0.89	0.21	0.89	0.23	0.04	0.61	0.80
CAC 40	0.95	16	0.12	0.89	0.29	0.90	0.02	0.12	0.06	0.12	33	0.01	0.15	0.01	0.16	0.02	0.01	0.13	0.25
	0.975	9	0.14	0.37	0.23	0.38	0.15	0.15	0.44	0.84	22	0.00	0.13	0.00	0.13	0.03	0.00	0.03	0.06
	0.99	3	0.57	0.77	0.82	0.77	0.60	0.47	0.89	0.22	9	0.04	0.18	0.05	0.18	0.02	0.02	0.20	0.38
	0.999	0	0.51	1.00	0.81	1.00	1.00	1.00	1.00	1.00	1	0.44	0.94	0.74	0.94	0.38	0.30	0.03	0.04
HANG	0.95	29	0.00	0.10	0.00	0.11	0.00	0.00	0.01	0.02	41	0.00	0.61	0.00	0.61	0.06	0.00	0.05	0.10
	0.975	11	0.03	0.11	0.03	0.11	0.01	0.02	0.24	0.48	15	0.18	0.56	0.34	0.56	0.06	0.15	0.01	0.02
	0.99	2	0.93	0.85	0.98	0.85	0.11	0.83	0.12	0.22	7	0.20	0.62	0.40	0.63	0.33	0.20	0.32	0.63
	0.999	0	0.51	1.00	0.81	1.00	1.00	1.00	1.00	1.00	1	0.44	0.94	0.74	0.94	0.32	0.26	0.44	0.86
IBEX 35	0.95	30	0.00	0.68	0.00	0.68	0.00	0.00	0.16	0.29	37	0.00	0.12	0.00	0.13	0.00	0.00	0.14	0.28
	0.975	12	0.01	0.16	0.02	0.16	0.05	0.01	0.28	0.57	18	0.03	0.22	0.05	0.22	0.01	0.02	0.73	0.58
	0.99	2	0.93	0.85	0.98	0.85	0.97	0.99	0.17	0.34	5	0.69	0.73	0.87	0.73	0.42	0.79	0.35	0.69
	0.999	1	0.22	0.92	0.47	0.92	0.39	0.31	0.23	0.46	1	0.44	0.94	0.74	0.94	0.99	0.60	0.03	0.05
STOXX 50	0.95	23	0.00	0.28	0.00	0.29	0.05	0.00	0.07	0.14	34	0.01	0.18	0.01	0.19	0.06	0.01	0.03	0.06
	0.975	8	0.27	0.29	0.31	0.29	0.09	0.21	0.21	0.41	19	0.02	0.27	0.03	0.27	0.23	0.02	0.41	0.83
	0.99	3	0.57	0.77	0.82	0.77	0.61	0.39	0.89	0.22	5	0.69	0.73	0.87	0.73	0.19	0.68	0.79	0.45
	0.999	0	0.51	1.00	0.81	1.00	1.00	1.00	1.00	1.00	1	0.44	0.94	0.74	0.94	0.56	0.29	0.03	0.05
AEX	0.95	26	0.00	0.61	0.00	0.62	0.35	0.00	0.41	0.79	35	0.00	0.08	0.00	0.09	0.16	0.00	0.04	0.08
	0.975	8	0.27	0.43	0.40	0.44	0.14	0.24	0.13	0.26	15	0.18	0.11	0.11	0.11	0.02	0.16	0.08	0.15
	0.99	2	0.93	0.85	0.98	0.85	0.58	1.00	0.82	0.38	6	0.40	0.68	0.64	0.68	0.48	0.30	0.05	0.10
	0.999	0	0.51	1.00	0.81	1.00	1.00	1.00	1.00	1.00	2	0.08	0.89	0.21	0.89	0.98	0.05	0.45	0.88
BVSP	0.95	15	0.20	0.37	0.29	0.38	0.08	0.23	0.12	0.23	34	0.01	0.89	0.02	0.89	0.16	0.01	0.00	0.01
	0.975	6	0.77	0.55	0.80	0.56	0.17	0.59	0.16	0.34	11	0.86	0.44	0.73	0.45	0.27	0.92	0.33	0.65
	0.99	2	0.93	0.85	0.98	0.85	0.15	0.74	0.79	0.43	2	0.23	0.89	0.49	0.89	0.15	0.19	0.80	0.40
	0.999	1	0.22	0.92	0.47	0.92	0.61	0.26	0.63	0.75	1	0.44	0.94	0.74	0.94	0.58	0.36	0.81	0.38
			2017								2017-2018								
	α	Exc.	LR_{uc}	LR_{ind}	LR_{cc}	DQ_{hit}	DQ_{VaR}	MCS_{uc}	MCS_{ind}	MCS_{cc}	Exc.	LR_{uc}	LR_{ind}	LR_{cc}	DQ_{hit}	DQ_{VaR}	MCS_{uc}	MCS_{ind}	MCS_{cc}
rBPOT																			
DAX	0.95	45	0.00	0.07	0.00	0.07	0.08	0.00	0.14	0.22	60	0.00	0.56	0.00	0.56	0.84	0.00	0.08	0.14
	0.975	24	0.00	0.66	0.00	0.67	0.91	0.00	0.34	0.66	37	0.00	0.12	0.00	0.13	0.30	0.00	0.54	0.97
	0.99	13	0.00	0.19	0.00	0.20	0.28	0.00	0.72	0.59	21	0.00	0.14	0.00	0.14	0.32	0.00	0.69	0.64
	0.999	1	0.22	0.92	0.47	0.92	0.57	0.27	0.14	0.28	1	0.44	0.94	0.74	0.94	0.99	0.45	0.02	0.05
FTSE 100	0.95	42	0.00	0.77	0.00	0.76	0.55	0.00	0.94	0.19	53	0.00	0.07	0.00	0.08	0.09	0.00	0.06	0.12
	0.975	25	0.00	0.21	0.00	0.21	0.10	0.00	0.14	0.26	38	0.00	0.01	0.00	0.02	0.01	0.00	0.09	0.17
	0.99	15	0.00	0.37	0.00	0.37	0.42	0.00	0.28	0.57	18	0.00	0.80	0.00	0.80	0.48	0.00	0.64	0.75
	0.999	2	0.02	0.85	0.07	0.85	0.39	0.02	0.75	0.50	4	0.00	0.78	0.00	0.78	0.80	0.00	0.48	0.95
NIKKEI 225	0.95	27	0.00	0.84	0.00	0.85	0.98	0.00	0.11	0.21	46	0.00	0.36	0.00	0.37	0.66	0.00	0.10	0.19
	0.975	15	0.00	0.13	0.00	0.14	0.32	0.00	0.31	0.65	27	0.00	0.35	0.00	0.36	0.65	0.00	0.28	0.55
	0.99	7	0.01	0.49	0.02	0.49	0.38	0.01	0.67	0.66	13	0.00	0.41	0.00	0.41	0.57	0.00	0.80	0.41
	0.999	1	0.22	0.92	0.47	0.92	0.66	0.36	0.78	0.45	1	0.44	0.94	0.74	0.94	0.94	0.59	0.37	0.75
S&P 500	0.95	111	0.00	0.14	0.00	0.14	0.00	0.00	0.09	0.00	84	0.00	0.22	0.00	0.24	0.06	0.00	0.75	0.65
	0.975	63	0.00	0.60	0.00	0.59	0.00	0.00	0.07	0.08	43	0.00	0.81	0.00	0.82	0.29	0.00	0.66	0.69
	0.99	26	0.00	0.11	0.00	0.12	0.00	0.00	0.62	0.82	18	0.00	0.80	0.00	0.80	0.46	0.00	0.84	0.33
	0.999	4	0.00	0.69	0.00	0.70	0.60	0.00	0.76	0.46	5	0.00	0.73	0.00	0.73	0.25	0.00	0.11	0.23
CAC 40	0.95	41	0.00	0.58	0.00	0.58	0.83	0.00	0.17	0.30	43	0.00	0.18	0.00	0.19	0.40	0.00	0.07	0.13
	0.975	18	0.00	0.08	0.00	0.08	0.21	0.00	0.74	0.54	29	0.00	0.05	0.00	0.05	0.16	0.00	0.17	0.33
	0.99	9	0.00	0.37	0.00	0.38	0.67	0.00	0.59	0.82	12	0.00	0.40	0.01	0.40	0.67	0.00	0.56	0.88
	0.999	1	0.22	0.92	0.47	0.92	0.31	0.26	0.63	0.73	2	0.08	0.89	0.21	0.89	0.91	0.13	0.13	0.25
HANG	0.95	35	0.00	0.91	0.00	0.90	0.22	0.00	0.49	0.92	40	0.00	0.93	0.00	0.93	0.99	0.00	0.65	0.73
	0.975	16	0.00	0.83	0.00	0.84	0.70	0.00	0.76	0.48	21	0.00	0.14	0.00	0.14	0.32	0.00	0.99	0.02
	0.99	7	0.01	0.49	0.02	0.49	0.75	0.01	0.76	0.46	10	0.02	0.48	0.04	0.49	0.78	0.02	0.14	0.29
	0.999	1	0.22	0.92	0.47	0.92	0.03	0.29	0.19	0.38	2	0.08	0.89	0.21	0.89	0.75	0.05	0.44	0.89
IBEX 35	0.95	40	0.00	0.87	0.00	0.88	0.19	0.00	0.83	0.41	44	0.00	0.09	0.00	0.10	0.01	0.00	0.21	0.38
	0.975	14	0.00	0.29	0.00	0.29	0.04	0.00	0.72	0.55	25	0.00	0.06	0.00	0.06	0.03	0.00	0.68	0.63
	0.99	7	0.01	0.49	0.02	0.49	0.40	0.01	0.68	0.64	10	0.02	0.48	0.04	0.49	0.21	0.01	0.86	0.28
	0.999	1	0.22	0.92	0.47	0.92	0.32	0.21	0.23	0.45	2	0.08	0.89	0.21	0.89	0.99	0.10	0.42	0.82
STOXX 50	0.95	54	0.00	0.05	0.00	0.05	0.03	0.00	0.95	0.21	59	0.00	0.25	0.00	0.29	0.04	0.00	0.04	0.07
	0.975	25	0.00	0.45	0.00	0.45	0.26	0.00	0.23	0.41	36	0.00	0.27	0.00	0.28	0.43	0.00	0.08	0.16
	0.99	11	0.00	0.27	0.00	0.28	0.21	0.00	0.44	0.86	12	0.00	0.40	0.01	0.40	0.64	0.00	0.70	0.60
	0.999	1	0.22	0.92	0.47	0.92	0.39	0.06	0.63	0.74	1	0.44	0.94	0.74	0.94	0.99	0.35	0.03	0.05
AEX	0.95	68	0.00	0.31	0.00	0.30	0.00	0.00	0.94	0.41	74	0.00	0.19	0.00	0.22	0.01	0.00	0.48	0.86
	0.975	44	0.00	0.76	0.00	0.71	0.01	0.00	0.79	0.57	44	0.00	0.01	0.00	0.01	0.00	0.00	0.20	0.37
	0.99	21	0.00	0.45	0.00	0.50	0.00	0.00	0.10	0.20	18	0.00	0.76	0.00	0.80	0.68	0.00	0.24	0.48
	0.999	3	0.00	0.81	0.01	0.77	0.01	0.00	0.69	0.59	3	0.01	0.83	0.03	0.83	0.98	0.01	0.38	0.74
BVSP	0.95	23	0.00	0.73	0.00	0.73	0.44	0.00	0.76	0.50	34	0.01	0.89	0.02	0.89	0.68	0.00	0.15	0.29
	0.975	10	0.07	0.48	0.14	0.48	0.63	0.06	0.12	0.24	9	0.65	0.53	0.74	0.53	0.65	0.72	0.58	0.82
	0.99	2	0.93	0.85	0.98	0.85	0.91	0.97	0.79	0.43	3	0.54	0.83	0.81	0.84	0.67	0.79	0.64	0.72
	0.999	1	0.22	0.92	0.47	0.92	0.95	0.29	0.63	0.74	1	0.44	0.94	0.74	0.94	0.81	0.51	0.81	0.38

Table 7: VaR accuracy tests of the BPOT (top-panel) and the rBPOT (bottom-panel)) models for the out-sample periods,i.e, from January 4, 2017 until December 29, 2017 (only year 2017), and from January 4, 2017 until December 27, 2018 (2017-2018). Entries in the rows are the significance levels (p-values) of the respective tests, with the exception of the confidence level α for the VaR and the number of exceptions (Exc.).

			2017									2017-2018								
		α	Exc.	LR_{uc}	LR_{ind}	LR_{cc}	DQ_{hit}	DQ_{VaR}	MCS_{uc}	MCS_{ind}	MCS_{cc}	Exc.	LR_{uc}	LR_{ind}	LR_{cc}	DQ_{hit}	DQ_{VaR}	MCS_{uc}	MCS_{ind}	MCS_{cc}
MPOT	DAX	0.95	34	0.00	0.88	0.00	0.89	0.00	0.00	0.00	0.00	41	0.00	0.12	0.00	0.12	0.00	0.00	0.00	0.00
		0.975	10	0.07	0.48	0.14	0.48	1.00	0.08	0.01	0.02	16	0.10	0.64	0.24	0.64	0.01	0.12	0.13	0.25
		0.99	0	0.04	1.00	0.12	1.00	1.00	0.14	0.00	0.00	3	0.54	0.83	0.81	0.84	0.41	0.79	0.19	0.37
		0.999	0	0.51	1.00	0.81	1.00	1.00	1.00	1.00	1.00	0	0.36	1.00	0.66	1.00	1.00	1.00	1.00	1.00
	FTSE 100	0.95	39	0.00	0.01	0.00	0.01	0.00	0.00	0.00	0.00	67	0.00	0.00	0.00	0.00	0.00	0.00	0.00	0.00
		0.975	13	0.00	0.22	0.01	0.22	0.00	0.00	0.05	0.10	28	0.00	0.01	0.00	0.01	0.00	0.00	0.02	0.04
		0.99	1	0.39	0.92	0.68	0.92	0.97	0.28	0.70	0.58	4	0.93	0.78	0.96	0.78	1.00	0.81	0.19	0.38
		0.999	0	0.51	1.00	0.81	1.00	1.00	1.00	1.00	1.00	1	0.44	0.94	0.74	0.94	1.00	0.37	0.02	0.05
	NIKKEI 225	0.95	13	0.47	0.19	0.33	0.21	0.08	0.40	0.55	0.93	27	0.19	0.84	0.41	0.85	0.43	0.14	0.34	0.68
		0.975	3	0.27	0.77	0.52	0.77	0.70	0.29	0.67	0.66	10	0.89	0.23	0.48	0.23	0.33	0.86	0.02	0.04
		0.99	0	0.04	1.00	0.12	1.00	1.00	0.02	0.00	0.00	3	0.54	0.83	0.81	0.84	0.76	0.62	0.39	0.76
		0.999	0	0.51	1.00	0.81	1.00	1.00	1.00	1.00	1.00	0	0.36	1.00	0.66	1.00	1.00	1.00	1.00	1.00
	S&P 500	0.95	31	0.00	0.20	0.00	0.21	0.00	0.00	0.00	0.00	33	0.01	0.15	0.01	0.16	0.01	0.01	0.01	0.02
		0.975	3	0.27	0.77	0.52	0.77	0.60	0.37	0.71	0.57	9	0.65	0.18	0.36	0.18	0.06	0.71	0.10	0.20
		0.99	0	0.04	1.00	0.12	1.00	1.00	0.16	0.00	0.00	4	0.93	0.02	0.08	0.02	0.01	0.98	0.12	0.25
		0.999	0	0.51	1.00	0.81	1.00	1.00	1.00	1.00	1.00	1	0.44	0.94	0.74	0.94	1.00	0.39	0.43	0.86
	CAC 40	0.95	50	0.00	0.04	0.00	0.05	0.00	0.00	0.00	0.00	70	0.00	0.00	0.00	0.00	0.00	0.00	0.00	0.00
		0.975	14	0.00	0.04	0.00	0.05	0.00	0.00	0.01	0.03	26	0.00	0.02	0.00	0.02	0.00	0.00	0.01	0.01
		0.99	0	0.04	1.00	0.12	1.00	1.00	0.17	0.00	0.00	8	0.09	0.13	0.08	0.14	1.00	0.11	0.01	0.01
		0.999	0	0.51	1.00	0.81	1.00	1.00	1.00	1.00	1.00	1	0.44	0.94	0.74	0.94	0.56	0.64	0.02	0.05
	HANG	0.95	27	0.00	0.01	0.00	0.01	0.00	0.00	0.00	0.00	34	0.01	0.18	0.01	0.19	0.00	0.00	0.00	0.00
		0.975	6	0.77	0.14	0.33	0.15	1.00	0.69	0.00	0.00	14	0.29	0.08	0.12	0.08	0.00	0.21	0.02	0.03
		0.99	1	0.39	0.92	0.68	0.92	1.00	0.70	0.07	0.13	4	0.93	0.78	0.96	0.78	0.42	0.86	0.30	0.59
		0.999	0	0.51	1.00	0.81	1.00	1.00	1.00	1.00	1.00	1	0.44	0.94	0.74	0.94	1.00	0.34	0.44	0.88
	IBEX 35	0.95	37	0.00	0.04	0.00	0.05	0.00	0.00	0.00	0.00	40	0.00	0.01	0.00	0.01	0.00	0.00	0.00	0.01
		0.975	10	0.07	0.48	0.14	0.48	0.01	0.05	0.21	0.41	15	0.18	0.11	0.11	0.11	0.00	0.20	0.62	0.76
		0.99	1	0.39	0.92	0.68	0.92	1.00	0.75	0.22	0.46	3	0.54	0.83	0.81	0.84	0.37	0.54	0.59	0.83
		0.999	0	0.51	1.00	0.81	1.00	1.00	1.00	1.00	1.00	0	0.36	1.00	0.66	1.00	1.00	1.00	1.00	1.00
	STOXX 50	0.95	48	0.00	0.04	0.00	0.05	0.00	0.00	0.00	0.00	69	0.00	0.01	0.00	0.01	0.00	0.00	0.00	0.00
		0.975	13	0.00	0.03	0.00	0.03	0.00	0.01	0.02	0.05	19	0.02	0.01	0.00	0.01	0.00	0.02	0.04	0.07
		0.99	0	0.04	1.00	0.12	1.00	1.00	0.20	0.00	0.00	3	0.54	0.83	0.81	0.84	1.00	0.72	0.18	0.37
		0.999	0	0.51	1.00	0.81	1.00	1.00	1.00	1.00	1.00	1	0.44	0.94	0.74	0.94	1.00	0.36	0.02	0.05
	AEX	0.95	42	0.00	0.01	0.00	0.02	0.00	0.00	0.00	0.00	50	0.00	0.01	0.00	0.01	0.00	0.00	0.00	0.00
		0.975	4	0.54	0.69	0.77	0.70	1.00	0.69	0.36	0.73	12	0.63	0.04	0.11	0.04	0.00	0.70	0.16	0.32
		0.99	0	0.04	1.00	0.12	1.00	1.00	0.15	0.00	0.00	3	0.54	0.83	0.81	0.84	0.63	0.44	0.27	0.54
		0.999	0	0.51	1.00	0.81	1.00	1.00	1.00	1.00	1.00	0	0.36	1.00	0.66	1.00	1.00	1.00	1.00	1.00
	BVSP	0.95	15	0.20	0.37	0.29	0.38	0.01	0.20	0.04	0.08	31	0.03	0.64	0.09	0.64	0.02	0.03	0.16	0.33
		0.975	4	0.54	0.69	0.77	0.70	0.11	0.66	0.25	0.51	6	0.13	0.68	0.29	0.68	0.14	0.15	0.77	0.45
		0.99	1	0.39	0.92	0.68	0.92	0.71	0.40	0.63	0.74	2	0.23	0.89	0.49	0.89	1.00	0.36	0.80	0.39
		0.999	1	0.22	0.92	0.47	0.92	0.73	0.04	0.63	0.75	1	0.44	0.94	0.74	0.94	0.89	0.44	0.81	0.38

			2017									2017-2018								
		α	Exc.	LR_{uc}	LR_{ind}	LR_{cc}	DQ_{hit}	DQ_{VaR}	MCS_{uc}	MCS_{ind}	MCS_{cc}	Exc.	LR_{uc}	LR_{ind}	LR_{cc}	DQ_{hit}	DQ_{VaR}	MCS_{uc}	MCS_{ind}	MCS_{cc}
rMPOT	DAX	0.95	30	0.00	0.51	0.00	0.53	0.52	0.00	0.36	0.70	49	0.00	0.87	0.00	0.87	0.84	0.00	0.30	0.57
		0.975	18	0.00	0.62	0.00	0.63	0.73	0.00	0.45	0.91	31	0.00	0.32	0.00	0.33	0.61	0.00	0.31	0.63
		0.99	9	0.00	0.37	0.00	0.38	0.36	0.00	0.52	0.97	16	0.00	0.26	0.00	0.26	0.51	0.00	0.86	0.29
		0.999	0	0.51	1.00	0.81	1.00	1.00	1.00	1.00	1.00	1	0.44	0.94	0.74	0.94	1.00	0.19	0.02	0.05
	FTSE 100	0.95	37	0.00	0.24	0.00	0.25	0.29	0.00	0.75	0.59	47	0.00	0.01	0.00	0.01	0.01	0.00	0.01	0.03
		0.975	18	0.00	0.69	0.00	0.69	0.70	0.00	0.42	0.83	31	0.00	0.02	0.00	0.02	0.02	0.00	0.07	0.12
		0.99	12	0.00	0.70	0.00	0.70	0.49	0.00	0.58	0.85	14	0.00	0.48	0.00	0.48	0.26	0.00	0.86	0.30
		0.999	1	0.22	0.92	0.47	0.92	0.98	0.16	0.71	0.59	3	0.01	0.83	0.03	0.83	0.97	0.01	0.54	0.92
	NIKKEI 225	0.95	25	0.00	0.97	0.00	0.96	0.90	0.00	0.22	0.42	42	0.00	0.69	0.00	0.69	0.75	0.00	0.19	0.37
		0.975	14	0.00	0.16	0.00	0.17	0.35	0.00	0.44	0.87	27	0.00	0.35	0.00	0.36	0.62	0.00	0.18	0.37
		0.99	6	0.03	0.55	0.08	0.56	0.11	0.03	0.77	0.45	12	0.00	0.35	0.00	0.35	0.54	0.00	0.56	0.85
		0.999	1	0.22	0.92	0.47	0.92	0.59	0.36	0.78	0.44	1	0.44	0.94	0.74	0.94	1.00	0.41	0.37	0.76
	S&P 500	0.95	32	0.00	0.93	0.00	0.92	0.00	0.00	0.58	0.89	51	0.00	0.23	0.00	0.24	0.51	0.00	0.00	0.00
		0.975	15	0.00	0.13	0.00	0.14	0.19	0.00	0.74	0.54	23	0.00	0.16	0.00	0.16	0.38	0.00	0.04	0.07
		0.99	8	0.00	0.43	0.01	0.43	0.55	0.00	0.42	0.84	10	0.02	0.23	0.03	0.23	0.46	0.02	0.33	0.67
		0.999	3	0.00	0.77	0.01	0.77	0.61	0.00	0.71	0.58	3	0.01	0.83	0.03	0.83	0.94	0.01	0.85	0.28
	CAC 40	0.95	31	0.00	0.74	0.00	0.73	0.63	0.00	0.42	0.79	40	0.00	0.09	0.00	0.10	0.25	0.00	0.09	0.18
		0.975	14	0.00	0.16	0.00	0.17	0.37	0.00	0.56	0.91	27	0.00	0.03	0.00	0.03	0.09	0.00	0.02	0.05
		0.99	7	0.01	0.49	0.02	0.49	0.78	0.01	0.41	0.84	9	0.04	0.53	0.10	0.53	0.81	0.03	0.19	0.39
		0.999	1	0.22	0.92	0.47	0.92	0.30	0.31	0.63	0.74	1	0.44	0.94	0.74	0.94	0.98	0.17	0.03	0.05
	HANG	0.95	27	0.00	0.78	0.00	0.80	0.32	0.00	0.35	0.68	35	0.00	0.97	0.01	0.97	1.00	0.00	0.69	0.63
		0.975	12	0.01	0.23	0.02	0.24	0.45	0.01	0.92	0.17	18	0.03	0.20	0.04	0.21	0.45	0.03	0.76	0.48
		0.99	4	0.25	0.69	0.48	0.70	0.93	0.23	0.47	0.96	8	0.09	0.58	0.21	0.58	0.86	0.07	0.16	0.32
		0.999	1	0.22	0.92	0.47	0.92	0.03	0.37	0.19	0.38	2	0.08	0.89	0.21	0.89	0.91	0.08	0.44	0.89
	IBEX 35	0.95	36	0.00	0.61	0.00	0.61	0.02	0.00	0.78	0.51	41	0.00	0.12	0.00	0.12	0.01	0.00	0.32	0.62
		0.975	15	0.00	0.37	0.00	0.38	0.07	0.00	0.61	0.78	24	0.00	0.04	0.00	0.04	0.02	0.00	0.49	0.97
		0.99	6	0.03	0.55	0.08	0.56	0.16	0.04	0.56	0.87	10	0.02	0.48	0.04	0.49	0.17	0.02	0.86	0.28
		0.999	1	0.22	0.92	0.47	0.92	0.33	0.12	0.23	0.46	2	0.08	0.89	0.21	0.89	0.97	0.12	0.42	0.84
	STOXX 50	0.95	42	0.00	0.96	0.00	0.96	0.03	0.00	0.33	0.59	47	0.00	0.08	0.00	0.09	0.04	0.00	0.12	0.23
		0.975	18	0.00	0.63	0.00	0.63	0.49	0.00	0.32	0.63	29	0.00	0.18	0.00	0.18	0.20	0.00	0.23	0.46
		0.99	8	0.00	0.43	0.01	0.43	0.64	0.00	0.72	0.55	10	0.02	0.48	0.04	0.49	0.63	0.02	0.90	0.20
		0.999	0	0.51	1.00	0.81	1.00	1.00	1.00	1.00	1.00	1	0.44	0.94	0.74	0.94	0.99	0.57	0.02	0.05
	AEX	0.95	46	0.00	0.99	0.00	0.97	0.25	0.00	0.60	0.96	49	0.00	0.01	0.00	0.01	0.01	0.00	0.17	0.35
		0.975	25	0.00	0.97	0.00	0.96	0.65	0.00	0.74	0.54	23	0.00	0.01	0.00	0.01	0.02	0.00	0.05	0.10
		0.99	5	0.09	0.62	0.22	0.63	0.85	0.09	0.69	0.64	12	0.00	0.40	0.01	0.40	0.70	0.00	0.45	0.90
		0.999	0	0.51	1.00	0.81	1.00	1.00	1.00	1.00	1.00	2	0.08	0.89	0.21	0.89	0.99	0.03	0.45	0.89
	BVSP	0.95	22	0.00	0.24	0.00	0.25	0.38	0.00	0.71	0.59	29	0.08	0.99	0.22	0.99	0.90	0.09	0.05	0.09
		0.975	8	0.27	0.29	0.31	0.29	0.36	0.33	0.26	0.53	11	0.86	0.44	0.73	0.45	0.56	0.93	0.47	0.92
		0.99	2	0.93	0.85	0.98	0.85	0.56	0.71	0.61	0.79	2	0.23	0.89	0.49	0.89	0.73	0.31	0.80	0.40
		0.999	1	0.22	0.92	0.47	0.92	0.94	0.05	0.63	0.75	1	0.44	0.94	0.74	0.94	0.77	0.62	0.81	0.39

Table 8: VaR accuracy tests of the MPOT (top-panel) and the rMPOT (bottom-panel) models for the out-sample periods,i.e, from January 4, 2017 until December 29, 2017 (only year 2017), and from January 4, 2017 until December 27, 2018 (2017-2018). Entries in the rows are the significance levels (p-values) of the respective tests, with the exception of the confidence level α for the VaR and the number of exceptions (Exc.).

	SPOT								rSPOT							
	2017				2017-2018				2017				2017-2018			
	$\alpha = 0.95$	$\alpha = 0.975$	$\alpha = 0.99$	$\alpha = 0.999$	$\alpha = 0.95$	$\alpha = 0.975$	$\alpha = 0.99$	$\alpha = 0.999$	$\alpha = 0.95$	$\alpha = 0.975$	$\alpha = 0.99$	$\alpha = 0.999$	$\alpha = 0.95$	$\alpha = 0.975$	$\alpha = 0.99$	$\alpha = 0.999$
DAX	0.913	0.898	0.879	0.917	0.992	0.969	0.944	0.95	1.000	1.000	1.000	1.000	1.000	1.000	1.000	1.000
FTSE 100	0.813	0.798	0.808	0.862	0.912	0.899	0.894	0.901	1.000	1.000	1.000	1.000	1.000	1.000	1.000	1.000
NIKKEI 225	0.877	0.878	0.881	0.93	0.971	0.951	0.935	0.943	1.000	1.000	1.000	1.000	1.000	1.000	1.000	1.000
S&P 500	0.9	0.885	0.888	0.942	1.045	0.969	0.898	0.883	1.000	1.000	1.000	1.000	1.000	1.000	1.000	1.000
CAC 40	0.913	0.898	0.876	0.886	1.014	0.993	0.949	0.913	1.000	1.000	1.000	1.000	1.000	1.000	1.000	1.000
HANG SENG	0.876	0.86	0.847	0.886	0.944	0.921	0.905	0.913	1.000	1.000	1.000	1.000	1.000	1.000	1.000	1.000
IBEX 35	0.793	0.781	0.784	0.867	0.878	0.865	0.859	0.893	1.000	1.000	1.000	1.000	1.000	1.000	1.000	1.000
STOXX 50	0.877	0.863	0.839	0.873	0.996	0.961	0.917	0.901	1.000	1.000	1.000	1.000	1.000	1.000	1.000	1.000
AEX	0.743	0.729	0.72	0.797	0.907	0.875	0.833	0.828	1.000	1.000	1.000	1.000	1.000	1.000	1.000	1.000
BVSP	0.772	0.783	0.815	0.888	0.9	0.897	0.899	0.919	1.000	1.000	1.000	1.000	1.000	1.000	1.000	1.000
	BPOT								rBPOT							
	2017				2017-2018				2017				2017-2018			
	$\alpha = 0.95$	$\alpha = 0.975$	$\alpha = 0.99$	$\alpha = 0.999$	$\alpha = 0.95$	$\alpha = 0.975$	$\alpha = 0.99$	$\alpha = 0.999$	$\alpha = 0.95$	$\alpha = 0.975$	$\alpha = 0.99$	$\alpha = 0.999$	$\alpha = 0.95$	$\alpha = 0.975$	$\alpha = 0.99$	$\alpha = 0.999$
DAX	0.978	0.984	0.984	0.984	1.057	1.045	1.03	1.006	1.070	1.038	1.019	1.003	1.107	1.077	1.051	1.019
FTSE 100	0.716	0.751	0.804	0.883	0.875	0.886	0.907	0.928	0.934	0.902	0.897	0.921	1.041	1.017	0.994	0.967
NIKKEI 225	0.897	0.933	0.975	1.028	1.024	1.036	1.04	1.042	0.957	0.969	0.996	1.041	1.085	1.075	1.067	1.058
S&P 500	0.79	0.828	0.879	0.947	1.039	1.004	0.957	0.915	1.818	0.907	0.851	0.947	1.123	1.039	0.975	0.924
CAC 40	0.881	0.893	0.906	0.925	1.029	1.022	0.994	0.956	0.978	0.957	0.95	0.949	1.102	1.08	1.037	0.981
HANG SENG	0.833	0.848	0.892	0.961	0.95	0.955	0.971	0.989	0.965	0.944	0.956	0.995	1.033	1.018	1.012	1.010
IBEX 35	0.823	0.848	0.895	0.958	0.913	0.928	0.948	0.967	0.884	0.889	0.922	0.971	0.966	0.966	0.972	0.978
STOXX 50	0.851	0.876	0.904	0.939	1.015	1.003	0.985	0.963	0.886	0.878	0.897	0.937	1.04	1.014	0.99	0.965
AEX	0.746	0.773	0.819	0.881	0.961	0.96	0.946	0.909	0.875	0.819	0.827	0.887	1.016	0.986	0.959	0.916
BVSP	0.812	0.837	0.878	0.936	0.931	0.943	0.954	0.962	0.849	0.866	0.899	0.948	0.954	0.963	0.969	0.97
	MPOT								rMPOT							
	2017				2017-2018				2017				2017-2018			
	$\alpha = 0.95$	$\alpha = 0.975$	$\alpha = 0.99$	$\alpha = 0.999$	$\alpha = 0.95$	$\alpha = 0.975$	$\alpha = 0.99$	$\alpha = 0.999$	$\alpha = 0.95$	$\alpha = 0.975$	$\alpha = 0.99$	$\alpha = 0.999$	$\alpha = 0.95$	$\alpha = 0.975$	$\alpha = 0.99$	$\alpha = 0.999$
DAX	0.7	0.757	0.821	0.885	0.862	0.881	0.905	0.922	1.068	1.05	1.032	1.013	1.111	1.085	1.060	1.025
FTSE 100	0.584	0.625	0.695	0.789	0.726	0.745	0.787	0.831	0.916	0.894	0.896	0.923	1.031	1.012	0.995	0.969
NIKKEI 225	0.729	0.768	0.818	0.882	0.902	0.9	0.901	0.905	0.966	0.966	0.977	1.004	1.082	1.058	1.038	1.017
S&P 500	0.637	0.729	0.821	0.921	0.874	0.894	0.891	0.885	0.937	0.924	0.942	0.980	1.147	1.072	0.999	0.937
CAC 40	0.666	0.694	0.759	0.828	0.817	0.835	0.853	0.864	0.979	0.966	0.959	0.955	1.106	1.087	1.044	0.986
HANG SENG	0.71	0.713	0.748	0.807	0.841	0.825	0.827	0.837	0.955	0.944	0.959	0.994	1.029	1.015	1.009	1.007
IBEX 35	0.682	0.723	0.795	0.876	0.792	0.82	0.856	0.89	0.874	0.878	0.911	0.962	0.963	0.962	0.968	0.973
STOXX 50	0.623	0.673	0.758	0.844	0.808	0.829	0.856	0.877	0.907	0.904	0.92	0.949	1.062	1.038	1.011	0.977
AEX	0.555	0.611	0.692	0.786	0.77	0.798	0.818	0.818	0.841	0.833	0.856	0.902	1.029	1.008	0.979	0.926
BVSP	0.691	0.749	0.814	0.899	0.842	0.874	0.903	0.931	0.844	0.861	0.894	0.943	0.949	0.956	0.963	0.964

Table 9: Ratios of the FZL functions described in (11) for the SPOT, the competing models (BPOT and MPOT and their realized versions) with respect to the rSPOT model at different confidence levels α. The backtesting periods span from January 4, 2017 until December 29, 2017 (only year 2017), and from January 4, 2017 until December 27, 2018 (2017-2018). Values smaller than one indicate that the rSPOT model outperforms the competing models in terms of the FZL function. The results for the Model Confidence Set procedure are highlighted in gray color for the best performing specifications included in the superior set at the $\alpha' = 0.05$ significant level. For instance, the superior set for the DAX during the one year backtesting period at the confidence level $\alpha = 0.99$ is composed by the rSPOT, rBPOT and rMPOT specification.

Apéndice D. Assessing Systemic Risk with Score-driven Extreme Value Models

Assessing Systemic Risk with Score-driven Extreme Value Models

- Correo electrónico confirmación artículo enviado a la revista
- Artículo enviado

RV: A manuscript number has been assigned: JBF-D-20-01464

-----Mensaje original-----
De: em.jbf.0.6fdab0.76b1cffe@editorialmanager.com
<em.jbf.0.6fdab0.76b1cffe@editorialmanager.com> En nombre de Journal of Banking and Finance
Enviado el: Wednesday, December 09, 2020 2:10 AM
Para: Rodrigo Sebastian Herrera Leiva <rodrigo.herrera@utalca.cl>
Asunto: A manuscript number has been assigned: JBF-D-20-01464

Ms. Ref. No.: JBF-D-20-01464
Title: Assessing Systemic Risk with Score-driven Extreme Value Models Journal of Banking and Finance

Dear Dr. Rodrigo Herrera,
Your submission "Assessing Systemic Risk with Score-driven Extreme Value Models" has been assigned manuscript number JBF-D-20-01464.

To track the status of your paper, please do the following:

1. Go to this URL: https://www.editorialmanager.com/jbf/
2. Enter your login details

3. Click [Author Login]
This takes you to the Author Main Menu.

4. Click [Submissions Being Processed]

Thank you for submitting your work to Journal of Banking and Finance.

Kind regards,

Surendar Muthu
Journal Manager
Journal of Banking and Finance
==========

For further assistance, please visit our customer support site at http://help.elsevier.com/app/answers/list/p/7923. Here you can search for solutions on a range of topics, find answers to frequently asked questions and learn more about EM via interactive tutorials. You will also find our 24/7 support contact details should you need any further assistance from one of our customer support representatives.

In compliance with data protection regulations, you may request that we remove your personal registration details at any time. (Use the following URL: https://www.editorialmanager.com/jbf/login.asp?a=r). Please contact the publication office if you have any questions.

Journal of Banking and Finance

Assessing Systemic Risk with Score-driven Extreme Value Models

--Manuscript Draft--

Manuscript Number:	JBF-D-20-01464
Article Type:	Full Length Article
Keywords:	extreme value theory; Banks; Tail Risk; Systemic Risk; Score-driven models
Corresponding Author:	Rodrigo Herrera, Ph.D Universidad de Talca Talca, CHILE
First Author:	Fernanda Fuentes, Msc
Order of Authors:	Fernanda Fuentes, Msc
	Rodrigo Herrera, Ph.D
	Adam Clements, PhD
Abstract:	This paper proposes a new class of marked point process models to capture the clustering behaviour in extreme financial events. The idea of multiple dynamic parameters embedded in the context of score driven models is utilized to estimate a dynamic extreme value approach, labelled as the Generalized Score-Driven Peaks Over Threshold model. A Monte-Carlo study is conducted to investigate different time-varying parameter specifications. The results show that this approach can capture a range of different dynamics for the parameters. The presence of systematic tail risk in the cross section of returns of 16 constituents of the S&P Banks Index by means of a dynamic tail-β risk measure generated under the proposed approach. It is shown that hedging against tail risk in portfolios of bank stocks bring several benefits in the prediction of future performance of their returns during periods of financial turmoil.

Powered by Editorial Manager® and ProduXion Manager® from Aries Systems Corporation

Cover Letter

Editors of
Journal of Banking and Finance

Dr. Rodrigo Herrera
Professor of Economics

Facultad de Economía y Negocios
Universidad de Talca, Chile.
Avenida Lircay s/n

Phone: +56 71 2200308
Email : rodrigo.herrera@utalca.cl

Chile, 12.08.2020

Dear Prof. Geert Bekaert

Attached to this letter you will find our manuscript titled, *Assessing Systemic Risk with Score-driven Extreme Value Models*, co-authored with Fernanda Fuentes and Adam Clements.

This paper proposes a new class of marked point process models to capture the clustering behaviour in extreme financial events. The idea of multiple dynamic parameters embedded in the context of score driven models is utilized to estimate a dynamic extreme value approach, labelled as the Generalized Score-Driven Peaks Over Threshold model. A Monte-Carlo study is conducted to investigate different time-varying parameter specifications. The results show that this approach can capture a range of different dynamics for the parameters. The presence of systematic tail risk in the cross section of returns of 16 constituents of the S&P Banks Index by means of a dynamic tail-β risk measure generated under the proposed approach. It is shown that hedging against tail risk in portfolios of bank stocks bring several benefits in the prediction of future performance of their returns during periods of financial turmoil.

We hope this manuscript would be of interest to the readership of your journal. Thank you in advance for your time in considering this submission.

Best Wishes,

Rodrigo Herrera

Title Page (with authors and affiliations)

Assessing Systemic Risk with Score-driven Extreme Value Models

Fernanda Fuentes[b], Rodrigo Herrera[a,*], Adam Clements[c]

[a]*Facultad de Economía y Negocios, Universidad de Talca, Av. Lircay s/n- Talca. Chile.*
[b]*Facultad de Ingeniería, Universidad de Talca, Camino a los Niches km.1-Curicó. Chile.*
[c]*School of Economics and Finance, Queensland University of Technology, Brisbane, Australia.*

Abstract

This paper proposes a new class of marked point process models to capture the clustering behaviour in extreme financial events. The idea of multiple dynamic parameters embedded in the context of score driven models is utilized to estimate a dynamic extreme value approach, labelled as the Generalized Score-Driven Peaks Over Threshold model. A Monte-Carlo study is conducted to investigate different time-varying parameter specifications. The results show that this approach can capture a range of different dynamics for the parameters. The presence of systematic tail risk in the cross section of returns of 16 constituents of the S&P Banks Index by means of a dynamic tail-β risk measure generated under the proposed approach. It is shown that hedging against tail risk in portfolios of bank stocks bring several benefits in the prediction of future performance of their returns during periods of financial turmoil.

JEL classification: C58; C22; F30; G17

Keywords: Extreme value theory, Banks, Tail Risk, Systemic Risk, Score-driven models.

*Corresponding author

Email addresses: ferfuentes@utalca.cl (Fernanda Fuentes), rodriherrera@utalca.cl (Rodrigo Herrera), a.clements@qut.edu.au (Adam Clements)

Manucript Click here to view linked References

Assessing Systemic Risk with Score-driven Extreme Value Models

Abstract

This paper proposes a new class of marked point process models to capture the clustering behaviour in extreme financial events. The idea of multiple dynamic parameters embedded in the context of score driven models is utilized to estimate a dynamic extreme value approach, labelled as the Generalized Score-Driven Peaks Over Threshold model. A Monte-Carlo study is conducted to investigate different time-varying parameter specifications. The results show that this approach can capture a range of different dynamics for the parameters. The presence of systematic tail risk in the cross section of returns of 16 constituents of the S&P Banks Index by means of a dynamic tail-β risk measure generated under the proposed approach. It is shown that hedging against tail risk in portfolios of bank stocks bring several benefits in the prediction of future performance of their returns during periods of financial turmoil.

JEL classification: C58; C22; F30; G17

Keywords: Extreme value theory, Banks, Tail Risk, Systemic Risk, Score-driven models.

1. Introduction

The subprime, and associated Global Financial Crisis has highlighted the impact of the banking system on the stability of the whole financial system, and has motivated a renewed interest in systemic risk, as the primary ingredient to understand financial crises. Recent literature on systemic risk focuses on global measures of systemic risk integrating simultaneously microprudential as well as macroprudential perspectives (see Benoit et al., 2017). The most widely utilized global measures of systemic risk approaches are the marginal expected shortfall (MES) of Acharya et al. (2017), the SRISK measure proposed by Brownlees and Engle (2016) and the CoVaR measure of Tobias and Brunnermeier (2016). An important feature that these models share is that they try to harness the information contained in the banks' extreme losses or returns.

The class of score-driven time series models developed by Creal et al. (2013) and Harvey (2013), on the other hand, have recently become popular in systemic risk modeling (see for instance Harvey and Lange, 2017; Gorgi et al., 2018; Bernardi and Catania, 2018). Although, the literature on systemic risk based on score-driven extreme value approaches is scarce, a small number of studies have considered models with only one (scale or shape) time-varying parameter (e.g., Bee et al., 2019; Zhang and Bernd, 2016; Massacci, 2016). This paper contributes to the systemic risk literature by introducing a score-driven extreme value model with all parameters varying over the sample period. The resulting model is labeled as Generalized score-driven Peaks-over-Threshold (GSPOT) model. Here, generalized relates to the generalization to multiple time-varying parameters that are orthogonal to the conditional Fisher information matrix, score-driven relates to each parameter being time-varying and driven by its own score from the information in past observations, and Peaks-over-Threshold relates to the extreme value method that utilize observations exceeding a sufficiently high threshold. It is shown that this approach performs well under a number of scenarios in a Monte-Carlo study.

The GSPOT approach is used to extend the tail-β risk measure recently proposed by Van Oordt and Zhou (2017) to a dynamic one. This measure decomposes the behavior of extremely adverse returns in the financial system into two main source of risk. One associated with the tail distribution function of the bank stocks, and other harnessing the tail dependence structure of the whole banking system. Furthermore, this measure of systemic risk encompasses other common ones, such as the Exposure CoVaR measure of Tobias and Brunnermeier (2016), the SRISK measure proposed by Brownlees and Engle (2016), and the most recent measure of systemic risk the Marginal Expected Shortfall (MES) of Acharya et al. (2017) (see Van Oordt and Zhou, 2019). Utilizing the tail-β risk measure we are able to not only to understand the dynamics of bank's risk individually, but also see if strong systemic linkages are associated with the stability of the global financial system.

The empirical analysis considers tail-β risk measures over time for the constituents of the S&P Banks Index, which consists of large market capitalization banks in the S&P 500 index. The empirical results reveal a number of interesting findings. First, the GSPOT approach is able to capture well-known stylized facts present in the asset returns such as extreme clustering, persistence and heavy tails. Both the exceedances of the extreme events, and the inter-exceedance times provide important information to describe the dynamics of extreme events in bank stock returns during periods of turmoil. Further, while, the tail-β risk estimates and the rolling beta estimates share similar dynamics for each bank, important differences are revealed, especially during periods of financial crisis. Finally, utilizing information contained in the tail-β risk measures, along with estimating a dynamic version of the MES risk measure, it is shown that investors can diversify their bank portfolios to hedge against tail risk, obtaining advantages in terms of expected portfolio returns.

The paper is organized as follows. In Section 2 introduces the basis of extreme value theory and outlines the Generalized Score-driven POT approach. Section 3 provides evidence from an extensive Monte Carlo study. Section 4 presents the results of our empirical study to

U.S Banks. Section 5 concludes.

2. Methodology

In this section we formulate the generalized score-driven Peaks-over-Threshold (GSPOT) model. First, we discuss the standard conditional POT approach from the point of view of marked point process theory, which is the basis of our framework.

2.1. The Conditional Peaks over Threshold (POT) Approach

Let $y_t \in \mathbb{R}$ be a random variable with a continuous distribution function F and upper support point of y_0 such that $\lim_{y \to y_0} F(y) = 1$. For instance, these random variables could be negative log-returns of any asset. In this framework, a marked point process (MPP) of exceedances $N(A)$ is a sequence of random pairs $\{(t_i, z_i)\}$ on $A \subset \mathbb{R}_+ \times \mathbb{R}_+$ with ordered event times $0 < t_1 < t_2 < \cdots < t_n < t$ describing the occurrence times of extreme returns exceeding a high threshold $u > 0$ whose exceedances or marks are $z_i = y_{t_i} - u$. Furthermore, for any MPP of exceedances the occurrence times $\{t_i\}$ are themselves a well-defined point process on $\mathbb{R}_+$ and accordingly are denoted by N_g and refereed as the ground process.

This stochastic process can be completely characterized by the inter-exceedance times between extreme events if the tail of F is in the domain of attraction of one of the extreme value distributions. In particular, the tail of F can be decomposed as follows

$$P(Y_t > y \mid \mathcal{H}_t) = P(Y_t > u \mid \mathcal{H}_t)\, P(Y_t > y \mid Y_t > u \mid \mathcal{H}_t),$$

where $\mathcal{H}_t = \{(t_i, z_i)\ \forall i : t_i < t\}$ is the sigma algebra generated by this process. Notice that the tail $P(Y_t > u \mid \mathcal{H}_t)$ is equivalent to the probability of observing an extreme event in the interval $(t_n, t]$, that is

$$P(Y_t > u \mid \mathcal{H}_t) = 1 - P\left(N_g(t) - N_g(t_n) = 0 \mid \mathcal{H}_t\right). \tag{1}$$

In the case of iid random variables, the exceedances times follows a Poisson process. On the other hand, according to the Pickand-Balkema-de Haan Theorem (Balkema and De Haan, 1974; Pickands, 1975), the distribution of the marks

$$P\left(Y_t > y \mid Y_t > u \mid \mathcal{H}_t\right) = P\left(Y_t - u > y - u \mid Y_t > u \mid \mathcal{H}_t\right) =: \overline{F}_u\left(y - u\right),$$

is well approximated by the generalized Pareto distribution

$$F_u\left(z_i\right) \to G\left(z_i; \beta, \xi\right) = \begin{cases} 1 - \left(1 + \xi \frac{z_i}{\beta}\right)^{-\frac{1}{\xi}} & \text{for } \xi \neq 0 \\ 1 - \exp\left(-\frac{z_i}{\beta}\right) & \text{for } \xi = 0, \end{cases} \tag{2}$$

as the threshold $u \to \infty$ for $0 \leq y \leq y_0 - u$, with scale parameter $\beta > 0$ and shape parameter $\xi \in \mathbb{R}$. Thus, for extreme events observed during the interval $(0, t]$, the joint log-likelihood function is given by

$$\sum_{i=1}^{N_g(t)} \ln\left\{p\left(t_i \mid \mathcal{H}_t\right) + P\left(Y_{N_g(t)+1} > t \mid \mathcal{H}_t\right)\right\} + \ln g\left(z_i \mid t_i, \mathcal{H}_t\right) \tag{3}$$

where, with a slight misuse of notation $p\left(t_i \mid \mathcal{H}_t\right)$ is the probability density function of the occurrence time of the extreme event i introduced in Eq.(1) and $g\left(z_i \mid t_i, \mathcal{H}_t\right)$ the probability density function of the marks defined in Eq(2), both conditional on the history $\mathcal{H}_t$. $P\left(Y_{N_g(t)+1} > t \mid \mathcal{H}_t\right)$ ensure merely the distribution of a regular point process[1]. Notice that the probability of occurrence of the extreme events is conditionally independent of the size of the marks.

[1] See Proposition 7.2.I in Daley and Vere-Jones (2003)

2.2. Generalized Score-driven POT (GSPOT)

The main novelty of the GSPOT approach, is that the dynamics of extreme events are captured continuously each time that an extreme event is observed by means of all parameters involved in the specification. In this way, it is possible to reflect the dynamics of the occurrence of extreme events and their magnitudes in the current parameters, using as information,lagged dependent variables and the score function.

Consider a set of orthogonal time-varying parameters $\boldsymbol{f}_i := \left\{\boldsymbol{f}_i^{\star} \cup \boldsymbol{f}_i^{*}\right\}$ defined by two disjoints sets $\boldsymbol{f}_i^{\star} := \left(f_i^1, \ldots, f_i^{k_1}\right)$ and $\boldsymbol{f}_i^{*} := \left(f_i^{k_1+1}, \ldots, f_i^{k_1+k_2}\right)$, with k_1 and k_2 being the number of time-varying parameters involved in stochastic process of occurrence of the extreme events and their magnitudes, respectively. Orthogonal parameters are easy to deal with as they ensure that maximum log-likelihood optimization is well behaved, since the conditional Fisher matrix will be diagonal, and therefore, easily invertible. Now, let $\mathcal{H}_i^{\star} = \left\{\left(t_s, f_s^{\star}\right)\ \forall s : s < i\right\}$ and $\mathcal{H}_i^{*} = \left\{\left(z_s, f_s^{*}\right)\ \forall s : s < i\right\}$ be the available information sets just before the occurrence of the extreme event i, of the occurrence times of the extreme events and their magnitudes, respectively. Furthermore, we define $\mathcal{H}_i := \mathcal{H}_i^{\star} \cup \mathcal{H}_i^{*}$ as the available information set of both process with $\mathcal{H}_i \subseteq \mathcal{H}_t$. Notice that we have simplified the notation in two ways. First, we have divided the information set into two parts, and second, we have discretized these in relation to the occurrence of extreme events and not to calendar time.

In order to introduce the GSPOT approach, we specify the dynamic of extreme events in terms of their conditional intensity functions (see Chavez-Demoulin and McGill 2012; Gresnigt et al. 2016; Hautsch and Herrera 2020), instead of specifying them equivalently by means of their conditional probability density functions as in Eq.(3)

$$\lambda\left(t_i, z_i \mid \mathcal{H}_i, \boldsymbol{f}_i\right) = \tau\left(t_i \mid \mathcal{H}_i^{\star}, \boldsymbol{f}_i^{\star}\right) g\left(z_i \mid t_i, \mathcal{H}_i^{*}, \boldsymbol{f}_i^{*}\right), \tag{4}$$

where the stochastic process $\tau\left(t_i \mid \mathcal{H}_i^{\star}, \boldsymbol{f}_i^{\star}\right)$ corresponds to the ground conditional intensity

associated with the occurrence time of an extreme event i, and therefore, the ground process N_g. This ground conditional intensity is characterized in our our framework by a conditional hazard function with

$$p\left(t \mid \mathcal{H}_i^{\star}, \boldsymbol{f}_i^{\star}\right) = \tau\left(t \mid \mathcal{H}_i^{\star}, \boldsymbol{f}_i^{\star}\right) \exp\left\{-\int_{t_n}^{t} \tau\left(s \mid \mathcal{H}_{N_g(s)}^{\star}, \boldsymbol{f}_{N_g(s)}^{\star}\right) ds\right\}$$

being equivalent to the probability density function of the occurrence times described in Eq.(3). On the other hand, the stochastic process $g\left(z_i \mid t_i, \mathcal{H}_i^{*}, \boldsymbol{f}_i^{*}\right)$ denotes again the conditional probability density function of the generalized Pareto distribution described in Eq.(2).

In this framework, each time-varying parameter f_i^j with $j = 1, \ldots, k_1 + k_2$, has first order score-driven dynamics following Harvey (2013) and Creal et al. (2013):

$$f_{i+1}^j = \omega_j + \psi_j s_i^j + \phi_j f_i^j \tag{5}$$

$$s_i^j = S_i^j \nabla_i^j = E_{i-1}\left[-\frac{\partial^2 \mathcal{L}_i\left(\boldsymbol{f}_i\right)}{\partial f_i^{j2}}\right]^{-1} \frac{\partial \mathcal{L}_i\left(\boldsymbol{f}_i\right)}{\partial f_i^j} \tag{6}$$

$$\mathcal{L}_i\left(\boldsymbol{f}_i\right) = \mathcal{L}_i\left(\boldsymbol{f}_i^{\star}\right) + \mathcal{L}_i\left(\boldsymbol{f}_i^{*}\right) \tag{7}$$

where $\boldsymbol{\theta} := \left\{\boldsymbol{\theta}^{\star} \cup \boldsymbol{\theta}^{*}\right\}$ denotes a set of (unrestricted) static coefficients for each time-varying parameter present in the specification, with $\boldsymbol{\theta}^{\star} := \left\{\left(\omega_j, \psi_j, \phi_j\right)\right\}_{j=1}^{k_1}$ and $\boldsymbol{\theta}^{*} := \left\{\left(\omega_j, \psi_j, \phi_j\right)\right\}_{j=k_1+1}^{k_1+k_2}$. Further, $\mathcal{L}_i\left(\boldsymbol{f}_i\right)$ corresponds to the contribution of each event i to the log-likelihood function, which can be also split into two conditionally independent components

$$\mathcal{L}_i\left(\boldsymbol{f}_i^{\star}\right) = \left\{\ln \tau\left(t_i \mid \mathcal{H}_i^{\star}, \boldsymbol{f}_i^{\star}; \boldsymbol{\theta}^{\star}\right) - \int_{t_{i-1}}^{t_i} \tau\left(s \mid \mathcal{H}_{N_g(s)}^{\star}, \boldsymbol{f}_{N_g(s)}^{\star}; \boldsymbol{\theta}^{\star}\right) ds\right\}$$

and

$$\mathcal{L}_i\left(\boldsymbol{f}_i^{*}\right) = \ln g\left(z_i \mid t_i, \mathcal{H}_i^{*}, \boldsymbol{f}_i^{*}; \boldsymbol{\theta}^{*}\right).$$

One is associated with the occurrence times of the extreme events, and the other with the

magnitude of the marks. Moreover, $\nabla_i^j = \frac{\partial \mathcal{L}_i(f_i)}{\partial f_i^j}$ is the j-th element of the conditional score $\boldsymbol{\nabla}_i \in \mathbb{R}^{k_1+k_2}$, and S_i^j is the diagonal entry with respect to the parameter j of the inverse conditional Fisher information $\boldsymbol{S}_i \in \mathbb{R}^{(k_1+k_2)\times(k_1+k_2)}$, starting in the upper left corner.

One important consequence of the orthogonality of the parameters is that the maximum likelihood estimates are independent, guaranteeing the convergence of the maximization of the log-likelihood function. In practice, the following Proposition, is a generalization of that from Cox and Reid (1987), and provides the path to build orthogonal time-varying parameters in our context:

Proposition 1. *Let* $\mathcal{L}_i\left(\boldsymbol{\varphi}_i\right) = \mathcal{L}_i\left(\boldsymbol{\varphi}_i^{\star}\right) + \mathcal{L}_i\left(\boldsymbol{\varphi}_i^{*}\right)$ *be the non-orthogonal log-likelihood function of a GSPOT specification with time-varying parameters* $\boldsymbol{\varphi}_i := \left\{\boldsymbol{\varphi}_i^{\star} \cup \boldsymbol{\varphi}_i^{*}\right\}$*, with*

$$\boldsymbol{\varphi}_i^{\star} := \left(\varphi_i^1, \ldots, \varphi_i^{k_1}\right) \text{ and } \boldsymbol{\varphi}_i^{*} := \left(\varphi_i^{k_1+1}, \ldots, \varphi_i^{k_1+k_2}\right).$$

Rewrite these log-likelihoods in function of other time-varying parameters $\boldsymbol{f}_i := \left\{\boldsymbol{f}_i^{\star} \cup \boldsymbol{f}_i^{*}\right\}$*, with* $\boldsymbol{f}_i^{\star} := \left(f_i^1, \ldots, f_i^{k_1}\right)$, $\boldsymbol{f}_i^{*} := \left(f_i^{k_1+1}, \ldots, f_i^{k_1+k_2}\right)$, $\boldsymbol{f}_i^{-\star} := \boldsymbol{f}_i^{\star} \setminus \left\{f_i^1\right\}$ *and* $\boldsymbol{f}_i^{-*} := \boldsymbol{f}_i^{*} \setminus \left\{f_i^{k_1+1}\right\}$*, as follows:*

$$\begin{aligned}\mathcal{L}_i\left(f_i^1, f_i^{k_1+1}, \boldsymbol{f}_i^{-\star}, \boldsymbol{f}_i^{-*}\right) =& \mathcal{L}_i^{\star}\left(f_i^1, \varphi_i^2\left(f_i^1, \boldsymbol{f}_i^{-\star}\right), \ldots, \varphi_i^{k_1}\left(f_i^1, \boldsymbol{f}_i^{-\star}\right)\right) \\ &+ \mathcal{L}_i^{*}\left(f_i^{k_1+1}, \varphi_i^{k_1+2}\left(f_i^{k_1+1}, \boldsymbol{f}_i^{-*}\right), \ldots, \varphi_i^{k_1+k_2}\left(f_i^{k_1+1}, \boldsymbol{f}_i^{-*}\right)\right).\end{aligned} \tag{8}$$

Then, the new parameterization is orthogonal, if and only if there is a solution to the following partial differential equations:

$$\sum_{r=2}^{k_1} \ell^{\star}\left(\varphi_i^r, \varphi_i^s\right) \frac{\partial \varphi_i^r}{\partial f_i^1} = -\ell^{\star}\left(f_i^1, \varphi_i^s\right), \quad s = 2, \ldots, k_1. \tag{9}$$

and

$$\sum_{r=k_1+2}^{k_1+k_2} \ell^* \left(\varphi_i^r, \varphi_i^s\right) \frac{\partial \varphi_i^r}{\partial f_i^{k_1+1}} = -\ell^* \left(f_i^{k_1+1}, \varphi_i^s\right), \quad s = k_1+2, \ldots, k_1+k_2, \tag{10}$$

where $\ell^\star \left(\varphi_i^r, \varphi_i^s\right) := E_{i-1}\left[\frac{\partial^2 \mathcal{L}_i^\star}{\partial \varphi_i^r \partial \varphi_i^s}\right]$ *and* $\ell^* \left(\varphi_i^r, \varphi_i^s\right) := E_{i-1}\left[\frac{\partial^2 \mathcal{L}_i^*}{\partial \varphi_i^r \partial \varphi_i^s}\right]$ *are measures of expectation of the conditional Fisher information matrix.*

2.3. The Weibull GSPOT specification

The usefulness of Proposition 1 is demonstrated by considering a specification whose ground conditional intensity follows a Weibull hazard function:

$$\tau \left(t_i \mid \mathcal{H}_i, \boldsymbol{\varphi}_i^\star\right) = \delta_i^{-k_i} k_i \left(t_i - t_{i-1}\right)^{k_i - 1}, \tag{11}$$

where $\boldsymbol{\varphi}_i^\star := (k_i, \delta_i)$ with $\delta_i > 0$, $k_i > 0$, while the dynamics of the marks still following a generalized Pareto density function:

$$g \left(z_i \mid t_i, \mathcal{H}_t, \boldsymbol{\varphi}_i^*\right) = \frac{1}{\beta_i} \left(1 + \xi_i \frac{z_i}{\beta_i}\right)^{-\frac{1}{\xi_i} - 1}, \tag{12}$$

where $\boldsymbol{\varphi}_i^* := (\xi_i, \beta_i)$ with $\xi_i > 0$, $\beta_i > 0$.

As noted above, the GSPOT approach consists of two main steps. First, finding an orthogonal specification, and second, equipping the parameters with a score-driven dynamic. Then, starting with Eq.(4), the (non-orthogonal) conditional intensity takes the following parametric form:

$$\lambda \left(t_i, z_i \mid \mathcal{H}_t, \boldsymbol{\varphi}_i\right) = \frac{\delta_i^{-k_i} k_i \left(t_i - t_{i-1}\right)^{k_i - 1}}{\beta_i} \left(1 + \xi_i \frac{z_i}{\beta_i}\right)^{-\frac{1}{\xi_i} - 1},$$

where $\boldsymbol{\varphi}_i := \left\{\boldsymbol{\varphi}_i^\star \cup \boldsymbol{\varphi}_i^*\right\}$ is the set of non-orthogonal time-varying parameters. According to Proposition 1, in order to find the orthogonal parameterization one must solve the following two differential equations. The first associated to the ground conditional intensity

$$\ell^{\star}(\delta_i, k_i)\frac{\partial \delta_i}{\partial k_i} = -\ell^{\star}(k_i, k_i)$$
$$\frac{k_i^2}{\delta_i^2}\frac{\partial \delta_i}{\partial k_i} = -\frac{\gamma - 1}{\delta_i}$$

and the second to the density probability function of the marks

$$\ell^{*}(\beta_i, \xi_i)\frac{\partial \beta_i}{\partial \xi_i} = -\ell^{*}(\xi_i, \xi_i)$$
$$\frac{1}{\beta_i^2(1+2\xi_i)}\frac{\partial \beta_i}{\partial \xi_i} = -\frac{1}{\beta_i(1+2\xi_i)(1+\xi_i)}$$

whose solutions are:

$$v_i = \ln\left\{\delta_i \exp\left(\tfrac{1-\gamma}{k_i}\right)\right\} \qquad w_i = \ln\left\{\beta_i(1+\xi_i)\right\}.$$

Thus, the new orthogonal specification is:

$$\lambda\left(t_i, z_i \mid \mathcal{H}_i, \boldsymbol{f}_i\right) = \frac{\exp(v_i)^{-k_i}\exp(1-\gamma)\,k_i\,(t_i - t_{i-1})^{k_i-1}(1+\xi_i)}{\exp(w_i)}\left(1+\xi_i\frac{z_i(1+\xi_i)}{\exp(w_i)}\right)^{-\frac{1}{\xi_i}-1}. \tag{13}$$

In the second step, it is necessary to equip the parameters of this conditional intensity with the score-driven dynamics. The sets of time-varying parameters are given by $\boldsymbol{f}_i^{\star} := \left\{f_i^1, f_i^2\right\} = \{v_i, \ln k_i\}$, which correspond to the scale and shape parameters in the ground conditional intensity described in Eq.(11), while $\boldsymbol{f}_i^{*} := \left\{f_i^3, f_i^4\right\} = \{w_i, \ln\xi_i\}$ represent the scale and shape parameters in Eq.(12). Corollary 2 provides the scaled scores to fully define the the score-driven dynamic of the Weibull GSPOT specification.

Corollary 2. *For the Weibull GSPOT specification proposed in Eq.(13) the scaled score is estimated by* $\boldsymbol{s}_i = \boldsymbol{\nabla}_i \boldsymbol{S}_i$*, where the score is given by* $\boldsymbol{\nabla}_i := \left\{\nabla_i^1, \ldots, \nabla_i^4\right\}$ *with:*

$$
\begin{aligned}
\nabla_i^1 := \frac{\partial \mathcal{L}_i\left(\boldsymbol{f}_i\right)}{\partial v_i}\frac{\mathrm{d}v_i}{\mathrm{d}f_i^1} &= k_i\left\{\zeta_i\left(t_i - t_{i-1}\right)\right\}^{k_i} - k_i \\
\nabla_i^2 := \frac{\partial \mathcal{L}_i\left(\boldsymbol{f}_i\right)}{\partial k_i}\frac{\mathrm{d}k_i}{\mathrm{d}f_i^2} &= \gamma + k_i \ln\left\{\zeta_i\left(t_i - t_{i-1}\right)\right\} - \left\{\zeta_i\left(t_i - t_{i-1}\right)\right\}^{k_i}\left(\gamma + k_i \ln\left\{\zeta_i\left(t_i - t_{i-1}\right)\right\} - 1\right) \\
\nabla_i^3 := \frac{\partial \mathcal{L}_i\left(\boldsymbol{f}_i\right)}{\partial w_i}\frac{\mathrm{d}w_i}{\mathrm{d}f_i^3} &= \frac{\left(1+\xi_i\right)z_i - \exp\left(w_i\right)}{\left(\xi_i + \xi_i^2\right)z_i + \exp\left(w_i\right)} \\
\nabla_i^4 := \frac{\partial \mathcal{L}_i\left(\boldsymbol{f}_i\right)}{\partial \xi_i}\frac{\mathrm{d}\xi_i}{\mathrm{d}f_i^4} &= \frac{\xi_i}{1+\xi_i} + \frac{\ln\left\{1+\exp\left(-w_i\right)\left(\xi_i+\xi_i^2\right)z_i\right\}}{\xi_i} + \frac{\left(1+\xi_i\right)\left(1+2\xi_i\right)z_i}{\left(\xi_i+\xi_i^2\right)z_i + \exp\left(w_i\right)},
\end{aligned}
$$

where $\zeta_i = \exp\left(\frac{1-\gamma}{k_i} - v_i\right)$ *and* γ *is the Euler–Mascheroni constant. On the other hand, the information quantity is given by:*

$$
\operatorname{diag}\left\{\boldsymbol{S}_i\right\} = \left\{S_i^1, \ldots, S_i^4\right\} = \left\{k_i^{-2}, 6\pi^{-2}, 1+2\xi_i, \left(\frac{1+\xi_i}{\xi_i}\right)^2\right\}. \tag{14}
$$

As noted in Eq.(14), asymptotically independent estimates of time-varying parameters implies that the conditional Fisher information matrix is diagonal, therefore the dynamics parameters in Eq.(5) are only dependent on past information and not contemporaneous spillovers from other processes[2].

Finally, one of the main purposes of the application of extreme value theory in quantitative finance is to be able to make inference associated with events taking place at the tail of the distribution of a stochastic process. Risk measures frequently used in this case are Value at Risk (VaR) and Expected Shortfall (ES). In addition, these risk measures are an essential component when obtaining other systemic risk measures such as CoVaR and MES. In the case of the GSPOT specification described in Eq.(13), the VaR for a confidence level of α, and given that $t_i < t$, can be obtained as follows

[2]The definition of orthogonality can be extended to more than two sets of parameters, however, complexity increases with the number of time-varying parameters (see Cox and Reid, 1987).

$$VaR_t(\alpha) = u + \frac{\exp(w_i)}{\xi_i(1+\xi_i)}\left\{\left(\frac{1-\alpha}{\exp(v_i)^{-k_i}\exp(1-\gamma)\,k_i\,(t-t_i)^{k_i-1}}\right)^{-\xi_i} - 1\right\}. \quad (15)$$

Similarly, the conditional ES is computed as

$$ES_t(\alpha) = \frac{1}{1-\alpha}\int_{\alpha}^{1} VaR_t(s)\,ds = \frac{VaR_t(\alpha)}{1-\xi_i} + \frac{\exp(w_i) - \xi_i(1+\xi_i)\,u}{(1-\xi_i^2)}. \quad (16)$$

A detailed derivation of these risk measures can be obtained following the results of Chavez-Demoulin and McGill (2012); Herrera and Clements (2018).

3. Monte-Carlo Analysis

This section illustrates the finite sample performance of estimators based on Weibull GSPOT or simply GSPOT models. To this end, we conducted a Monte Carlo study for a range of data generating processes. In the first experiment, samples of extreme events of length $n = \{250, 500, 750, 1000\}$ are generated, sample sizes often encountered in stock market returns. Three sets of static parameters $\boldsymbol{\theta} := \left\{\left(\omega_j, \psi_j, \phi_j\right)\right\}_{j=1}^{j=k_1+k_2}$, with $\left\{\psi_j\right\} = \{0.1, 0.5, 0.9\}$, $\left\{\omega_j\right\} = -0.1$ and $\left\{\phi_j\right\} = 0.05$ are considered, implying low, average, and high persistence. The number of replications is 1000 for each of the scenarios. Based on the maximum likelihood estimate $\hat{\boldsymbol{\theta}}_{\boldsymbol{n}}$ of $\boldsymbol{\theta}$ we develop measures of performance for the filtered estimates $\hat{f}_i^j$, which are obtained from Eq.(5) and capture the parameter uncertainty about the true value of $\boldsymbol{\theta}$. The mean error (ME) and the mean square error (MSE) of the time-varying parameters are reported as measures of central tendency and dispersion, respectively, i.e.;

$$ME = \frac{1}{n}\sum_{i=1}^{n}\left(\hat{\rho}_i^j - \rho_i^j\right) \quad \text{and} \quad MSE = \frac{1}{n}\sum_{i=1}^{n}\left(\hat{\rho}_i^j - \rho_i^j\right),^2$$

where ρ_i^j is an orthogonalized time-varying parameter.

Table B.1 reports the simulation results, concentrating on the results for the persistence

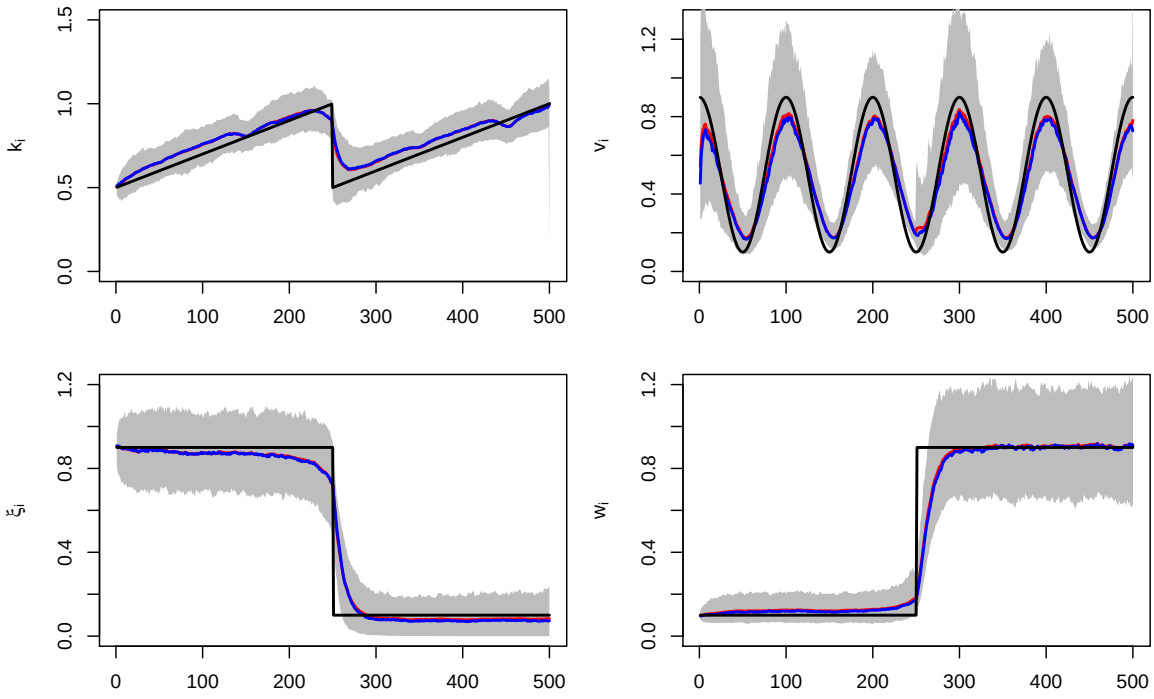

Figure 1: Simulation study with deterministic orthogonalized time-varying parameters estimated using the GSPOT approach based on 1000 simulations. The sample size is 500. Black lines denote the true deterministic function, while the red and blue lines correspond to the mean and median estimates of the time-varying parameters, respectively, obtained over all simulations. The grey bands correspond to the estimated 95% confidence interval.

parameters of both processes. When non-negativity conditions are imposed for small $\psi_j^j = 0.1$, the filtered estimates of $\hat{f}_i^j$ are slightly positively biased for small samples. On the other hand, when higher persistence is present ($\psi_j^j = 0.9$) in the shape parameters, the MSE increases mainly due to possibly infinite second moments ($\hat{\xi}_i > 0.5$ and $\hat{k}_i \to 0$), increasing the dispersion of their estimates. However, in all other case, estimation is consistent given that the ME and MSE drop considerably with sample sizes larger than 500.

In the second experiment, the type of misspecification involves the use of deterministic time-varying parameters. We generate 1000 simulations of sample size $n = 500$. The dynamics of the parameters evolve over time based on different patterns, exhibiting abrupt, rapid and

gradual changes:[3]

- Ramp $k_i = (i/250 - \lfloor i \rfloor /250)\, 0.5 + 0.5$
- Cosine $\alpha_i = 0.5 + 0.4 \cos(2\pi i/100)$
- Sudden drop $\xi_i = 0.9 - 0.8 \mathbb{1}_{i>250}$
- Sudden jump $\delta_i = 0.9 - 0.8 \mathbb{1}_{i<250}$

Figure 1 shows the estimates for the four time-varying parameters. Black lines denote the true deterministic function, while the red and blue lines correspond to the mean and median estimates of the time-varying parameters. The gray bands correspond to the estimated 95% confidence interval. Overall, maximum likelihood provides satisfactory parameter estimates in all the cases considered.

4. Tail-β risk dynamics for U.S Banks

The empirical analysis centers on the tail-β risk measure recently proposed by Van Oordt and Zhou (2017), which utilizes results from extreme value theory to decompose the behavior of extremely adverse returns in the financial system into two main source of risk. One is associated with the tail distribution function of the bank stocks, and the other harnessing the tail dependence structure of the whole banking system.

Under this framework the lower tail of the excess returns of bank stock j, $R_j^e = R_j - R_f$, are driven by the tail behavior of the excess returns of the market portfolio m, $R_m^e = R_m - R_f$, as follows:

$$R_j^e = \beta_j^T R_m^e + \varepsilon_j, \quad \text{for } R_m^e < -VaR_m(\alpha),$$

[3] Various other different specifications for the dynamic of the time varying parameters were utilized, however the results were quite similar to those presented.

where R_j and R_m correspond to stock returns of bank j and the market portfolio m, while R_f is the risk-free rate. Here the condition $R_m^e < -VaR_m(\alpha)$ indicates that the relationship between the excess returns of bank j and the market m, captured by the tail beta coefficient β_j^T, is only justified under the occurrence of extremely adverse extreme events in market m, i.e., above the VaR at the α- confidence level, hence the index T. Finally, ε_j denotes the asset specific risk which is assumed to be independent of the overall risk in the banking sector. Under some mild conditions, Van Oordt and Zhou (2017) show that, for extreme return events obeying a power law, the estimator of the tail beta coefficient β_j^T is given by

$$\beta_j^T = \lim_{\alpha \to 0} \Lambda_j(\alpha)^{1/\xi_m} \frac{VaR_j(\alpha)}{VaR_m(\alpha)}, \tag{17}$$

where ξ_m is the shape parameter of the market m, $\Lambda_j(\alpha) := P\left(R_j^e < -VaR_j(\alpha) \mid R_m^e < -VaR_m(\alpha)\right)$ is the coefficient of tail dependence between R_j and R_m, while $VaR_j(\alpha)$ and $VaR_m(\alpha)$ correspond to the VaR of R_j and R_m, respectively. Further, Van Oordt and Zhou (2019) show that the tail-β risk estimator is related to several other measures of systemic risk, such as Exposure CoVaR, SRISK and the most recent measure of systemic risk the Marginal Expected Shortfall (MES) of Acharya et al. (2017). Indeed, the MES measure is related to the tail-β risk measure as

$$MES_j(\alpha) := \beta_j^T ES_m(\alpha), \tag{18}$$

where $ES_m(\alpha)$ denotes the expected shortfall of the market portfolio m. Hence, the tail-β risk measure seems to be a sufficiently flexible methodology to capture systemic risk and extrapolate to other alternative risk measures.

Using the methodology proposed in section 2.3, Eq.(17) is extended to a dynamic alternative

$$\beta_{jt}^T := \hat{\Lambda}_{jt}(\alpha)^{1/\hat{\xi}_{mt}} \frac{\widehat{VaR_{jt}}(\alpha)}{\widehat{VaR_{mt}}(\alpha)}, \tag{19}$$

where $\widehat{VaR_{jt}}(\alpha)$ and $\widehat{VaR_{mt}}(\alpha)$ are the dynamic VaR estimates of the returns R_j and R_m, and $\hat{\xi}_{mt}$ is the estimator of the shape parameter of the market portfolio m. All VaR estimates are obtained by means of Eq.(15). Finally, a simple rolling window estimator of the coefficient of tail dependence is also constructed from the semiparametric specification

$$\hat{\Lambda}_{jt}(\alpha) := \alpha(t-\omega) \sum_{k=t-\omega}^{t} \mathbb{1}_{\left(R^e_{jk} < -\widehat{VaR_{jk}}(\alpha) \text{ and } R^e_{mk} < -\widehat{VaR_{mk}}(\alpha)\right)},$$

where ω is the length of the window used. Using this dynamic approach a deeper understanding of the systemic risk in the banking sector can be obtained.

4.1. Data Description

The empirical analysis is based on constituents of the S&P Banks Index, which are also large market capitalization members of the S&P 500 index. The sample consists of daily returns for 16 banks, spanning the period, January 4, 1999 to December 31, 2013 for the in-sample period, while the backtesting period is from January 4, 2014 to December 31, 2018. Three banks were excluded from the sample because of missing data. Moreover, we use daily US 3-month treasury bill rate as a proxy for the risk-free rate R_f and the S&P 500 index returns as proxy for market return R_m. A list with the names of all banks utilized together with some descriptive statistics for the bank returns are provided in Table B.2.

4.2. Empirical Results

Here, the negative losses that exceed the 90% quantile of negative log-returns are treated as extreme events. The choice of this threshold is always somewhat contentious. However, a large number of studies show that a choice between 5% and 10% of the tail distribution seems to be good compromise between bias and variance (see Chavez-Demoulin et al. 2014; Bee et al. 2017; Herrera and Clements 2018). Table B.3 reports the results of the estimation of the GSPOT model for all the bank returns, also including results for the S&P 500 index

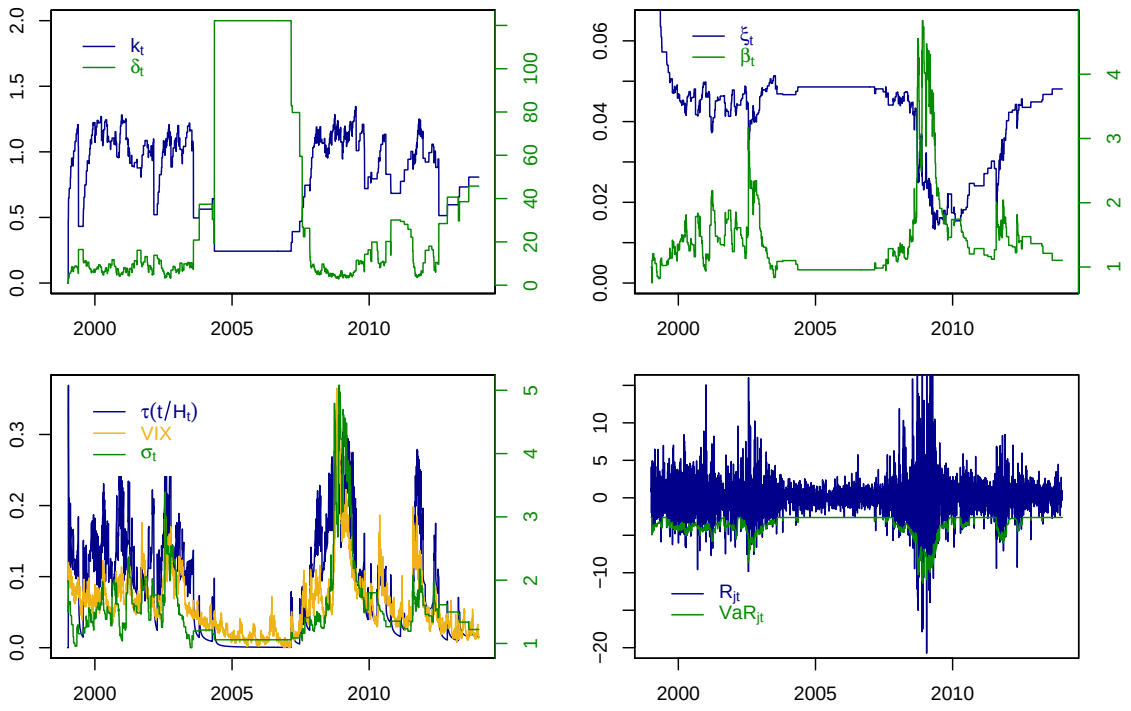

Figure 2: Dynamic behavior of the extreme negative returns of the JP Morgan Chase & Co stock return index through the sample period from January 4, 1999 to December 31, 2013. Top-left: the dynamic of the time-varying parameters of the ground process (k_t and δ_t). Top-right: the dynamic parameters of associated to the generalized Pareto distribution (ξ_t and β_t). Bottom-left: the VIX index, the ground conditional intensity $\tau(t \mid \mathcal{H}_t)$ and the extreme volatility σ_t obtained from the magnitude of the exceedances. Bottom-right: VaR estimates at the 0.95 confidence level for the negative log-returns.

returns. According to these results, in most cases, the parameter estimates are statistically significant. Further, we see that the persistence parameters ϕ_i^j tend to be high for most of the banks. In particular, this persistence is stronger for scale than for shape parameters, although in all cases the time-varying parameters are observed to be mean-reverting (ϕ_i^j less than one).

In order to provide deeper insight into the dynamics of the parameters, Figure 2 illustrates the behavior of extreme returns associated with one of the largest banks in the United States, the JPMorgan Chase & Co[4]. In particular, Figure 2 exhibits the time-varying parameters of the ground process (top-left panel), the dynamic parameters of the generalized Pareto distribution

[4]JP Morgan Chase & Co is a leading global financial services firm with assets of $2.6 trillion in 2019

(top-right), the ground conditional intensity together with the extreme volatility obtained from the magnitude of the exceedances[5] and the VIX index as measure of expectation of market risk (bottom-left).

Finally, VaR estimates at the 0.95 confidence level for the negative log-returns are displayed (bottom-right). Both parameters associated with the conditional intensity of the ground process (k_t and δ_t) and those associated with the probability density function of the marks (ξ_t and β_t), manage to reflect well-known stylized facts present in the asset returns like extreme clustering, persistence and heavy tails. This result is very important, given that both the exceedances of the extreme events and the inter-exceedance times provide relevant information to describe the dynamics of extreme events of financial crises. As a consequence of the proposed dynamics, there is a direct relationship between the ground conditional intensity defined in Eq.(11) and the volatility of extreme events σ_t during turbulent periods. Indeed, our approach provides complementary information to that contained in other measures of market risk, e.g., the VIX index, as is highlighted in Figure 2, with the difference being that the proposed risk measures only focus on tail risk dynamics.

Moving beyond the univariate risk dynamics, next, estimates for the tail-β risk measures over time are presented for each of the bank returns, utilizing the results of the estimates in Table B.3. The VaR estimates for each bank's return are calculated at the 0.95- confidence level, while the windows choose to estimate the dynamic tail dependence is 2 years (500 trading days). As a benchmark model, we also estimate a dynamic-rolling beta model β^r_{jt}, from a standard CAPM specification, by means of a regression model utilizing a window of 3 months (approximately 63 trading days) for each bank's return R^e_j against the market return

[5] According to the generalized Pareto distribution this is defined as follows:

$$\sigma_t = \frac{w_t}{(1-\xi_t)\sqrt{(1-2\xi_t)}},$$

for $\xi_t > 0.5$.

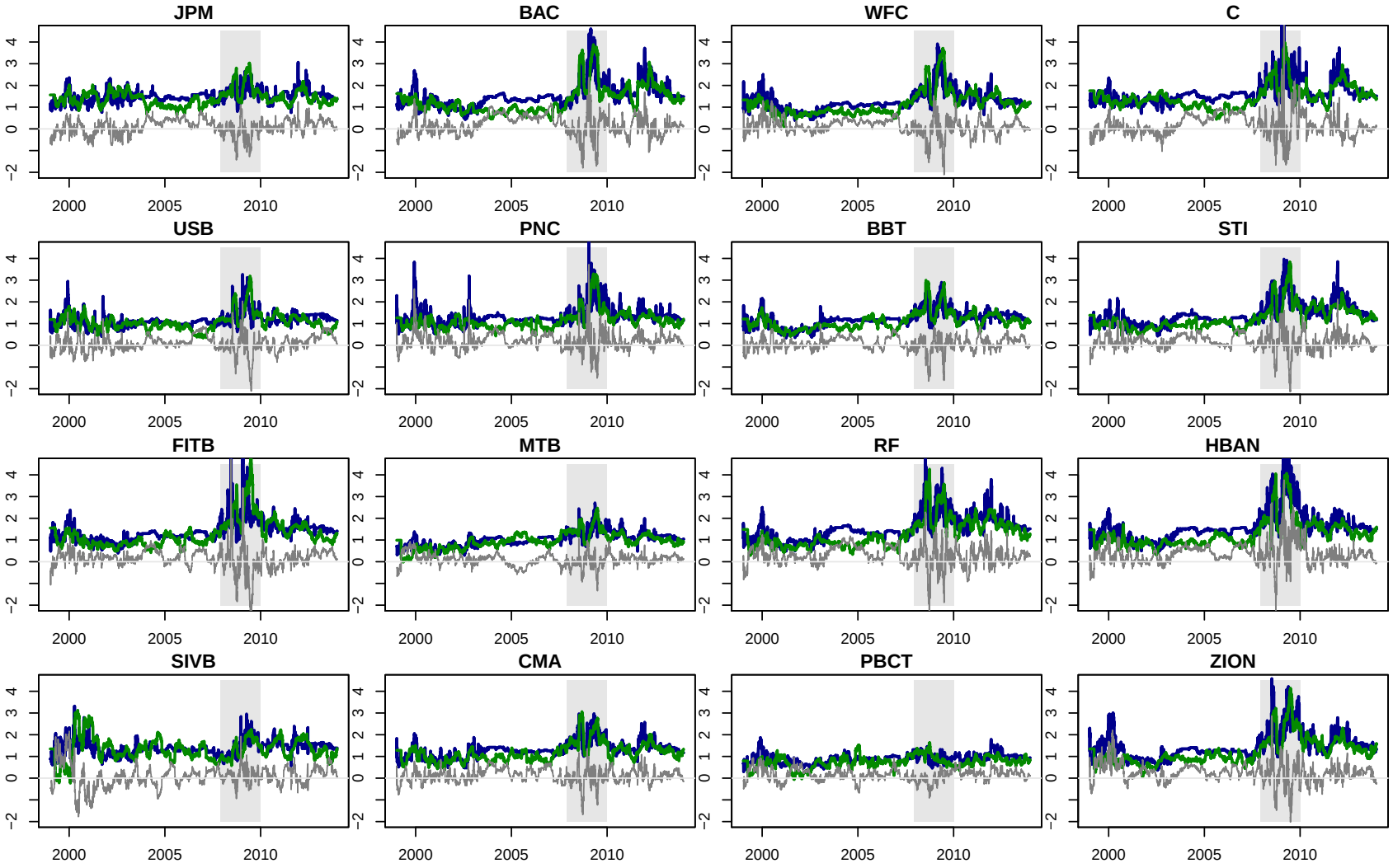

Figure 3: Dynamic estimates of tail-β risk β^T_{jt}, rolling betas β^r_{jt}, and tail beta spread $(\beta^T_{jt} - \beta^r_{jt})$ for bank stocks through the sample period from January 4, 1999 to December 31, 2013.

R^e_m. The results of these estimations are displayed in Figure 3 for each bank in the sample in the same order (from top-left to bottom-right) as described in Table B.2. Blue and green lines correspond to tail-β risks and rolling betas, respectively, while gray lines correspond to the tail beta spread ($\beta^T_{jt} - \beta^r_{jt}$), i.e., the spread between tail betas and the rolling betas.

We find that the tail-β risk estimates as well as the rolling beta estimates share similar dynamics across banks, although we identify some differences between them, especially during periods of turmoil. On average, tail-β risk estimates are 15% higher than the rolling beta estimates and about 6% less volatile. Furthermore, during the subprime crisis we observe a higher dispersion of the tail beta spread, which is highlighted (by a dark gray background) in Figure 3 between December 2007 and December 2009.

In the next section we propose different portfolio optimization strategies based on the results of the tail-β risk estimates. We investigate whether these strategies are informative regarding the dynamics of extreme events and can help to maximize the expected returns of a portfolio in times of high risk in the markets.

4.3. Portfolio optimization scenarios at U.S Banks

One of the key points in modern financial theory is the need for diversification strategies that account for downside risks during periods of turmoil. In order to analyze the extent to which tail-β risk estimates are useful for selecting portfolios of stock banks, a similar approach to Van Oordt and Zhou (2017) is taken with twelve equally-weighted portfolios constructed under two different scenarios.

In the first scenario, *the non-overlapped portfolios*, a bank can only be a member of one portfolio. We build four groups of banks from largest to smallest magnitude of the risk measure utilized. Each group has four bank stocks. Subsequently, we build six portfolios with the different combinations of two groups. In this way, we explore the different forms of diversification that could occur when mixing tail betas of different magnitudes. To identify the groups within a portfolio $\mathcal{P}$ we use subindices from 1 to 4. Thus, for example, a portfolio

with subscripts 1 and 4, $\mathcal{P}_{1,4}$, would indicate that this portfolio is the union of groups 1 and 4, with the highest and lowest average of the risk measure utilized, respectively.

In the second scenario with also six portfolios, *the overlapped portfolios*, there can be an overlap of banks between the portfolios, i.e., a bank stock can be part of more than one portfolio. In both strategies banks are ranked based on the average of different risk measures based on tail-β risk estimates over the whole sample period during which they were held, a period of one month (about 21 trading days). After this period, the portfolios are rebalanced according to the new average of these risk measures from the holding period. For overlapped portfolios, the sub-indeces simply indicate the ranking of the bank stock that belongs to the portfolio in relation to the risk measure utilized. For example, a portfolio with subscripts from 1 to 6, $\mathcal{P}_{1:6}$, is a portfolio composed by the first six bank's stock returns whose risk measures are the highest during the holding period. Again, the confidence level for VaR and ES measures utilized is at the 0.95 confidence level[6].

4.4. Portfolio optimization based on Tail-β risk and Marginal expected shortfall

Under the first strategy, the risk measures used are the dynamic estimates of tail-β risk, the tail-β spreads, and the absolute value of tail-β spreads. For this exercise we calculate rolling betas β^r_{jt} utilizing a window of 1, 2 and 3 months for each bank's return R^e_j against the market return R^e_m. In a second strategy, we consider a dynamic version of the MES risk measure proposed in Eq.(18)

$$MES_{jt}(\alpha) := \beta^T_{jt} ES_{mt}(\alpha), \tag{20}$$

where $ES_{mt}(\alpha)$ is estimated utilizing the results of Eq.(16). In addition, in order to capture the cross-sectional variation in MES for each stock bank j, we also consider the spread

[6]Similar results are obtained for others confidence levels.

between the MES and the ES, and the absolute value of this spread. The main advantage of this approach in comparison with that above is that we do need to calculate rolling betas, and therefore, the uncertainty related to to windows span is not relevant.

Table B.4 reports the results in- and out-of-sample for the first strategy with the respective average in percentage of the portfolio returns (ret%). We denote by $\underset{j\in\mathcal{P}}{E}$ the average of the risk measure utilized for the bank stock returns j that belong to the portfolio $\mathcal{P}$. Using only the information related to the tail-β risk measures, we observe that for the overlapped as well as the non-overlapped portfolios is not possible to find a clear pattern, independent of the window used in to estimate the rolling betas. Better results are obtained when instead we use the spread as a risk measure to rank stock banks (from third to sixth column). In general, there is a positive relationship between a low or negative spread and a high portfolio return. Another interesting result is that there seems to be some diversification when we use portfolios with high and low spreads in the same portfolio, e.g., $\mathcal{P}_{1,4}$ which is a portfolio that is composed by group 1 (highest spreads) and group 4 (lowest spreads) of stock banks. Regardless of these estimates, the most consistent results are obtained when we use instead the absolute spread value as a risk measure. These results suggest that sorting risky portfolios by means of absolute tail beta spread, i.e., portfolios composed of stocks whose tail-β risk measure are decoupled from the rolling betas, tend to have higher expected returns.

In order to give greater robustness to the results based on the tail-β risk estimates and to discard that these are not a consequence of the window utilized in the rolling beta estimates, we explore in the second strategy whether the cross-sectional variation in the MES measure can help to identify the risk premium. Table B.5 describes the results for the three risk measures based on MES as proposed in Eq.(20). In particular, the $\underset{j\in\mathcal{P}}{E}\left[\overline{MES_j}\right]$ the average of each MES_{jt} of bank stock j that belongs to the portfolio $\mathcal{P}$ during the holding period. Similarly, we denote by $\underset{j\in\mathcal{P}}{E}\left[\overline{MES_j}-\overline{ES_j}\right]$ and $\underset{j\in\mathcal{P}}{E}\left[\left|\overline{MES_j}-\overline{ES_j}\right|\right]$ the average of each

spread and absolute value of the spread, respectively[7]. Like the previous results, when using only the MES measure and the spread, it is not possible to obtain advantages in terms of portfolio returns. However, when the absolute value of the spread is used as risk measure, clear advantages appear when this value is minimized. Observe that assuming independence between the average of tail-β risk measures and the ES of the market portfolio, the the absolute value of the spread is reduced when the product of the average of tail-β risk measures and the ES of the market portfolio is similar to the average ES of the chosen portfolio $\mathcal{P}$, that is, $\left|\overline{MES_j} - \overline{ES_j}\right| = \left|\overline{\beta_j^T ES_m} - \overline{ES_j}\right| = \left|\overline{\beta_j^T}\,\overline{ES_m} - \overline{ES_j}\right|$.

5. Conclusion

This paper has proposed a novel time-varying score-driven extreme value model, which is labeled as Generalized score-driven Peaks-over-Threshold (GSPOT). The dynamics of the parameters are orthogonal to the conditional Fisher information matrix, with updating only based on the score from past observations. A Monte-Carlo study showed that this approach can capture a range of different dynamics for the parameters. An empirical study at U.S stock banks returns showed that this model adequately captures the behaviour of extreme events during periods of financial distress. Furthermore, by means of the GSPOT model we estimate a dynamic version of the tail-β risk measures of Van Oordt and Zhou (2017) and the Marginal Expected Shortfall (MES) of Acharya et al. (2017) for these stock bank returns. The empirical results show that the tail-β risk estimates as well as the dynamic version of the MES risk measure are useful in portfolio optimization by hedging against tail risk, obtaining advantages in terms of expected portfolio returns.

[7] The confidence level has been dropped for easy of the exposition.

References

Acharya, V. V., Pedersen, L. H., Philippon, T., Richardson, M., 2017. Measuring systemic risk. The Review of Financial Studies 30 (1), 2–47.

Balkema, A. A., De Haan, L., 1974. Residual life time at great age. The Annals of Probability 5 (2), 792 – 804.

Bee, M., Dupuis, D. J., Trapin, L., 2017. Realized extreme quantile: A joint model for conditional quantiles and measures of volatility with evt refinements. Journal of Applied Econometrics.

Bee, M., Dupuis, D. J., Trapin, L., 2019. Realized peaks over threshold: A time-varying extreme value approach with high-frequency-based measures. Journal of Financial Econometrics 17 (2), 254–283.

Benoit, S., Colliard, J.-E., Hurlin, C., Pérignon, C., 2017. Where the risks lie: A survey on systemic risk. Review of Finance 21 (1), 109–152.

Bernardi, M., Catania, L., 2018. Switching generalized autoregressive score copula models with application to systemic risk. Journal of Applied Econometrics (May), 1–23.

Brownlees, C., Engle, R. F., 2016. Srisk: A conditional capital shortfall measure of systemic risk. The Review of Financial Studies 30 (1), 48–79.

Chavez-Demoulin, V., Embrechts, P., Sardy, S., 2014. Extreme-quantile tracking for financial time series. Journal of Econometrics 181 (1), 44–52.

Chavez-Demoulin, V., McGill, J., 2012. High-frequency financial data modeling using hawkes processes. Journal of Banking & Finance 36 (12), 3415–3426.

Cox, D. R., Reid, N., 1987. Parameter orthogonality and approximate conditional inference. Journal of the Royal Statistical Society: Series B (Methodological) 49 (1), 1–18.

Creal, D., Koopman, S. J., Lucas, A., 2013. Generalized autoregressive score models with applications. Journal of Applied Econometrics 28 (5), 777–795.

Daley, D., Vere-Jones, D., 2003. An Introduction to the Theory of Point Processes. Springer Series in Statistics.

Gorgi, P., Hansen, P., Janus, P., Koopman, S., 2018. Realized wishart-garch: A score-driven multi-asset volatility model. Journal of Financial Econometrics.

Gresnigt, F., Kole, E., Franses, P. H., 2016. Specification testing in hawkes models. Journal of Financial Econometrics 15 (1), 139–171.

Harvey, A., Lange, R.-J., 2017. Volatility modeling with a generalized t distribution. Journal of Time Series Analysis 38 (2), 175–190.

Harvey, A. C., 2013. Dynamic models for volatility and heavy tails: with applications to financial and economic time series. Vol. 52. Cambridge University Press.

Hautsch, N., Herrera, R., dec 2020. Multivariate dynamic intensity peaks-over-threshold models. Journal of Applied Econometrics 35 (2), 248–272.

Herrera, R., Clements, A., 2018. Point process models for extreme returns: Harnessing implied volatility. Journal of Banking & Finance 88, 161–175.

Massacci, D., 2016. Tail risk dynamics in stock returns: Links to the macroeconomy and global markets connectedness. Management Science 63 (9), 3072–3089.

Pickands, J., 1975. Statistical inference using extreme order statistics. The Annals of Statistics, 119 – 131.

Tobias, A., Brunnermeier, M. K., 2016. Covar. The American Economic Review 106 (7), 1705.

Van Oordt, M., Zhou, C., 2019. Systemic risk and bank business models. Journal of Applied Econometrics 34 (3), 365–384.

Van Oordt, M. R., Zhou, C., 2017. Estimating systematic risk under extremely adverse market conditions. Journal of Financial Econometrics 17 (3), 432–461.

Zhang, X., Bernd, S., 2016. Tail risk in government bond markets and ECB unconventional policies. Tech. rep., Working paper.

Appendix A. Proofs

Proof. **Proposition** 1. The time-varying parameters $\boldsymbol{f}_i$ are orthogonal if the off-diagonal elements of the conditional Fisher information matrix are zero. From Eq.(8) we can obtain the second derivatives for time-varying parameters j with respect to f_i^1:

$$\frac{\partial^2 \mathcal{L}_i^\star}{\partial f_i^1 \partial f_i^j} = \sum_{s=2}^{k_1} \frac{\partial^2 \mathcal{L}_i^\star}{\partial f_i^1 \partial \varphi_i^s} \frac{\partial \varphi_i^s}{\partial f_i^j} + \sum_{r=2}^{k_1} \frac{\partial^2 \mathcal{L}_i^\star}{\partial \varphi_i^r \partial \varphi_i^s} \frac{\partial \varphi_i^s}{\partial f_i^j} \frac{\partial \varphi_i^r}{\partial f_i^1} + \sum_{r=2}^{k_1} \frac{\partial \mathcal{L}_i^\star}{\partial \varphi_i^r} \frac{\partial \varphi_i^r}{\partial f_i^1 \partial f_i^j}.$$

Now it is sufficient to check that off-diagonal elements of the Fisher information matrix are zero, where the last term vanishes, because the expected value of the derivative of the log-likelihood of the sample evaluated at the true value, equals zero. Rearranging terms gives:

$$\sum_{s=2}^{k_1} \frac{\partial \varphi_i^s}{\partial f_i^j} \left\{ E_{i-1}\left[\frac{\partial^2 \mathcal{L}_i^\star}{\partial f_i^1 \partial \varphi_i^s} \right] + \sum_{r=2}^{k_1} E_{i-1}\left[\frac{\partial^2 \mathcal{L}_i^\star}{\partial \varphi_i^r \partial \varphi_i^s} \right] \frac{\partial \varphi_i^r}{\partial f_i^1} \right\} = 0,$$

which requires that

$$E_{i-1}\left[\frac{\partial^2 \mathcal{L}_i^\star}{\partial f_i^1 \partial \varphi_i^s} \right] + \sum_{r=2}^{k_1} E_{i-1}\left[\frac{\partial^2 \mathcal{L}_i^\star}{\partial \varphi_i^r \partial \varphi_i^s} \right] \frac{\partial \varphi_i^r}{\partial f_i^1} = 0, \quad s = 2, \ldots, k_1.$$

This is equivalent to the result stated in Eq.(9). Similar results can be obtained for Eq.(10). □

Appendix B. Tables

	$\hat{v}_i = \hat{f}_i^1$						$\hat{k}_i = \exp(\hat{f}_i^2)$					
	$\psi_1 = 0.1$		$\psi_1 = 0.5$		$\psi_1 = 0.9$		$\psi_2 = 0.1$		$\psi_2 = 0.5$		$\psi_2 = 0.9$	
Sample size	MSE	ME	MSE	ME	MSE	ME	MSE	ME	MSE	ME	MSE	ME
250	0.035	-0.046	0.002	-0.015	0.016	-0.020	0.003	-0.036	0.010	-0.049	0.156	-0.007
500	0.001	0.001	0.002	0.014	0.002	0.017	0.000	-0.009	0.004	0.038	0.402	-0.166
750	0.001	-0.001	0.004	-0.018	0.002	-0.002	0.001	-0.005	0.005	-0.023	0.142	0.037
1000	0.001	0.000	0.003	0.021	0.002	-0.023	0.001	0.005	0.006	0.016	0.210	0.003
	$\hat{w}_i = \hat{f}_i^3$						$\hat{\xi}_i = \exp(\hat{f}_i^4)$					
	$\psi_3 = 0.1$		$\psi_3 = 0.5$		$\psi_3 = 0.9$		$\psi_4 = 0.1$		$\psi_4 = 0.5$		$\psi_4 = 0.9$	
Sample size	MSE	ME	MSE	ME	MSE	ME	MSE	ME	MSE	ME	MSE	ME
250	0.006	-0.012	0.062	-0.114	0.007	0.013	0.010	-0.002	0.541	0.520	0.333	-0.038
500	0.001	0.009	0.000	0.015	0.003	0.016	0.005	0.039	0.303	-0.101	0.351	0.014
750	0.007	-0.042	0.000	0.007	0.001	-0.002	0.001	0.002	0.655	-0.068	0.225	0.146
1000	0.003	-0.035	0.000	-0.009	0.005	0.023	0.002	-0.015	0.402	-0.067	0.572	-0.162

Table B.1: Mean error (ME) and the mean square error (MSE) of the time-varying parameters obtained from the Monte Carlo study, with samples size of extreme events $n = \{250, 500, 750, 1000\}$. The estimations are obtained with 1000 replications. We consider three different scenarios for the static parameters $\boldsymbol{\theta} := \left\{(\omega_j, \psi_j, \phi_j)\right\}_{j=1}^{j=k_1+k_2}$, with $\left\{\psi_j\right\} = \{0.1, 0.5, 0.9\}$, $\left\{\omega_j\right\} = -0.1$ and $\left\{\phi_j\right\} = 0.05$ generating processes reflecting low, average, and high persistence.

Ticker symbol	Company name
JPM	JP Morgan Chase & Co.
BAC	Bank of America
WFC	Wells Fargo & Co
C	Citigroup
USB	US Bancorp
PNC	PNC Financial Services Group
BBT	BB&T
STI	Suntrust Banks
FITB	Fifth Third Bancorp
MTB	M&T Bank
RF	Regions Financial Corporation
HBAN	Huntington Bcsh.
SIVB	SVB Financial Group
CMA	Comerica
PBCT	Peoples United Financial
ZION	Zions Bancorporation

Table B.2: Bank stocks in the data sample

Ticker	Ground conditional intensity							Generalized Pareto distribution						
	Scale ($\hat{v}_i = \hat{f}_i^1$)			Shape ($\hat{k}_i = \exp(\hat{f}_i^2)$)			Log-lik	Scale ($\hat{w}_i = \hat{f}_i^3$)			Shape ($\hat{\xi}_i = \exp(\hat{f}_i^4)$)			Log-lik
	ω_1	ψ_1	ϕ_1	ω_2	ψ_2	ϕ_2		ω_3	ψ_3	ϕ_3	ω_4	ψ_4	ϕ_4	
S&P500	0.129	0.169	0.949	0.001	0.039	0.941	-1213.56	-0.578	1.435	0.932	0.485	0.071	0.220	-687.20
	(2.80)	(6.13)	(50.31)	(0.20)	(2.12)	(24.32)		(-26.72)	(74.98)	(11.53)	(33.78)	(60.15)	(13.63)	
JPM	0.203	0.214	0.914	0.002	0.108	0.855	-1156.09	0.022	0.098	0.962	-0.121	0.001	0.942	-607.88
	(3.34)	(6.11)	(33.93)	(0.25)	(3.67)	(12.57)		(22.27)	(19.69)	(86.92)	(-25.79)	(25.98)	(44.07)	
BAC	0.163	0.200	0.931	-0.002	0.053	0.930	-1144.06	0.018	0.116	0.975	0.008	0.001	0.904	-673.66
	(2.96)	(6.61)	(38.19)	(-0.35)	(2.28)	(24.80)		(78.16)	(12.68)	(11.56)	(22.77)	(23.24)	(15.32)	
WFC	0.134	0.199	0.942	0.002	0.065	0.939	-1132.66	0.897	0.769	0.902	0.191	0.971	0.847	-626.49
	(2.87)	(6.24)	(44.55)	(0.46)	(2.89)	(29.62)		(64.39)	(14.10)	(16.15)	(10.14)	(82.57)	(51.06)	
C	0.194	0.223	0.919	0.004	0.074	0.620	-1161.49	0.434	0.447	0.709	-0.163	-0.015	0.270	-741.76
	(3.40)	(7.01)	(38.18)	(0.25)	(1.61)	(3.44)		(10.68)	(32.47)	(16.08)	(-17.32)	(-27.80)	(28.66)	
USB	0.258	0.261	0.891	0.012	0.080	0.734	-1146.38	0.190	0.715	0.206	0.192	-0.027	-0.010	-715.81
	(3.65)	(6.71)	(29.63)	(0.82)	(2.34)	(4.95)		(17.05)	(27.67)	(49.95)	(44.79)	(-52.71)	(-21.13)	
PNC	0.131	0.199	0.946	-0.001	0.073	0.926	-1161.93	0.014	0.109	0.969	-0.303	0.001	0.996	-583.10
	(2.99)	(6.85)	(49.52)	(-0.05)	(2.85)	(22.80)		(69.51)	(22.55)	(69.51)	(-69.51)	(8.49)	(23.84)	
BBT	0.085	0.193	0.963	0.001	0.047	0.972	-1147.26	0.011	0.081	0.978	-0.129	0.001	0.929	-571.31
	(2.65)	(6.92)	(65.32)	(0.34)	(3.75)	(73.03)		(70.17)	(16.52)	(10.37)	(-61.22)	(27.38)	(30.61)	
STI	0.146	0.220	0.934	0.007	0.068	0.910	-1134.44	0.015	0.109	0.979	-0.187	0.001	0.914	-677.53
	(3.17)	(6.50)	(44.70)	(1.08)	(2.88)	(21.04)		(35.15)	(30.58)	(12.34)	(-67.01)	(47.87)	(59.14)	
FITB	0.130	0.197	0.945	-0.001	0.075	0.895	-1141.39	0.679	0.729	0.883	0.333	-0.041	0.576	-811.80
	(3.08)	(6.69)	(49.31)	(-0.01)	(2.41)	(16.00)		(0.93)	(2.65)	(-0.07)	(92.88)	(-68.79)	(34.72)	
MTB	0.108	0.211	0.954	0.004	0.051	0.955	-1184.55	0.013	0.132	0.961	-1.323	0.001	0.666	-525.82
	(2.56)	(6.64)	(51.20)	(0.98)	(2.88)	(38.69)		(16.78)	(17.62)	(57.86)	(-11.81)	(13.08)	(22.60)	
RF	0.119	0.225	0.945	0.003	0.057	0.953	-1106.98	0.029	0.132	0.970	-2.482	0.001	0.679	-717.50
	(3.08)	(6.97)	(50.98)	(0.77)	(3.49)	(42.28)		(17.45)	(12.40)	(83.11)	(-53.79)	(75.00)	(90.47)	
HBAN	0.089	0.207	0.961	0.001	0.074	0.957	-1117.57	0.018	0.107	0.980	0.011	0.001	0.977	-740.65
	(2.68)	(6.79)	(59.67)	(0.04)	(3.49)	(42.12)		(7.73)	(5.46)	(13.23)	(17.89)	(29.80)	(27.81)	
SIVB	0.150	0.210	0.939	-0.016	0.031	-0.892	-1179.35	0.833	0.075	0.021	0.509	-0.035	0.055	-796.69
	(2.80)	(6.72)	(42.37)	(-0.23)	(1.70)	(-18.77)		(78.42)	(11.32)	(31.70)	(17.35)	(-10.27)	(58.57)	
CMA	0.130	0.222	0.947	-0.001	0.051	0.951	-1169.47	0.018	0.101	0.970	-0.292	0.001	0.833	-620.70
	(2.46)	(6.08)	(40.48)	(-0.03)	(2.96)	(31.45)		(5.23)	(22.40)	(96.50)	(-7.26)	(-7.71)	(30.76)	
PBCT	0.207	0.184	0.918	0.005	0.071	0.840	-1230.43	0.011	0.098	0.926	-0.384	-0.001	0.799	-450.48
	(2.85)	(5.86)	(31.57)	(0.55)	(1.82)	(7.35)		(10.40)	(54.03)	(27.09)	(-34.67)	(-23.66)	(32.59)	
ZION	0.223	0.272	0.902	0.011	0.044	0.837	-1125.32	0.024	0.115	0.973	0.007	0.001	0.931	-743.31
	(4.06)	(7.17)	(37.98)	(0.95)	(1.57)	(6.30)		(16.23)	(19.17)	(12.23)	(11.69)	(18.77)	(12.17)	

Table B.3: GSPOT estimates of the ground conditional intensity and the generalized Pareto distribution for bank stocks. The table reports the estimated coefficients and t-statistics (in parentheses). Log-lik corresponds to the value of the log-likelihood.

Portfolios			1-Month					2-Months				3-Months			
	$\underset{j\in\mathcal{P}}{E}\left[\overline{\beta_j^T}\right]$		$\underset{j\in\mathcal{P}}{E}\left[\overline{\beta_j^T}-\overline{\beta_j^r}\right]$		$\underset{j\in\mathcal{P}}{E}\left[\left\|\overline{\beta_j^T}-\overline{\beta_j^r}\right\|\right]$		$\underset{j\in\mathcal{P}}{E}\left[\overline{\beta_j^T}-\overline{\beta_j^r}\right]$		$\underset{j\in\mathcal{P}}{E}\left[\left\|\overline{\beta_j^T}-\overline{\beta_j^r}\right\|\right]$		$\underset{j\in\mathcal{P}}{E}\left[\overline{\beta_j^T}-\overline{\beta_j^r}\right]$		$\underset{j\in\mathcal{P}}{E}\left[\left\|\overline{\beta_j^T}-\overline{\beta_j^r}\right\|\right]$	
	rank	ret%	rank	ret%	rank	ret%	rank	ret%	rank	ret%	rank	ret%	rank	ret%
Non-overlapped portfolios in-sample														
$\mathcal{P}_{1,2}$	1.570	2.701	0.385	1.775	1.422	5.027	0.361	2.360	1.438	4.806	0.356	2.093	1.400	4.770
$\mathcal{P}_{1,3}$	1.487	2.513	0.301	3.330	1.293	4.128	0.285	2.965	1.300	4.274	0.281	3.066	1.267	4.152
$\mathcal{P}_{1,4}$	1.371	3.306	0.166	5.591	1.128	5.283	0.165	4.632	1.132	4.607	0.170	5.275	1.104	5.116
$\mathcal{P}_{2,3}$	1.343	4.261	0.160	1.976	1.038	2.284	0.158	2.935	1.038	2.960	0.159	2.292	1.020	2.451
$\mathcal{P}_{2,4}$	1.227	5.054	0.025	4.237	0.873	3.439	0.038	4.602	0.871	3.294	0.048	4.501	0.857	3.415
$\mathcal{P}_{3,4}$	1.144	4.866	-0.059	5.792	0.744	2.540	-0.038	5.207	0.732	2.761	-0.027	5.474	0.723	2.797
Overlapped Portfolios in-sample														
$\mathcal{P}_{1:6}$	1.634	1.537	0.447	2.084	1.531	5.733	0.417	2.952	1.551	5.481	0.410	2.038	1.506	5.407
$\mathcal{P}_{3:8}$	1.484	3.248	0.296	1.068	1.260	4.606	0.281	2.294	1.270	4.370	0.281	1.956	1.242	3.859
$\mathcal{P}_{5:10}$	1.385	4.671	0.203	1.476	1.103	2.845	0.197	1.742	1.106	3.299	0.197	0.950	1.086	3.309
$\mathcal{P}_{7:12}$	1.299	4.779	0.116	2.636	0.971	1.892	0.119	2.555	0.966	2.545	0.121	2.929	0.952	2.175
$\mathcal{P}_{9:14}$	1.215	5.561	0.024	4.773	0.838	2.064	0.036	4.420	0.829	2.654	0.041	4.055	0.817	2.563
$\mathcal{P}_{11:16}$	1.091	4.783	-0.119	6.528	0.667	2.664	-0.091	6.753	0.655	2.710	-0.077	7.228	0.647	2.466
Non-overlapped portfolios out-of-sample														
$\mathcal{P}_{1,2}$	1.519	1.505	0.271	1.626	0.583	2.276	0.252	1.417	0.502	2.440	0.234	1.598	0.456	1.897
$\mathcal{P}_{1,3}$	1.438	2.946	0.195	1.690	0.529	2.838	0.187	2.264	0.452	2.344	0.171	2.246	0.407	2.654
$\mathcal{P}_{1,4}$	1.349	2.653	0.085	2.758	0.468	2.966	0.085	3.176	0.400	3.316	0.079	2.836	0.359	2.789
$\mathcal{P}_{2,3}$	1.310	2.975	0.076	2.870	0.422	2.662	0.075	2.452	0.348	2.311	0.068	2.792	0.313	2.839
$\mathcal{P}_{2,4}$	1.221	2.682	-0.034	3.938	0.360	2.790	-0.026	3.364	0.296	3.284	-0.024	3.382	0.266	2.974
$\mathcal{P}_{3,4}$	1.139	4.123	-0.110	4.002	0.307	3.352	-0.091	4.211	0.246	3.188	-0.087	4.030	0.217	3.731
Overlapped Portfolios out-of-sample														
$\mathcal{P}_{1:6}$	1.577	1.638	0.323	1.620	0.629	2.587	0.301	1.392	0.547	2.417	0.279	1.530	0.497	2.034
$\mathcal{P}_{3:8}$	1.441	1.177	0.199	2.304	0.516	2.834	0.186	1.659	0.438	2.454	0.174	2.341	0.398	1.819
$\mathcal{P}_{5:10}$	1.349	2.476	0.114	2.757	0.449	2.238	0.108	2.209	0.372	2.036	0.100	2.382	0.336	2.351
$\mathcal{P}_{7:12}$	1.267	3.313	0.038	2.504	0.394	2.596	0.041	2.696	0.321	2.313	0.036	2.894	0.287	2.893
$\mathcal{P}_{9:14}$	1.189	4.410	-0.044	3.811	0.340	3.356	-0.030	3.789	0.275	3.197	-0.032	3.334	0.244	3.860
$\mathcal{P}_{11:16}$	1.097	4.044	-0.159	4.449	0.277	3.632	-0.136	4.475	0.221	3.820	-0.128	4.420	0.195	4.012

Table B.4: Results in- and out-of-sample for the bank portfolios using as strategy three risk measures based on dynamic tail-β . The in-sample period spans from January 4, 1999 to December 31, 2013, while the backtesting period is from January 4, 2014 to December 31, 2018. We denote by $\underset{j\in\mathcal{P}}{E}\left[\overline{\beta_j^T}\right]$ the average of each tail beta β_{jt}^T of bank stock j that belongs to the portfolio $\mathcal{P}$ during the holding period. Similarly, we denote by $\underset{j\in\mathcal{P}}{E}\left[\overline{\beta_j^T}-\overline{\beta_j^r}\right]$ and $\underset{j\in\mathcal{P}}{E}\left[\left|\overline{\beta_j^T}-\overline{\beta_j^r}\right|\right]$ the average of each spread and absolute value of the spread, respectively. The portfolio returns in percentage is denoted by ret% during the holding period. The column labeled 1-Month, 2-Months, and 3-Months reports the number of months utilized to estimate the rolling betas β_{jt}^r.

Portfolios	$\underset{j\in\mathcal{P}}{E}\left[\overline{MES_j}\right]$		$\underset{j\in\mathcal{P}}{E}\left[\overline{MES_j}-\overline{ES_j}\right]$		$\underset{j\in\mathcal{P}}{E}\left[\left\|\overline{MES_j}-\overline{ES_j}\right\|\right]$		$\underset{j\in\mathcal{P}}{E}\left[\overline{MES_j}\right]$		$\underset{j\in\mathcal{P}}{E}\left[\overline{MES_j}-\overline{ES_j}\right]$		$\underset{j\in\mathcal{P}}{E}\left[\left\|\overline{MES_j}-\overline{ES_j}\right\|\right]$	
	rank	ret%	rank	ret%	rank	ret%	rank	ret%	rank	ret%	rank	ret%
	Non-overlapped portfolios in-sample						*Non-overlapped portfolios out-of-sample*					
$\mathcal{P}_{1,2}$	8.274	2.700	2.588	3.843	2.696	3.301	5.682	1.577	1.795	2.137	2.858	2.032
$\mathcal{P}_{1,3}$	7.808	2.593	2.357	3.120	2.480	3.504	5.367	2.769	1.544	2.414	2.619	1.500
$\mathcal{P}_{1,4}$	7.163	3.277	1.964	3.483	2.192	3.673	5.034	2.539	0.121	2.813	2.400	3.376
$\mathcal{P}_{2,3}$	6.974	4.290	1.969	4.084	2.076	3.894	4.886	3.089	1.138	2.815	1.417	2.252
$\mathcal{P}_{2,4}$	6.329	4.974	1.576	4.447	1.787	4.063	4.553	2.859	-0.285	3.214	1.198	4.128
$\mathcal{P}_{3,4}$	5.863	4.867	1.345	3.724	1.571	4.266	4.238	4.051	-0.536	3.491	0.959	3.596
	Overlapped Portfolios in-sample						*Overlapped Portfolios out-of-sample*					
$\mathcal{P}_{1:6}$	8.642	1.433	2.760	3.339	2.871	3.128	5.903	1.440	1.972	2.164	3.307	1.612
$\mathcal{P}_{3:8}$	7.768	3.243	2.346	4.538	2.435	3.662	5.394	1.398	1.541	2.356	1.804	1.659
$\mathcal{P}_{5:10}$	7.208	4.581	2.088	4.300	2.186	3.700	5.038	2.609	1.263	2.248	1.536	2.269
$\mathcal{P}_{7:12}$	6.729	4.956	1.850	4.026	1.964	4.005	4.720	3.516	1.013	2.746	1.290	2.244
$\mathcal{P}_{9:14}$	6.263	5.562	1.597	3.922	1.740	4.181	4.422	4.315	0.740	3.337	1.072	3.310
$\mathcal{P}_{11:16}$	5.570	4.840	1.172	3.870	1.438	4.449	4.080	4.057	-1.052	4.098	0.847	4.382

Table B.5: Results in- and out-of-sample for the bank portfolios using as strategy three risk measures based on the Marginal Expected Shortfall (MES). The in-sample period spans from January 4, 1999 to December 31, 2013, while the backtesting period is from January 4, 2014 to December 31, 2018. We denote by $\underset{j\in\mathcal{P}}{E}\left[\overline{MES_j}\right]$ the average of each MES_{jt} of bank stock j that belongs to the portfolio $\mathcal{P}$ during the holding period. Similarly, we denote by $\underset{j\in\mathcal{P}}{E}\left[\overline{MES_j}-\overline{ES_j}\right]$ and $\underset{j\in\mathcal{P}}{E}\left[\left|\overline{MES_j}-\overline{ES_j}\right|\right]$ the average of each spread and absolute value of the spread, respectively. The portfolio returns in percentage is denoted by ret% during the holding period.